

DIRECTED EVOLUTION OF D-AMINO ACID OXIDASE FOR THE
OXIDATION OF NON-PROTEINOGENIC AMINO ACIDS

Yvonne Martha Wilson



PhD

The University of Edinburgh

2009



Biocatalysts are powerful tools in the synthesis of enantiomerically pure chiral compounds. The properties of enzymes can be improved and novel activities obtained through the application of directed evolution techniques. A key element in this process is the screening technology applied for detection of the desired properties.

This project has focused on amino acid oxidase enzymes with activity towards non-proteinogenic amino acids. Two sources of amino acid oxidases were investigated. A culture collection containing 500 microorganisms was screened for activity towards two β -amino acids. However, no observable oxidase activity was detected towards these substrates. In addition, known amino acid oxidase enzymes were subjected to both random and single-site saturation mutagenesis with the aim of producing novel activity.

Random mutagenesis libraries were prepared by propagating the *Trigonopsis variabilis* D-amino acid oxidase (TvDAAO) gene in a mutator strain and by performing error-prone PCR (epPCR) on the *Rhodotorula gracilis* D-amino acid oxidase (RgDAAO) gene. These libraries were initially screened using a solid-phase assay for detection of activity towards β -amino acids. To overcome reproducibility problems, a high-throughput liquid-phase screening method in 96-well plate format was developed, evaluated and used to screen the RgDAAO epPCR library.

In the absence of any detectable activity towards the selected β -amino acid substrates, an alternative strategy, which minimised the variant library size and increased the range of substrates, was applied. Single site saturation libraries were generated by saturation mutagenesis PCR at the RgDAAO active site residues F58, M213, Y238 and R285. The resulting variant libraries were screened in the liquid-phase for activity towards a range of proteinogenic and non-proteinogenic amino acids.

Saturation mutagenesis at the conserved active site residues Y238 and R285 produced mainly deleterious exchanges. Reduced oxidase activity was observed towards good substrates for the parental enzyme and no novel oxidase activity was detected for substrates towards which the parental enzyme is inactive.

However, saturation at the active site residues F58 and M213 produced a range of beneficial and deleterious variants, allowing substrate profiles to be produced for each. Evaluation of these profiles permitted the identification of individual variants.

Although no oxidase activity was observed towards β -amino acids, improved activity was observed in both the F58 and M213 saturation mutagenesis libraries towards several proteinogenic and non-proteinogenic substrates. The improved activity detected in the assay for the variants F58L and F58I towards (*rac*)-tetrahydroisoquinoline-3-carboxylic acid and for F58M towards (*R*)-pipecolic acid was confirmed by performing whole cell biotransformations and analysing the progression of the reactions by HPLC.

I would like to thank my supervisor Professor Nick Turner for his guidance and the opportunity to carry out this work. I am grateful for advice and supervision from Professor Bob Baxter.

My industrial supervisor, Dr Rich Lloyd has been extremely helpful and I am indebted to him for his time and advice. I also thank the biocatalysis group at Chirotech, particularly Dr Ian Taylor for their helpfulness and sharing their knowledge.

I am grateful to Ingenza for providing me with their pPOT3 plasmid containing the RgDAAO gene and friendly assistance.

Dr Jemma Morgan provided me with the pJLM402 plasmid containing the TvDAAO gene and supported me during my PhD. I am grateful to Dr Renate Reiss for her time, advice and friendship. I appreciate the support and friendliness of the Turner/Flitsch group members.

Many thanks to Dr Renate Reiss, Dr Valentin Koehler and Dr Bettina Nestl for proof-reading this thesis.

Thank you to my parents and to Callum for their encouragement and backing. Thanks also to Sue for persuading me to return to education.

I am grateful to the BBSRC and Chirotech for funding.

ABBREVIATIONS

AAP	4-aminoantipyrine
% v/v	% by volume
[X]	concentration of X, in units given
AMP	Ampicillin
AU	Absorbance units
BCA	Bicinchoninic acid
Bp	Base pair
BSA	Bovine Serum Albumin
CAP	Chloramphenicol
CFE	Cell free extract
Cfu	colony forming unit
dCMP	deoxycytidine monophosphate
dGMP	deoxyguanosine monophosphate
DI	Deionised
DKR	Dynamic kinetic resolution
DNA	Deoxyribonucleic acid
dNTP	Deoxyribonucleotide triphosphate (generic)
e.e.	enantiomeric excess
EC number	Enzyme Commission number
EDTA	Ethylene diamine tetraacetic acid
epPCR	error-prone polymerase chain reaction
EtBr	Ethidium bromide
FAD	flavin adenine dinucleotide
HRP	Horseradish peroxidase
ICMB	Institute of Cell and Molecular Biology
KAN	Kanamycin
Kb	kilobases
LB	Luria-Bertani broth

ABBREVIATIONS

M. Wt	molecular weight
MEGAWHOP	megaprimer PCR of whole plasmid
NEB	New England Biolabs
PBS	Phosphate buffered saline
PCR	Polymerase chain reaction
PDB	Protein Data Bank
PVDF	Polyvinylidene fluoride
RgDAAO	<i>Rhodotorula gracilis</i> D-amino acid oxidase
RO	Reverse osmosis
Rpm	revolutions per minute
RV	resuspension volume
SDS PAGE	sodium dodecylsulfate polyacrylamide gel electrophoresis
SOB	Super optimal broth
SOC	SOB medium + glucose
TAE	Tris acetate EDTA
<i>Taq</i>	<i>Thermus aquaticus</i>
TBHBA	2,4,6-tribromo-3-hydroxybenzoic acid
TEAA	Triethyl ammonium acetate buffer
T _m	Melting temperature
Tris	Tris(hydroxymethyl) aminomethane
Ts	transition (nucleotide exchange)
TS(B)	Tryptone soya (broth)
Tv	transversion (nucleotide exchange)
TvDAAO	<i>Trigonopsis variabilis</i> D-amino acid oxidase
UV	Ultraviolet

Declaration	2
Abstract	3
Acknowledgements	4
Abbreviations	5
Contents	7
1 INTRODUCTION	10
1.1 SYNTHESIS OF CHIRAL AMINO ACIDS	10
1.1.1 Biocatalytic routes to optically pure non-proteinogenic amino acids	11
1.2 D-AMINO ACID OXIDASE	18
1.3 DIRECTED EVOLUTION	19
1.3.1 Random Variant Libraries and Bias	21
1.3.2 Assessment of random libraries	26
1.3.3 Activity Screening	27
1.4 SUMMARY AND AIMS	30
2 RESULTS AND DISCUSSION	31
2.1 SCREENING MICROORGANISMS FOR ACTIVITY TOWARDS β-AMINO ACIDS	31
2.2 CHARACTERISATION OF PARENTAL OXIDASE ENZYMES	34
2.2.1 Confirmation of parental gene sequences	34
2.2.2 Comparison of the RgDAAO and TvDAAO amino acid sequences	34
2.2.3 Parental oxidase activity towards proteinogenic and non-proteinogenic amino acids	35
2.2.4 Conclusions	43
2.3 DIRECTED EVOLUTION OF D-AAO	44
2.3.1 Mutator strain library TvDAAO	44
2.3.2 epPCR library RgDAAO	45
2.3.3 Screening the RgDAAO epPCR library	54
2.3.4 Conclusions	86
2.4 SATURATION MUTAGENESIS OF PARENTAL <i>RHODOTORULA GRACILIS</i> D-AMINO ACID OXIDASE	89
2.4.1 Selection of key residues for saturation mutagenesis	89
2.4.2 Preparation of saturation mutagenesis libraries	91
2.4.3 Verification of RgDAAO saturation mutagenesis libraries	92
2.4.4 Growth and expression of RgDAAO saturation mutagenesis variants	94
2.4.5 Process for screening of RgDAAO saturation mutagenesis variants	96
2.4.6 Screening of RgDAAO saturation mutagenesis libraries	116
2.4.7 Conclusions	128

2.5	BIOTRANSFORMATIONS USING VARIANT ENZYMES	132
2.5.1	Biotransformation of pipercolinic acid.....	132
2.5.2	Biotransformation of (<i>R</i>)-tiq	135
2.5.3	Conclusions.....	138
2.6	OVERALL CONCLUSIONS	140
2.7	OVERALL FUTURE WORK.....	143
3	EXPERIMENTAL	145
3.1	INSTRUMENTS.....	145
3.2	METHODS.....	146
3.2.1	DNA purification and manipulation	146
3.2.2	Mutation Protocols.....	149
3.2.3	Transformation, growth and protein expression methods	154
3.2.4	Protein purification and analysis.....	159
3.2.5	Colorimetric assays.....	161
3.2.6	Biotransformations.....	163
3.2.7	Buffer and reagent recipes	164
4	REFERENCES.....	167
5	APPENDICES	172
5.1	PARENTAL DNA SEQUENCES.....	172
5.1.1	<i>R. gracilis</i> DAAO	172
5.1.2	<i>T. variabilis</i> DAAO	173
5.2	PRIMERS.....	174
5.2.1	Sequencing primers.....	174
5.2.2	epPCR Primers.....	174
5.2.3	Saturation mutagenesis primers	175
5.3	VECTOR MAPS.....	175
5.3.1	pJLM402.....	175
5.4	GENOTYPES OF <i>E. COLI</i> STRAINS USED	176
5.4.1	TOP10.....	176
5.4.2	BL21 (DE3)	176
5.4.3	XL1-Blue	176
5.4.4	XL1-Red	176
5.5	SYMBOLS OF THE NATURALLY OCCURRING AMINO ACIDS	176
5.6	SINGLE LETTER NUCLEOTIDE CODES.....	177
5.7	CALCULATIONS	177
5.7.1	Pearson Product moment correlation coefficient (R^2).....	177
5.7.2	Beer-Lambert Law	178
5.8	MICROORGANISMS SCREENED FOR ACTIVITY TOWARDS (<i>RAC</i>)-β- PHENYLALANINE AND (<i>RAC</i>)-β-HOMOPHENYLALANINE.....	178

5.9	PROFILES AND HIGHEST NORMALISED RATES FOR RGDAAO SATURATION	
	MUTAGENESIS LIBRARIES	182
5.9.1	RgDAAO F58: (<i>R</i>)-alanine	182
5.9.2	RgDAAO F58: (<i>rac</i>)-tetrahydroisoquinoline-3-carboxylic acid.....	185
5.9.3	RgDAAO F58: (<i>rac</i>)- <i>allo</i> -threonine	188
5.9.4	RgDAAO F58: (<i>R</i>)-threonine.....	189
5.9.5	RgDAAO F58: (<i>S</i>)-alanine	191
5.9.6	RgDAAO F58: (<i>R</i>)-pipecolinic acid	193
5.9.7	RgDAAO F58: (<i>rac</i>)- β -homophenylalanine	195
5.9.8	RgDAAO F58: (<i>rac</i>)- <i>tert</i> -leucine	197
5.9.9	RgDAAO F58:(<i>rac</i>)- 3-aminobutyric acid.....	199
5.9.10	RgDAAO F58: (<i>rac</i>)- β -phenylalanine	200
5.9.11	RgDAAO M213: (<i>rac</i>)-tetrahydroisoquinoline-3-carboxylic acid.....	201
5.9.12	RgDAAO M213: (<i>R</i>)-serine	203
5.9.13	RgDAAO M213: (<i>rac</i>)- β -pyridylalanine	205
5.9.14	RgDAAO M213: (<i>rac</i>)-homophenylalanine	207
5.9.15	RgDAAO M213: (<i>rac</i>)-phenylalanine	209
5.9.16	RgDAAO M213: (<i>rac</i>)- β -methylphenylalanine.....	211
5.9.17	RgDAAO M213: (<i>rac</i>)- β -homophenylalanine.....	213
5.9.18	RgDAAO M213: (<i>rac</i>)- 3-aminobutyric acid	215
5.9.19	RgDAAO M213: (<i>rac</i>)- β -phenylalanine.....	216
5.9.20	RgDAAO R285: (<i>R</i>)-alanine.....	217
5.9.21	RgDAAO R285: (<i>S</i>)-alanine	219
5.9.22	RgDAAO R285: (<i>rac</i>)-tetrahydroisoquinoline-3-carboxylic acid.....	221
5.9.23	RgDAAO R285: (<i>R</i>)-pipecolinic acid	223
5.9.24	RgDAAO R285: (<i>rac</i>)- <i>allo</i> -threonine	225
5.9.25	RgDAAO R285: (<i>rac</i>)- β -homophenylalanine.....	227
5.9.26	RgDAAO R285: (<i>rac</i>)- 3-aminobutyric acid	229
5.9.27	RgDAAO R285: (<i>rac</i>)- β -phenylalanine.....	230
5.9.28	RgDAAO Y238: Rates shown prior to normalisation.....	231

1 INTRODUCTION

1.1 SYNTHESIS OF CHIRAL AMINO ACIDS

Amino acids have a large range of industrial applications and some proteinogenic amino acids are produced in significant volumes. For example, in 1999 650 000 tons of glutamic acid were produced for use in the food industry.⁽¹⁾ Non-proteinogenic amino acids are also important for use as synthetic building blocks for fine chemicals and pharmaceutical intermediates. Examples of pharmaceuticals incorporating non-proteinogenic amino acid moieties are the β -lactam antibiotic, amoxicillin produced by GSK and taltobulin, an antimetabolic produced by Wyeth shown in Figure 1.1.

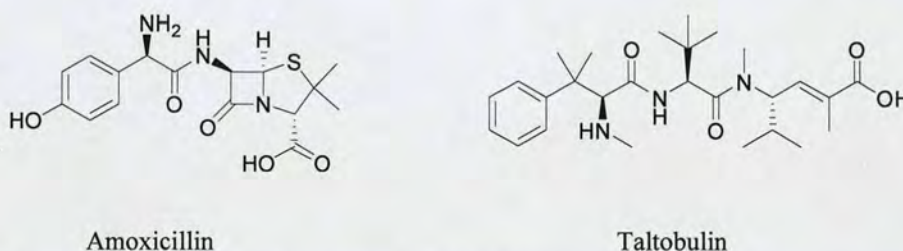
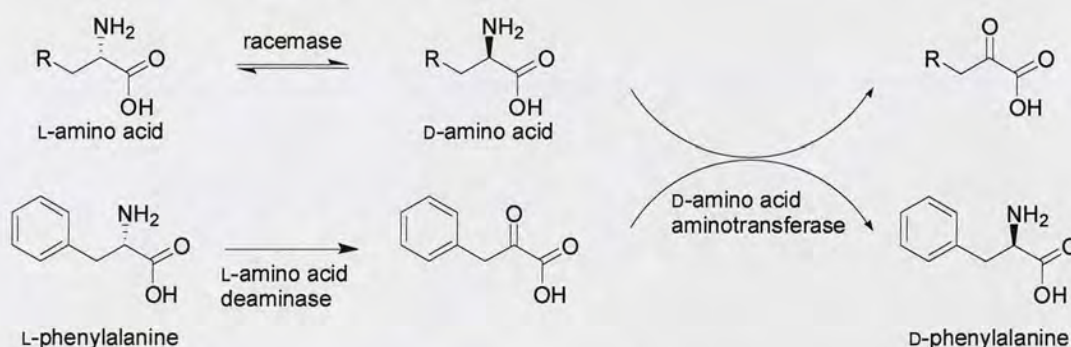


Figure 1.1 – Active compounds containing non-proteinogenic amino acids.

Amino acids are obtained by extraction (proteinogenic amino acids) or by chemical or biological synthesis. Where one epimer in an active compound does not confer the desired activity, production of enantiomerically pure compounds, rather than racemic mixtures is desired. Manufacturers are required to research and characterise the physiological activity of each enantiomer in any chiral drug to be marketed as a mixture, as the distomer may cause adverse effects. For example, (*S*)-penicillamine has antiarthritic activity while the (*R*)-enantiomer is toxic.⁽²⁾ In addition, asymmetric production routes reduce cost and waste. There are many chemical methods for the asymmetric synthesis of amino acids, for example asymmetric Strecker reaction, α -alkylation of glycine derivatives and asymmetric hydrogenation.^(3,4) However, as biocatalysts offer high chemo-, enantio- and regio-selectivity, catalyse a broad spectrum of reactions, are degradable and operate at physiological temperature and pH, these present attractive routes to chiral amino acids.

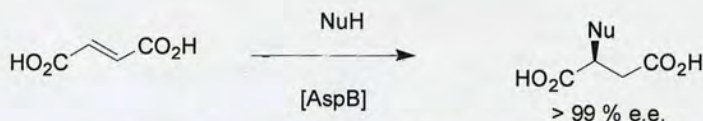
1.1.1 Biocatalytic routes to optically pure non-proteinogenic amino acids

Several enzymes have been investigated for their use in the production of chiral amino acids, for example hydantoinases combined with carbamoylases, acylases, amidases, lipases, lyases, transaminases and dehydrogenases. Hauer *et al.* published a review in 2004 on industrial production of optically active compounds including biocatalytic routes to amino acids⁽¹⁾ in which several fermentation and biotransformation methods are described. An example of a fermentation method used industrially is the production of (*R*)-phenylalanine by Monsanto.⁽⁵⁾ The microorganisms used have been modified such that they produce a racemase, L-amino acid deaminase and D-amino acid aminotransferase but no D-amino acid deaminases. L-phenylalanine is produced endogenously and the L-amino acid amino-donor group is added to the growth medium. The α -keto acid produced by deamination of the donor group is metabolised to CO₂ and H₂O (Scheme 1.1).



Scheme 1.1 – Fermentation process for the production of D-phenylalanine using modified microorganisms.⁽⁵⁾

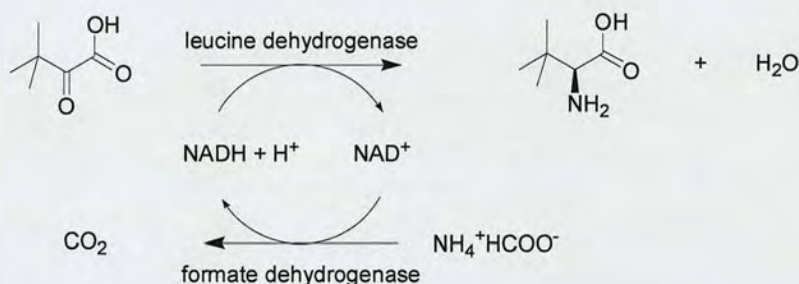
Hauer's review also describes the commercial production of L-aspartic acid by the desymmetrisation of fumaric acid using ammonia as nucleophile catalysed by L-aspartate ammonia lyase (AspA, EC 4.3.1.1). AspA is very substrate specific and no useful alternative nucleophiles have been identified. More recently, Feringa *et al.* described the cloning and overexpression of aspartate ammonia lyase (AspB) from *Bacillus* sp.YM55-1. This group found that AspB which, in contrast to AspA can accept nucleophiles other than ammonia⁽⁶⁾ as shown in Scheme 1.2.



Nu = HNOH, MeONH, HNNH₂ or MeNH

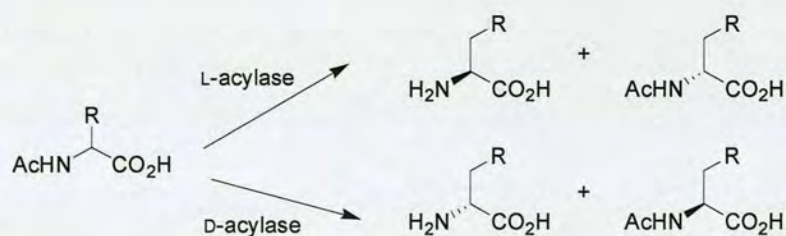
Scheme 1.2 – AspB catalysed Michael addition of a nucleophile (Nu) to fumarate. Enantiomeric excesses > 99 % were achieved with 100 % conversion at 42 mM substrate concentration over reaction times ranging from 20 min to 7 days.⁽⁶⁾

An industrial example which makes use of a dehydrogenase is the Degussa process for the production of *L-tert-leucine* which uses *L-leucine* dehydrogenase for the reductive amination of the corresponding 2-oxocarboxylic acid as shown in Scheme 1.3.⁽⁷⁾ This reaction requires a cofactor such as NADH which is regenerated by the dehydrogenation of ammonium formate, catalysed by formate dehydrogenase.



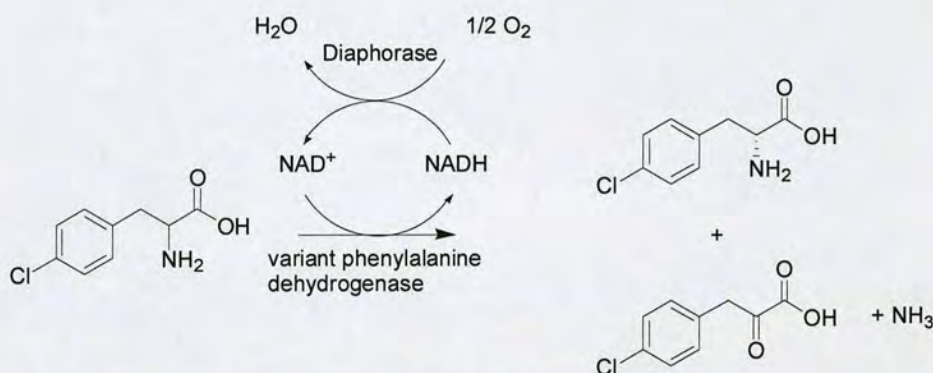
Scheme 1.3 – Reductive amination by leucine dehydrogenase.⁽⁷⁾

There are many examples of enzymes applied in kinetic resolutions from racemates to produce chiral amino acids. For example acylases are used to selectively hydrolyse the amide bond in one enantiomer, leaving the other unreacted as shown in Scheme 1.4.



Scheme 1.4 – Acylase-catalysed kinetic resolution of amino acids.

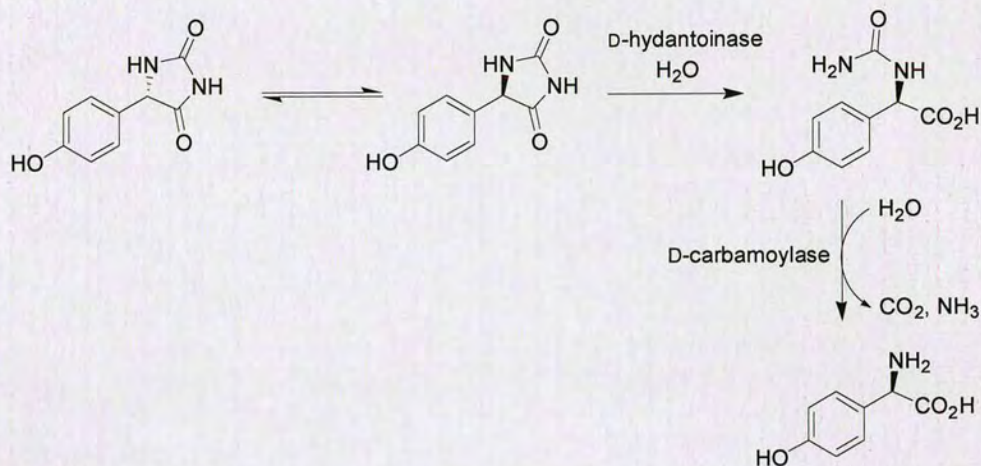
A recent example published by Engel *et al.* describes the kinetic resolution of D-4-chlorophenylalanine⁽⁷⁾ using an engineered L-phenylalanine dehydrogenase. Cofactor regeneration is catalysed by diaphorase. The high stereoselectivity of the enzyme leaves the D-enantiomer basically unreacted even at high conversions.



Scheme 1.5 – Kinetic resolution of (*rac*)-4-Cl-phenylalanine (5-10 mM). 99 % conversion of the (*S*)-enantiomer after 40 h.⁽⁷⁾

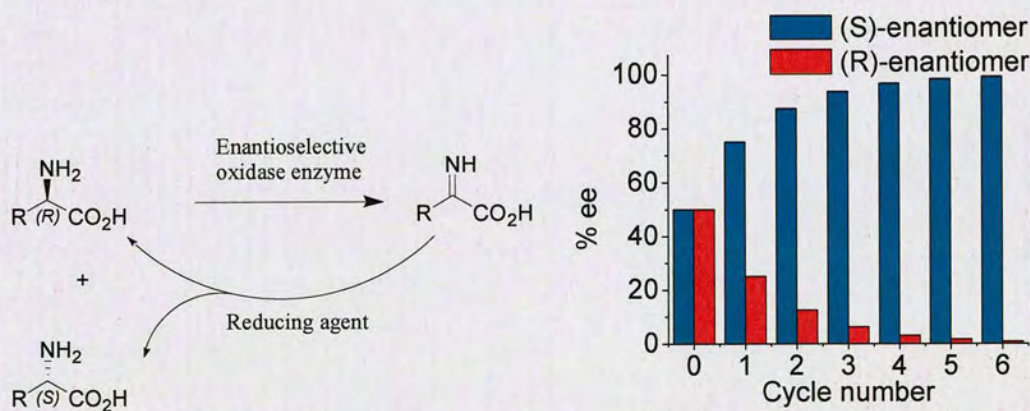
A limitation in kinetic resolutions is the 50 % theoretical yield which may be obtained. To overcome this limitation strategies such as dynamic kinetic resolution or cyclic deracemisation have been applied in some cases.

A commercial example of a dynamic kinetic resolution used in the production of amino acids is the Kanegafuchi synthesis of D-*p*-hydroxyphenylglycine shown in Scheme 1.6.⁽⁸⁾ D-5-(*p*-hydroxy)-phenylhydantoin is selectively hydrolysed by D-hydantoinase to *N*-carbamoyl-*p*-hydroxy-D-phenylglycine. Under alkaline conditions the racemic hydantoin starting material is racemised thus enabling a theoretical yield of the carbamoylated D-amino acid of 100 %. Decarbamoylation to the amino acid is performed by a D-carbamoylase.



Scheme 1.6 – Dynamic kinetic resolution of a racemic hydantoin used in the production of *D-p*-hydroxyphenylglycine.

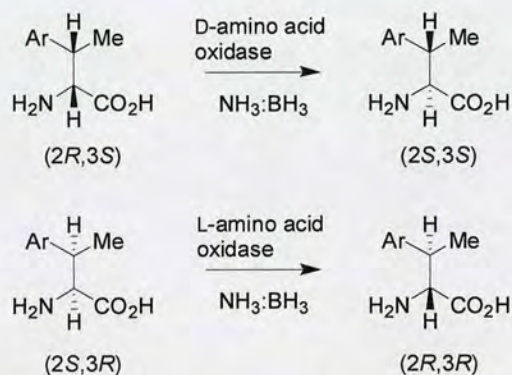
An alternative strategy researched in the group of Nicholas J. Turner combines an enantioselective enzyme-catalysed oxidation reaction with a non-selective, non-enzymatic reduction reaction, as shown in Scheme 1.7.



Scheme 1.7 – Cyclic deracemisation of amino acids.

Given ideal conditions, it can be seen that 7 cycles of the above scheme will produce a single enantiomer in >99 % e.e. This oxidation-reduction sequence has been successfully used within the Turner group for the deracemisation of chiral α -amino acids⁽⁹⁻¹¹⁾ and has been extended to chiral amines⁽¹²⁾.

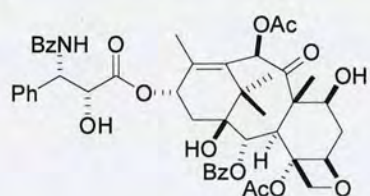
The former method was used in combination with asymmetric hydrogenation to access all four diastereomers of a range of β -methyl- β -arylalanine analogues as shown in Scheme 1.8.⁽¹⁰⁾



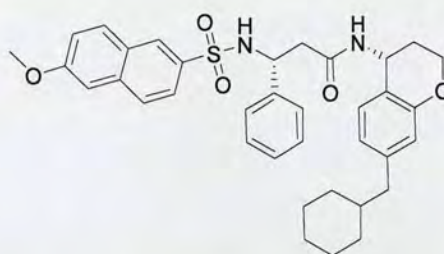
Scheme 1.8 – Deracemisation of β -methyl- β -arylalanine analogues.⁽¹⁰⁾

It was found that, although, the $(2S,3R)$ and $(2R,3S)$ diastereomers were easily accessed by asymmetric hydrogenation of didehydroamino acids, this was not the case for the $(2R,3R)$ and $(2S,3S)$ diastereomers. Cyclic deracemisation of the $(2S,3R)$ diastereomers using L-amino acid oxidase, combined with ammonia borane as reducing agent, provided the $(2R,3R)$ diastereomers in yields of between 68-81 % and > 99 % de. Deracemisation of the $(2R,3S)$ diastereomers using D-amino acid oxidase provided the $(2S,3S)$ diastereomers with yields of 80-92 % and > 99 % de.

β -amino acids are much less abundant than their α -counterparts but they do occur in nature in free form and as substructures of peptides and alkaloids. Naturally occurring β -amino acids include β -lysine, β -alanine and β -tyrosine.⁽¹³⁾ β -Alanine, for example, is a precursor to pantothenic acid, an intermediate in coenzyme A biosynthesis.⁽¹⁴⁾ Free β -amino acid and natural products containing β -amino acids have been found to display antibiotic, antifungal, cytotoxic or other pharmacological properties. Examples are the antitumor agent paclitaxel, the α -hydroxy β -amino acid side chain of which has been shown to be necessary for activity⁽¹⁵⁾ and the bradykinin B1 receptor antagonist, both shown in Figure 1.2.



Paclitaxel

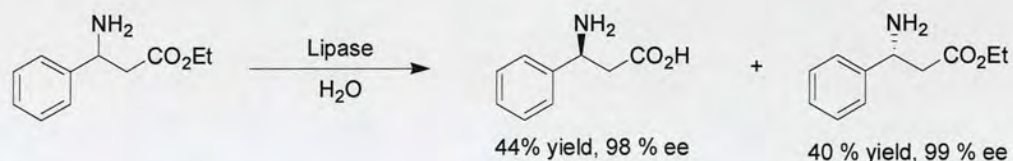


Bradykinin B1 receptor antagonist

Figure 1.2 – Structures of the mitotic inhibitor Paclitaxel⁽¹⁵⁾ and a bradykinin B1 receptor antagonist⁽¹⁶⁾.

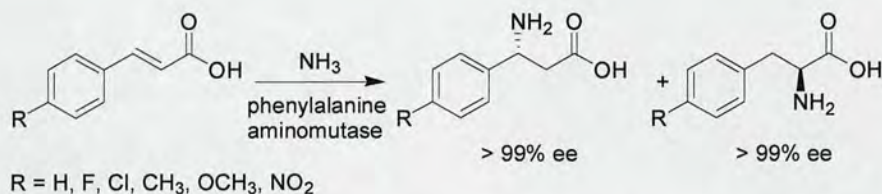
β -Amino acids are also important as synthetic precursors to β -lactams, which include β -lactamase inhibitors, human leukocyte elastase inhibitors and have been shown to possess antibiotic activity and influence cholesterol uptake.⁽¹⁵⁾ Peptidases are unable to cleave amide bonds adjacent to a β -amino acid, thus peptides containing β -amino acids are more stable to enzymatic hydrolysis and can therefore be used in the preparation of modified peptides with increased *in vivo* stability.^{(17),(18)}

Most biocatalytic routes to enantiomerically pure β -amino acids involve kinetic resolutions using hydrolytic enzymes. Many examples in the literature make use of penicillin acylase (PA) from *Escherichia coli* (*E. coli*) which is interesting because most amidases are substrate specific and β -amino acids are not the natural substrates.⁽¹⁵⁾ An efficient and scaleable example of a lipase catalysed resolution of β -aryl- β -amino acids described by Faulconbridge *et al.* is shown in Scheme 1.9.⁽¹⁹⁾



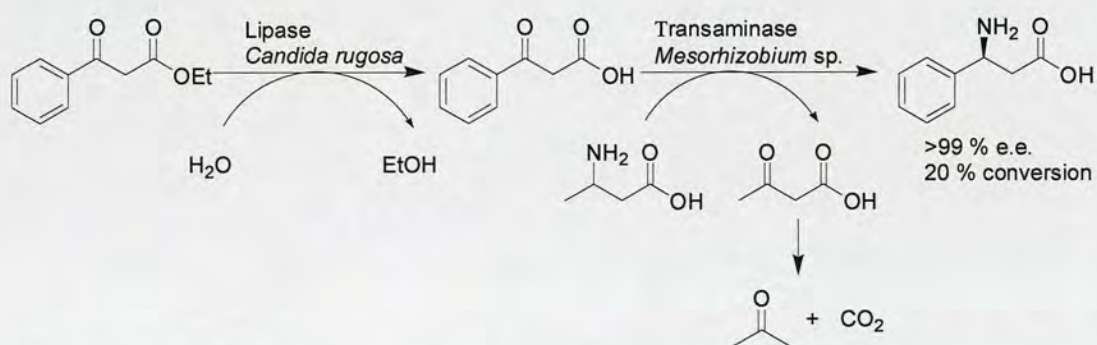
Scheme 1.9 – A lipase-catalysed resolution of β -aryl- β -amino acid esters performed at 200 g L⁻¹ substrate concentration and providing 44 % yield, 98 % e.e. The lipase accepts a variety of β -aryl- β -amino acid ester analogues.⁽¹⁹⁾

A recent paper by Janssen *et al.* describes the phenylalanine aminomutase catalysed amination of substituted cinnamic acids to produce enantioselectively α - and β -phenylalanine derivatives.⁽²⁰⁾



Scheme 1.10 – Aminomutase catalysed formation of α - and β -phenylalanine derivatives. The regioselectivity of the addition reaction is affected by the electronic nature of the aromatic substituent. Electron-donating groups promote formation of the β -amino acid.

Transaminases have been identified for the transamination of both aliphatic and aromatic β -keto acids. An example is the transaminase from *Mesorhizobium* sp. strain LUK which has been cloned and characterised by Kim *et al.*⁽²¹⁾ The transamination of benzoylacetate is shown in Scheme 1.11. To prevent problems caused by the decarboxylation of the β -keto acid substrate, Kim *et al.* generated it *in situ* by lipase-catalysed hydrolysis of the β -keto ester. Inhibition of the transaminase by the β -keto acid product of the amino donor was observed for several donors and was overcome by the use of 3-aminobutyric acid, the product of which decomposes to acetone and CO₂.

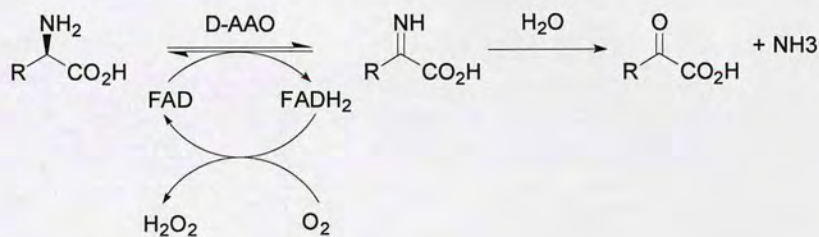
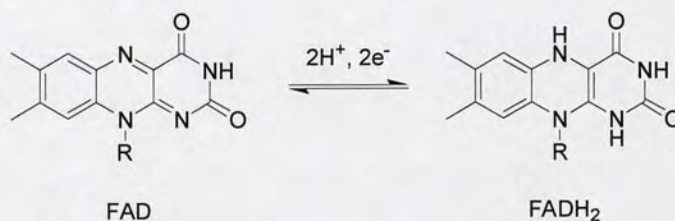


Scheme 1.11 – Transaminase-mediated transformation of benzoylacetate to (S)- β -phenylalanine.

Several biocatalytic routes to both proteinogenic and non-proteinogenic amino acids have been described. However, it was hoped that the oxidation-reduction strategy used in the Turner group for the deracemisation of α -amino acids could be further developed to include new examples of non-proteinogenic α -amino acids and in particular β -amino acids. A suitable enzyme for the enantioselective oxidation of β -amino acids was therefore required. Possible starting points for this project were A) to screen for existing β -amino acid oxidase activity from a collection of microorganisms, B) to screen α -amino acid oxidase enzymes for activity towards β -amino acids and C) to assess the ability of monoamine oxidase-N to accept β -amino acid substrates. Activity detected from any of these sources would be further developed by directed evolution.

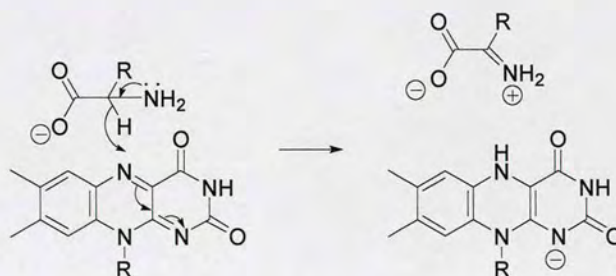
1.2 D-AMINO ACID OXIDASE

The cloned D-Amino acid oxidase (DAAO, EC 1.4.3.3) genes from *Trigonopsis variabilis* (TvDAAO) and *Rhodotorula gracilis* (RgDAAO) were available for this project. D-Amino acid oxidase flavoproteins have been known since the 1930s when they were discovered by Krebs⁽²²⁾ and these enzymes have been found in both prokaryotic and eukaryotic organisms, including mammals⁽²³⁾. A review of the physiological functions of DAAOs was published by Pollegioni in 2007.⁽²⁴⁾ The functions are wide-ranging and include catabolic, detoxification, biosynthesis and regulatory roles. The EC classification 1.4.3.3 describes the oxidoreductase group of enzymes which act on CH-NH₂ donors and use oxygen as acceptor. As shown in Scheme 1.12, the amino acid is enzymatically dehydrogenated to the corresponding imino acid. This is coupled to the reduction of the flavin adenine dinucleotide (FAD) cofactor which reoxidises spontaneously in the presence of molecular oxygen, with the concomitant formation of hydrogen peroxide. FAD reduction and reoxidation is shown in Scheme 1.13. The imino acid is non-enzymatically hydrolysed to the keto acid and ammonia. Hydrogen peroxide can be detected in colorimetric assays, providing a convenient screening method and access to kinetic data.⁽²⁵⁾

Scheme 1.12 - Oxidation of α -amino acids by DAAO

Scheme 1.13 - FAD reduction/oxidation

The mechanism for the oxidation of D-amino acids by TvDAAO and RgDAAO was disputed for some time, however, more recently evidence drawn from structural, computational and kinetic isotope studies suggest a direct hydride transfer mechanism as shown in Scheme 1.14.⁽²⁶⁾

Scheme 1.14 – Proposed hydride transfer mechanism of DAAO.⁽²⁶⁾

1.3 DIRECTED EVOLUTION

A powerful method for the engineering of enzymes is directed evolution, an approach which has grown rapidly since the 1990s. Improved mutation and screening

methods have been developed, for example, by Arnold and Stemmer^(27,28) and directed evolution techniques have become a standard tool for biocatalyst development.

Directed evolution is based on the *in vitro* evolution of biomolecules through successive cycles of variation and selection (see Figure 1.3).

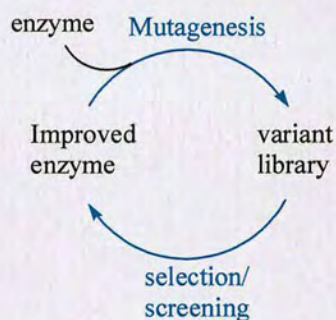


Figure 1.3 - Simplified schematic of steps involved in directed evolution

In the case of enzymes improved properties would include substrate specificity, stability, enantioselectivity or activity. Given a reliable and high-throughput screening/selection process, beneficial mutations can be easily selected and deleterious ones discarded. Significant advantages of this approach over rational design are that a detailed knowledge of the enzyme active site and of the reaction mechanism are not required.

A good example of the improvement which can be obtained by this method is the evolution of an aspartate transaminase with 2.6×10^6 -fold higher activity towards the non-native substrate valine. This was achieved through the cumulative effects of mutations distributed over much of the enzyme structure. In this case, the majority of the substituted amino acids are not in contact with the substrate or cofactor. This highlights the advantage of directed evolution over rational design which relies on the ability to predict useful mutations and will mainly concentrate on active site residues.⁽²⁹⁾

The parental gene which codes for the enzyme in question is subjected to random mutagenesis and a mutant library is generated. The mutant genes are then transformed into a host, often *E. coli*, for gene expression and screening. Colonies identified as showing improved activity during the screening process are selected and subjected to another round of mutagenesis in an iterative process towards the optimised variant (Figure 1.4).

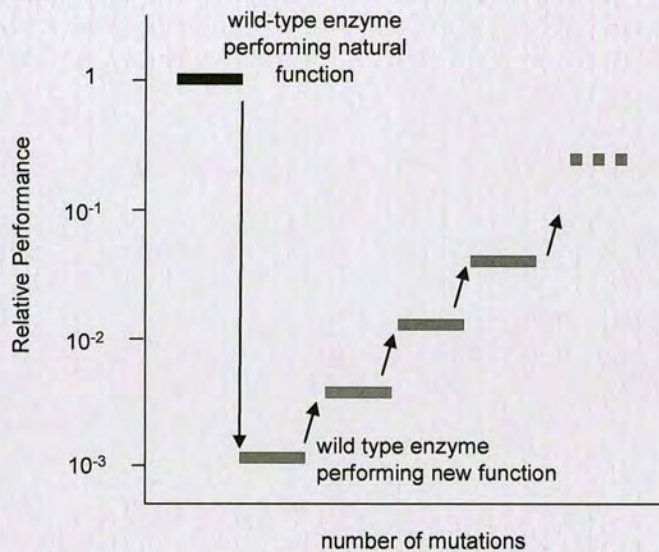


Figure 1.4 - Increase in performance during iterative process

1.3.1 Random Variant Libraries and Bias

In an ideal random library of mutants, each possible mutation should be as likely to occur as any other. This is usually not the case and instead some mutants will be significantly more represented than others and some might not occur at all. The library will therefore demonstrate bias in favour of certain mutants. Numerous methods for producing libraries have been developed, often with the aim of reducing this bias, and the advantages and disadvantages of these will be discussed. First the inherent bias of key methods such as error-prone PCR (epPCR) and the use of mutator strains, which introduce single point mutations, are described.

One significant reason for bias in a library with single-point mutations arises from the nature of nucleotide exchanges. Two types of single base-pair exchanges can occur, transitions and transversions. Transitions are purine to purine ($A \leftrightarrow G$) or pyrimidine to pyrimidine ($T \leftrightarrow C$) exchanges. Transversions are purine to pyrimidine (A or $G \rightarrow T$ or C) or pyrimidine to purine (T or $C \rightarrow A$ or G) exchanges. The DNA bases are shown in Figure 1.5 and it can be seen that there are twice as many possible transversions as transitions. For example, the three possible exchanges of the nucleotide A result in one transition (A to G) and two transversions (A to T or C). However, transitions naturally occur more frequently than transversions.⁽³⁰⁾ The molecular cause of point mutations can be found in tautomerisation, oxidative deamination or oxidation of the bases, and these most often result in a transition. An example is the amino-imino tautomerisation of adenine shown in Figure 1.6 along with the resulting non-complementary base-pairing which arises due to the altered position of favourable hydrogen bonds. Figure 1.7 shows the outcome of the alternative base-pairing, that is, an $A \rightarrow G$ transition in one strand and a $T \rightarrow C$ transition in the other.

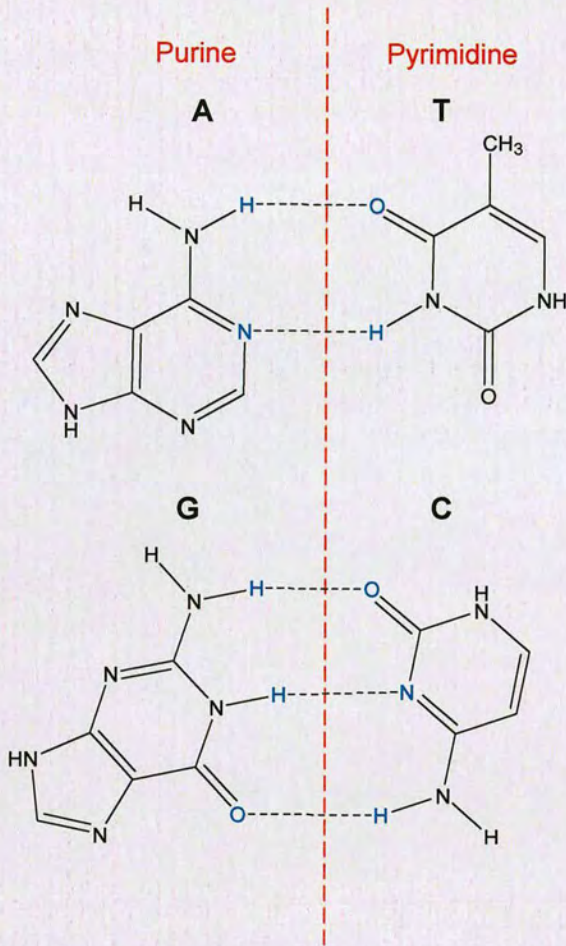


Figure 1.5 – Purine bases adenine (A) and guanine (G) are shown to the left of the central red line and pyrimidine bases thymine (T) and Cytosine (C) to the right. A purine to purine exchange or a pyrimidine to pyrimidine exchange is called a transition. An exchange of a purine base for a pyrimidine base or *vice versa* is called a transversion.

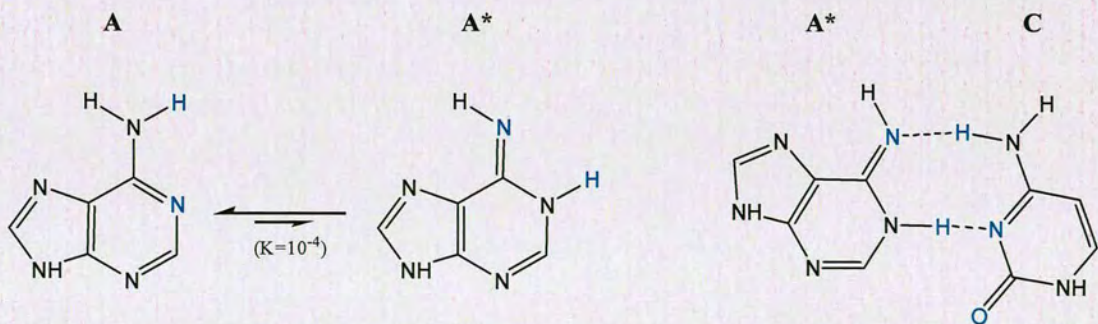


Figure 1.6 – Relationship between adenine (A) and its imino tautomer (A*) and the resulting non-complementary base-pairing relationship with cytosine (C).⁽³¹⁾

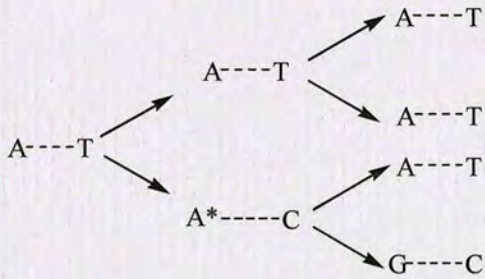


Figure 1.7 – Tautomerism in the adenine base leads to an A→G transition in one strand and a T→C transition in the other.⁽³¹⁾ (A* = tautomer of adenine.)

In addition to the higher frequency of transitional exchanges over transversional exchanges, the degeneracy in the genetic code (Table 1.1) means that some amino acid exchanges are more likely to occur than others. For example, 6 codons encode a leucine residue while only one encodes a methionine residue. The table also shows that an exchange at the 3rd position of a codon often does not result in a change to the encoded amino acid (synonymous exchange). This is particularly true for transitions at the 3rd position where only $ATA \leftrightarrow ATG$ and $TGA(\text{Ter}) \leftrightarrow TGG$ result in a change to the amino acid encoded.

Further, transitions occurring at the first codon position are likely to result in a chemically similar amino acid residue.⁽³²⁾ The chemical groupings are shown by colour code in Table 1.1. These are aromatic (F, W, Y); aliphatic (G, A, V, L, I); neutral (C, M, P, S, T, N, Q); and charged (D, E, H, K, R). For example, the codons of the hydrophobic amino acids A, V, L or I cannot be mutated by a single nucleotide exchange to codons of the charged amino acids D, E, K or R.⁽³²⁾ It is statistically unlikely that more than one nucleotide per codon will be exchanged and, therefore, even under the assumption that each nucleotide exchange at each codon position is equally likely, the possible exchanges for a given amino acid residue drop from 19 to an average of 7.5.⁽³²⁾ In natural evolution degeneracy minimises the consequences of single point mutations but this results in a lack of diversity in a directed evolution experiment.

Table 1.1 - The genetic code. The colour codes represent the chemical group of the encoded amino acid. Pink = aromatic, green = aliphatic, blue = neutral, red = charged. The one letter amino acid codes are given in the Appendix. Ter = terminator codon.

Pos ⁿ 2 \ Pos ⁿ 1	T	C	A	G
T	TTT F TTC F TTA L TTG L	TCT S TCC S TCA S TCG S	TAT Y TAC Y TAA Ter TAG Ter	TGT C TGC C TGA Ter TGG W
C	CTT L CTC L CTA L CTG L	CCT P CCC P CCA P CCG P	CAT H CAC H CAA Q CAG Q	CGT R CGC R CGA R CGG R
A	ATT I ATC I ATA I ATG M	ACT T ACC T ACA T ACG T	AAT N AAC N AAA K AAG K	AGT S AGC S AGA R AGG R
G	GTT V GTC V GTA V GTG V	GCT A GCC A GCA A GCG A	GAT D GAC D GAA E GAG E	GGT G GGC G GGA G GGG G

Mutator Strains

The gene of interest is cloned and propagated in a host strain engineered to cause faults in DNA replication and repair. One example is the *E. coli* host XL1-Red which contains three mutations, *mutS*, *mutD* and *mutT*, affecting the DNA repair pathways.⁽³³⁾ This generates a mutation rate approximately 5000-fold greater than wild-type and results in approximately 1 nucleotide mutations/kb. The main advantage of this method is the lack of a sub-cloning step. However, mutations are not restricted to the gene of interest but can occur elsewhere in the plasmid, for example mutations in the promoter region may lead to expression variants. In addition, the process is time consuming and yields a low mutation rate. Only single point mutations are produced with amplification of those errors generated early in the propagation process.

Error-prone Polymerase Chain Reaction (epPCR)

By changing the standard PCR reaction components and conditions, for example, the use of *Thermus aquaticus* (Taq) polymerase which has a naturally high error rate, increased Mg^{2+} concentration, addition of Mn^{2+} and altering the balance of dNTPs added, the fidelity of the reaction is decreased so as to cause one or more amino acid substitutions in the encoded protein.⁽³⁴⁾ The mutation frequency can be adjusted and rates of 1-10 nucleotides per kb can be obtained. An additional advantage is that the mutations generated are contained within the gene of interest. However, epPCR is susceptible to the mutational bias discussed above. Another disadvantage is that a sub-cloning step must be included. In addition, Taq polymerase is 4 times more likely to mutate As and Ts.

1.3.2 Assessment of random libraries

Schwaneberg *et al.*⁽³⁵⁾ make the point that the traditional method of assessing the quality of a random library, that is by taking the Ts/Tv ratio and the ratio of AT→GC/GC→AT transitions, is limited. An ideal mutational method would produce values of 0.5 and 1 for the above ratios respectively, with the value of 0.5 arising for Ts/Tv because there are 4 possible transitions and 8 possible transversions. However, the degeneracy in the genetic code and the low probability of exchanging more than one nucleotide per codon mean that, a library displaying these ideal ratios will not show ideal diversity in the amino acid sequences encoded.

For the above reasons, three alternative indicators of the quality of a random mutagenesis library were suggested.

- An amino acid diversity indicator to assess the average number of amino acid substitutions per residue and the probability of producing variants with preserved amino acid sequences.

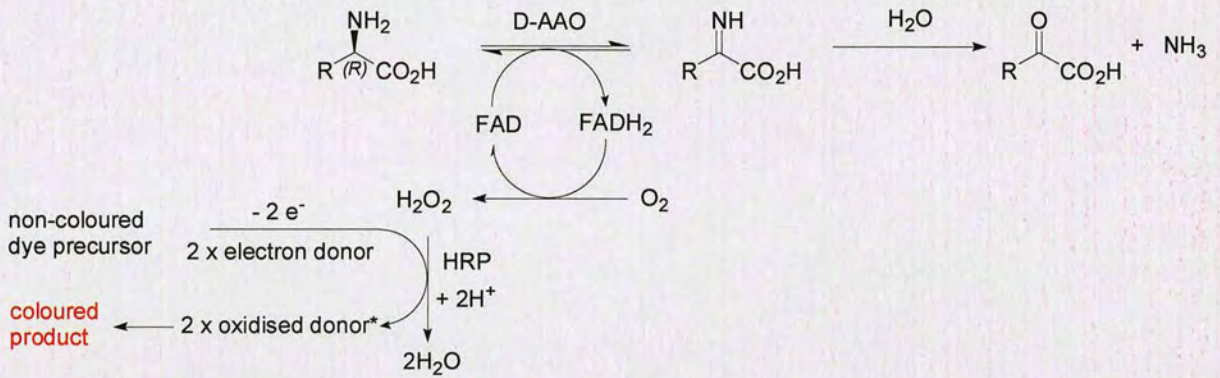
- A chemical diversity indicator to analyse the substituted amino acid residues according to the groupings aliphatic, aromatic, charged and neutral.
- Finally, a protein structure indicator to indicate the statistical likelihood of generating stop, glycine or proline producing codons. Glycine and proline residues destabilise helical structures while stop codons produce truncated proteins and all may result in inactive variants.

This group have produced an analysis tool, named MAP⁽³⁶⁾ which takes an input gene sequence and, based on these 3 factors and the mutational spectra of 19 different mutational methods (including enzymatic, chemical and whole cell), provides a prediction of the library composition. In assessing the random single nucleotide exchange libraries of 4 genes from different organisms (to account for codon usage) they provide a predicted spectrum for a non-biased library (non-biased mutational spectrum with each nucleotide equally targeted). This would produce 21-25.8 % preserved amino acids, an average of 7 possible amino acid substitutions per residue (instead of the full 19), 55.5 % amino acids with chemically different side chains, 2.9-4.7 % stop codons and 11.1-16.0 % glycine/proline residues.

1.3.3 Activity Screening

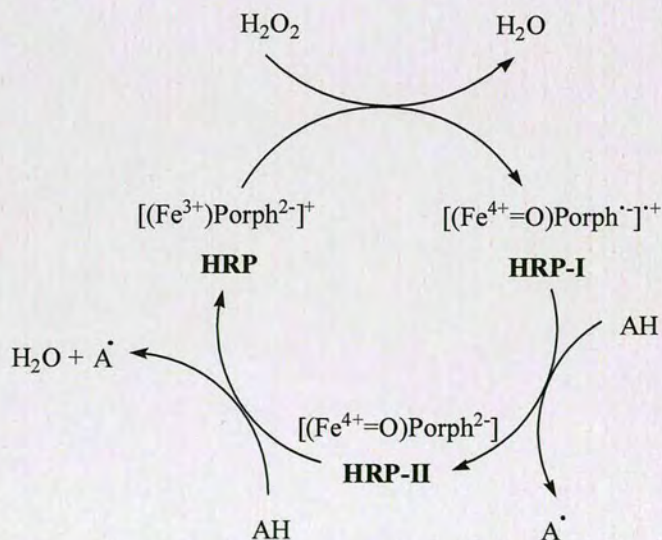
Horseradish Peroxidase Colorimetric Assay

A coupled colorimetric screen was used to detect turnover of amino acids by D-amino acid oxidase. Scheme 1.15 shows the DAAO catalysed oxidation of an amino acid to the corresponding imino acid and the resulting reduction of the flavin cofactor. The cofactor is reoxidised by molecular oxygen to form hydrogen peroxide, which can be detected using an horseradish peroxidase (HRP, EC number 1.11.1.7) coupled assay.



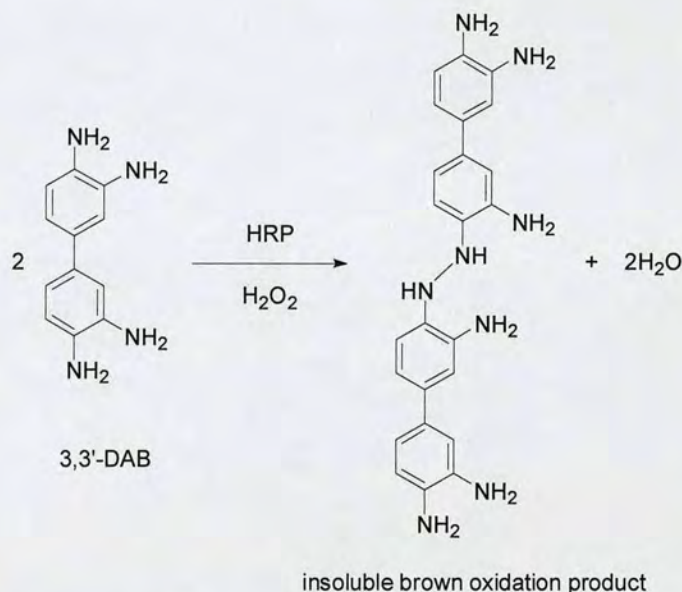
Scheme 1.15 – The principle of the HRP coupled colorimetric assay for detection of DAAO activity. The flavin cofactor is reduced upon oxidation of amino acids by DAAO. Recycling of the cofactor by molecular oxygen produces hydrogen peroxide which is detected using an HRP based screen.

HRP catalyses the reduction of hydrogen peroxide to water. This involves a two electron oxidation of HRP by hydrogen peroxide, followed by two one electron reductions of the enzyme by electron donors, such as aromatic amines or phenolic compounds, to return the enzyme to its resting state.⁽³⁷⁾ The reaction cycle is shown in Scheme 1.16.



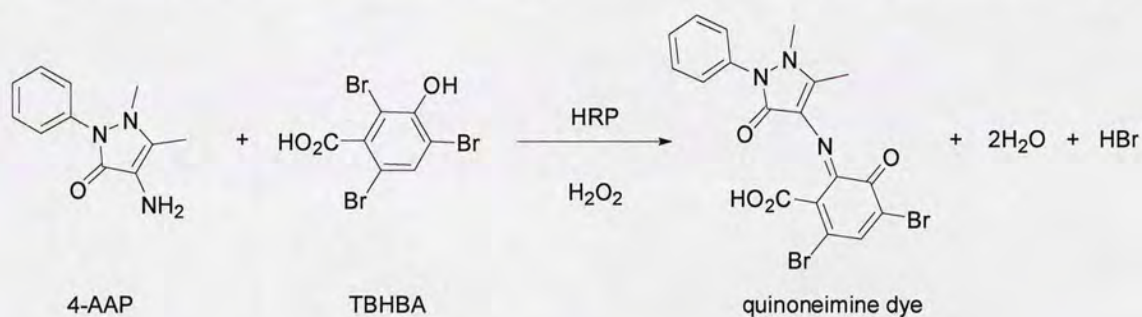
Scheme 1.16 – HRP reaction cycle.⁽³⁷⁾ First, a two electron oxidation of HRP by hydrogen peroxide to HRP-I (Porph = porphyrin). This is followed by two one electron reductions of the enzyme by electron donors (accompanied by HRP assisted proton transfers). (AH = electron donor).

To enable detection of H_2O_2 formation, chromogenic electron donors are selected which form a coloured product after coupling of their oxidised radical forms. The electron donor substrate in the solid-phase assay is 3,3'-diaminobenzidine (3,3'-DAB), which produces a brown-coloured product (Scheme 1.17).



Scheme 1.17 – Peroxidase catalysed oxidation of 3,3'-DAB in the solid-phase produces a brown-coloured oxidation product within the colonies. The qualitative solid-phase assay is a high-throughput method which was used in this work to screen epPCR RgDAAO libraries for improved activity towards non-proteinogenic amino acids.⁽³⁸⁾

The colour-forming substrates in the HRP-coupled solution phase assay are 4-aminoantipyrine (4-AAP) and 2,4,6-tribromohydrobenzoic acid (TBHBA). These combine to give a soluble, red quinoneimine dye (Scheme 1.18) which is detected using light with a wavelength of 510 nm.



Scheme 1.18 - Peroxidase catalysed formation of quinoneimine dye in the liquid-phase assay was performed in 96-well microtitre plates. The quantitative liquid-phase assay employing 4-AAP and TBHBA as dye components was used in this work to screen epPCR RgDAAO libraries for improved activity towards non-proteinogenic amino acids. Colour formation was followed at 510 nm.

1.4 SUMMARY AND AIMS

Biocatalysts are attractive for the asymmetric synthesis of chiral compounds due to their potential chemo-, regio- and stereo-selectivity as well as the mild reaction conditions they require. There are a number of biocatalytic methods for the synthesis of optically pure proteinogenic and non-proteinogenic amino acids. The aim of this project was to develop an enzyme for the oxidation of non-proteinogenic amino acids which could be used in future deracemisation reactions to provide a theoretical 100 % yield of the desired enantiomer. The substrates investigated were therein non-proteinogenic α -amino acids and β -amino acids. Methods employed to reach this goal included screening of microbial libraries and random mutagenesis as well as site directed mutagenesis of DAAO.

2 RESULTS AND DISCUSSION

2.1 SCREENING MICROORGANISMS FOR ACTIVITY TOWARDS β -AMINO ACIDS

With the aim of detecting any existing β -amino acid oxidase activity, a culture collection containing 535 microorganisms (see Appendix 5.8) was screened using the HRP-coupled liquid phase assay described in Section 1.3.3. The culture collection was obtained in the form of lyophilised powder in 15 x 96-well storage plates, with each microorganism present in duplicate on a single plate.

A Tecan Genesis Workstation 150, comprising a robotic arm, liquid handler, plate reader and storage carousel was programmed to perform the following protocol:-

1. Suspend the lyophilised microorganisms in buffer.
2. Transfer cell suspension, assay mix (HRP, 4-AAP and TBHBA) and substrate to black polystyrene, 96-well assay plates.
3. Measure absorbance at 510 nm in an integrated plate reader (time = 0).
4. Lid assay plate 1 and move to a storage carousel for room temperature incubation.
5. Remeasure absorbance at 510 nm (time = 2 and 20 h).

Two β -amino acid substrates were assayed against the culture collection: (*rac*)- β -phenylalanine and (*rac*)- β -homophenylalanine (see Figure 2.1). An additional assay was measured where substrate was replaced with water to provide a negative control.

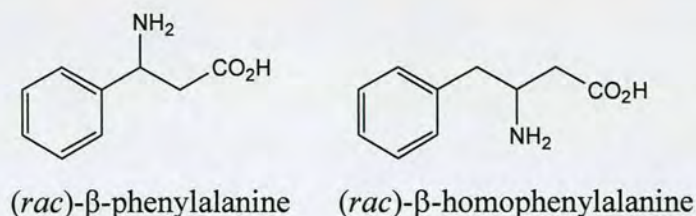


Figure 2.1 - β -Phenylalanine and β -homophenylalanine.

It was anticipated that any β -amino acid oxidase activity would be present at very low levels and therefore endpoint absorbance measurements were taken at 2 and 20 h. However, a number of wells on some plates responded to the assay with rapid colour formation both in the presence and in the absence of substrate. The results obtained from the assay of one plate of microorganisms against (*rac*)- β -homophenylalanine are shown in Figure 2.2.

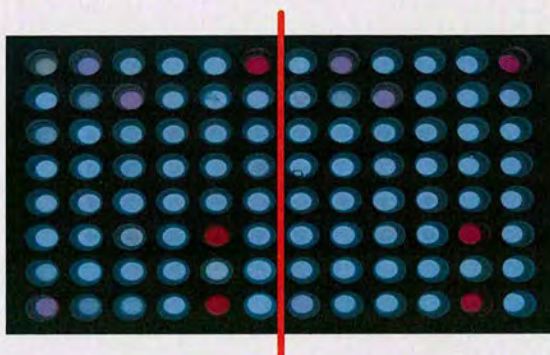


Figure 2.2 – The results produced from the assay of one plate of microorganisms against (*rac*)- β -homophenylalanine following a 2 h room temperature incubation. The microorganisms have been plated such that the left hand side of the plate, A1 to H6, is identical to the right hand side of the plate, A7 to H12.

The absorbances measured at 2 and at 20 h were corrected by subtracting the absorbance recorded at time = 0. The data for each substrate were compared with the negative control data. All the wells containing microorganisms which showed an increase in absorbance at 510 nm in response to the assay mixture with substrate also produced an increase in absorbance in response to the negative control assay mixture where substrate had been replaced with water. This false positive response was observed for prokaryotic and eukaryotic microorganisms alike. The oxidation of the dye precursors TBHBA and 4-AAP could be caused by other enzymatic sources of hydrogen peroxide in these particular microorganisms but could otherwise be due to alternative oxidising systems which result in the oxidation of the dye precursors to the quinoneimine dye.

No β -amino acid oxidase activity was detected within the microorganism collection by the HRP-coupled liquid-phase assay. The method could be improved by measuring the initial rate, rather than endpoint absorbance. In view of the fact that

some microorganisms respond to the TBHBA, 4-AAP, HRP assay mixture in the absence of an externally added substrate, an alternative detection system would be preferable. Consumption of β -amino acid could be detected by HPLC analysis, although this would reduce screening throughput.

A broader substrate spectrum of β -amino acids screened could have allowed detection of β -amino acid oxidase activity. This could be done by applying a substrate cocktail containing various β -amino acid substrates and subsequent identification of the substrate responsible for any oxidase activity identified.

Due to the lack of detectable β -amino acid oxidase activity in the microorganisms screened, it was decided to subject known amino acid oxidase enzymes to directed evolution with the aim of producing novel oxidase activity towards β -amino acids.

2.2 CHARACTERISATION OF PARENTAL OXIDASE ENZYMES

2.2.1 Confirmation of parental gene sequences

The following two D-amino acid oxidase (DAAO) enzymes were used in this work. *Rhodotorula gracilis* DAAO (RgDAAO) and *Trigonopsis variabilis* DAAO (TvDAAO). The corresponding genes were obtained as cloned plasmids; RgDAAO in pPOT3 from Ingenza, Edinburgh and TvDAAO in pJLM402 from Dr Jemma Morgan.⁽³⁹⁾ The plasmid maps and parental gene sequences are shown in the Appendix (Section 5.3).

The parental sequences of both genes were sequenced and the nucleotide sequences thus obtained were compared with published sequences.

RgDAAO

The parental RgDAAO sequence consists of 1107 bp and differs from the published nucleotide sequence (Pollegioni *et al.* ⁽⁴⁰⁾, GenBank/EMBL accession number U60066) at 4 nucleotide positions: 217T>C, 597G>C, 882T>C and 1006G>A. Two of these nucleotide differences 597G>C and 882T>C, result in no change to the amino acid sequence, whereas 217T>C gives rise to proline in place of serine 73 (S73P) and 1006G>A to threonine in place of alanine 336 (A336T). Residue 73 is located on the outer surface of the enzyme, while residue 336 is located in the active site (it has been reported that serine 335 is involved in hydrogen bonding to the α -amino group of amino acid substrates⁽⁴¹⁾).

TvDAAO

The nucleotide sequence of the TvDAAO gene provided consists of 1071 bp and is identical to that published by Alonso,⁽⁴²⁾ GenBank/EMBL accession number Z80895.

2.2.2 Comparison of the RgDAAO and TvDAAO amino acid sequences

The RgDAAO and TvDAAO amino acid sequences resulting from the genes used were aligned using the BLOSUM62 matrix and are compared in Figure 2.3. Similarities in the amino acid residue sequences of various DAAO enzymes have

been discussed by, for example, Faotto⁽⁴³⁾ and Pilone⁽²³⁾ and regions common to many DAAO enzymes are highlighted (numbered I to VI) in Figure 2.3. The 3 conserved active site residues discussed by Pilone⁽²³⁾ are marked with a red star. In RgDAAO these are Y223, Y238 and R285, corresponding to Y243, F258 and R301 in TvDAAO. The alignment of the two amino acid sequences yielded 29.8 % identity (yellow) and 46.0 % identity or similarity (blue).

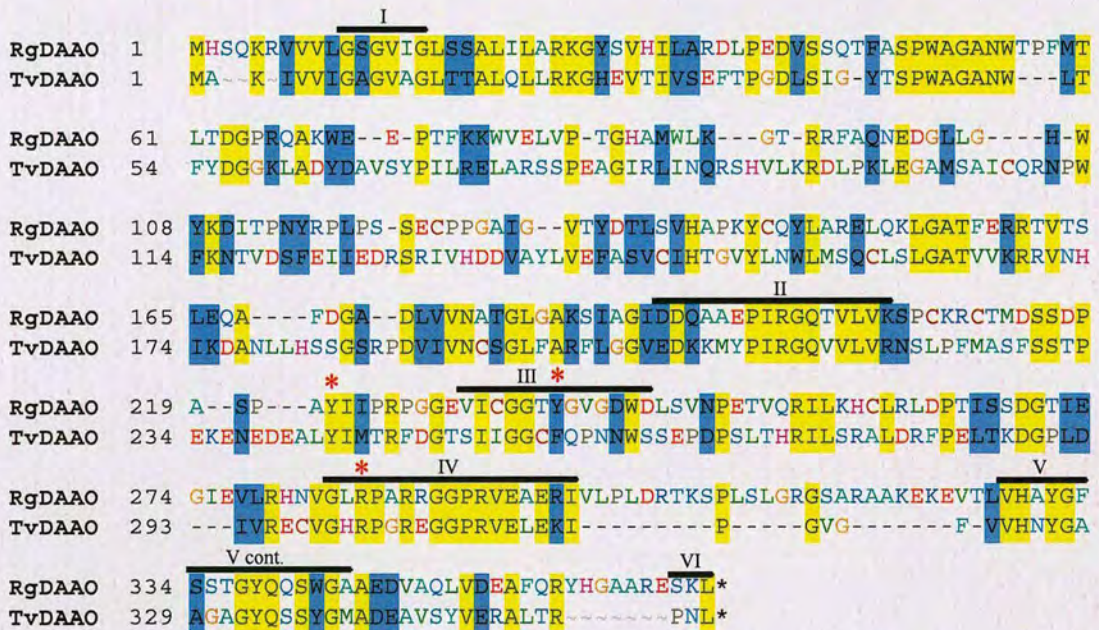


Figure 2.3 - Alignment of the amino acid residue sequences of RgDAAO and TvDAAO. The alignment was performed using the BLOSUM62 matrix which yields 29.8 % identity (yellow) and 46.0 % identity or similarity (blue) between the two sequences. Regions I and III are involved in FAD binding, with I showing the typical motif, GxGxxG. Regions II, IV and V are DAAO active site regions. Region VI in RgDAAO shows the type 1 peroxisomal targeting signal SK/HL, which is not present in TvDAAO. Red stars mark conserved residues as proposed by Pilone⁽²³⁾.

2.2.3 Parental oxidase activity towards proteinogenic and non-proteinogenic amino acids

The HRP-coupled solid- and liquid-phase colorimetric assays described in Section 1.3.3 were used for the detection of parental oxidase activity.

Liquid-phase assay substrate screen

The liquid-phase assay was performed in 96-well microtitre plates using cell free extract (CFE) obtained from cells expressing TvDAAO or RgDAAO. The HRP substrates were 4-aminoantipyrine (4-AAP) and tribromohydroxybenzoic acid (TBHBA). The increase in absorbance at 510 nm was monitored over time using a plate reader. A panel of proteinogenic and non-proteinogenic substrates was monitored against TvDAAO and RgDAAO. Figure 2.4 shows the parental activity spectra for both enzymes. Substrates towards which both enzymes proved inactive are listed in Table 2.1. As both DAAOs showed good activity towards (*R*)-methionine, rates are given relative to the rate obtained for this substrate (100 %).

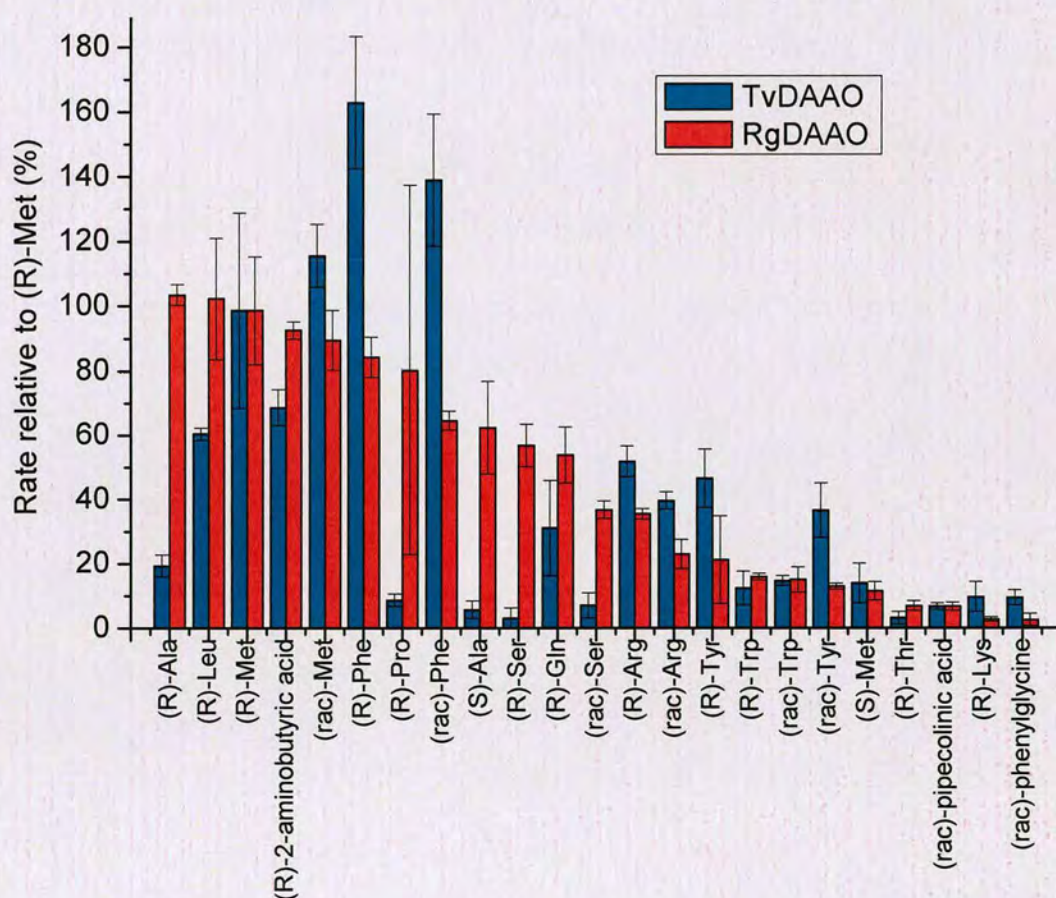


Figure 2.4 – Recorded activity rates for the TvDAAO and RgDAAO liquid-phase assays against a panel of substrates. Rates are given relative to that obtained for (*R*)-methionine (100 % = 1.9×10^{-1} and 1.6 mAU s^{-1} for TvDAAO and RgDAAO respectively). The assays were performed in 96 well microtitre plates with each well containing buffer, HRP, TBHBA, 4-AAP, substrate

(20 mM racemate or 10 mM single enantiomer) and CFE obtained from cells expressing either RgDAAO or TvDAAO. The rate of increase in absorbance at 510 nm was measured for 55 min. Both assays were performed in triplicate and the results are shown \pm one standard deviation.

Table 2.1 – Substrates towards which RgDAAO and TvDAAO showed no activity. * = TvDAAO activity was not measured. ** = β -amino acid

γ -amino- <i>n</i> -butyric acid	(<i>S</i>)-cysteine (D-cysteine)
β -glutamic acid**	(<i>S</i>)-azetidine-2-carboxylic acid*
β -alanine**	(<i>S</i>)-aspartic acid
glycine	(<i>S</i>)-arginine
ethyl-4-aminobutyrate	(<i>S</i>)-2-aminobutyric acid
(<i>rac</i>)- <i>cis</i> -2-Aminocyclopentanecarboxylic acid **	(<i>rac</i>)- β -homophenylalanine**
(<i>rac</i>)- <i>cis</i> -2-Aminocyclohexanecarboxylic acid **	(<i>rac</i>)- β -homoleucine**
(<i>rac</i>)- <i>cis</i> -2-Aminocyclohex-3-enecarboxylic acid**	(<i>rac</i>)- <i>tert</i> -leucine*
anthranilic acid	(<i>rac</i>)- <i>p</i> -methyl-3-amino-3-phenyl propionic acid**
(<i>S</i>)-tyrosine	(<i>rac</i>)- <i>p</i> -methoxy-3-amino-3-phenyl propionic acid**
(<i>S</i>)-tryptophan	(<i>rac</i>)- <i>p</i> -fluoro-3-amino-3-phenyl propionic acid**
(<i>S</i>)-threonine*	(<i>rac</i>)- <i>p</i> -chloro-3-amino-3-phenyl propionic acid**
(<i>S</i>)-serine	(<i>rac</i>)-nipecotic acid**
(<i>S</i>)-proline	(<i>rac</i>)-ethylpipecolinate
(<i>S</i>)-pipecolinic acid*	(<i>rac</i>)-ethyl-3-aminobutyrate*
(<i>S</i>)-phenylalanine	(<i>rac</i>)-cysteine
(<i>S</i>)-ornithine	(<i>rac</i>)-3-aminobutyric acid**
(<i>S</i>)-lysine	(<i>rac</i>)-3-amino-3-phenyl propionic acid (β -phenylalanine)**
(<i>S</i>)-leucine	(<i>rac</i>)-3-amino-3-cyclohexane propionic acid**
(<i>S</i>)-isoleucine	(<i>rac</i>)-3-amino-3-cyclohex-6-ene propionic acid**
(<i>S</i>)-histidine	(<i>R</i>)- α -methylbenzylamine*
(<i>S</i>)-glutamine	(<i>R</i>)-glutamic acid
(<i>S</i>)-glutamic acid	(<i>R</i>)-2-amino-1-propanol*

In accordance with literature data(26,44), hydrophobic α -amino acids are the best substrates for both TvDAAO and RgDAAO. However, some discrepancies appear in Figure 2.4 compared with literature values. The most conspicuous of these is the observation of 60 % relative activity of RgDAAO towards (*S*)-alanine. The literature explicitly states that L-amino acids, such as (*S*)-alanine, are not substrates for DAAOs(26). Due to the high stereoselectivity of RgDAAO, it has been developed as a biosensor for the detection of D-amino acids, including (*R*)-alanine, in food.⁽⁴⁵⁾ No RgDAAO activity was expected towards (*S*)-alanine or, additionally, (*S*)-methionine

for which relative rates of 9 and 12 % were obtained for TvDAAO and RgDAAO respectively. The observed colour formation may be due to racemisation of these substrates in the presence of CFE or perhaps to a change in enantioselectivity of RgDAAO caused by the T336A mutation described in Section 2.2.1. No analysis to assess the enantiopurity of the substrates was undertaken. No activity was shown towards other L-amino acids tested (see Table 2.1).

Tishkov presents a comparison of the relative rates from literature for various DAAOs.⁽⁴⁴⁾ When these values are compared with the data presented here, the significant differences are relative rates observed in this work for TvDAAO towards (*R*)-alanine, (*R*)-phenylalanine and (*R*)-glutamine of 20 %, 160 % and 30 % respectively compared with literature values of 120 %, 50 % and 100 % respectively. In addition, a relative rate of 37 % was obtained for RgDAAO towards (*R*)-arginine in this work but is reported as 2 % in the literature. Tishkov advises that discrepancies in relative rates reported in the literature are due to the use of different assay procedures under different experimental conditions. Additionally, results can be influenced by the presence of catalase in cell preparations and by the fact that the concentration of oxygen in water under normal experimental conditions can be lower than its K_m value for some of the enzymes. For example, the concentration of oxygen in water at atmospheric pressure of air is 0.21 mM at pH 8.0 and 37°C under equilibrium conditions and the K_m value of oxygen for TvDAAO is 0.72 mM.⁽⁴⁴⁾

The data presented here show that both TvDAAO and RgDAAO are active towards (*R*)-phenylalanine but show poor activity towards (*rac*)-phenylglycine. Several β -analogues of phenylalanine, for example, (*rac*)- β -phenylalanine and (*rac*)- β -homophenylalanine (Figure 2.1), were included in the screen but no activity was shown by either enzyme towards these substrates.

(*R*)-Serine is a substrate for RgDAAO but not for TvDAAO, whereas both enzymes show poor activity towards (*R*)-threonine.

Neither DAAO demonstrated activity towards any of the β -amino acids tested (marked ** in Table 2.1). Additionally, no oxidase activity was observed towards γ -amino-*n*-butyric acid, (*R*)-2-amino-1-propanol or (*R*)- α -methylbenzylamine.

Anthranilic acid is known to be a competitive inhibitor of RgDAAO⁽⁴¹⁾ and has the structure shown in Figure 2.5. The substrates (*rac*)-*cis*-2-aminocyclohexanecarboxylic acid, (*rac*)-*cis*-2-aminocyclohex-3-enecarboxylic acid and (*rac*)-*cis*-2-aminocyclopentanecarboxylic acid were added to the substrate panel. No activity was observed towards these substrates.

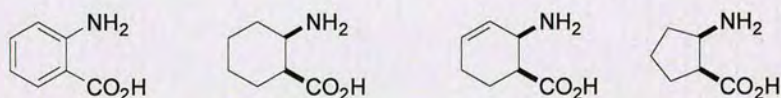


Figure 2.5 – Cyclic β -amino acids included in the screen against RgDAAO and TvDAAO. Anthranilic acid, (*rac*)-*cis*-2-aminocyclohexanecarboxylic acid, (*rac*)-*cis*-2-aminocyclohex-3-enecarboxylic acid and (*rac*)-*cis*-2-aminocyclopentanecarboxylic acid.

RgDAAO displayed 80 % relative activity towards (*R*)-proline and 8 % relative activity towards the 6-membered ring homologue, (*rac*)-pipecolinic acid. However, no oxidase activity was observed towards the β -analogue of (*rac*)-pipecolinic acid, (*rac*)-nipecotic acid, nor towards the ethyl ester of (*rac*)-pipecolinic acid (Figure 2.6). In a second round of substrate screening (see Figure 2.7), RgDAAO showed 4 % relative activity towards (*rac*)-tetrahydroisoquinoline-3-carboxylic acid.

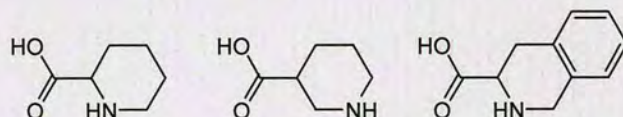


Figure 2.6 – Heterocyclic amino acids screened against RgDAAO. (*rac*)-Pipecolinic acid, (*rac*)-nipecotic acid and (*rac*)-tetrahydroisoquinoline-3-carboxylic acid.

The second substrate panel was assessed against RgDAAO only and the data are shown in Figure 2.7. These substrates were measured in duplicate and the rates obtained are again given relative to (*R*)-methionine.

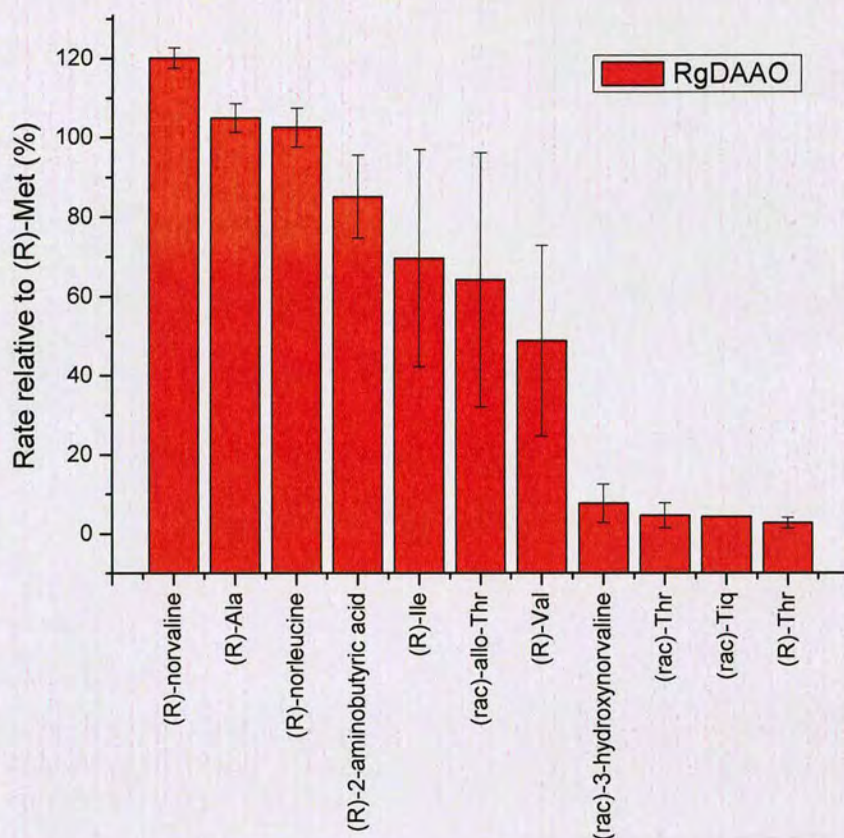


Figure 2.7 – Results of the RgDAAO liquid-phase assay against a secondary panel of substrates. The assays were performed in 96 well microtitre plates with each well containing buffer, HRP, TBHBA, 4-AAP, substrate (20 mM racemate or 10 mM single enantiomer; (*rac*)-tetrahydroisoquinoline-3-carboxylic acid = 10 mM) and CFE obtained from cells expressing RgDAAO. The rate of increase in absorbance at 510 nm was measured for 55 min. Rates are given relative to that obtained for (*R*)-methionine (100 % = 1.6 mAU s⁻¹). The data were measured in duplicate and are shown \pm one standard deviation. Tiq = tetrahydroisoquinoline-3-carboxylic acid.

A relative activity of 49 % was observed for RgDAAO towards (*R*)-valine. This increased to 120 % for the straight-chain aliphatic amino acid (*R*)-norvaline, whereas the relative rate obtained towards (*rac*)-3-hydroxynorvaline was just 8 %. The relative activities demonstrated by RgDAAO towards the leucine series were: (*R*)-leucine 104 %; (*R*)-norleucine 103 %; (*R*)-isoleucine 70 % but the enzyme was inactive towards (*rac*)-*tert*-leucine and β -homoleucine. (*Rac*)-*allo*-threonine was oxidised considerably faster (64 % relative rate) than (*rac*)-threonine (3 % relative rate).

Solid-phase assays

The solid-phase assay discussed in Section 1.3.3 was used to screen TvDAAO and RgDAAO for activity towards the β -amino acids: (*rac*)- β -phenylalanine, (*rac*)- β -homophenylalanine, β -homoleucine and β -homomethionine. Cells expressing RgDAAO, TvDAAO or containing plasmid with no gene insert (empty vector) were grown and induced on nitrocellulose membranes and sections of these membranes were transferred to assay plates containing a filter paper soaked with HRP-assay mixture and substrate, as shown in Figure 2.8. This figure shows the results of the assays using **A**) (*rac*)- β -homoleucine and **B**) (*R*)-alanine as substrate.

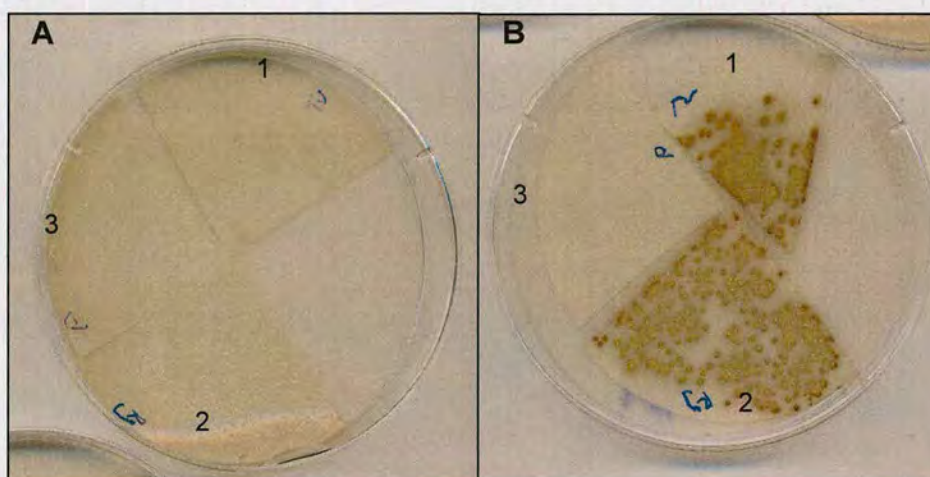


Figure 2.8 – DAAO solid-phase assay. Each assay plate contained a filter paper soaked in assay mix consisting of buffer, substrate (20 mM racemate or 10 mM single enantiomer), HRP and 3,3'-DAB. Substrate A = (*rac*)- β -homo-leucine and substrate B = (*R*)-alanine. Colonies were grown on nitrocellulose membranes which were cut into sections and placed in the assay plates. Membranes numbered 1 held TvDAAO expressing colonies, 2 held RgDAAO expressing colonies and 3 held colonies containing empty vector.

Figure 2.8 **B**) shows that, as expected, colonies expressing TvDAAO (membrane 1) or RgDAAO (membrane 2) turn a red/brown colour as the hydrogen peroxide produced in the reoxidation of the cofactor of DAAO leads to the oxidation of 3,3'-DAB in a HRP-catalysed reaction. The empty vector colonies (membrane 3) remain uncoloured as there is no DAAO present to oxidise (*R*)-alanine and therefore no H_2O_2 produced. The substrate in Figure 2.8 **A**) is (*rac*)- β -homoleucine and lack of colour formation in the colonies on all three membrane sections indicates that (*rac*)-

β -homoleucine is not a substrate for either RgDAAO or TvDAAO, as confirmed in the liquid-phase assay discussed above. This assay was repeated using (*rac*)- β -phenylalanine, (*rac*)- β -homophenylalanine, and β -homomethionine with no indication of oxidation by either TvDAAO or RgDAAO.

The solid-phase assay was also used to assess the potential of a variant monoamine oxidase-N from *Aspergillus niger* (MAO-N, variant D5⁽⁴⁶⁾) which oxidises amines, for activity towards these four β -amino acid substrates. The assay was performed using an identical protocol to that described above but the positive control substrate in this case was (*rac*)- α -methylbenzylamine ((*rac*)- α -MBA). The results of the solid-phase assay towards (*rac*)- β -homoleucine and (*rac*)- α -MBA are shown in Figure 2.9 A) and B) respectively.

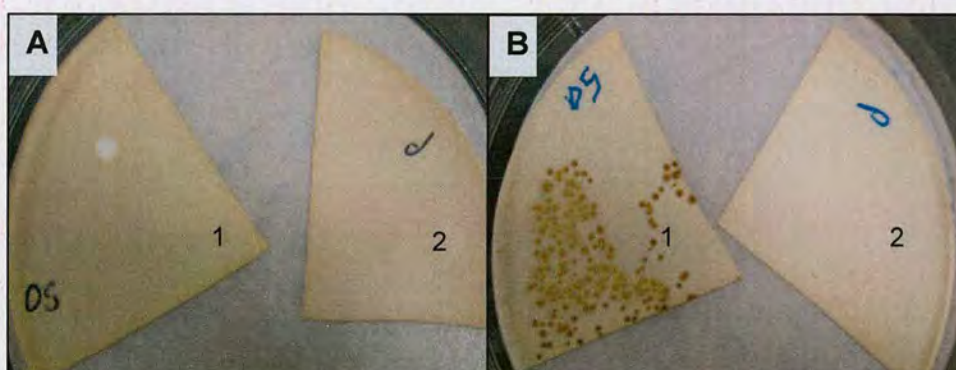


Figure 2.9 – MAO-N solid-phase assay. These assay plates were prepared as for the assay shown in Figure 2.8. Substrate A = (*rac*)- β -homo-leucine and substrate B = (*rac*)- α -MBA. Membranes numbered 1 contained MAO-N expressing colonies and membranes numbered 2 contained empty vector colonies.

Figure 2.9 B) shows that MAO-N producing colonies on membrane 1 lead, when exposed to (*rac*)- α -MBA and assay mix, to colour formation, while the empty vector colonies showed no colour formation. In Figure 2.9 A), neither the MAO-N producing colonies on membrane 1 nor the empty vector colonies on membrane 2 coloured up during incubation with (*rac*)- β -homoleucine and assay mix, indicating that β -homoleucine is not a substrate for MAO-N. This assay was repeated using (*rac*)- β -phenylalanine, (*rac*)- β -homophenylalanine and β -homomethionine as substrates and no colour formation was observed.

2.2.4 Conclusions

The gene sequences of TvDAAO and RgDAAO were obtained and their amino acid sequences aligned and compared. Regions of the two sequences which are conserved in DAAOs were highlighted.

A panel of substrates was assayed in the liquid-phase to give an overview of the parental activity profiles of both TvDAAO and RgDAAO and these were compared with relative rates presented in the literature. Although some discrepancies appeared between the data presented here and literature values, it was confirmed that amino acids with hydrophobic side chains are the best substrates for both enzymes. No oxidase activity was detected towards β -amino acids or towards other amino-containing compounds without a carboxylic acid functionality at the α -carbon. Some activity was observed towards the non-proteinogenic α -amino acids (*rac*)-pipecolic acid and (*rac*)-1,2,3,4-tetrahydroisoquinoline-3-carboxylic acid.

In accordance, a solid-phase screen showed no RgDAAO or TvDAAO activity towards the β -amino acids (*rac*)- β -phenylalanine, (*rac*)- β -homophenylalanine, (*rac*)- β -homoleucine or (*rac*)- β -homomethionine. Additionally, solid-phase screening of a MAO-N variant against the same β -amino acid substrates showed no observable oxidase activity.

It was expected that directed evolution of the TvDAAO or RgDAAO genes would produce variant enzymes acting as β -amino acid oxidases which could be detected using a solid-phase assay against the β -amino acid, (*rac*)- β -homophenylalanine.

2.3 DIRECTED EVOLUTION OF D-AAO

2.3.1 Mutator strain library TvDAAO

The starting point for directed evolution in this project was to generate a TvDAAO random library through the use of the mutator strain XL1-Red as discussed in Section 1.3.1. Fresh plasmid DNA was isolated from a single TOP10 *E. coli* colony and used to transform XL1-Red *E. coli* cells which were grown as described in Experimental Sections 3.2.2 and 3.2.3 to generate a library of variants.

Verification of Mutator Strain Library

Plasmid DNA extracted from the mutator strain library was used to transform *E. coli* BL21(DE3) cells which were grown on LB agar plates containing antibiotic. Twenty of the resulting colonies were selected and cultured overnight. The plasmid DNA was extracted and sequenced as described in Section 3.2.1. Full sequences were obtained for 14 genes and more than 50 % of each of the remaining genes was captured. The nucleotide mutation 3G>T was observed in 18 of the 20 TvDAAO nucleotide sequences and the other two genes were not sequenced in this region. This nucleotide exchange results in the exchange of the start codon, methionine (ATG), for an isoleucine (ATT). The absence of the start codon means that the TvDAAO enzyme will not be expressed by the cell. No other mutations were observed in any of the sequenced genes. The original plasmid DNA used to transform the XL1-Red cells was checked by sequencing and found to contain the start codon ATG. It was therefore assumed that the mutation to ATT was generated early during the propagation cycles and became dominant in the culture.

A repeat of the mutator strain experiment was considered but, as a result of the very low mutation rates achieved, it was decided to perform epPCR with the aim of producing a higher mutation rate.

In the meantime, the RgDAAO gene cloned into the vector pPOT3 was obtained from Dr Annette Turner of Ingenza, Edinburgh. As a crystal structure is available for this enzyme,⁽⁴⁷⁾ this gene was used for epPCR in preference over TvDAAO.

Knowledge of the structure would allow a more detailed analysis of any mutants which displayed improved activities towards unnatural amino acids.

2.3.2 epPCR library RgDAAO

An epPCR was performed with the aim of producing an RgDAAO variant library with a mutation rate of 2-3 nucleotide exchanges per gene for subsequent screening against a range of β -amino acids. Fresh RgDAAO plasmid was prepared from TOP10 cells and an epPCR was performed using this as template at four different annealing temperatures (50.0, 56.1, 60.2 and 65.5 °C). The gene was successfully amplified in all cases as shown in Figure 2.10.

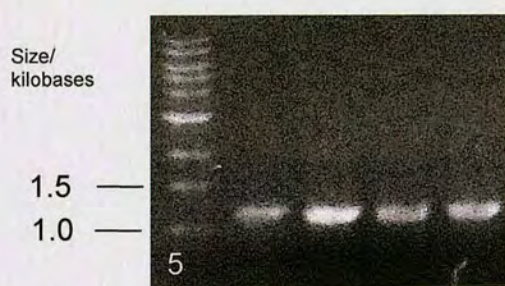


Figure 2.10 - epPCR products (1107 bp) following agarose gel electrophoresis. Lane 1 DNA ladder, lanes 2 to 5 ep products from 50.0, 56.1, 60.2 and 65.6 °C epPCRs respectively.

The products were combined and used as megaprimers in a PCR with parental RgDAAO/pPOT3 as template to subclone the library into the pPOT3 vector. The PCR was carried out with mass ratios ($\text{ng } \mu\text{L}^{-1}$ reaction volume) of 0.5, 1 and 2 times megaprimer to template DNA. The products of these PCRs were digested with the restriction enzyme DpnI to remove methylated parental DNA as explained in Section 3.2.1. The digested products were used to transform highly competent XL1-Blue cells which repair the nicked DNA produced in the PCR reaction. The transformants were grown on LB or TSB agar plates treated with chloramphenicol (CAP). As the plasmid confers CAP resistance to the cells, only cells successfully transformed with plasmid DNA grew. Figure 2.11 shows the number of XL1-Blue colonies produced per 100 μL transformation mixture in each case (in duplicate). A ratio of megaprimer to template DNA of 1-2 to 1 by mass produced good results.

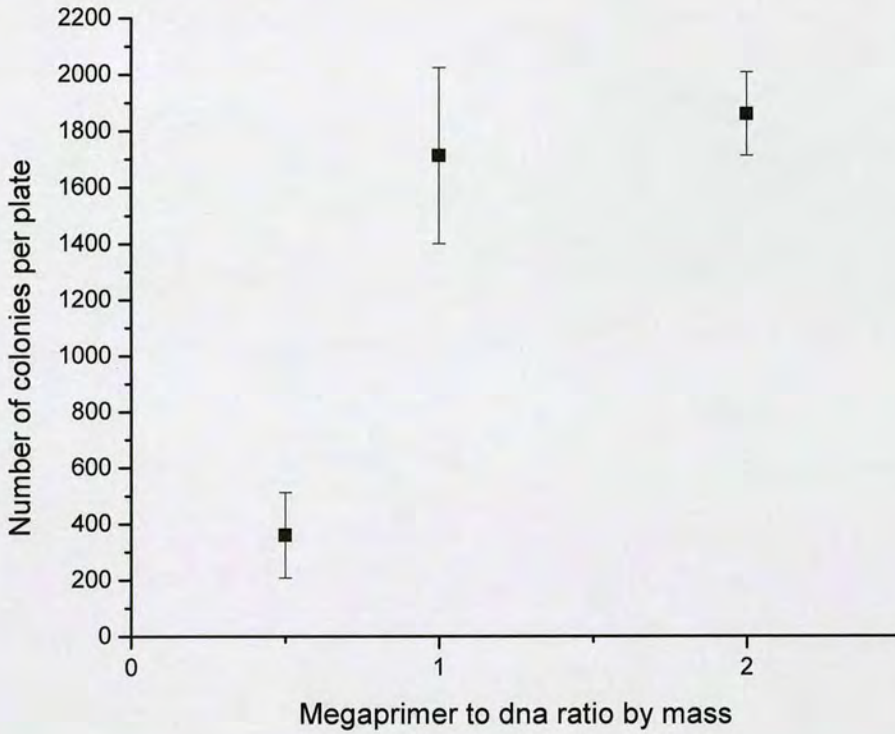


Figure 2.11 - XL1-Blue transformation efficiency by mass ratio of megaprimer to DNA template used for whole plasmid extension. Data points represent the mean values \pm standard deviation obtained from duplicate plates.

Verification of epPCR Library

The library was analysed for the number and diversity of mutations it contained. Twenty XL1-Blue colonies were selected and cultured overnight. The plasmid DNA was extracted and sequenced as described in Section 3.2.1. The primers used for the amplification captured approximately 85 % of each of the sequenced genes. Eighteen of the sequenced samples contained the DAAO gene and two were circular plasmid with no gene insert. The number of nucleotide exchanges per gene in the sample were calculated and resulted in an average number of nucleotide mutations per gene of 2.7 as shown in Figure 2.12.

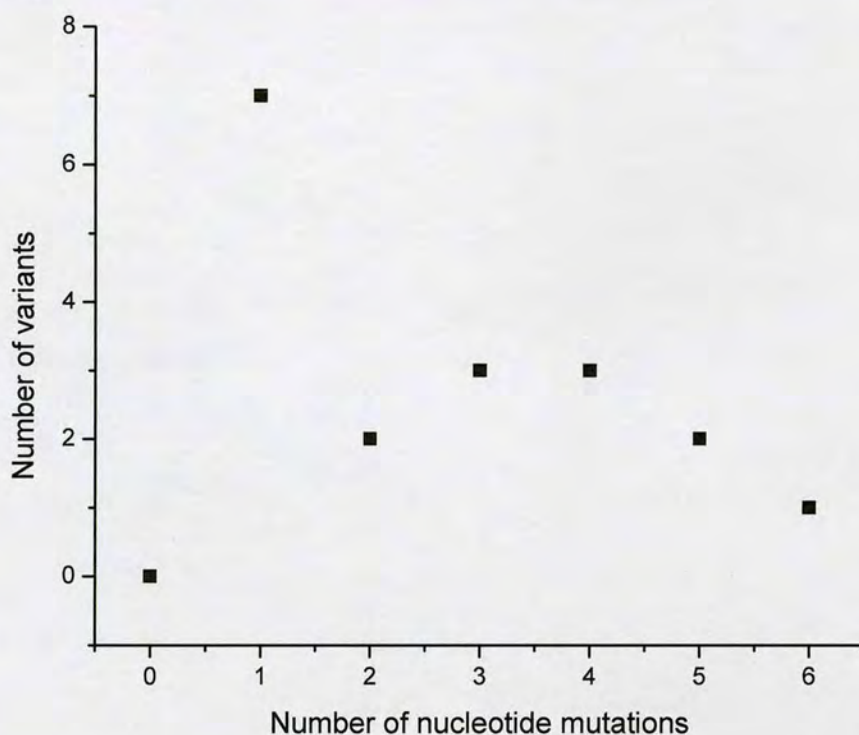


Figure 2.12 - Number of nucleotide mutations per gene observed in a sample of 20 sequenced variants from the RgDAAO epPCR library. Average number of mutations per gene = $(7 \times 1 + 2 \times 2 + 3 \times 3 + 3 \times 4 + 2 \times 5 + 1 \times 6) / 18 = 2.7$.

A summary of the observed nucleotide mutations in 18 randomly picked samples are shown in Table 2.2. Point insertions and deletions are normally not beneficial as they cause a shift in the reading frame of the sequence and are likely to generate inactive variant enzymes. No insertions were detected but the tested samples contained 3 point deletions over 2 genes.

Table 2.2- Analysis of mutations in sample of RgDAAO epPCR library. (Sample size = 18 variants.)

Type of mutation	Number	Percentage of total mutations
nucleotide exchanges	45	94 %
nucleotide deletions	3	6 %
nucleotide insertions	0	0 %

A common method of assessing diversity in a random library is to take the transition to transversion (Ts/Tv) and AT→GC/GC→AT transition ratios. Transitions are purine to purine (A↔G) or pyrimidine to pyrimidine (T↔C) exchanges. Transversions are purine to pyrimidine (A or G → T or C) or pyrimidine to purine (T or C → A or G) exchanges. In this context, a library is considered to be free from bias when each type of nucleotide exchange occurs with an equal frequency. As there are twice as many possible transversions as transitions, the Ts/Tv ratio should be 0.5. The number of AT→GC transitions should equal the number of GC→AT transitions and the ratio should be 1. The values observed in the RgDAAO library and the non-biased values produced by a similar method were compared. Schwaneberg *et al.*⁽³⁵⁾ compared the Ts/Tv and AT→GC/GC→AT ratios generated by a range of mutagenesis protocols. Of these, the most similar to that used in this work was an epPCR method presented by Shafikhani *et al.*,⁽⁴⁸⁾ which includes a *Thermus aquaticus* (*Taq*) PCR in the presence of Mn²⁺ and dNTPs with the balance dGTP=dATP<dCTP=dTTP. However, 1.25-fold more of each primer and 10-fold more MnCl₂ were used than in this work which was adapted from a procedure taken from Escalettes and Turner.⁽⁴⁹⁾ The values obtained for Ts/Tv and AT→GC/GC→AT ratios by each method are shown in Table 2.3.

Table 2.3 - Quality of RgDAAO library expressed by nucleotide exchange ratios. (Sample size = 18 variants.)

	Non-biased	Comparison epPCR ^[a]	RgDAAO epPCR
Ts/Tv	0.5	0.8	2.5
AT→GC/GC→AT	1.0	2.0	2.2

[a] see reference (35)

It can be seen that the comparison epPCR results and the experimental results deviate from the ideal, with both showing higher Ts/Tv and AT→GC/GC→AT ratios. In relation to the comparison method, the RgDAAO epPCR library produced here generated a similar AT→GC/GC→AT ratio but a 3-fold higher Ts/Tv ratio. This was investigated further by comparing each exchange type as shown in Table 2.4. There were 2.3 times fewer A→T and T→A transversions and approximately 1.7 times more A→G and T→C transitions produced in this library than by the comparison

method. The effect of manganese concentration was considered. The comparison epPCR method used 500 μM Mn^{2+} , whereas the method employed here used only 50 μM . At 50 μM Mn^{2+} , the mechanism of manganese-induced mutagenesis involves Mn^{2+} binding to the DNA template which causes misinsertions to occur.⁽⁵⁰⁾ Additional mechanisms begin to feature at concentrations of Mn^{2+} above 500 μM (Mn^{2+} association with either single stranded regions of DNA or with the polymerase)⁽⁵⁰⁾ and it is possible that these have some influence on the mutagenic profile of the comparison epPCR.

Table 2.4 shows that neither the comparison epPCR method, nor the epPCR method used here, produced unbiased nucleotide exchange libraries. The impact of this bias was assessed by studying the amino acid sequences encoded.

Table 2.4 - Detailed analysis of nucleotide exchanges in RgDAAO epPCR library (sample size = 18 variants).

Type of exchange	Exchange	non-biased (%)	comparison epPCR ^[a] (%)	observed (%)
transitions	A to G	8	14	22
	T to C	8	14	27
	G to A	8	7	9
	C to T	8	7	13
transversions	A to T	8	21	9
	T to A	8	21	9
	A to C	8	4	2
	T to G	8	4	2
	G to C	8	1	2
	C to G	8	1	0
	G to T	8	2	2
	C to A	8	2	2
	Total	96	98	99

[a] see reference (35)

The distribution of amino acid substitutions among the variants selected for sequencing is shown in Figure 2.13. The average number of amino acid substitutions per variant is 1.4 (from 2.7 nucleotide exchanges per gene). This moderate mutation rate is a useful starting point for investigating the effects of mutating RgDAAO on its ability to oxidise unnatural amino acids. However, 4 of the 18 variants contained

synonymous nucleotide mutations with no change occurring in the amino acid sequence. This had to be taken into account when the number of colonies which must be screened to cover the majority of sequences present in the library is considered. The number of colonies to be screened will be discussed in more detail later in this Section.

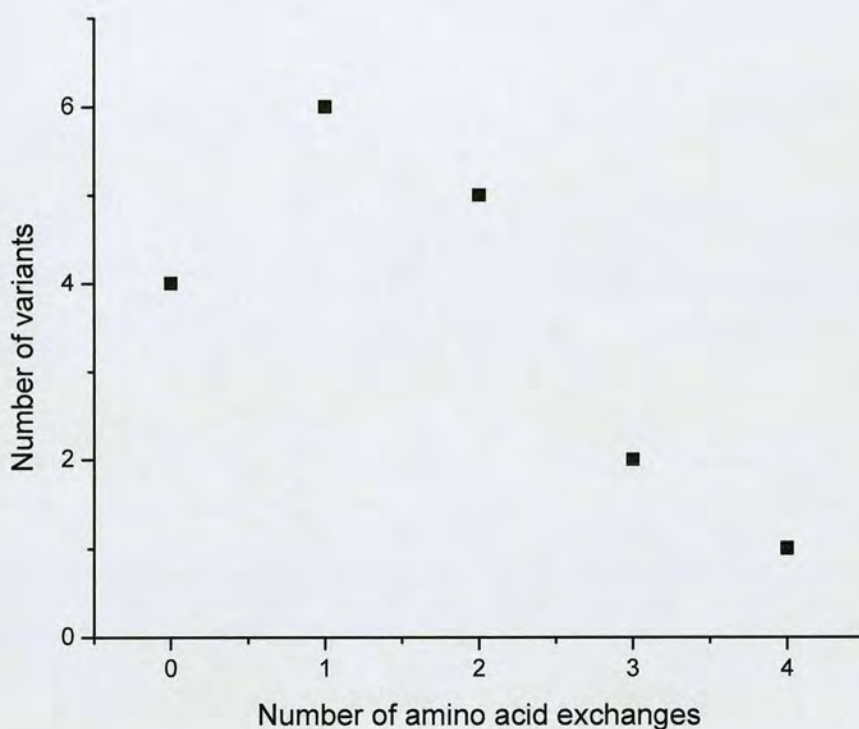


Figure 2.13 - Distribution of amino acid exchanges in RgDAAO epPCR library. Sample size = 18 variants with an average amino acid exchange per gene of $1.4 (6x1 + 5x2 + 2x3 + 1x4)/18$.

It is useful to discuss the range of amino acid exchanges observed in the context of a set of diversity indicators proposed by Schwaneberg *et al.*⁽³⁵⁾ as these provide an overview of the library composition which can then be compared to the ideal library composition. Schwaneberg also analysed a range of mutagenic methods and produced a statistical tool (MAP) which predicts the mutagenic profile (amino acid exchanges) for a particular gene when subjected to each of these methods. The

method most similar to that used to create the RgDAAO epPCR library is the Shafikhani *et al.* epPCR method discussed above. Despite the difference in manganese concentrations used, the results of a MAP prediction of the mutagenic profile of the RgDAAO gene using the Shafikhani epPCR method are also compared with the ideal and observed results. In addition, the mutagenic profile predicted by MAP for a non-biased nucleotide library of the RgDAAO gene is included in the comparison. The data from the two RgDAAO MAP analyses are referred to as the ‘predicted’ and ‘non-biased’ results, respectively, in the discussion below. The three diversity indicators are chemical diversity indicator, protein structure indicator and amino acid diversity indicator.

- Chemical diversity indicator:

The “ideal chemical distribution” of amino acid substitutions is shown in Table 2.5 and is simply based on the number of amino acids in each chemical category: 25 % charged (D, E, H, K, R), 35 % neutral (C, M, P, S, T, N, Q), 15 % aromatic (F, Y, W) and 25 % aliphatic (G, A, V, L, I). This distribution describes a situation where each category of amino acid is targeted with the appropriate frequency, for example 25 % of the newly substituted residues will be charged. The category of the residue displaced is not considered.

The ideal figures (Table 2.5) are compared with the distribution which would have been obtained had a non-biased nucleotide exchange library of this gene been produced and with the predicted and observed distributions. It can be seen that a non-biased nucleotide exchange library cannot access each amino acid exchange equally. As discussed in the Introduction, this is due to the degeneracy of the genetic code and the fact that it is statistically unlikely to exchange more than one nucleotide per codon. The observed amino acid exchanges reasonably match the ideal chemical distribution but with a loss of aromatic substitutions in favour of aliphatic substitutions. The percentage of aromatic substitutions in the library generated is also lower than in the predicted library. This observation could be due to the small sample size (26 amino acid exchanges from 18 sequenced variants) giving a non-



representative reflection of the data or to the increased manganese concentration in the method used for prediction purposes.

In summary, in comparison with the ideal chemical distribution of the replacement amino acid residues the RgDAAO epPCR library contains 2 percentage points fewer charged substitutions, 4 percentage points fewer neutral substitutions and 11 percentage points fewer aromatic substitutions. In contrast, there are 14 percentage points more aliphatic substitutions and 4 percentage points more stop codons than would be shown by an ideal distribution.

Table 2.5 – The ideal chemical diversity of substituted amino acids in a random library and values produced from MAP analyses for ‘non-biased’ and ‘predicted’ RgDAAO libraries compared with the observed diversity in the RgDAAO epPCR library.

	Charged (%)	Neutral (%)	Aromatic (%)	Aliphatic (%)
Ideal chemical distribution	25	35	15	25
Non-biased	23	32	6	35
Predicted	22	32	7	34
Observed (18 sequenced variants)	23	31	4	38

- Protein structure indicator:

This investigates mutated codons which are likely to introduce structural changes in the protein and may lead to inactive variants, for example stop codons or those encoding glycine or proline residues which destabilise helical structures. Ideally, no stop codons would be introduced to the gene. However, 4 % of the amino acid exchanges in the sequenced samples yield stop codons as shown in Table 2.6. This value is consistent with the MAP analyses for the ‘predicted’ and ‘non-biased’ RgDAAO libraries. In the case of Gly and Pro residues, the observed value of 23 % is higher than both the predicted and non-biased values (13 and 14 % respectively). However, Gly and Pro residues will only destabilise the protein structure when they occur within a helical region. A cartoon representation (generated using PyMOL) of the RgDAAO monomer⁽⁴⁷⁾ is shown in Figure 2.14 with helices coloured blue and strands coloured red. The Protein Data Bank (PDB) entry (1C0P) shows that RgDAAO contains 36 % helical structures. This means that any Gly and Pro residues

introduced have approximately 36 % likelihood of causing destabilisation. This reduces both predicted values of potentially destabilising mutations to 9 % (4 % stop and 5 % Pro/Gly) and the observed value to 12 % (4 % stop and 8 % Pro/Gly).

Table 2.6 – Exchanges with potential to adversely affect protein secondary structure.

	Stop (%)	Gly/Pro (%)
Ideal chemical distribution	0	10
Non-biased	4	14
Predicted	4	13
Observed (18 sequenced variants)	4	23

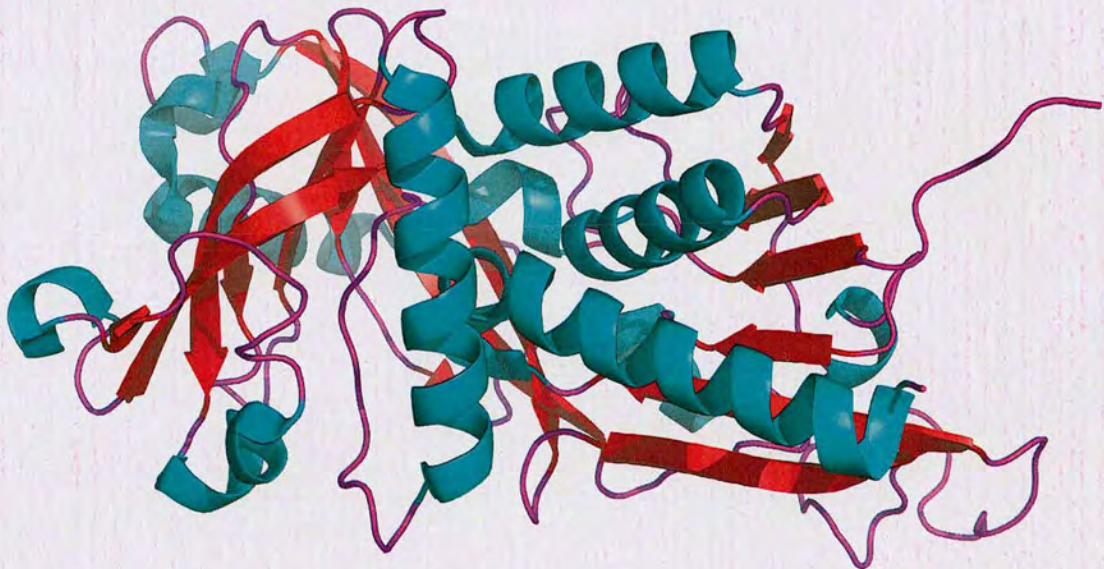


Figure 2.14 – PyMOL cartoon representation of the RgDAAO monomer.⁽⁴⁷⁾ PDB ID code 1c0p. Helices are shown in blue and strands are shown in red. The monomer contains 36 % helical structures and exchanges to Pro or Gly residues in these regions may cause structural destabilisations which result in inactive enzymes.

- Amino acid diversity indicator:

The amino acid diversity indicator assesses the number of variants with synonymous nucleotide exchanges and the average possible amino acid substitutions per residue (assuming a single nucleotide exchange within each codon). The MAP analysis predicted 23 % synonymous exchanges but only 9 % were observed. The analysis

also showed that the average possible amino acid substitutions available per residue when mutating the RgDAAO gene using the most similar epPCR conditions is 7.5. The minimum predicted for this gene using any of the seven *Taq*-based epPCR methods described in the MAP analysis programme is 5.5 and it would therefore be expected that the actual number lies within this range. The maximum possible average diversity per residue achievable by any of the single point mutational methods is 7.5 (with the exception of those methods which actively increase the likelihood of yielding more than one exchange per codon). The limitations are again due to the degeneracy of the genetic code and the statistical likelihood that only one nucleotide per codon will be exchanged.

Overall, the generated RgDAAO epPCR library contained an average of 1.4 amino acid substitutions per variant. Amino acid exchanges to all chemical groupings were observed and the mutational profile compared well with the ideal chemical distribution with the exception of a reduced percentage of exchanges to aromatic residues. A MAP analysis of the gene showed that the library is likely to target an average of between 5.5 and 7.5 amino acids per residue (28.9 - 39.5 % of the natural diversity). The number of amino acid exchanges which may lead to enzyme inactivity for structural reasons was estimated to be 12 % which is reasonably close to both the 'predicted' and 'non-biased' values. Any single nucleotide exchange method of mutagenesis will introduce some form of bias to the library generated and although the limitations of the RgDAAO epPCR library must be considered, the library is appropriate for screening for variant DAAO activity towards new substrates.

2.3.3 Screening the RgDAAO epPCR library

Using the equations described by Patrick *et al.*,⁽⁵¹⁾ the number of variants which should be selected in order to have a 95 % likelihood of screening 100 % of the possible sequences is given by Equation 1. L is the number of variants to be screened, the probability (P_c) is 0.95 and V is the total number of possible sequences. V is determined from the number of possible codons (64) and the average number of

nucleotide exchanges/gene (2.7). In the case of this epPCR library, V has a value of $64^{2.7}$ or 75 281, resulting in the number of colonies to be screened (L) of $\sim 1\,069\,000$.

$$L = -V \ln(-\ln P_c / V)$$

Equation 1 – L = number of variants to be screened, P_c = probability, V = total number of possible sequences.

This calculated figure includes the deletions observed in the sequenced sample but not the 2 sequences in which empty plasmids were observed. As these account for 10 % of the sample, the screening efforts should be increased accordingly to $\sim 1\,176\,000$. With these numbers, the screen to be used for the detection of improved variants in random libraries must be robust and high-throughput.

Solid-phase screen and limitations

Initially the RgDAAO epPCR library was screened for novel activity using the HRP-coupled solid-phase assay described in Section 1.3.3. A solid-phase screen has been successfully used in the Turner and other groups for detecting desired improvements in oxidases towards substrates of interest.^(49,52) Figure 2.15 shows an example of the detection of MAO-N variants with improved activity towards chiral amines.⁽⁵³⁾



Figure 2.15 – Detection of improved oxidase activity by solid-phase HRP-coupled screen⁽⁵³⁾. The brown coloured colonies indicate oxidase activity towards the substrate screened.

Approximately 50 000 RgDAAO epPCR variants were screened on solid-phase against β -amino acid substrates. No activity was detected. This was not conclusive because it became evident that the solid-phase screen was not consistent or robust enough to screen the large numbers of colonies required. To demonstrate the problem

two transformations of *E. coli* BL21(DE3) cells were carried out, one using the parental RgDAAO/pPOT3 and the other using MAO-N variant/pET16b.⁽⁵⁴⁾ The transformants were grown on nitrocellulose membranes and are shown in Figure 2.16. Membrane A contains colonies expressing RgDAAO and membrane B contains colonies expressing MAO-N. Both membranes were treated with an HRP assay mixture containing active substrate ((*R*)-alanine for RgDAAO and α -methyl benzylamine for MAO-N). The colonies on each membrane should have developed colour under these conditions. All MAO-N producing colonies on membrane B coloured as expected. However, on membrane A many of the parental RgDAAO producing colonies showed no colour formation, although this should have been observed. This was a recurring problem with RgDAAO producing colonies in the solid-phase assay. Given the number of colonies required for full screening of the library, it was decided that this solid-phase assay was not a useful method for RgDAAO screening. Therefore, a new assay method was required.

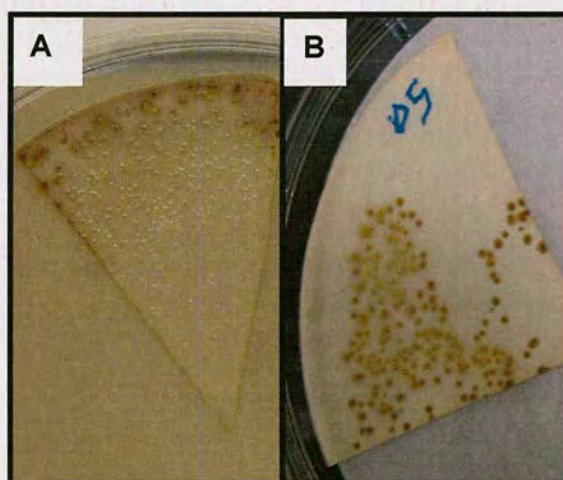


Figure 2.16 - Solid-phase HRP coupled assay. A = Transformants expressing RgDAAO, treated with HRP, 3,3'-DAB and (*R*)-alanine, B = transformants expressing MAO-N (D5) treated with HRP, 3,3'-DAB and α -MBA. Not all identical colonies on membrane A showed colour formation as observed on membrane B.

Liquid-phase assay and validation

Solid-phase assays only allow a qualitative evaluation of activity. In contrast, screening in liquid-phase is more quantifiable as colour formation is measured

spectrophotometrically and does not rely on detection by eye. The sensitivity, reproducibility, accuracy and robustness of the assay can be easily evaluated.

As described in Section 2.1 some microorganisms cause the oxidation of the dye precursors 4-AAP and TBHBA in the HRP-coupled liquid phase assay in the absence of an externally added amino acid, which made controls impossible. Figure 2.17 shows an example of the positive and negative controls used for liquid-phase screening of the RgDAAO epPCR library. The positive controls in wells 1 to 3 contain cells transformed with RgDAAO/pPOT3 and the negative controls in wells 4 to 6 cells contain cells transformed with pPOT3 (empty vector). All the wells contain HRP, 4-AAP, TBHBA and (*R*)-alanine. No colour formation is observed in the negative control wells in contrast to the positive controls.



Figure 2.17 - Liquid-phase HRP coupled assay. Wells 1-3 are positive controls which contain cells producing RgDAAO, HRP, 4-AAP, TBHBA and (*R*)-alanine. Wells 4-6 contain empty vector cells, HRP, 4-AAP, TBHBA and (*R*)-alanine.

Determination of total protein concentration in cell free extracts

In the liquid-phase assay, RgDAAO was used either as whole cells or in the form of CFE. Total protein concentration of CFE from different cell growths and extractions was estimated and compared. The methods used for determination of the total protein concentration of the prepared samples were UV absorbance at 260 and 280 nm and bicinchoninic acid (BCA) assay. The principles of these two methods are described in Section 3.2.4. An example of the standard curve produced when using the BCA assay is shown in Figure 2.18.

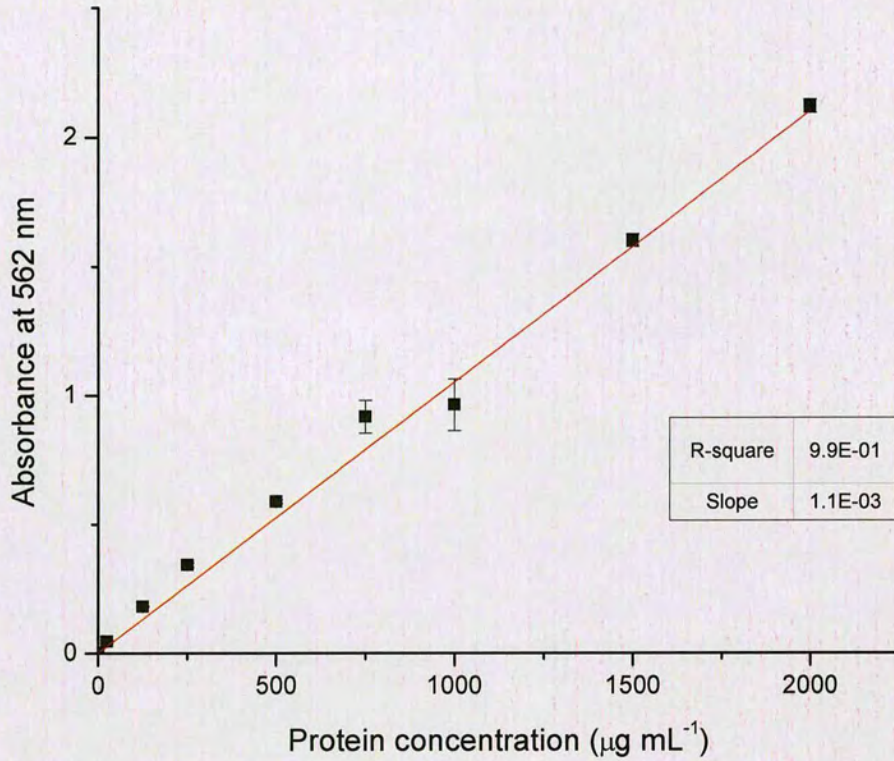


Figure 2.18 – BCA standard curve for determination of total protein concentration of CFE produced using BSA of known concentration. Each sample and standard was measured in triplicate and data points represent the mean values \pm standard deviation. Background was removed by subtracting a control which contained no BSA.

The values for total protein content in cell free extracts by UV spectrophotometry and by BCA assay were compared. Protein concentrations from various *E. coli* BL21(DE3) fermentations were determined. The results are shown in Table 2.7.

Table 2.7 – Comparison of total protein concentration obtained from cells containing different plasmids. Empty vector = pPOT3 plasmid with no gene insert. (1) and (2) represent extracts from different cell growths. UV absorbance was measured using a 1 in 20 dilution of the CFEs to measure within the linear detection range. CFE used in the BCA assay was diluted 1 in 5 to measure within the range of the standards

	Concentration UV absorbance approximation (mg mL ⁻¹)	Concentration BCA assay (mg mL ⁻¹)
Empty vector (pPOT3) (1)	5.1	4.2
Empty vector (pPOT3) (2)	n/m	4.7
TvDAAO/pPOT3 (1)	5.7	4.9
TvDAAO/pPOT3 (2)	n/m	4.7
RgDAAO/pPOT3 (1)	5.3	3.9
RgDAAO/pPOT3 (2)	5.2	4.2

Estimating the protein concentration using UV absorbance gives higher values than by BCA assay. However, similar concentrations are obtained within each of the individual methods.

Robustness of the liquid-phase assay

An easily calculated parameter is the Z factor, Z'. This is a "screening window coefficient" described by Zhang *et al.*⁽⁵⁵⁾ which is calculated using the average positive control (μ_{c+}), average negative control (μ_{c-}) and the standard deviations obtained for each (σ_{c+} and σ_{c-} respectively) in Equation :

$$Z' = 1 - \frac{(3\sigma_{c+} + 3\sigma_{c-})}{|\mu_{c+} - \mu_{c-}|}$$

Equation 2 - Z' = screening window coefficient, μ_{c+} and μ_{c-} = averages of the positive and negative controls respectively, σ_{c+} and σ_{c-} = standard deviations of the positive and negative controls respectively.

The Z' factor describes the separation of the distributions of the positive and negative controls. A Z' value of between 0.5 and 1 means that the separation band is large and indicates that the assay will be useful for screening. Assays showing lower Z' values have to be examined more carefully but can still produce meaningful results. Figure 2.19 shows Z' calculated over the time-course of an HRP-coupled liquid-phase assay detecting parental RgDAAO activity against (R)-alanine as the positive control. The

assay was performed using CFE. Two different negative controls were used for the calculation, absence of substrate (blue line) or absence of enzyme (pink line). Both sets of data give values close to 1, confirming that the assay will be useful for screening purposes and that either negative control can be used. With increasing colour formation the Z' value improves rapidly.

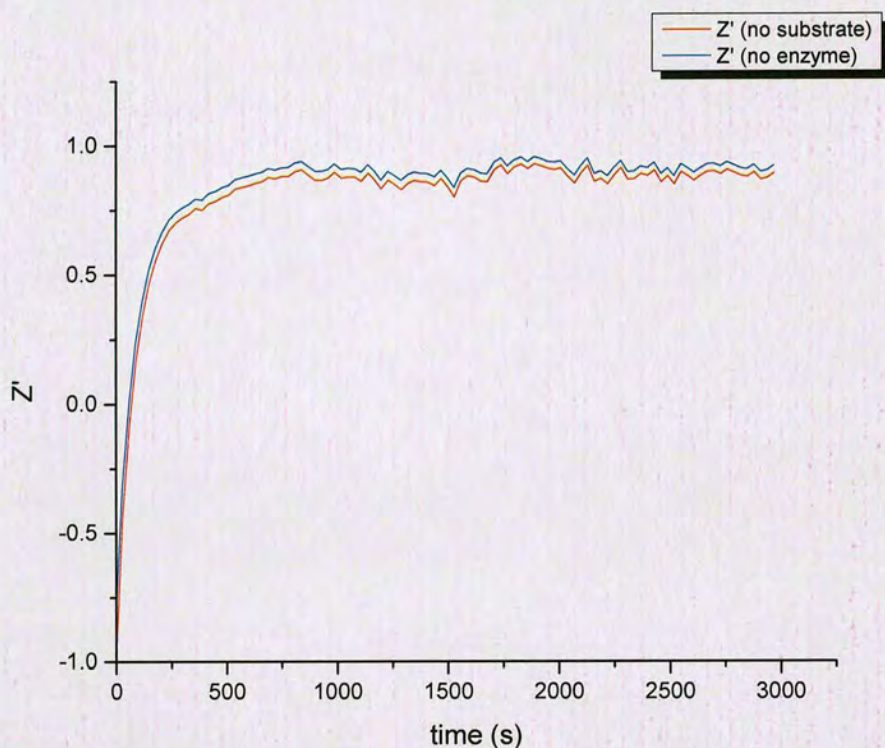


Figure 2.19 – Z' calculated for an HRP-coupled assay detecting parental RgDAAO cell free extract (cfe) activity against (*R*)-alanine as the positive control. Two different negative controls are compared, absence of substrate (red line) and absence of enzyme (blue line).

Light Sensitivity of Liquid-phase Assay

The HRP substrate, 4-AAP, used in the liquid-phase assay is light sensitive and a solution containing 4-AAP, TBHBA and HRP will colour pink over time when exposed to light. This causes an increase in the recorded absorption which must be subtracted as background. The wells around the edge of a 96-well plate are more likely to be exposed to light than those at the centre and the background response is not identical for each well. In addition, as the project was concerned with detecting novel and potentially very low activities, it was useful to allow long-term

development of the assay. This timescale increased the impact of background colour formation on the assay results.

Three HRP-coupled assays were performed under different conditions over 15 h to assess the background colour formation. Three microtitre plates were prepared with triplicate positive (+) and negative (-) controls. The positive controls were whole cells expressing RgDAAO assayed against (*R*)-alanine and the negative controls were whole cells transformed with empty plasmid also assayed against (*R*)-alanine. Plate A was a normal transparent polystyrene microtitre plate which was covered with a transparent lid between measurements. Plate B was an identical transparent plate which was covered with foil while not being measured. Plate C was a black polystyrene microtitre plate (with transparent base to allow absorbance measurement) which was covered with a black polystyrene lid while not being measured. The absorbance at 510 nm was measured after 1, 3 and 15 hours and the results from each triplicate averaged. A plot of the results is shown in Figure 2.20.

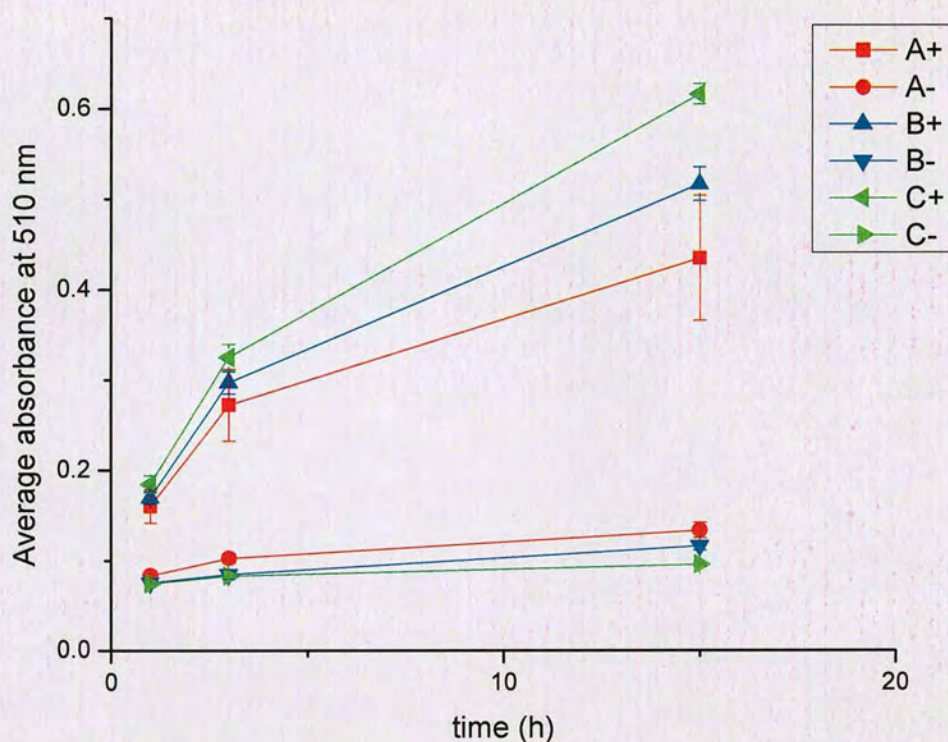


Figure 2.20 - Light sensitivity of liquid-phase assay. Plate A = transparent plate, plate B = foil-covered transparent plate, C = black polystyrene plate with black lid. Squares show the averaged absorbance of positive controls and triangles the averaged absorbance of negative controls. All points are shown ± 1 standard deviation.

As expected, the positive controls all show a significantly better response than their respective negative controls. The standard deviation (shown by the error bars) in the data from the plate left open to light were much greater than in plates B and C for both the positive and negative controls. The increase in absorbance due to the influence of light was investigated by comparing the rate obtained for each negative control.

The results are shown in Table 2.8 and demonstrate that the smallest background colour formation is given when using a black microtitre plate covered with a lid with a rate of $1.4 \times 10^{-3} \text{ AU}\cdot\text{h}^{-1}$.

Table 2.8 – slope of the negative control response over 15 hours for plates A, B and C. Plate A = transparent plate, plate B = foil-covered transparent plate, C = black polystyrene plate with black lid.

Plate	A	B	C
AU.h ⁻¹	$3.2 \times 10^{-3} \pm 2.7 \times 10^{-4}$	$2.8 \times 10^{-3} \pm 2.2 \times 10^{-4}$	$1.4 \times 10^{-3} \pm 1.5 \times 10^{-4}$

The Z factor was used to further investigate the impact of light exposure on the assay. Z' values were calculated for each of the three plates and are shown plotted against time in Figure 2.21. Given that Z' values above 0.5 indicate a good screening assay, it is clear that an uncovered transparent plate (A) is an unsuitable method for screening, while either a black plate and lid (C) or a foil-covered plate (B) give good separation of the positive and negative controls with Z' values of between 0.65 and 0.90. This experiment also demonstrates that assays using whole cells give satisfactory values for Z'.

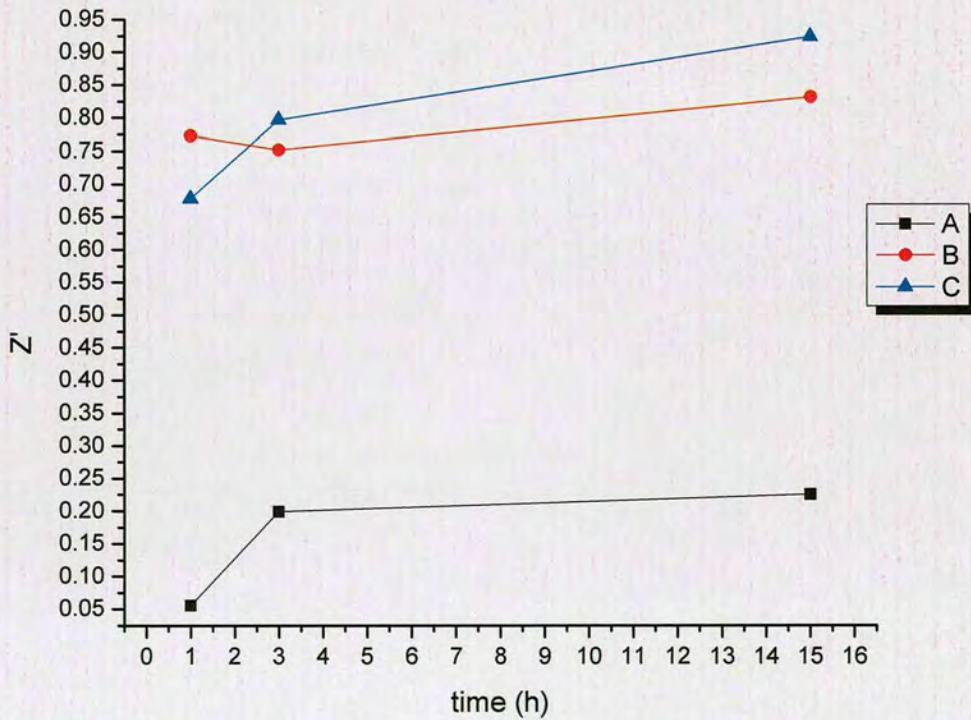


Figure 2.21 – Sensitivity of liquid-phase assay towards light expressed by Z'. (A) = transparent plate left open to light, (B) = transparent plate covered from light and (C) = black plate with lid.

Linearity and detection limit of the liquid-phase assay

The sensitivity of the HRP assay was assessed by performing a serial dilution of hydrogen peroxide in a microtitre plate. This assay used HRP, 4-AAP, TBHBA and H₂O₂, with no RgDAAO or substrate present.

The concentration of an approximately 30 % w/v solution of H₂O₂ was determined by titration against KMnO₄ and was found to be 5.30 M (18.0 % w/w), according to Equation 3.

**Equation 3**

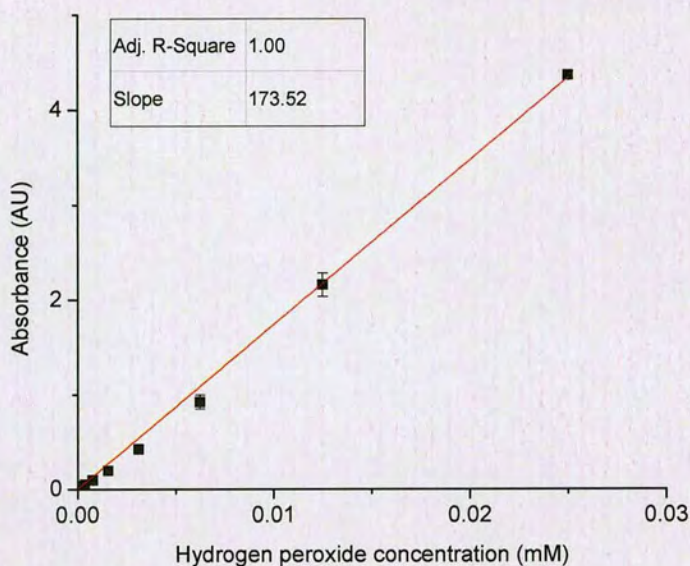
The maximum concentration of H₂O₂ was 25 μM which was reduced in a series of 1 in 2 dilutions as shown in Table 2.9. The assay was repeated 8 times and the data for each dilution averaged. The absorbance obtained for the well containing no H₂O₂ was used to blank the other results which are plotted as absorbance against H₂O₂ concentration in Figure 2.22. The plot marked (A) in this figure shows the full range of dilutions measured, while the plot marked (B) shows only the lowest concentrations.

Table 2.9 – A serial dilution of H₂O₂ was performed to determine the detection limits of the colorimetric assay.

Position	1	2	3	4	5	6	7	8	9	10	11
H ₂ O ₂ (μM)	25.00	12.50	6.25	3.13	1.56	0.78	0.39	0.20	0.10	0.05	0.00

The maximum reading on the plate reader used (Fluostar Optima) was 4.5 AU at 510 nm). Figure 2.22 (A) shows that detection of colour formation is linear up to this maximum which occurs at a concentration of 25 μM H₂O₂. An R² value (see Section 5.7) of 1.00 was obtained for the linear regression. Figure 2.22 (B) shows only the data for the five lowest H₂O₂ concentrations. The linear dependence of colour formation on H₂O₂ concentration is maintained, with an R² value of 0.92, and concentrations as low as 0.05 μM can be detected by the HRP-dye system. This represents an excellent linear relationship between absorbance measurement and H₂O₂ concentration.

(A)



(B)

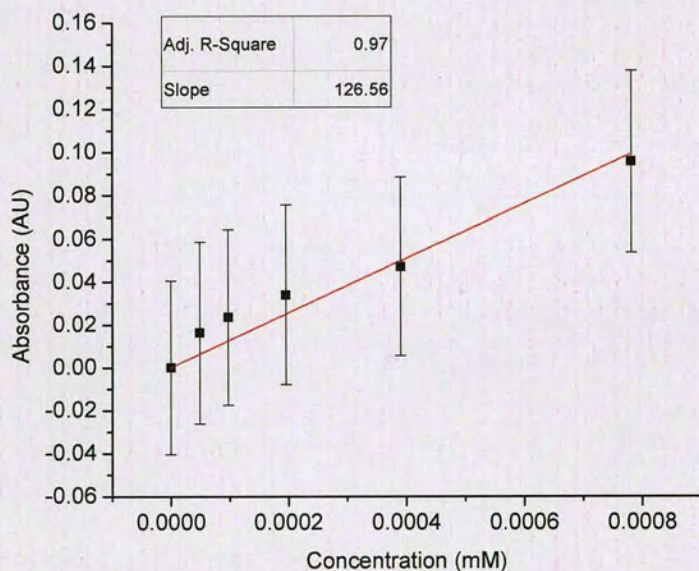


Figure 2.22 – Plots of averaged endpoint absorbance (minus blank) against H_2O_2 concentration for an assay also containing HRP, 4-AAP and TBHBA. (A) shows the full range of dilutions measured and (B) shows only the lowest concentrations. All data points represent mean values from reactions repeated 8 times and are given \pm one standard deviation.

The HRP-coupled liquid-phase assay was assessed further by performing a series of dilutions of both substrate (*(R)*-alanine) and cell free extract (from cells expressing RgDAAO). A liquid-handler was used to perform the dilutions. The total volume of

the wells was 200 μL , the maximum concentration of CFE added was 50 % v/v (A1-A12) and the maximum concentration of (*R*)-alanine was 10 mM (A1-H1). Figure 2.23 shows the layout of the 96-well plate with increasing substrate concentration towards the top of the plate and increasing CFE volume to the right. All wells contained HRP, 4-AAP, TBHBA and dilutions of RgDAAO CFE and (*R*)-alanine with the exceptions of H1-H12 (no RgDAAO CFE) and A12-H12 (no (*R*)-alanine). Table 2.10 gives the concentrations of CFE and (*R*)-alanine in each well.

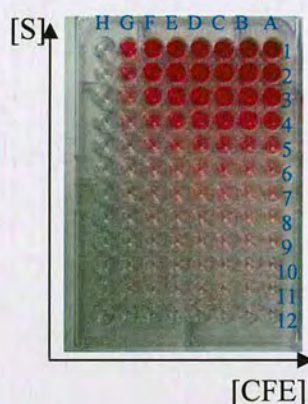


Figure 2.23 – Layout of serial dilution plate used to estimate the detection limit of HRP-coupled liquid-phase assay. All wells contain RgDAAO CFE, HRP, 4-AAP, TBHBA and (*R*)-alanine with the exceptions of H1-H12 (no RgDAAO CFE) and A12-H12 (no (*R*)-alanine). The well numbers are labelled in blue. Total well volume = 200 μL .

Table 2.10 – Concentrations of RgDAAO CFE and (*R*)-alanine used in serial dilutions assay. The assay was performed in triplicate and measured over 50 minutes.

Column	[CFE] (% v/v)	Row	[Substrate] (mM)
A	50.0	1	10.00
B	25.0	2	5.00
C	12.5	3	2.50
D	6.3	4	1.25
E	3.1	5	0.63
F	1.6	6	0.31
G	0.8	7	0.16
H	0	8	0.08
		9	0.04
		10	0.02
		11	0.01
		12	0.00

The assay was performed in triplicate and measured over 50 minutes. The rate of change in absorbance (mAU s^{-1}) was calculated for each well. The data were

averaged and are shown in Figure 2.24 as rate against the substrate concentration. Error bars (\pm one standard deviation) are shown only for 1.6 and 50 % v/v CFE. This figure shows that the increase in rate due to substrate concentration is approximately linear until a plateau is reached between 0.63 and 2.5 mM (*R*)-alanine.

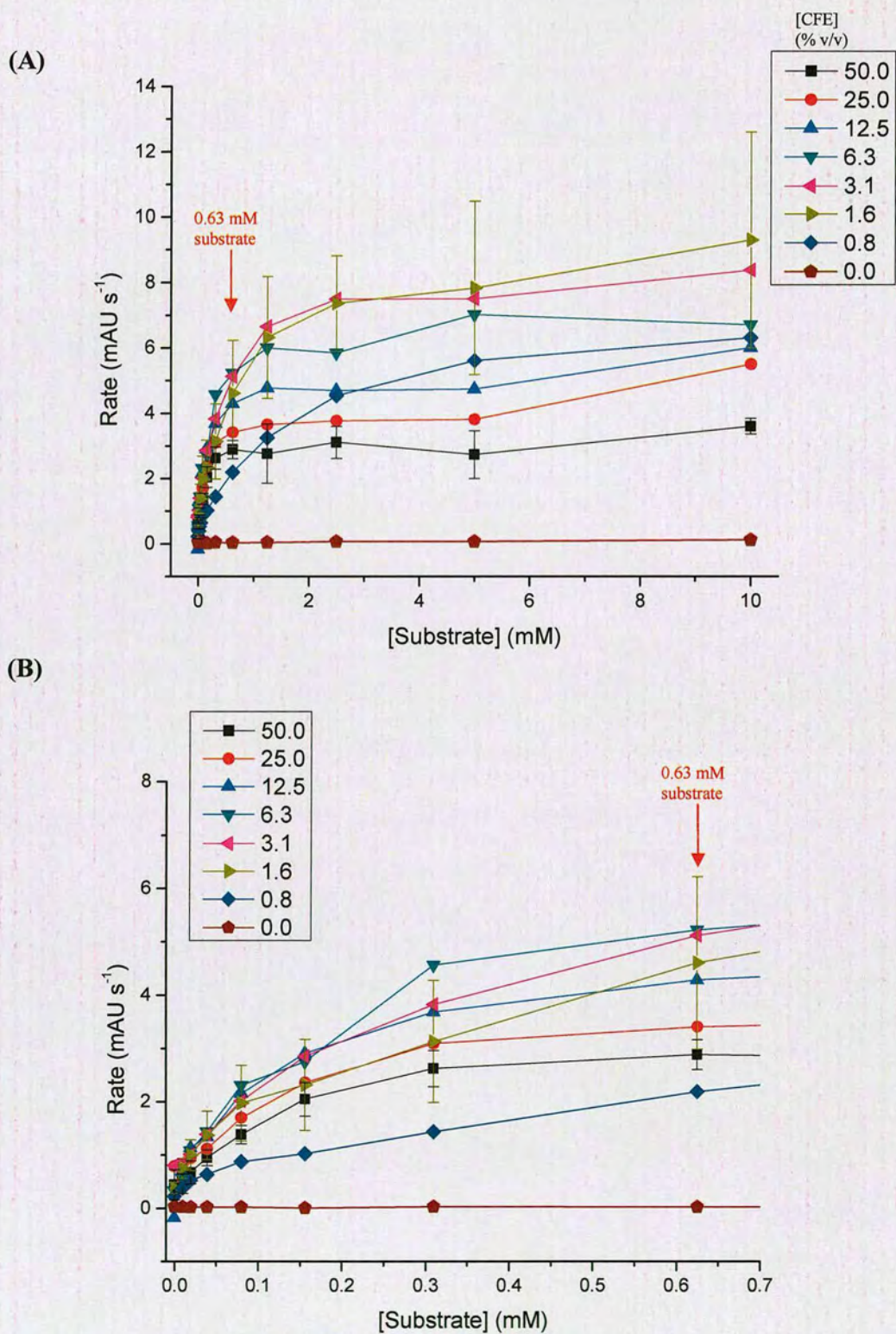
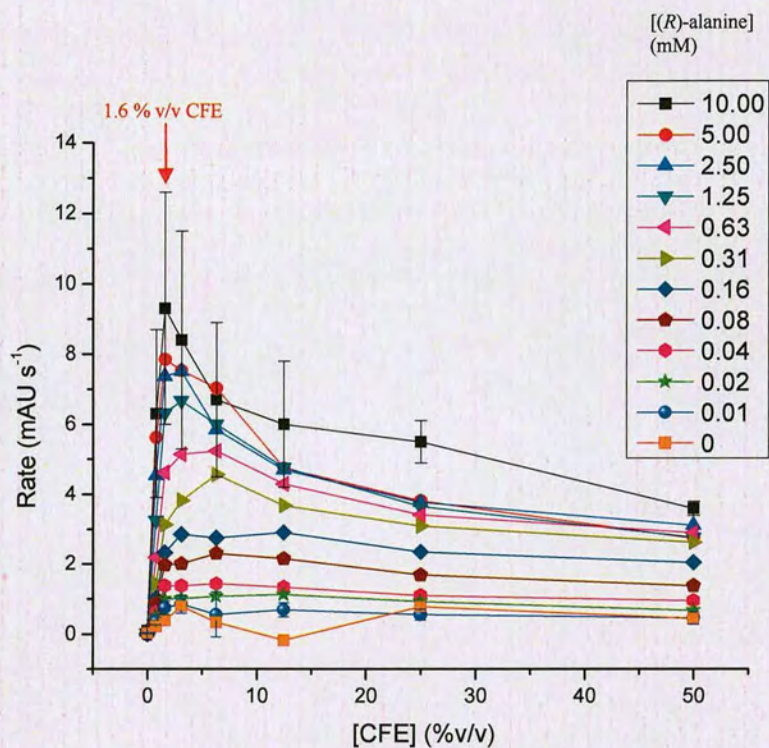


Figure 2.24 – Liquid-phase serial dilutions assay. Data points represent mean values from triplicate reactions. Plot of maximum rate of change in absorbance against substrate concentration for various concentrations of RgDAAO CFE. (A) shows the full range of data

collected while (B) shows only the rates obtained for substrate concentrations up to 0.63 mM. The curves produced for 1.6 and 50 % v/v CFE are shown \pm one standard deviation. CFE serial dilutions were made by manual pipetting and substrate dilutions by means of a liquid handler (Tecan Genesis). Assay mix was also added by the liquid handler. The order of addition was: CFE, assay mix, (R)-alanine.

The data were also plotted in the alternative representation shown in Figure 2.25 with the rate plotted against CFE concentration. Error bars (\pm one standard deviation) are shown for 10.0 and 0.01 mM substrate. This figure indicates a high degree of inaccuracy at low CFE and high substrate concentrations within the chosen experimental setup. The increase in rate due to CFE concentration is linear until a steep decrease at around 1.6 % v/v CFE. V_{\max} (AU s^{-1}) should increase with increasing CFE concentrations. However the opposite trend was observed for concentrations of CFE higher than 1.6 % v/v. The highest values for V_{\max} were given by 0.8 to 1.6 % v/v CFE and the lowest by 50 % v/v. It was assumed that this decrease was caused by either protein precipitation or other CFE enzymes affecting either the RgDAAO system or the HRP system. Future assays were carried out with CFE concentrations of ≤ 5 % v/v.

A)



B)

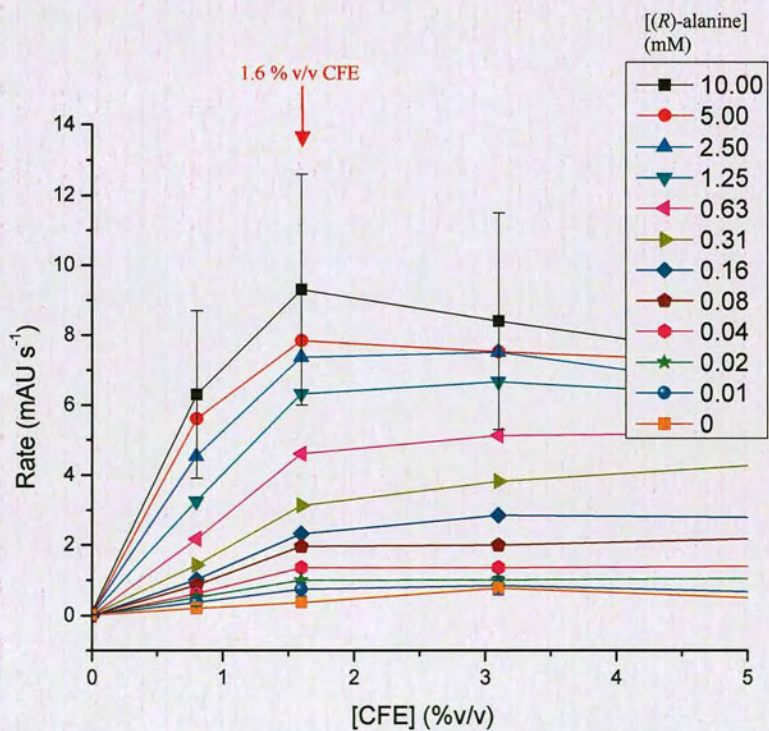


Figure 2.25 - Liquid-phase serial dilutions assay. Data points represent mean values from triplicate reactions. Plot of maximum rate against CFE concentration for various concentrations of substrate. (A) shows the full range of data collected while (B) shows only the rates obtained

for CFE concentrations up to 3.1 %v/v. The curves produced for 10.0 and 0.01 mM (*R*)-alanine are shown \pm one standard deviation. CFE serial dilutions were made by manual pipetting and substrate dilutions by means of a liquid handler (Tecan Genesis). Assay mix was also added by the liquid handler. The order of addition was: CFE, assay mix, (*R*)-alanine.

The Michaelis constant (K_m) is the substrate concentration at half the maximum velocity and should remain constant at all enzyme concentrations. K_m values can be calculated either from Michaelis-Menten plots such as those shown in Figure 2.24 or from double-reciprocal (Lineweaver-Burk) plots such as those shown in Figure 2.26 where $1/V$ has been plotted against $1/[S]$. These double-reciprocal plots should produce a linear relationship from which K_m can be determined via extrapolation to the intercept on the x-axis. Figure 2.26 (A) shows the double-reciprocal plot obtained using 50 % v/v CFE and (B), for comparison, shows that obtained using 0.8 % v/v CFE.

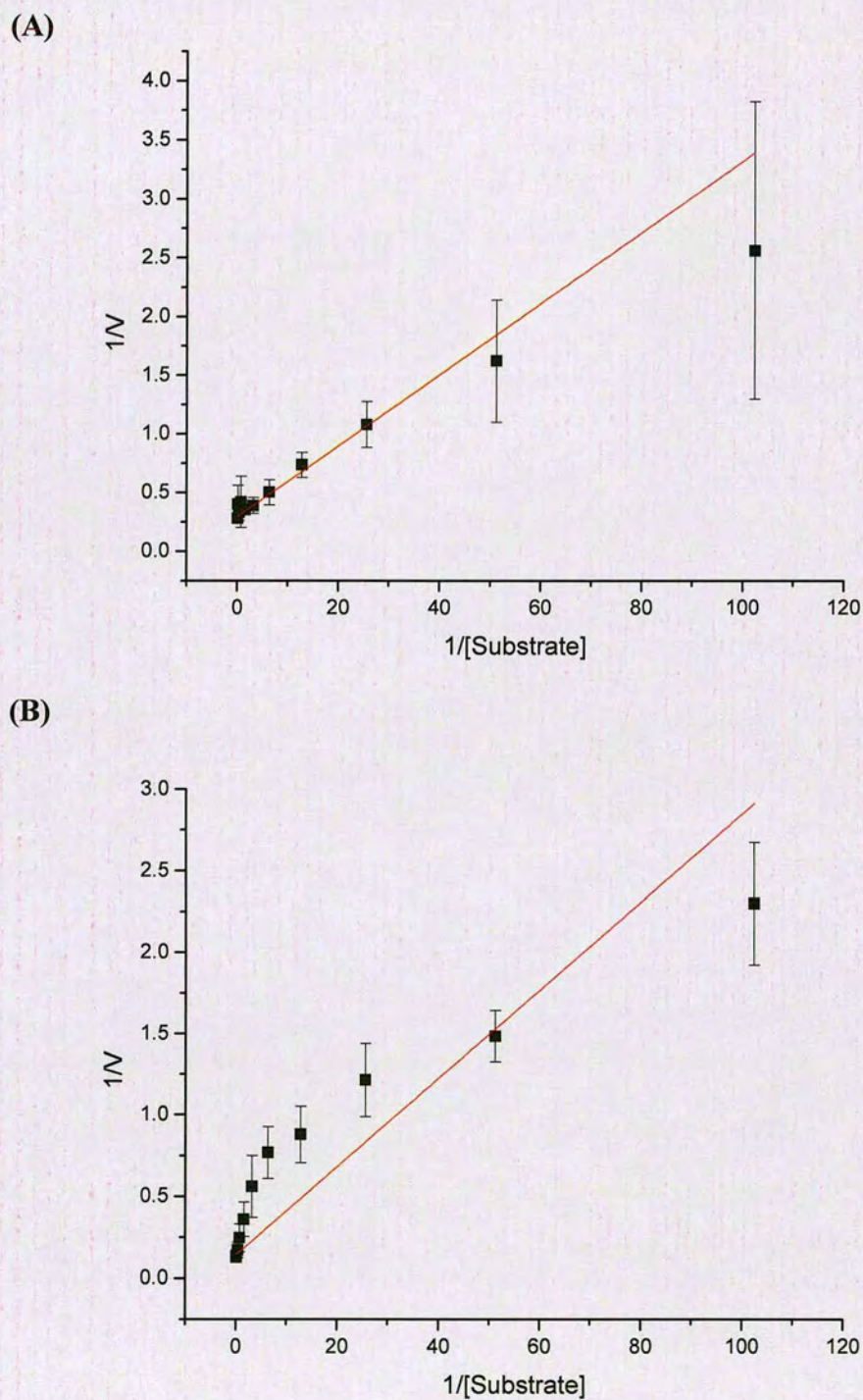


Figure 2.26 – Lineweaver-Burk plots for (A) 50 %v/v CFE and (B) 0.8 %v/v CFE. The inverse of the maximum rates ($1/V$, s AU⁻¹) are plotted against the inverse of substrate concentration ($1/[S]$, mM⁻¹). K_m can be extracted by extrapolation of the linear regression to the point where it intercepts the x-axis (at $-1/K_m$).

The programme OriginPro 8 was used to calculate the values obtained for K_m and V_{max} from both the Michaelis-Menten and the Lineweaver-Burk plots. This was done for each enzyme concentration and the results of these calculations are shown in Table 2.11.

Table 2.11 – V_{max} and K_m values calculated for various concentrations of RgDAAO against (*R*)-alanine (pH 7.6, 25 °C) using both Michaelis-Menten and Lineweaver-Burk plots.

[CFE] (%v/v)	Michaelis-Menten		Lineweaver-Burk	
	V_{max} (mAU s ⁻¹)	K_m (mM)	V_{max} (mAU s ⁻¹)	K_m (mM)
50.00	3.30 ± 0.32	0.10 ± 0.03	3.44 ± 0.11	0.10 ± 0.01
25.00	4.20 ± 0.30	0.12 ± 0.04	4.16 ± 0.23	0.09 ± 0.02
12.50	5.07 ± 0.19	0.10 ± 0.02	4.75 ± 0.15	0.07 ± 0.01
6.25	7.58 ± 1.46	0.22 ± 0.16	6.22 ± 0.32	0.11 ± 0.01
3.13	10.76 ± 3.16	0.72 ± 0.81	6.90 ± 0.64	0.11 ± 0.02
1.56	9.67 ± 4.40	0.59 ± 0.92	6.74 ± 0.78	0.11 ± 0.02
0.78	8.49 ± 0.85	0.85 ± 0.81	7.02 ± 0.91	0.19 ± 0.04

As discussed, the values obtained for V_{max} peak at CFE concentrations of approximately 1.6 to 3.1 % v/v, however the errors involved are very large at these lower CFE concentrations. The values obtained from the Michaelis-Menten plot give a maximum value for V_{max} of 10.76 mAU s⁻¹, whereas the maximum value produced using a Lineweaver-Burk plot is 7.02 mAU s⁻¹.

K_m values calculated from the Michaelis-Menten plots range between 0.10 and 0.85 mM but have extremely large errors attached to the higher values, which were obtained using the lower CFE concentrations. The values obtained using the Lineweaver-Burk plots range between 0.07 and 0.19 mM. The average value for K_m determined using the Lineweaver-Burk plots was 0.11 mM. This figure differs from literature values for RgDAAO against (*R*)-alanine which range from 0.8⁽⁵⁶⁾ to 2.6 mM.⁽⁵⁷⁾ Both of these literature figures were calculated at pH 8.5 and 25 °C using purified enzyme, whereas the data described here were collected at pH 7.6, 25 °C using CFE. It was assumed that inaccuracies were due to the use of CFE in this experiment and to reduced accuracy of rate determination at low substrate concentrations. A substrate concentration well above K_m was desired for screening purposes and all further assays were carried out at 10 mM (single enantiomer).

Summary of Liquid-phase Assay Investigations

The Z' factor was used to show that the HRP-coupled liquid-phase assay is a good screening assay, using either whole cells or CFE. The detection limits were determined, through a series of H_2O_2 dilutions, to be 25 to $< 0.05 \mu M$ with excellent linearity of absorbance measurement to concentration maintained between these points. As the stoichiometry of amino acid oxidation to H_2O_2 formation is one to one (Scheme 1.15), the reaction can be monitored for conversions up to $25 \mu M$. It should be noted however that the sensitivity decreases significantly when using whole cells as the background in this case is much higher. A series of dilutions of both (*R*)-alanine and CFE using the HRP-coupled assay indicate that rate of colour formation increases until V_{max} is reached at 0.63 mM substrate but that rate decreases at CFE concentrations above $1.6 \% \text{ v/v}$. Additionally, background colour formation due to the light sensitivity of assay components was minimised through the use of black polystyrene assay plates.

Development of high-throughput liquid-phase screen

The biggest disadvantage of the liquid-phase assay compared with the solid-phase assay is screening throughput. Thousands of colonies can easily be screened in a single solid-phase assay experiment but this is very labour intensive in 96-well plate format. For example, in order to screen the estimated 1 176 000 required to cover the entire RgDAAO epPCR library, 12 250 96-well plates will be required. In screening this RgDAAO epPCR library two main steps were taken to increase throughput. A) An increase in the number of colonies screened per well and B) automation of the screening process.

A) Growth of variant libraries in semi-solid agarose

One method of screening in the liquid-phase would be to transfer individual colonies from an agar plate containing a library of RgDAAO expressing variants to a 96-well culture plate and grow these as liquid cultures in preparation for screening. It was decided instead to grow the colonies in 96-well plate format using semi-solid agarose (SeaPrep Agarose from Lonza). The agarose contains enough gelling strength to hold the colonies and provide an equal and separated growing environment for each

individual but is liquid enough for the grown colonies and agarose to be separated by centrifugation. This presents a method of growing and screening more than one colony per well. The screening throughput is increased, for example, from 96 to 960 colonies per plate and the amount of substrate required is decreased. Figure 2.27 describes the overall process.

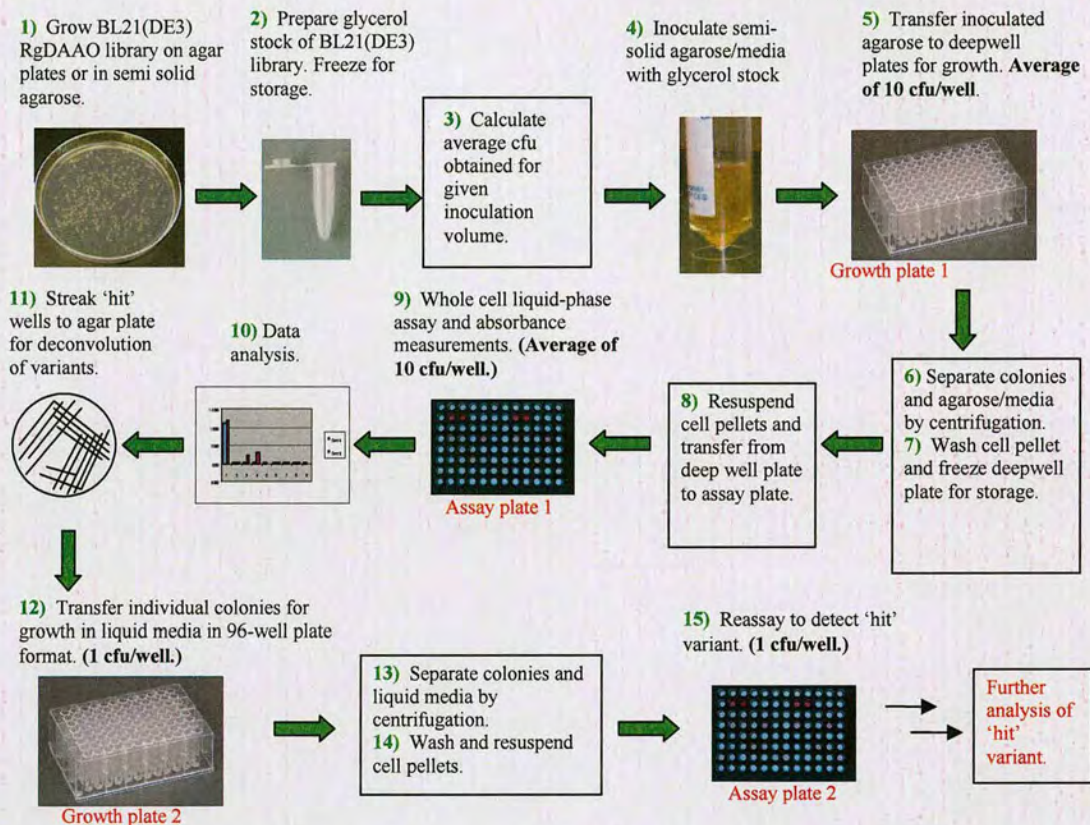


Figure 2.27 – Protocol for increasing throughput of the liquid-phase assay using growth of colonies in semi-solid agarose. CfU = colony forming unit. The steps 1 to 14 are described in more detail in the text below.

The steps in this figure are discussed in more detail through the use of one example which demonstrates the method from beginning to end.

- Figure 2.27: Steps 1 and 2

The RgDAAO epPCR library was used to transform the *E. coli* expression strain BL21(DE3) which was grown on agar plates and transferred to storage tubes as a glycerol stock.

- Figure 2.27: Steps 3 and 4

Prior to inoculation of the glycerol stock to semi-solid agarose two factors had to be determined: i) the minimum gel strength required to hold the growing colonies and ii) the appropriate inoculation volume of glycerol stock.

i) In order to determine the minimum strength of agarose which would hold the growing colonies, three gel strengths were prepared by the method described in Section 3.2.3 such that the final agarose concentration in a 1 to 1 agarose/media mixture was 0.45, 0.5 and 0.55 % w/v. 10 mL of each preparation was transferred to a sample tube and inoculated with RgDAAO BL21(DE3) glycerol stock. The liquid mixture gelled when cooled at 4 °C for 2 h and colonies formed overnight at 37 °C. The results are shown in Figure 2.28. Tube (A) contained 0.45 % w/v agarose and 'trails' can be seen where the colonies have slipped through the gel matrix as they grew. Individual colonies were observed in tubes (B) and (C) and 0.5 % w/v agarose was the minimum concentration of SeaPrep agarose which held the growing colonies but which was still liquid enough to be removed by centrifugation. This concentration was used for inoculation of the glycerol stock library.

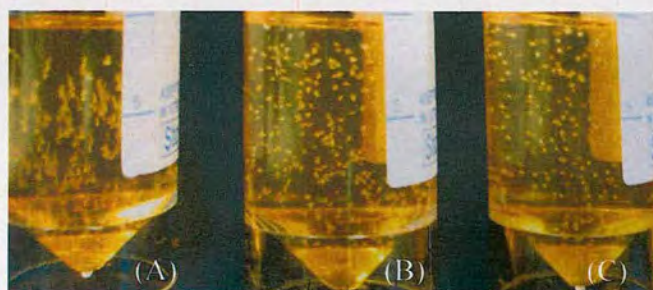


Figure 2.28 - Determination of percentage (w/v) SeaPrep Agarose required to hold growing colonies. A = 0.45 % w/v, B = 0.50 % w/v, C = 0.55 % w/v SeaPrep agarose.

ii) The appropriate volume of glycerol stock to be added to the SeaPrep agarose was assessed using similarly prepared glycerol stocks of parental (RgDAAO/pPOT3) BL21(DE3) and empty vector (pPOT3) BL21(DE3) cells. It was accepted that these results would represent an approximation of the library (epRgDAAO/pPOT3) BL21(DE3) glycerol stocks. Aliquots from one preparation of each of the three glycerol stocks were used in all the experiments performed. A series of dilutions (Table 2.12) of parental and empty vector glycerol stocks were prepared and 50 μ L of each was spread onto 90 mm TSB/agar plates in triplicate. The plates were incubated overnight and the number of colonies which formed on each is shown in Table 2.12. The averaged results are also shown in the plot in Figure 2.29.

Table 2.12 – Average numbers of colonies formed by spreading 50 μ L of a series of dilutions of parental and empty vector glycerol stocks onto agar plates. The experiment was repeated in triplicate and the data shown are the mean values obtained \pm one standard deviation. Samples E and H were measured in duplicate only.

		dilution factor	average number of colonies
RgDAAO	A	1×10^4	2581 ± 628
	B	1×10^6	451 ± 40
	C	1×10^8	85 ± 12
	D	1×10^{10}	18 ± 4
Empty Vector	E	1×10^4	1688 ± 88
	F	1×10^6	90 ± 20
	G	1×10^8	22 ± 7
	H	1×10^{10}	1 ± 1

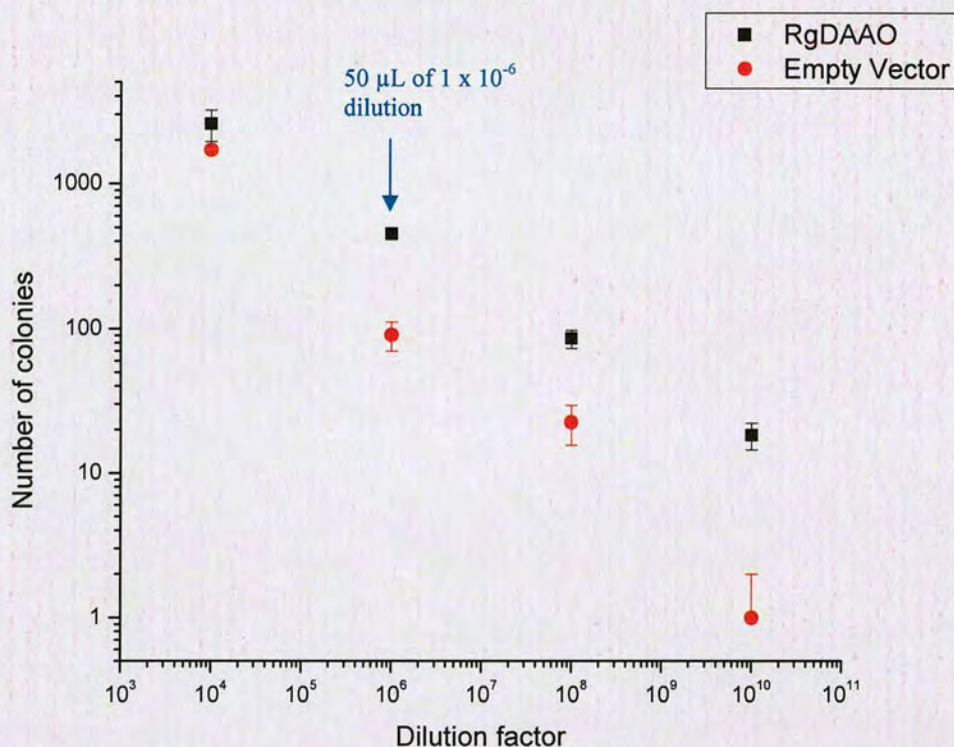


Figure 2.29 – Averaged numbers of colonies obtained by spreading 50 μL of each dilution of parental and empty vector working glycerol stocks onto TSB/agar plates. Data are the mean values obtained from triplicate measurements with the exceptions of empty vector 1×10^4 and 1×10^{10} dilutions which were measured in duplicate only. Each point is shown \pm one standard deviation.

It was decided to grow approximately 15 variant RgDAAO producing colonies in 500 μL SeaPrep agarose per well. This number reduces the number of 96-well plates to be screened for full coverage of the library from 12 250 to 817. In addition, this figure makes the deconvolution of a ‘hit’ well, to find the variant(s) responsible for the colour change, possible on one 96-well plate. According to Equation 1, the number of wells (1 colony per well) required to be statistically certain of re-screening each variant from the hit well is 85. Using Table 2.12 as guidance, 50 mL SeaPrep agarose was inoculated with 250 μL of a 1×10^6 dilution of RgDAAO glycerol stock. Positive and negative controls (cells producing parental RgDAAO and cells containing empty vector respectively) were prepared at the same time.

- Figure 2.27: Step 5

The inoculated agarose was transferred to a 1.1 mL plate, referred to as growth plate 1 in Figure 2.27, by multi-channel pipette (500 μ L per well). The colonies were grown and protein production induced as described in Section 3.2.3. The number of colonies observed per well was between 10 and 20 and the approximate overall numbers in each plate were monitored. Positive and negative controls were prepared similarly on a separate 1.1 mL plate.

- Figure 2.27: Steps 6 and 7

The semi-solid agarose was removed from the cells by centrifugation and the resulting cell pellets were washed with buffer (Section 3.2.3) and stored in 96-well format in the growth plates at -20 °C.

B) Automated screening process

Screening throughput was increased further through the use of a robot to perform the assay and measure the absorbance.

- Figure 2.27: Steps 8 and 9

A Tecan Genesis Workstation 150 was used to perform a similar protocol to that described in Section 2.1, using the following protocol:-

1. Resuspend the pelleted cells in growth plate 1.
2. Transfer cells, assay mix (HRP, 4-AAP and TBHBA) and substrate to black polystyrene, 96-well assay plates (assay plate 1 in Figure 2.27).
3. Move assay plate 1 to a plate reader and measure absorbance at 510 nm (time = 0).
4. Lid assay plate 1 and move to a storage carousel for room temperature incubation.
5. Move assay plate 1 to a plate reader and remeasure absorbance at 510 nm (time = 24 h).

The carousel on which the plates were stored allowed up to 50 plates to be assayed during each screening set. To screen the 817 plates required to cover the full library, 17 sets of 48 plates each were needed. The RgDAAO epPCR library was screened against 20 mM (*rac*)- β -homophenylalanine.

- Figure 2.27 Step 10: Data analysis

The absorbance measurement taken at time 0 was subtracted from the measurement taken at 24 h (Δ Abs). The data obtained for each plate were viewed as shown in Figure 2.30. The Δ Abs calculated for each well was plotted against the well location on the plate. The column numbers (1-12) are shown on the x-axis and the rows (A-H) are denoted as shown in the legend. For example, the point marked with a red circle shows the Δ Abs value for well D1 of this particular plate.

Z' was calculated using positive and negative controls (in triplicate) which were treated in exactly the same manner as the library plates and resulted in values of between 0.4 and 0.7. This range indicates that this method of growth and assaying reduces the accuracy of the assay but is still within the regions of a useful screening assay.

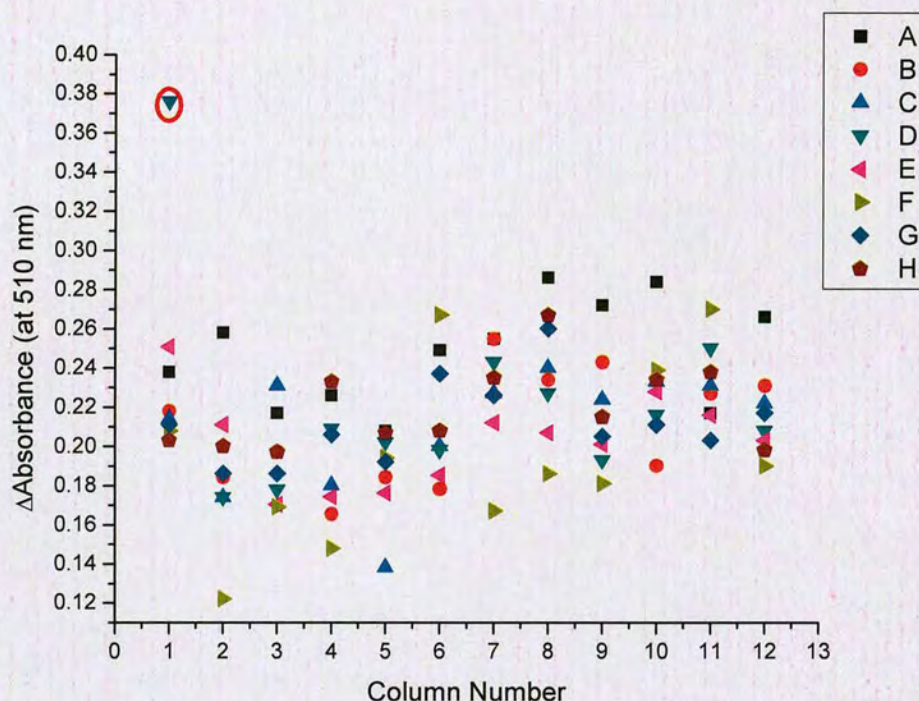


Figure 2.30 – Screening results for one plate of the RgDAAO epPCR library. The change in absorbance over 24 h (Δ Abs) for each of the 96 wells is plotted against well location. Column number (1-12) is shown on the x-axis and rows (A-H) are identified by the markings in the legend.

- Figure 2.27: Steps 11 to 14

'Hit' wells such as D1 in Figure 2.30, contained between 10 and 20 colonies and these had to be deconvoluted to select the active variant. A sample (50 μ L) was removed from well D1 of growth plate 1 and streaked onto a TSB/agar plate which was incubated overnight at 37 °C. 88 colonies were picked and transferred to liquid media in individual wells of a 96 x 1.1 mL plate (growth plate 2 in Figure 2.27) for growth and induction of protein expression.

- Figure 2.27: Step 15

The resulting cell pellets were resuspended and transferred to an assay plate (assay plate 2 in Figure 2.27). A re-assay was performed, using β -homophenylalanine as substrate with the aim of identifying the active variant from plate 1, well D1. The data from assay plate 2 were handled in the same way as for plate 1 and the results

are shown in Figure 2.31. Two wells on assay plate 2 showed some colour formation, C9 and G10. The change in absorbance measured for well E9 was also high but no colour formation was visible by eye. The cell pellet in this well was not fully resuspended and was not selected for further analysis as the higher absorbance reading was thought to be due to particulates rather than production of H_2O_2 .

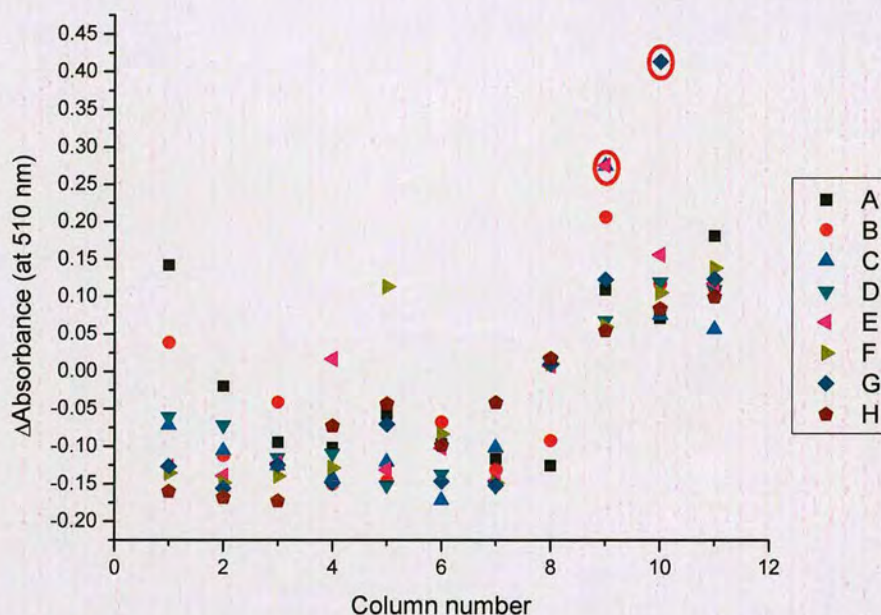


Figure 2.31 – Results for assay plate 2 (reassay of individual variants from plate 1, well D1). The change in absorbance over 24 h (Δ Abs) for each of the 96 wells is plotted against well location. Column number (1-12) is shown on the x-axis and rows (A-H) are identified by the markings in the legend.

Cells variants designated C9 and G10 were recultured in 50 mL volumes. Parental RgDAAO and cells containing empty vector were prepared similarly. A whole cell HRP-coupled assay was performed with the aim of comparing the activity of parental RgDAAO with C9 and G10. The substrates assayed were (*R*)-alanine, (*rac*)- β -phenylalanine and (*rac*)- β -homophenylalanine. The layout of the plate is shown in Figure 2.32 and the contents of each well are explained in the legend. Two negative controls were included, (i) cells containing empty vector were tested against each substrate and (ii) each cell preparation was tested in the absence of substrate. The

assay was performed in triplicate and repeated with separately prepared cell cultures. Both C9 and G10 retained activity towards (*R*)-alanine and G10 appeared to have increased activity towards both (*rac*)- β -homophenylalanine and (*rac*)- β -phenylalanine with respect to parental RgDAAO activity.

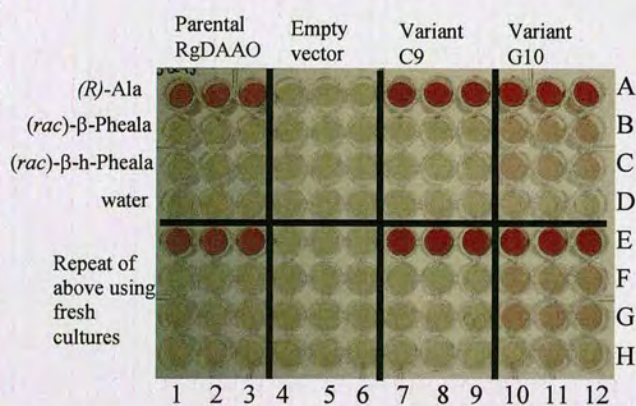


Figure 2.32 – Whole cell assay in triplicate. Each well contains HRP, 4-AAP and TBHBA. Columns 1-3 contain cells expressing parental RgDAAO, columns 4-6 cells transformed with empty vector, columns 7-9 cells expressing C9 and columns 10-12 cells expressing G10. The substrates used were (*R*)-alanine (10 mM, rows A and E), (*rac*)- β -phenylalanine ((*rac*)- β -Pheala, 20 mM, rows B and F) and (*rac*)- β -homophenylalanine ((*rac*)- β -h-Pheala, 20 mM, rows C and G). Rows D and H contained no substrate and the volume was adjusted in these wells with water. Rows E-H are a control duplicate of rows A-D using separately cultured cells.

The variants were investigated further using CFE obtained from cell cultures expressing parental RgDAAO and the G10 and C9 variants. Extracts were also obtained from cells which contained empty vector. These were assayed using the HRP-coupled assay against the substrates (*rac*)- β -phenylalanine and (*rac*)- β -homophenylalanine. The assay was performed in triplicate and Figure 2.33 shows the averaged absorbances measured over a period of 11.5 h. These plots show that the increase in absorbance for both C9 and G10 with each of the substrates is similar to that for parental RgDAAO but that in both cases this is greater than for the extracts from cells containing empty vector. Table 2.13 presents the rate of change in absorbance for each and confirms that the activities of C9 and G10 are similar to parental RgDAAO. The rates obtained using (*rac*)- β -homophenylalanine as substrate are between 1.5 and 2.0 times greater than for (*rac*)- β -phenylalanine in all three cases.

The genes producing C9 and G10 were sequenced and both proved to be the parental RgDAAO gene. This highlights the problem of attempting to detect small improvements in activity towards a substrate for which the parental enzyme has little or no activity. Absorbance values are likely to be close to the background levels and are easily misinterpreted.

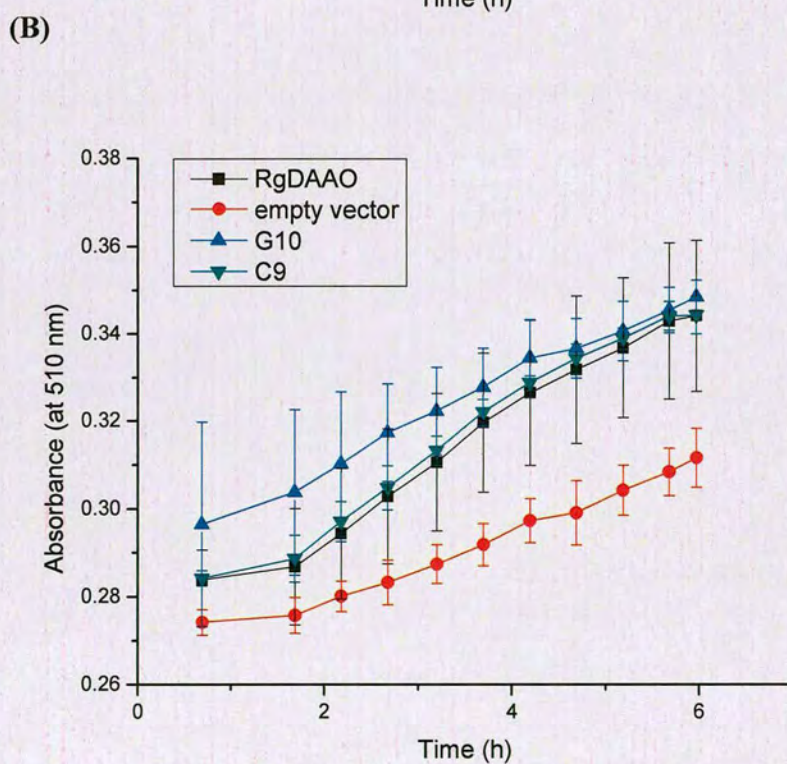
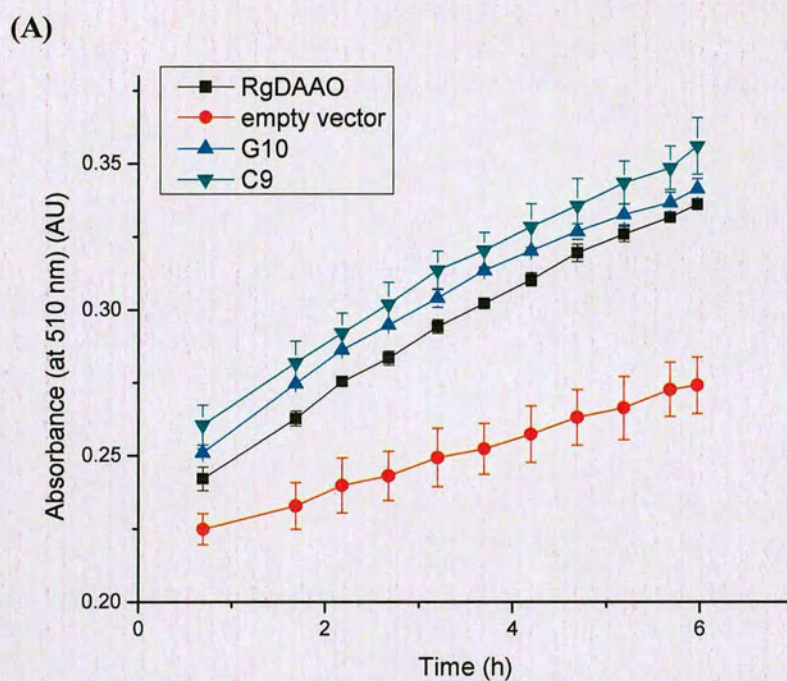


Figure 2.33 – Plots of absorbance against time for RgDAAO, G10, C9 and empty vector CFE assays. Each well contained CFE, HRP, 4-AAP, TBHBA and substrate (20 mM). (A) Substrate = (*rac*)-2, (B) substrate = (*rac*)-1. The assays were performed in triplicate and the averaged data is shown \pm one standard deviation.

Table 2.13 – Comparison of parental RgDAAO and variants using CFE HRP-coupled assay. Averaged rate of change in absorbance with time.

	RgDAAO (AU h ⁻¹)	G10 (AU h ⁻¹)	C9 (AU h ⁻¹)	empty vector (AU h ⁻¹)
(rac)-2	$1.8 \times 10^{-2} \pm 2.6 \times 10^{-4}$	$1.8 \times 10^{-2} \pm 6.4 \times 10^{-4}$	$1.8 \times 10^{-2} \pm 3.1 \times 10^{-4}$	$9.2 \times 10^{-3} \pm 8.9 \times 10^{-4}$
(rac)-1	$1.2 \times 10^{-2} \pm 1.9 \times 10^{-3}$	$1.0 \times 10^{-2} \pm 3.6 \times 10^{-3}$	$8.9 \times 10^{-3} \pm 5.4 \times 10^{-3}$	$6.9 \times 10^{-3} \pm 1.3 \times 10^{-3}$

To confirm (*rac*)- β -homophenylalanine oxidation by HPLC analysis, conversion of at least 5 % is required. The observed rate of 8.8×10^{-3} AU h⁻¹ (measured rate less empty vector rate) relates to a conversion of 5.1×10^{-5} mM h⁻¹ (see Figure 2.22) or 2.4×10^{-3} mM over 48 hours. This is just 0.02 % conversion and will not be accurately measurable by HPLC.

Approximately 72 000 colonies (50 plates) were screened using this liquid-phase assay and no activity resulting in colour formation sufficiently above the background activity was observed towards the tested substrates. The combined coverage of the liquid and solid-phase screening performed represents 10 % of the desired screening number (in order to be 95 % certain of viewing 100 % of the variants, see Equation 1). However, given the difficulty of detecting any improvement in RgDAAO activity towards substrates for which there is little or no parental activity it was decided to attempt a more directed approach and to select specific sites for saturation mutagenesis so that the screening efforts could be reduced.

2.3.4 Conclusions

Two random DAAO libraries were generated, a TvDAAO library through propagation in the mutator strain XL1-Red and an RgDAAO library by epPCR. The TvDAAO library was found to have a mutation in the start codon in at least 18 of the 20 genes sequenced and no other observable mutations. This library and method were therefore not considered for further work. The 20 genes sequenced from the RgDAAO library indicated 2.7 nucleotide exchanges per gene which yielded a similar amino acid exchange profile to that which was predicted by a MAP analysis of the RgDAAO gene using a similar epPCR method.

It was calculated that 1 176 000 colonies should be screened in order to be 95 % certain of covering 100 % of the library members. Although screening for improved variants on solid-phase is an established and powerful technique, the HRP-coupled solid-phase assay used in this work did not prove to be robust enough to screen this number of variants. An HRP-coupled liquid-phase assay was therefore investigated. This assay demonstrated good separation between the distributions of the positive and negative controls, giving a Z factor close to 1, and could therefore be considered a good screening assay. The detection limits for H_2O_2 were found to be between 25 and $0.05 \mu\text{M}$ with good linearity of absorbance measurements between these two points. A serial dilution of (*R*)-alanine showed that V_{max} was reached at 0.63 mM and K_{m} was estimated to be approximately 0.03 mM , although literature values are in the range 0.8 to 2.6 mM . Screening assays were carried out at 10 mM substrate concentration with the aim of assaying at a concentration above the K_{m} for various substrates. A similar set of dilutions of RgDAAO CFE showed that the rate of colour formation decreased at concentrations above $1.6 \% \text{ v/v}$ and therefore concentrations no greater than $5.0 \% \text{ v/v}$ CFE were used in further assays. It was also shown that background colour formation was minimised through the use of black polystyrene assay plates.

A method was developed for screening of the library in liquid-phase in 96-well plate format. Throughput was increased by increasing the number of colonies which could be screened in each well through growth of the variants in semi-solid agarose. This resulted in a reduction of the number of plates to be screened from 12 250 to 817. Further increases in throughput were made through automation of the assay process using a robot for resuspension of the cells, transfer of cells, assay mixture and substrate to the assay plate and measurement absorbance at 0 and 24 h.

Although this methodology did improve the screening rate, the precision and sensitivity of the assay was reduced and detecting small improvements towards substrates for which parental RgDAAO had little or no native activity was found to be extremely difficult. In total approximately 122 000 variants were screened by either solid or liquid-phase assay and although this was only 10 % of the desired

screening number, it was decided that a more useful approach may be to dramatically reduce the library size required for screening by focussing on selected active site residues.

As no improvements in RgDAAO activity towards the two β -amino acid substrates screened were observed in the epPCR library, it was considered that evolution of activity towards these substrates may not be feasible. In α -amino acids the carboxyl group and the amino group are adjacent to one another. In the RgDAAO active site the carboxyl group is involved in binding to the active site(26) and the amino group is then in good alignment with the flavin N5 in order for hydride transfer to occur. In β -amino acids, the presence of the methylene group between these functionalities will alter the ability of the bound substrate to be in correct alignment with the flavin to allow hydride transfer to occur. Therefore, in conjunction with reducing the library size by selecting active site residues, the substrates to be screened were broadened to include α -amino acids with the aim of producing an overview of the beneficial and deleterious amino acid exchanges at the selected sites towards a range of amino acid substrates.

2.4 SATURATION MUTAGENESIS OF PARENTAL *RHODOTORULA GRACILIS* D-AMINO ACID OXIDASE

Saturation mutagenesis at selected residues in the active site of RgDAAO was performed in order to reduce the size of the variant library which required to be screened. In addition, the substrate scope was broadened to include non-proteinogenic α -amino acids with the aim of producing an overview of the beneficial and deleterious amino acid exchanges at selected active site residues towards a range of amino acid substrates.

2.4.1 Selection of key residues for saturation mutagenesis

The crystal structure of RgDAAO in complex with (*R*)-alanine⁽⁴⁷⁾ was obtained from the RCSB Protein Data Bank (PDB ID code 1c0p). (*S*)- β -phenylalanine was superimposed onto (*R*)-alanine by overlaying the C(1)-C(2)-N bonds in (*R*)-alanine with the C(2)-C(3)-N bonds in the β -amino acid, as shown in Figure 2.34.

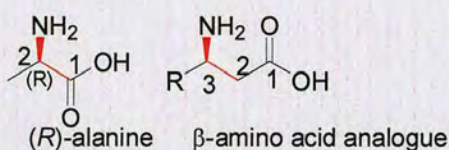
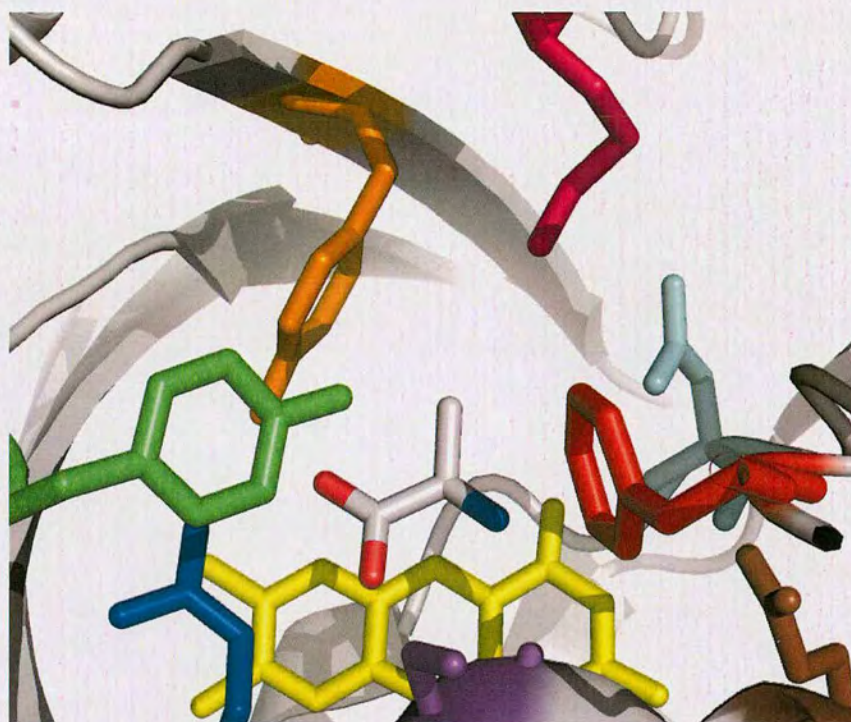


Figure 2.34 – β -amino acids were docked into the active site of the RgDAAO crystal structure by overlaying the bonds shown in red.

The amino acid residues closest to the substrate are shown in Figure 2.35. (A) shows the original structure with co-crystallised (*R*)-alanine in the active site and (B) shows the same structure with (*S*)- β -phenylalanine superimposed in place of (*R*)-alanine. In these representations, Y223, Y238 and R285, the 3 active site residues conserved in all DAAOs, are shown on the left of each picture. Single-site saturation libraries were prepared at two of these three residues (Y238 and R285, coloured green and blue respectively). Two further single-site saturation libraries were created at the active site residues F58 (red) and M213 (pink) which can be seen to the right of each picture in Figure 2.35.

(A)



(B)

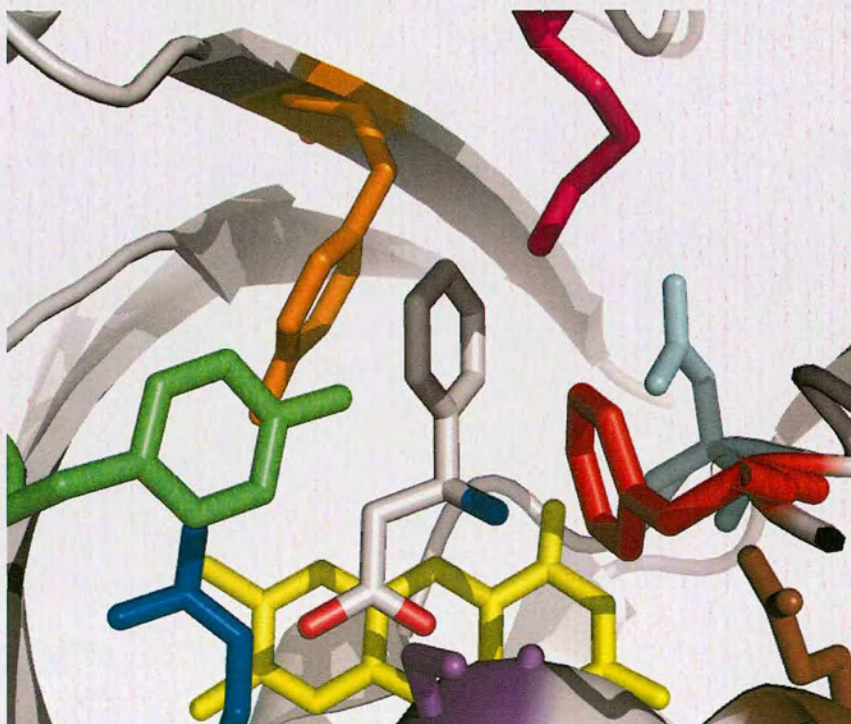


Figure 2.35 - RgDAAO crystal structure,⁽⁴⁷⁾ PDB ID code 1c0p. (A) co-crystallised with (*R*)-alanine, (B) (*S*)-1. Residue colour code: light blue = N54, red = F58, pink = M213, orange = Y223, green = Y238, blue = R285, purple = S335, brown = Q339. The flavin molecule is shown in yellow. Y223, Y238 and R285 are conserved residues. Y223, Y238, M213 and F58 were selected for single-site saturation mutagenesis.

Given an appropriate range of substrates (towards which RgDAAO shows good to low activity) saturation mutagenesis at this selection of residues will allow study of the effect of modifications around the active site, at both conserved and non-conserved residues. The substrates selected for screening of the libraries will be discussed separately for each library.

2.4.2 Preparation of saturation mutagenesis libraries

Fresh plasmid DNA (RgDAAO/pPOT3) was prepared from TOP10 *E. coli* cells and used in a saturation mutagenesis PCR (Section 3.2.2). The primers for this PCR contained a degenerate NNS codon at the site of interest (Section 5.2.3). N refers to any of the four DNA nucleotides and S to either a G or a C. NNS is therefore shorthand for the degenerate codon (A/T/G/C)(A/T/G/C)(G/C). The single letter nucleotide codes are shown in Section 5.6. Table 2.14 shows the genetic code (compare with Table 1.1) with those codons containing an A or a T at the third position removed. It can be seen that NNS degeneracy gives access to 32 codons covering all 20 amino acids.

Table 2.14 – Codons provided by the degenerate codon NNS. The amino acid residues encoded have been arbitrarily numbered (1-20) for clarity. Ter = terminator codon.

Pos ⁿ 2 \ Pos ⁿ 1	T	C	A	G
T	TTC F (1) TTG L (2)	TCC S (6) TCG S (6)	TAC Y (10) TAG Ter	TGC C (17) TGG W (18)
C	CTC L (2) CTG L (2)	CCC P (7) CCG P (7)	CAC H (11) CAG Q (12)	CGC R (19) CGG R (19)
A	ATC I (3) ATG M (4)	ACC T (8) ACG T (8)	AAC N (13) AAG K (14)	AGC S (6) AGG R (19)
G	GTC V (5) GTG V (5)	GCC A (9) GCG A (9)	GAC D (15) GAG E (16)	GGC G (20) GGG G (20)

Parental DNA was removed from the PCR products as described in Section 3.2.2 and the digested products were used for the transformation of XL1-Blue *E. coli*. Several transformations resulted in the colony numbers for each library shown in Table 2.15. According to Equation 1,⁽⁵¹⁾ the number of variants which should be screened in

order to ensure 99 % certainty of covering 100 % of the possible variants is 260. The numbers of colonies obtained were therefore sufficient to cover each library in its entirety apart from the Y238 library. Y238 RgDAAO colonies were difficult to produce and, as this mutagenesis site was at a conserved residue, it was decided that an initial screening of the 180 variants would be made prior to deciding whether to generate more colonies.

Table 2.15 – Number of colonies obtained for each single site saturation mutagenesis library.

Library	Number of XL1-Blue colonies
F58	480
M213	316
Y238	180
R285	1093

2.4.3 Verification of RgDAAO saturation mutagenesis libraries

Ten XL1-Blue colonies from each library were cultured overnight and the plasmid DNA extracted from these. The plasmid DNA was sequenced by MWG Biotech, Germany, using sequencing primers shown in Appendix 5.2.1. The results are shown in Table 2.16.

Table 2.16 - RgDAAO saturation mutagenesis results.

Position 1 (N)	Position 2 (N)	Position 3 (S)	Copies	Amino acid residue
Codon at amino acid position 58. Parent = TCC, Phe.				
T	T	G	3	Leu
T	A	C	1	Tyr
C	A	G	1	Gln
C	G	G	1	Arg
A	A	C	1	Asn
A	C	G	1	Thr
G	T	C	1	Val
G	T	G	1	Val
Codon at amino acid position 213. Parent = ATG, Met.				
T	T	G	1	Leu
T	G	G	1	Trp
C	T	C	3	Leu

Position 1 (N)	Position 2 (N)	Position 3 (S)	Copies	Amino acid residue
A	C	C	1	Thr
A	G	G	1	Arg
G	T	G	1	Val
G	T	C	1	Val
G	A	C	1	His
Codon at amino acid position 238. Parent = TAC, Tyr.				
T	T	G	1	Leu
T	C	C	3	Ser
C	T	G	1	Leu
C	G	C	1	Arg
A	C	G	1	Thr
A	A	G	3	Lys
Codon at amino acid position 285. Parent = CGA, Arg.				
T	C	C	1	Ser
T	C	G	1	Ser
T	A	G	2	Ter
T	G	C	1	Cys
C	A	C	1	His
C	T	G	1	Leu
A	T	G	1	Met
A	A	C	1	Asn
G	G	C	1	Gly

With the exception of saturation library Y238, the degenerate NNS codon designed into the primers for the saturation mutagenesis reaction provided the expected distribution of nucleotide exchanges in the sequenced colonies. Each of the 4 nucleotides can be found at positions 1 and 2 of the codon and a G or a C is seen at position 3. It was therefore statistically likely that the F58, M213 and R285 libraries contained all possible combinations of NNS and therefore the 32 available codons encoding all 20 possible amino acid residues, at the desired positions. In the sequenced sample of the Y238 library the nucleotide G was not observed at position 1 where it is part of the code for Val, Ala, Asp, Glu and Gly. However, as mentioned above, it was decided to review this library following the outcome of an initial screen.

2.4.4 Growth and expression of RgDAAO saturation mutagenesis variants

The libraries were transferred from XL1-Blue *E. coli* to BL21(DE3) *E. coli* for expression of protein by the method described in Section 3.2.2. The BL21(DE3) colonies were grown on agar plates as shown in (i) of Figure 2.36 which describes the procedure for the transfer of variant libraries from agar plates to 96-well plate format. A detailed description can be found in Section 3.2.3.

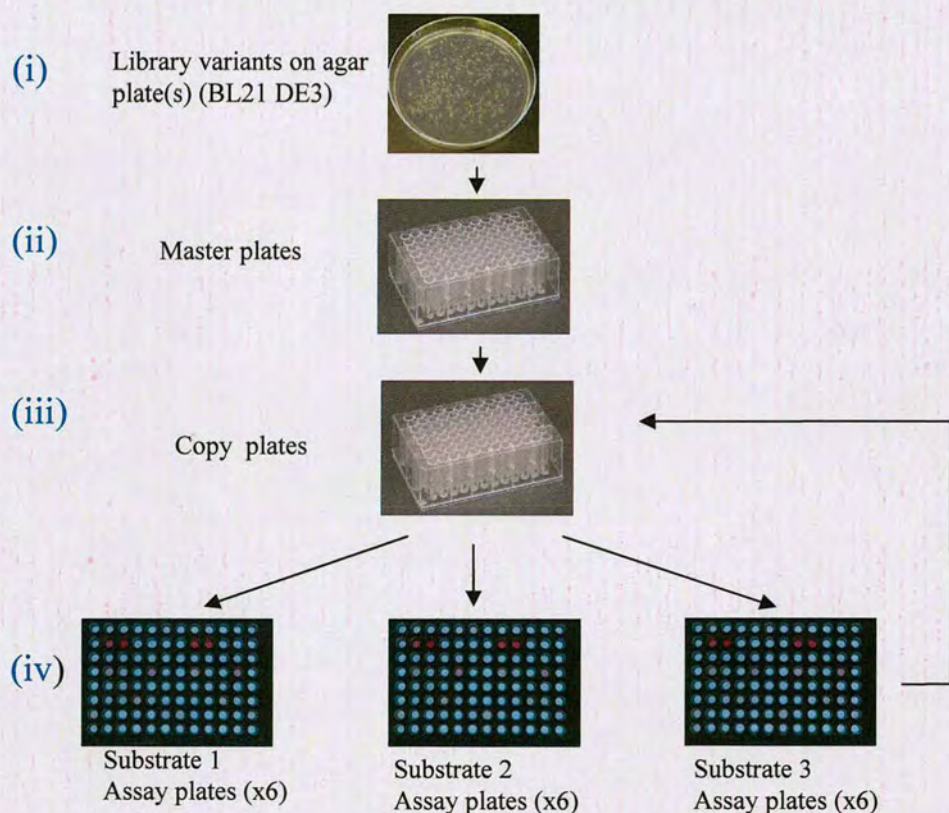


Figure 2.36 – Protocol for transfer of RgDAAO saturation mutagenesis variants from agar plate to 96-well plate format. (i) BL21(DE3) cells containing variant RgDAAO plasmid were cultured on agar plates. (ii) Individual variant colonies were picked and inoculated to 96 well, 2.2 mL master plates and cultured overnight. (iii) The overnight cultures were inoculated to copy plates. Protein expression was induced during growth in these plates and the cells were pelleted and resuspended in buffer. (iv) The resuspended cells were transferred to assay plates (one plate for each substrate tested). The master plate cultures were pelleted and glycerol stocks of these were prepared for storage and future use.

The layout of the master and copy plates is shown in Figure 2.37. Positive, negative and blank controls were included. The positive and negative controls were individually picked BL21(DE3) colonies containing parental RgDAAO plasmid and empty plasmid (no gene insert) respectively. Blank wells contained media but were

not inoculated with a colony. A diagonal of blank wells starting at A1 was created to provide a check for any cross-contamination between the wells during growth and transfer to the copy plates. Some cross-contamination was observed in the blank wells when media volumes of 1 mL were used for growth of the cultures in the master and copy plates. This problem could be solved by reduction to 800 μ L media volume. Six master plates were produced from the RgDAAO F58 library and 5 from each of the other libraries. This represents 480 variants from the F58 library and 400 from each of the other libraries. These numbers ensure adequate over-sampling of each variant library.

	1	2	3	4	5	6	7	8	9	10	11	12
A	B	v	v	v	v	v	v	v	v	v	v	P
B	v	B	v	v	v	v	v	v	v	v	v	P
C	v	v	B	v	v	v	v	v	v	v	v	P
D	v	v	v	B	v	v	v	v	v	v	v	N
E	v	v	v	v	B	v	v	v	v	v	v	N
F	v	v	v	v	v	B	v	v	v	v	v	N
G	v	v	v	v	v	v	B	v	v	v	v	B
H	v	v	v	v	v	v	v	B	v	v	v	B

Figure 2.37 – Layout of master plate for saturation mutagenesis libraries. B= blank, N = negative control (cells containing empty plasmid), P = positive control (cells containing parental plasmid) and v = RgDAAO variant.

To check for consistent growth in the copy plates, the relative OD₆₀₀ values of the resulting cultures were compared. Figure 2.38 shows the data for a single plate from the RgDAAO F58 library which indicates less growth in the wells to the top left of the plate. The average OD₆₀₀ was 1.4 with a standard deviation across the plate of 0.1. Maximum observed OD₆₀₀ divided by minimum observed OD₆₀₀ gave a value of 1.8 which was considered acceptable.

	1	2	3	4	5	6	7	8	9	10	11	12
A	B											P
B		B										P
C			B									P
D				B								N
E					B							N
F						B						N
G							B					B
H								B				B

Key: < 0.1 0.1 - 0.5 0.5 - 1.0 1.0 - 1.5

Figure 2.38 - Saturation mutagenesis plate layout for growth and expression. P = positive control (RgDAAO/pPOT3), N = negative control (pPOT3), B = blank. Colours relate to final OD₆₀₀ values.

2.4.5 Process for screening of RgDAAO saturation mutagenesis variants

The assay plates were direct transfers from the copy plate but additionally, cells expressing parental RgDAAO from wells 12A and 12B were added to wells 12G and 12H which had been blank in the copy plate. Two sets of assay mix were prepared, both containing HRP, 4-AAP and TBHBA. The substrate to be assayed (test substrate) was added to one of these and control substrate ((*R*)-serine unless otherwise mentioned) was added to the other. Assay mix containing test substrate was added to all wells in columns 1-11 and to wells 12G-H. The control substrate assay mix was added to wells 12A-F. The final concentration of substrate in each well was 10 mM single enantiomer or 20 mM racemate. Figure 2.39 shows the layout of the assay plates. The positive controls (parental RgDAAO assayed against (*R*)-serine) are boxed in red, the negative controls (empty vector assayed against (*R*)-serine) are boxed in blue and the parental comparison wells (parental RgDAAO assayed against test substrate) are boxed in green.

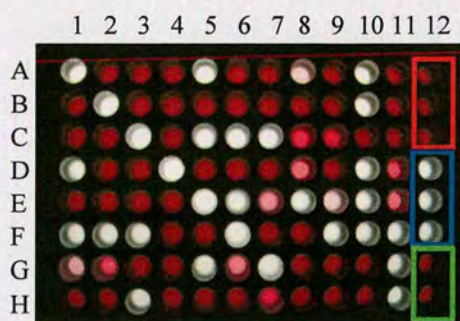


Figure 2.39 – Example of an F58 library plate assayed against (*R*)-alanine. The positive controls (parental RgDAAO assayed against (*R*)-serine) are boxed in red, the negative controls (empty vector cells assayed against (*R*)-serine) are boxed in blue and wells containing parental RgDAAO assayed against the test substrate are boxed in green. The blank wells 1A to 7G are clearly visible (8H was inoculated with a variant in this example). The remaining blank wells are the result of inactive variants.

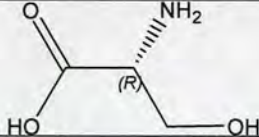
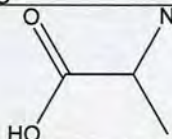
Following addition of assay mix and substrate, the plate was immediately transferred to a plate reader and the absorbance at 510 nm was recorded. The timescales over which further measurements were taken are discussed below. This process was repeated for each substrate.

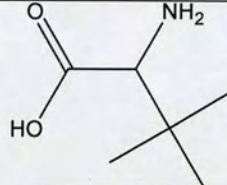
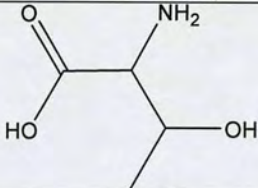
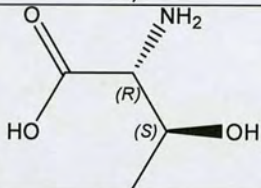
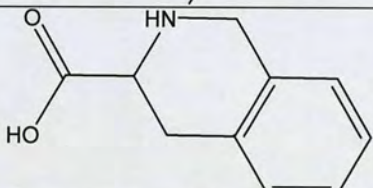
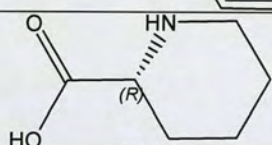
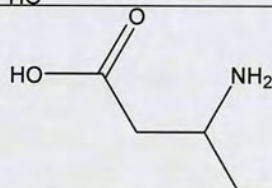
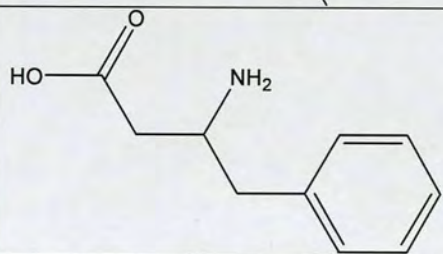
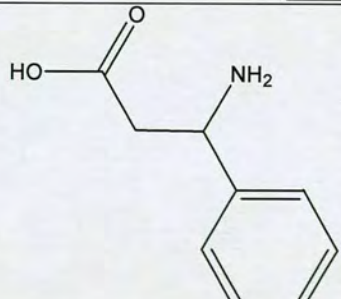
Substrate selection for screening of the RgDAAO F58 saturation mutagenesis library

Substrates were chosen for screening of the saturation mutagenesis libraries with the aim of detecting improved or novel oxidase activity but also with the purpose of revealing the beneficial and deleterious effects of substitutions at the selected residues. In order to develop a parental profile, substrates towards which RgDAAO showed a range of activities, from good to poor, were required. The substrate panel therefore included known α -amino acid substrates, non-proteinogenic α -amino acids and β -amino acids. The six RgDAAO F58 saturation library plates were screened against the 10 substrates shown in Table 2.17. (*R*)-serine was used as positive control because RgDAAO activity towards this substrate provides detectable colour development within 3 min which increases linearly over a period of approximately 2 h. (*R*)-serine is therefore a suitable positive control to use alongside test substrates towards which the parental enzyme shows a range of activities. Parental RgDAAO activity towards each test substrate is shown relative to activity towards (*R*)-serine.

Certain aliphatic α -amino acids are good substrates for RgDAAO (Section 2.2.3) and (*R*)-alanine with 246 % relative activity was selected as a probe for deleterious exchanges. Although the parent enzyme is highly (*R*)-selective in the case of larger amino acids, low activity has been demonstrated towards (*S*)-alanine which was added to the substrate panel to highlight any changes in enantioselectivity generated by saturation mutagenesis. RgDAAO shows no activity towards (*rac*)-*tert*-leucine and this substrate was chosen as a non-proteinogenic aliphatic α -amino acid towards which activity might be developed. The parent RgDAAO has a relative activity of 54 % towards (*R*)-*allo*-threonine which was included in the substrate panel to determine whether saturation mutagenesis at F58 would yield improvements towards a substrate with medium activity. RgDAAO shows good activity towards the cyclic amino acid (*R*)-proline but much lower activity towards the cyclic non-proteinogenic amino acids (*rac*)-tetrahydroisoquinoline-3-carboxylic acid (40 %) and (*R*)-pipecolinic acid (3 %). It was assumed that favourable exchanges might improve RgDAAO activity towards these two substrates. No RgDAAO activity has been detected towards β -amino acids. As the relative activity of **4** (246 % for (*R*)-alanine) is very high, the β -homo-analogue (*rac*)-3-aminobutyric acid (or β -homoalanine) was included in the substrate panel. In addition, the β -homo-analogue ((*rac*)- β -homophenylalanine) and β -isomer ((*rac*)- β -phenylalanine) of (*rac*)-phenylalanine for which RgDAAO has a relative activity of 130 % were added to the screen with the aim of detecting variant RgDAAO activity towards β -amino acids.

Table 2.17 – Substrates used for screening RgDAAO F58 saturation library

Structure	Name	Parental activity (relative to (<i>R</i>)-serine) (%)
	(<i>R</i>)-serine	100
	(<i>R</i>)-alanine	246
	(<i>S</i>)-alanine	6

Structure	Name	Parental activity (relative to (<i>R</i>)-serine) (%)
	(<i>rac</i>)- <i>tert</i> -leucine	0
	(<i>rac</i>)- <i>allo</i> -threonine (2 <i>R</i> ,3 <i>R</i> and 2 <i>S</i> ,3 <i>S</i>)	54
	(<i>R</i>)-threonine (2 <i>R</i> ,3 <i>S</i>)	6
	(<i>rac</i>)-tetrahydroisoquinoline-3- carboxylic acid	40
	(<i>R</i>)-pipecolic acid	3
	(<i>rac</i>)-3-aminobutyric acid	0
	(<i>rac</i>)- β -homophenylalanine	0
	(<i>rac</i>)- β -phenylalanine	0

Description of screening method using RgDAAO F58 library master plate 6

The libraries were prepared and screened using the above substrates. In addition, one plate, RgDAAO F58 library plate-6, was screened in triplicate to assess the screening method and data analysis. The averaged data from this plate will be used to describe the methods applied.

Three copies of the plate 6 variants were grown and pelleted according to step (iii) in Figure 2.36. These copy plates are referred to as F58 plate-6.2, -6.3 and -6.4 and each was assayed against the substrates in Table 2.17. The data collected from these plates were used to assess the assay method and data handling.

i) Assay duration

The activity range of RgDAAO variants towards the test substrates varied significantly and the timescale over which to measure colour formation therefore had to be appropriately chosen. Figure 2.40 shows the average rate of colour formation for a selection of F58 RgDAAO master plate 6 variants towards (*R*)-alanine, a good substrate for the parental enzyme. Rates determined for wells G1 to G12 from plates-6.2, -6.3 and -6.4 were averaged for comparison. Well G7 was a blank control containing no cells and well G12 contained parental RgDAAO. The remaining wells contained RgDAAO F58 variants which displayed different activities towards (*R*)-alanine.

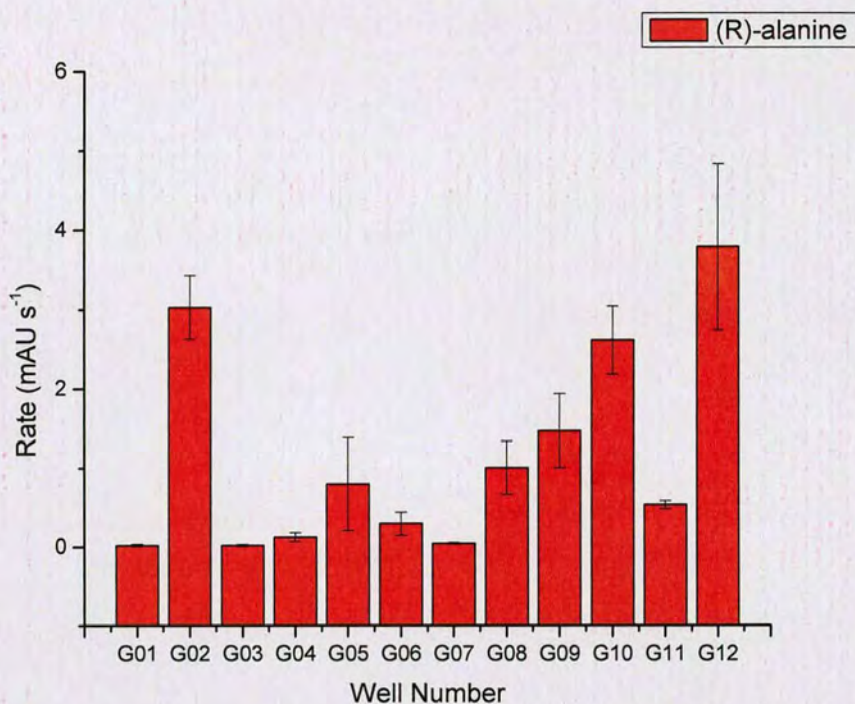


Figure 2.40 – Rate of colour formation per hour for wells G1 to G12 (RgDAAO F58 plates 6.2, 6.3 and 6.4) towards the substrate (*R*)-alanine. The average rate of colour formation for each well is shown and the error is given as \pm one standard deviation.

The rates observed with these variants towards (*R*)-alanine demonstrate that measurements at several timepoints must be taken in order to capture meaningful rate data. A balance is required between measuring the rate of very active variants, detecting the rate of poorly active variants and minimising plate time in the spectrophotometer in order to maximise the number of plates measured. In the case of very active enzymes, for example, the parent G12 and variant G2, the maximum absorbance reading measurable by the spectrophotometer detector (4.5 AU) is reached within approximately 20 min. The collection of rate data for these enzymes must therefore be complete within this period. However, the less active variant G4 required an incubation period of approximately 3 h before colour formation due to enzyme activity could be separated from the background colour formation observed in well G7. The incubation time required for clear separation of activity from background was greater still for substrates such as (*R*)-pipecolic acid towards which the RgDAAO F58 variants were less active. The absorbance on each plate was

therefore monitored over a 3 to 10 minute period at the start of the assay followed by two measurements taken after incubation periods of approximately 3 and 20 h.

ii) Rate calculations

The maximum slope for each curve over a selected number of data points was determined using Microsoft Excel. Figure 2.41 (A) shows the average rates obtained towards (*R*)-alanine for plates-6.2, -6.3 and 6.4 for selected wells where the rate calculation was made over 3, 5, 7 and 9 data points and plot (B) shows the average rate obtained towards (*R*)-pipercolinic acid for each of the wells with calculations made over 3, 5 and 7 data points (measurements were not taken over 9 data points for this substrate). The parental enzyme is very active towards (*R*)-alanine and poorly active towards (*R*)-pipercolinic acid. The wells shown all contained substrate and assay mix and included two different negative controls, well G7 which contained no cells and well F12 which contained empty vector cells. Well G12 contained parental enzyme and wells G4 and G9 contained variants displaying poor and medium activity towards (*R*)-alanine respectively.

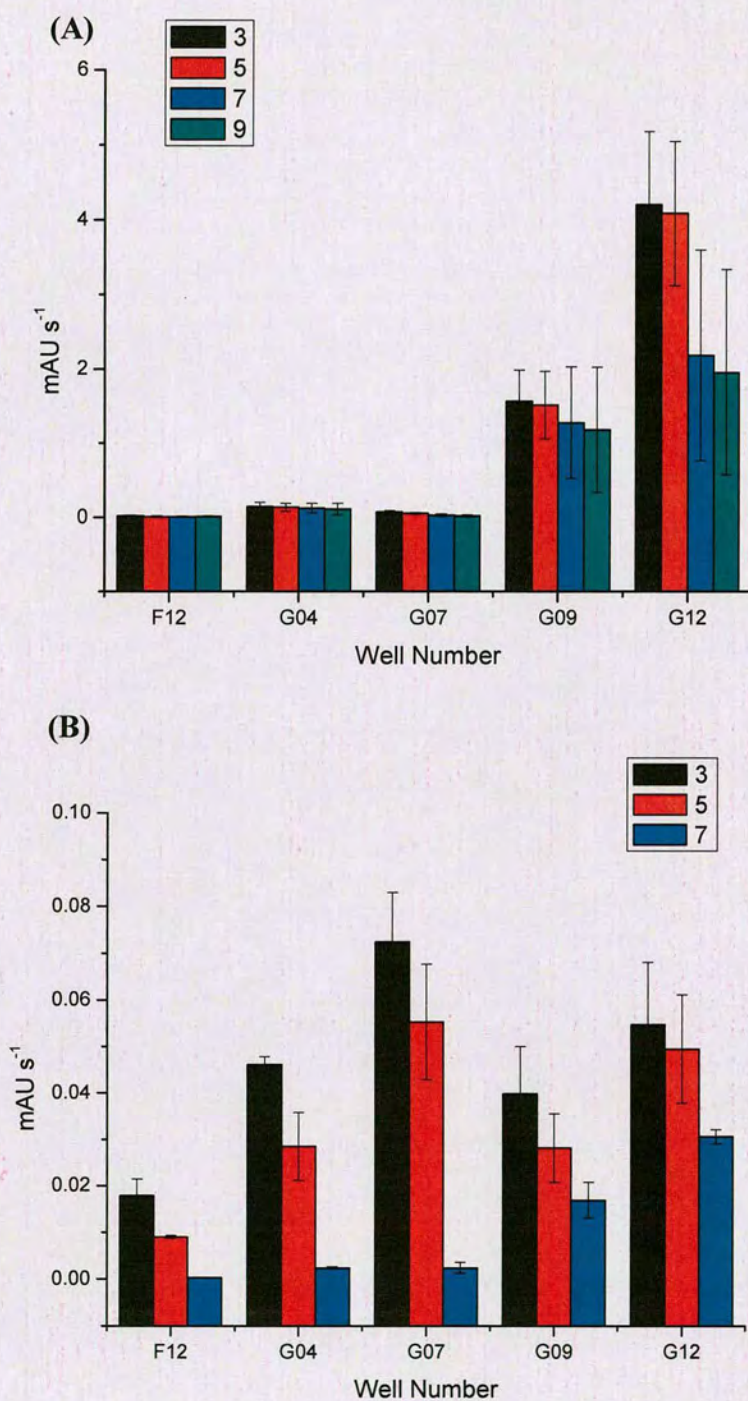


Figure 2.41 – Difference in maximum rate obtained by calculation over 3, 5, 7 and 9 data points for the substrate (*R*)-alanine (A) and over 3, 5 and 7 data points for the substrate (*R*)-pipercolinic acid (B). The rates obtained for wells G4 (variant RgDAAO), G7 (blank well containing no cells) and G12 (parental RgDAAO) (averaged data from plates 6.2, 6.3 and 6.4) are shown for comparison along with the associated error of \pm one standard deviation.

Plot (A) shows the rates obtained in response to (*R*)-alanine. The active enzymes in wells G9 and G12 show that the highest rates with smallest error are obtained when the calculation is taken over 3 to 5 data points. Lower rates with increased error over a larger number of data points are due to the detection maximum for the spectrophotometer having been reached within this number of data points. This is reflected by a reduction in the R^2 value calculated for each gradient. Table 2.18 compares the R^2 values of the slopes obtained for parental enzyme against (*R*)-alanine and against (*R*)-pipecolinic acid, calculated over a range of data points. The 'poorer' substrate (*R*)-pipecolinic acid stays within the linear range over the maximum number of data points, whereas the assay against (*R*)-alanine reaches the detector maximum and linearity decreases when the slope is calculated over the maximum number of data points.

Table 2.18 – R^2 values calculated from the gradients obtained for parental enzyme (well G12) assayed against both (*R*)-alanine and (*R*)-pipecolinic acid. n.m. = not measured. 3, 5, 7, and 9 represent the number of data points over which the slope calculation was made.

	3	5	7	9
(<i>R</i>)-pipecolinic acid	1.0	1.0	1.0	n.m.
(<i>R</i>)-alanine	1.0	1.0	0.9	0.8

Plot (B) in Figure 2.41 shows the rates calculated for the response of each selected well to (*R*)-pipecolinic acid. It should be noted that the y-axis scale in this plot is much lower than in plot (A). This plot demonstrates that it is not until the slope calculation is taken over 7 data points that the rates obtained for the active enzymes G9 and G12 reach higher values than for the negative control G7. The negative controls show an increase in absorbance due to mixing during the first 5 to 10 min of the assay but this increase is not continued throughout the remaining incubation time. In every case the mixing effect is more pronounced in wells containing no cells than in negative control wells containing empty vector cells. Although the effect is negligible when compared with active enzymes towards substrates for which they show reasonable activity, it becomes dominant in the case of less active variants towards poor substrates. The raw data for each of these wells (plate 6.3 only) is shown in Figure 2.42. When compared to the rate calculations shown in Figure 2.41 (B) it can be seen that the most accurate representation of relative colour formation

in the wells is given when the rates are calculated over the maximum number of data points.

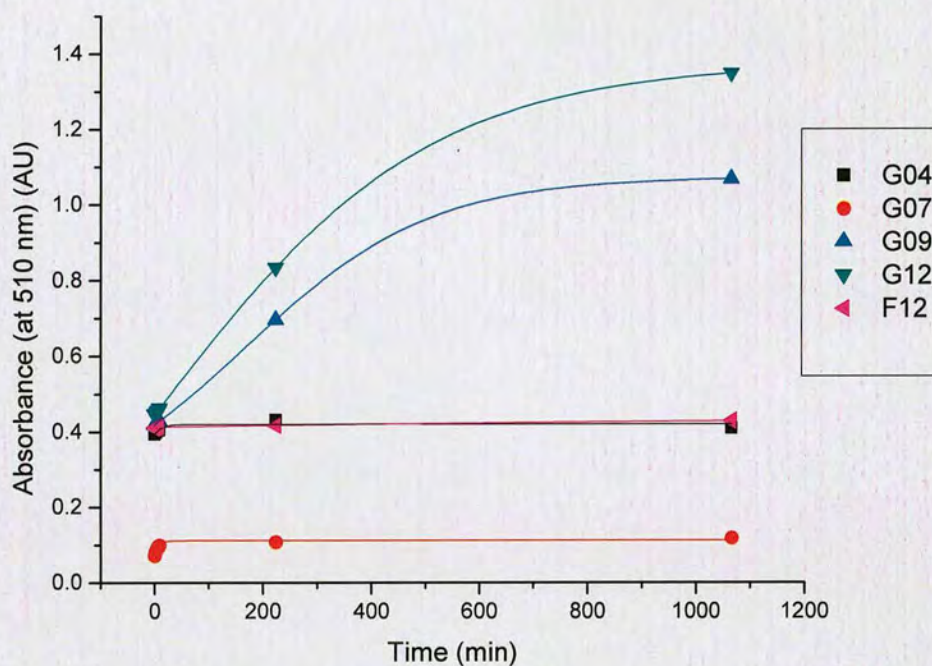


Figure 2.42 - Raw data for plate 6.3 wells G4 (variant RgDAAO), G7 (blank well containing no cells) and G12 (parental RgDAAO) assayed against (*R*)-pipecolinic acid and well F12 (empty vector cells) assayed against the control substrate (*R*)-serine.

It was decided that the most appropriate method of calculating meaningful rate data for each plate was to incorporate the maximum number of data points possible prior to any of the wells reaching the detector maximum of 4.5 AU. Where the positive controls resulted in significantly higher rates than the test substrate, that is for the substrates towards which the parental enzyme showed no activity, the data for the positive control wells were considered separately (the slope was calculated using only the data until the absorption maximum had been reached).

A small but continuous decrease in absorbance was observed over time for the substrates (*rac*)- β -phenylalanine, (*rac*)-3-aminobutyric acid, (*rac*)- β -homophenylalanine and (*rac*)-*tert*-leucine when in the presence of cells. The average

values are shown in Table 2.19. Given that the background initial absorbance readings of wells containing cells, assay mix and substrate is approximately 0.4 to 0.5 AU and the background initial reading for wells containing assay mix and substrate only is approximately 0.1 AU, the observed decrease in absorbance may be due to partial cell lysis caused by the presence of toxic substrates. In order to observe improvements in activity towards these substrates, the rate of increase in absorbance due to production of hydrogen peroxide will need to be greater than the rate of decrease in absorbance due to eventual cell lysis.

Table 2.19 – Average rates of decrease in absorbance observed in wells containing cells and non-active substrates. The measurements were made in triplicate and the error shown is \pm one standard deviation.

Substrate	$\mu\text{AU s}^{-1}$
<i>(rac)</i> - <i>tert</i> -leucine	-1.2 ± 0.2
<i>(rac)</i> - β -phenylalanine	-0.6 ± 0.2
<i>(rac)</i> - β -homophenylalanine	-0.4 ± 0.4
<i>(rac)</i> -3-aminobutyric acid	-0.8 ± 0.04

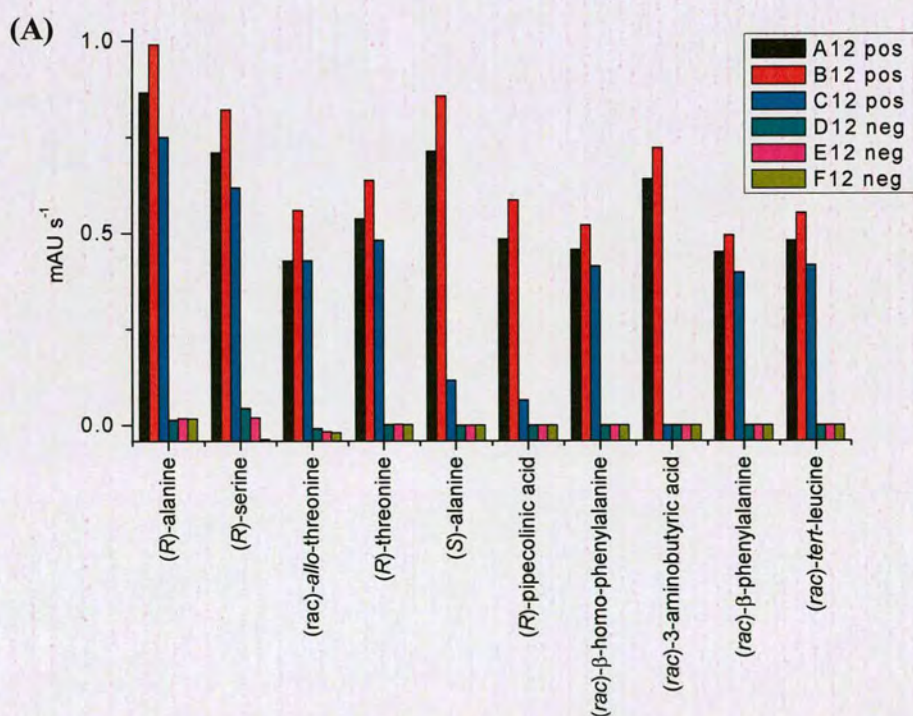
iii) Normalisation of data

Z' values were calculated for each assay plate with the purpose of providing an insight into differences in performance originating from growth in copy plates-6.2, -6.3 or -6.4 and into the performance of each individual assay plate. These values were calculated using the triplicate of positive and negative controls on each assay plate and are shown in Table 2.20.

Table 2.20 – Z' factor values calculated for each assay of plate-6.2, -6.3 or -6.4. n.m. = not measured.

Substrate	6.2	6.3	6.4
(<i>R</i>)-alanine	0.6	0.4	0.0
(<i>R</i>)-serine	0.5	0.3	n.m.
(<i>rac</i>)- <i>allo</i> -threonine	0.6	0.4	0.0
(<i>R</i>)-threonine	0.3	0.3	0.1
(<i>S</i>)-alanine	-0.7	0.3	0.2
(<i>R</i>)-pipecolic acid	-0.8	0.3	0.1
(<i>rac</i>)- β -homophenylalanine	0.7	0.3	0.1
(<i>rac</i>)-3-aminobutyric acid	-1.1	0.3	0.0
(<i>rac</i>)- β -phenylalanine	0.7	0.4	0.1
(<i>rac</i>)- <i>tert</i> -leucine	0.7	0.3	0.0
average	0.3	0.3	0.1

As discussed in Section 1.3.3, Z' values of greater than 0.5 indicate a good assay and although it was demonstrated in Section 2.3.3 that this assay can provide very good Z' values, overall these data are poor. It was decided to investigate this further by analysing the positive and negative control data generated for each source. These are shown in the plots in Figure 2.43 (A), (B) and (C).

**Figure 2.43 (A)**

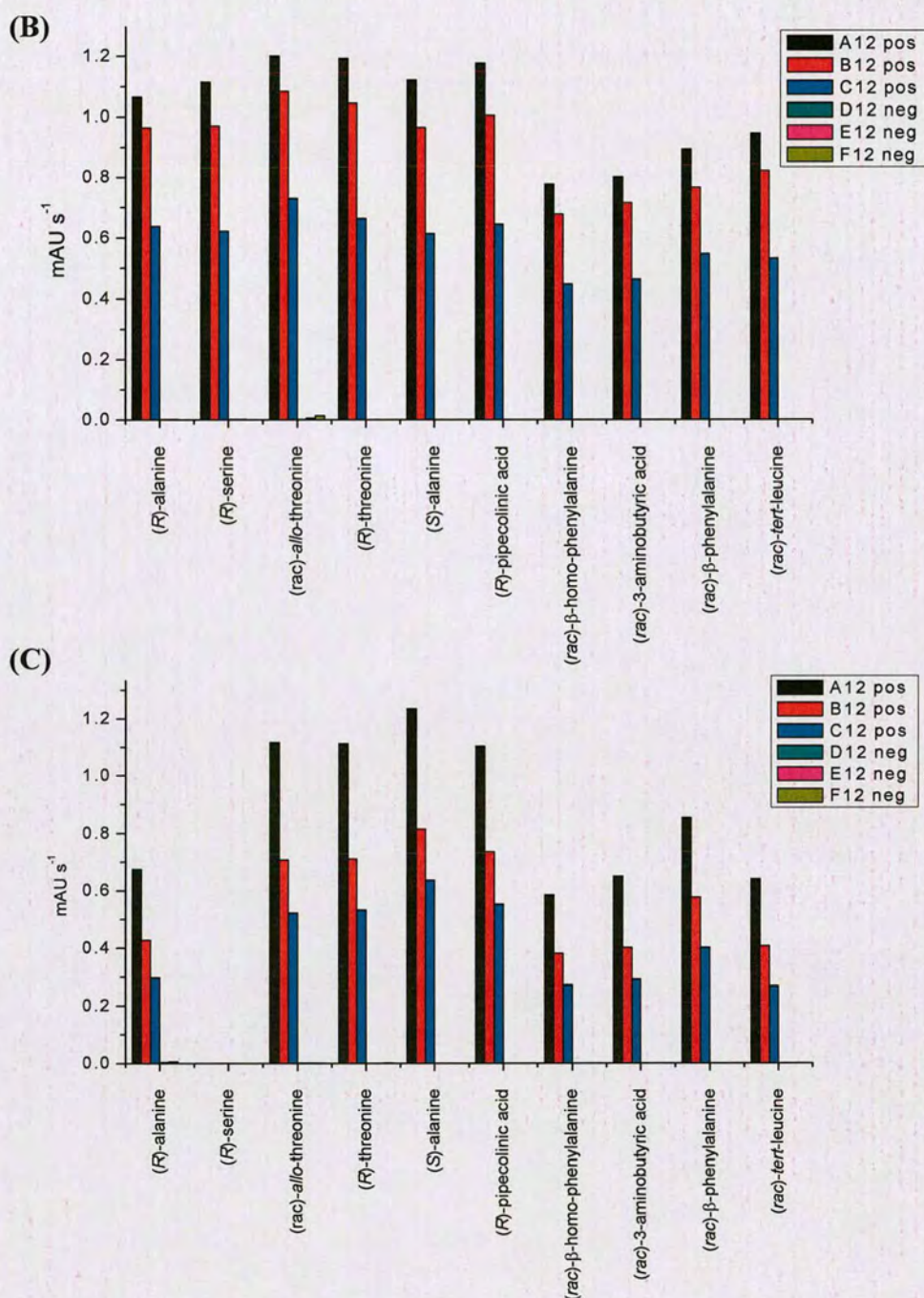


Figure 2.43 – Positive and negative control data collected for copy plates-6.2 (A), -6.3 (B) and -6.4 (C). Positive controls are parental RgDAAO and negative controls are empty vector cells. Both were assayed against (*R*)-serine. (The negative controls do not show in most of the plots.)

Compilation of the control data provides a significant amount of information. In most cases the performance order of the three positive controls on each plate is A12 and B12 > C12. In particular, the control well C12 performed very poorly on 3 of the

assay plates produced from copy plate-6.2 (see (*S*)-alanine, (*R*)-pipecolinic acid and (*rac*)-3-aminobutyric acid.). The poor performance of well C12, is seen in all three regrowth plates and may be due to a contamination carried forward from the master plate well. The literature K_m for the parental enzyme towards (*R*)-serine is 13.7 mM.⁽⁵⁷⁾ This means that, at the working concentration of 10 mM, the observed rate will be sensitive to any changes in substrate concentration. A systematic pipetting error was considered but a liquid handler was used to prepare the assay plates and no significant error was observed on checking the method. It was decided to omit data from control well C12 in all further calculations. The revised Z' values are shown in Table 2.21.

Table 2.21 – Revised Z' values (following removal of C12 data). n.m. = not measured.

Substrate	6.2	6.3	6.4
(<i>R</i>)-alanine	0.8	0.8	0.3
(<i>R</i>)-serine	0.6	0.8	n.m.
(<i>rac</i>)- <i>allo</i> -threonine	0.6	0.8	0.3
(<i>R</i>)-threonine	0.8	0.8	0.3
(<i>S</i>)-alanine	0.7	0.8	0.4
(<i>R</i>)-pipecolinic acid	0.7	0.8	0.4
(<i>rac</i>)- β -homophenylalanine	0.8	0.8	0.4
(<i>rac</i>)-3-aminobutyric acid	0.8	0.8	0.3
(<i>rac</i>)- β -phenylalanine	0.9	0.8	0.4
(<i>rac</i>)- <i>tert</i> -leucine	0.8	0.8	0.3
Average	0.8	0.8	0.4

The removal of control C12 data improves the Z' values significantly, although the values originating from copy plate-6.4 are still low. The information provided by the control data in Figure 2.43 shows that this is because the B12 wells also performed poorly on these plates. Despite this, B12 positive control wells were retained for data normalisation in order that manipulations for all plates were consistent.

To make the data between plates comparable, the data were normalised with the response of the control wells for each individual plate using the normalisation calculation shown in Equation 4. The variation observed in rates calculated for different assay plates which originated from the same copy plate (6.2, 6.3 or 6.4) is

partly due to the duration of initial absorbance measurements taken which is identical for all the wells on a particular plate. N is the average rate calculated for the triplicate of negative controls on the assay plate and P is the average rate calculated for the duplicate positive controls on the plate (well C12 not used).

$$\text{Normalised rate} = \frac{\text{rate} - N}{P - N}$$

Equation 4

A summary of the procedure used to assess the RgDAAO saturation mutagenesis libraries is shown below.

Table 2.22 – Data handling procedure used to assess the RgDAAO saturation mutagenesis libraries.

1	Assess linear region for the majority of the variants on the plate and calculate the maximum slope within this range. For substrates towards which the parental enzyme is inactive the positive controls on the plate must be considered separately.
2	Assess control data and Z' for each plate to provide an insight into the performance of the controls
3	Normalise the data using Equation 4.
4	Compare high results for each substrate of interest.

Substrate profiles

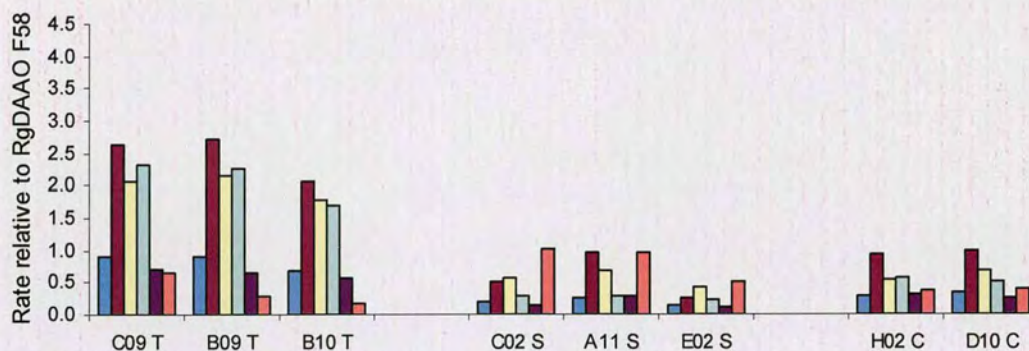
The data produced using the RgDAAO F58 copy plates-6.2, -6.3 and -6.4 were normalised as described and the results were averaged. In order to consider the data for all six active substrates on a single scale plot, the data were manipulated by dividing the normalised rates for a particular substrate by the average normalised rate obtained for the parental enzyme towards that substrate. The resulting data are therefore shown relative to the parental activity towards each substrate which is set equal to 1. Therefore any number greater than one implies improved activity over parental activity and any number smaller than one implies that the variant showed lower activity towards the test substrate than the parent. This manipulation could

only be performed for substrates towards which the parental enzyme showed reasonable activity. The parental RgDAAO activities obtained towards these substrates are shown relative to the rate obtained towards (*R*)-methionine in Table 2.23. For substrates towards which the parental enzyme showed only low activity the accuracy of the parental control data was not sufficient to provide meaningful relative rates. It was apparent from the data obtained for plate-6 that activity profiles for individual variants could be detected. The amino acid exchange at position 58 for selected variants was confirmed by gene-sequencing, and where more than one example of the same amino acid exchange was identified, the activity profiles were compared. Figure 2.44 shows the activity profiles of all the F58T, F58S, F58C, F58L and F58I variants sequenced from this plate. These profiles prove to be reproducible with the exception of well D01 which was shown by sequencing to be an RgDAAO F58L variant. In all three measurements of this well the variant performed poorly towards each substrate. The OD₆₀₀ values confirmed that the cells in this well had grown to a similar density as the rest of the wells in each of the growth plates and the poor response may have been due to a contamination carried to the copy wells from the master plate. The reproducibility is reduced in the case of less active variants such as F58S.

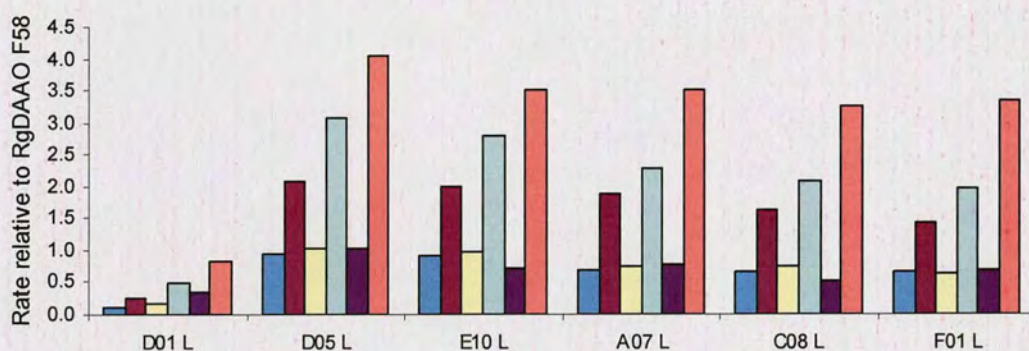
Table 2.23 – For reference: parental RgDAAO relative activities calculated for the profiling substrates. Shown relative to RgDAAO activity towards (*R*)-methionine (1.6 mAU s⁻¹).

Substrate	% Activity relative to (<i>R</i>)-methionine
(<i>R</i>)-alanine	105 %
(<i>S</i>)-alanine	64
(<i>rac</i>)- <i>allo</i> -threonine	64
(<i>R</i>)-threonine	8
(<i>R</i>)-serine	58
(<i>rac</i>)-pipecolinic acid	8

RgDAAO F58T, F58S and F58C



RgDAAO F58L



RgDAAO F58I

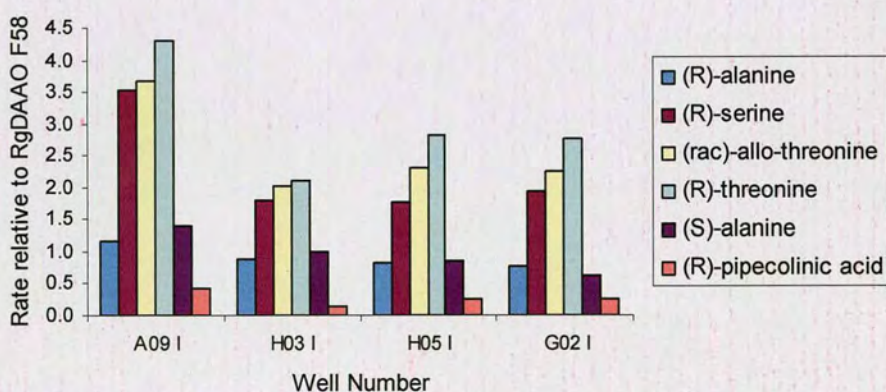


Figure 2.44 – Substrate profiles obtained for all F58T, F58S, F58C, F58L and F58I variants identified on plate-6 of the RgDAAO F58 saturation mutagenesis library. Parental RgDAAO activity is set as one. Any number greater than one implies improved activity over parental activity and any number smaller than one implies that the variant showed lower activity towards the test substrate than the parent.

The activity profiles obtained for each well on plate-6 (average of triplicate) were assessed and set into groups comprising identical or very similar profiles with the

aim of identifying the 20 possible activity profiles. These groupings produced the 23 activity profiles shown in Figure 2.45. The amino acid at position 58 is known for 14 of these profiles and variants with unknown amino acid exchanges are labelled U1 to U9. The reduced reproducibility observed in the activity profiles for less active variants means that these are more difficult to group and results in 23 observed profiles rather than the maximum of 20. This assumes that all possible amino acid exchanges were present on plate-6, which contained 88 variants.

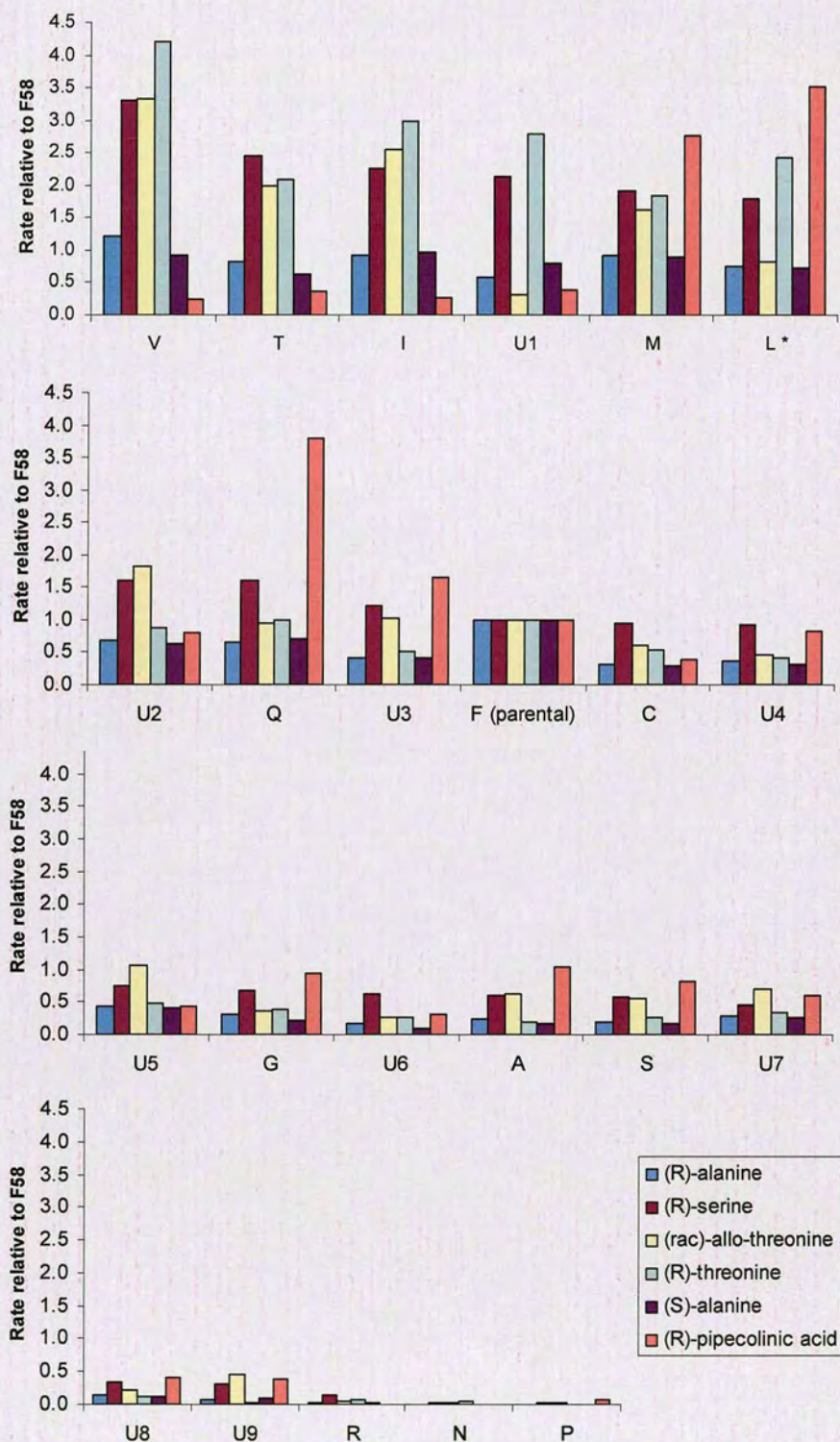


Figure 2.45 – 23 substrate profile patterns determined in F58 RgDAAO saturation mutagenesis library. * = well D01 not included in average. U1 to U9 = unknown amino acid exchanges. Parental RgDAAO activity is set as one. Any number greater than one implies improved activity over parental activity and any number smaller than one implies that the variant showed lower activity towards the test substrate than the parent.

In Figure 2.45, the activity profiles have been ordered in relation to their activity towards (*R*)-serine. No activity improvements were observed towards the substrates (*R*)- and (*S*)-alanine in this set of variants (plate 6, F58 RgDAAO).

It was observed in the variants identified by sequencing that exchanges from F58 to V, T, I, M, L and Q showed improved activity towards some of the substrates tested. However, exchanges to C, G and A led to variants with less activity than the parental enzyme towards most of the substrate set. Exchanges from F58 to R, N and P produced variants which were inactive towards all substrates tested.

Although the F58Q variant displays improved activity towards (*R*)-serine and (*R*)-pipecolinic acid and retains activity towards the remaining substrates, reduction of the residue length by one methylene group (change from glutamine to asparagine) in the F58N variant renders the enzyme inactive towards all the screened substrates. The impact of shortened residue length is also seen in the aliphatic group of residues. Both the F58G and F58A variants are less active than the parental enzyme towards the majority of substrates tested while the F58V, F58I, F58L and F58M variants all maintain or improve activity (with the exception that F58V and F58I show reduced activity towards (*R*)-pipecolinic acid).

The variants F58V and F58I have similar activity profiles, with 2- to 4-fold improved activity towards (*R*)-serine, (*rac*)-*allo*-threonine and (*R*)-threonine but reduced activity towards (*R*)-pipecolinic acid. In contrast, the F58L variant shows 2- to 4-fold improvements in activity towards (*R*)-serine, (*R*)-threonine and (*R*)-pipecolinic acid but no change in activity towards (*rac*)-*allo*-threonine. The responses of these three variants (F58V, F58I and F58L) towards the stereoisomers (*R*)-threonine and (*rac*)-*allo*-threonine were compared. Improved activity towards (*R*)-threonine over the parental response is observed for all three variants but only F58V and F58I show improved activity towards (*rac*)-*allo*-threonine. Both residues (valine and isoleucine) are branched at the β -carbon.

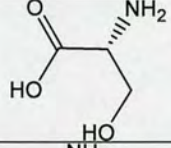
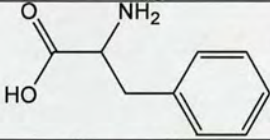
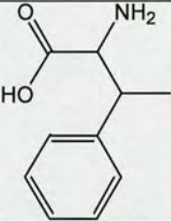
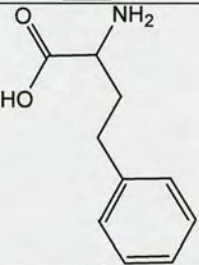
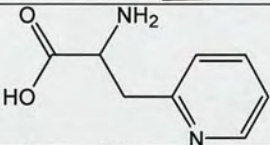
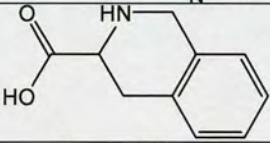
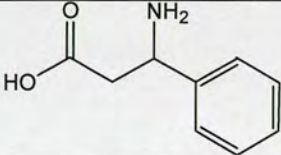
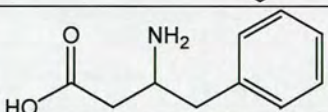
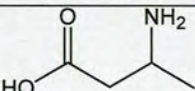
Additionally, variants with residues in position 58 that are branched at the β -carbon appear to be unfavourable for activity towards (*R*)-pipecolinic acid. Variants F58V, F58T and F58I all show reduced activity towards this substrate, whereas variants F58M, F58L and F58Q show improved activity (between 3- to 4-fold). The F58A, F58G and F58S variants approximately maintain the activity observed by the parental enzyme towards (*R*)-pipecolinic acid. In contrast to these results, variant F58C, which might be expected to behave similarly to the F58A or F58S variants, shows reduced activity.

Variant F58T has a fairly similar profile towards the substrates tested as that of the F58V variant and both exhibit improved activity towards the substrates (*R*)-serine, (*rac*)-*allo*-threonine and (*R*)-threonine. However, exchange of one methyl group in the residue F58V for a hydroxyl group in residue F58T somewhat reduces these improvements. In addition, comparing the F58T variant with F58S shows that the presence of the hydroxyl group alone, with no methyl group at the β -position of the residue, reduces the activity further. The F58S variant displays activity below that of the parental enzyme towards all of the substrates except (*R*)-pipecolinic acid, towards which the level of activity is maintained.

2.4.6 Screening of RgDAAO saturation mutagenesis libraries

The RgDAAO F58 saturation mutagenesis library was screened against the ten substrates described in Table 2.17. This set of substrates was also used for screening of the RgDAAO R285 library, with the exception of (*rac*)-*tert*-leucine. The Y238 library was screened against 4 substrates; (*R*)- and (*S*)-alanine, (*R*)-pipecolinic acid and (*rac*)-3-aminobutyric acid. However, the substrate set was altered to include more chromogenic compounds for screening of the M213 library. The purpose of this was to provide more straightforward HPLC analysis, should any of the variants be selected to perform biotransformation reactions on the compounds. The full set of substrates screened against RgDAAO M213 is shown in Table 2.24.

Table 2.24 - Substrates used for screening of RgDAAO M213 saturation mutagenesis library

Structure	Name	Activity (relative to (<i>R</i>)-serine, data extracted from controls used in screening assay) (%)
	(<i>R</i>)-serine	100
	(<i>rac</i>)-phenylalanine	593
	(<i>rac</i>)- β -methylphenylalanine	19
	(<i>rac</i>)-homophenylalanine	135
	(<i>rac</i>)- β -pyridylalanine	29
	(<i>rac</i>)-1,2,3,4-tetrahydroisoquinoline-3-carboxylic acid	6
	(<i>rac</i>)- β -phenylalanine	0
	(<i>rac</i>)- β -homophenylalanine	0
	(<i>rac</i>)-3-aminobutyric acid	0

The Z' values obtained for each plate assayed were calculated and are shown in Table 2.25. The growth in all the RgDAAO Y238 library plates was poor. This is reflected in the control data, and therefore in the values provided for Z' . The values calculated for plates F58-1.1, M213-4.1 and R285-4.1 were also poor but as these libraries were over-sampled and the remaining plates provided the statistical likelihood that every amino acid exchange would be covered, the data from these plates could be dismissed. The majority of the remaining Z' values are good, indicating that the assay has worked well on these plates.

Table 2.25 – Z' values obtained for each library plate. * = 1,2,3,4-tetrahydroisoquinoline-3-carboxylic acid. n.m. = not measured. **Well C12 positive control was removed from the Z' calculation for plate F58 3.1. Each library was prepared and stored on 5 or 6 microtitre plates. Copies of these master plates are referred to as copy plates 1.1 to 6.1.

F58 (positive control substrate = (R)-alanine)	1.1	2.1	3.1**	4.1	5.1	6.1
(R)-alanine	-0.1	1.0	0.9	0.8	0.6	1.0
(rac)-allo-threonine	0.0	0.9	0.8	0.9	0.7	0.9
(R)-threonine	-0.3	0.9	0.8	0.9	0.7	0.8
(S)-alanine	0.0	1.0	1.0	0.9	0.6	0.9
(R)-pipecolinic acid	-0.1	0.9	-0.1	0.8	0.7	0.8
(rac)-tiq*	-0.1	0.9	1.0	0.8	0.6	1.0
(rac)-3-aminobutyric acid	-0.1	0.8	0.8	0.8	0.8	0.9
(rac)- β -homophenylalanine	0.0	1.0	0.8	1.0	0.6	1.0
(rac)- β -phenylalanine	0.0	n.m.	0.6	0.7	0.7	0.9
(R)-tert-leucine	-0.3	0.9	0.9	0.7	0.6	0.9
R285 (positive control substrate = (R)-serine)	1.1	2.1	3.1	4.1	5.1	6.1
(R)-alanine	0.7	0.8	0.9	0.8	0.4	0.9
(rac)-allo-threonine	1.0	0.3	0.8	-0.3	0.6	0.6
(R)-threonine	0.4	n.m.	0.3	-2.1	0.4	0.2
(S)-alanine	0.8	0.7	0.9	0.9	0.7	0.5
(R)-pipecolinic acid	0.6	0.4	0.9	0.0	0.7	0.6
(rac)-tiq*	0.3	0.5	0.8	-0.1	0.5	0.6
(rac)-3-aminobutyric acid	0.5	0.9	0.0	0.2	0.4	0.4
(rac)- β -homophenylalanine	0.5	0.7	0.6	-0.6	1.0	0.6
(rac)- β -phenylalanine	0.7	0.8	0.7	-1.6	0.6	-0.3
M213 (positive control substrate = (R)-serine)	1.1	2.1	3.1	4.1	5.1	
(rac)-tiq*	0.8	0.5	0.6	-1.0	0.8	
(rac)- β -methylphenylalanine	0.7	0.8	0.3	-1.0	0.6	
(rac)-phenylalanine	0.8	0.4	0.3	-0.9	0.7	
(rac)- β -pyridylalanine	0.9	0.5	0.4	-2.2	0.8	
(R)-serine	0.6	0.2	0.9	-0.8	1.0	
(rac)-homophenylalanine	0.4	0.1	0.7	-1.4	0.6	
(rac)-3-aminobutyric acid	0.7	0.6	0.9	-1.5	0.7	
(rac)- β -homophenylalanine	0.6	0.4	0.0	-2.4	0.8	
(rac)- β -phenylalanine	0.8	0.8	0.7	-0.2	0.8	
Y238 (positive control substrate = (R)-serine)	1.1	2.1	3.1	4.1	5.1	
(R)-alanine	0.6	-0.1	-0.6	0.5	0.4	
(S)-alanine	0.0	-0.4	-0.8	-2.6	-0.1	
(R)-pipecolinic acid	0.8	0.5	-0.9	-0.6	0.4	
(rac)-3-aminobutyric acid	0.7	0.6	-0.6	-0.5	0.3	

The analysis procedure described in Table 2.22 was used to assess the RgDAAO F58, M213, Y238 and R285 libraries. In the case of these single measurements the profiles were not reproducible between plates from the same library, although similar profiles could be identified within the same plate. The profiles were calculated for the 10 highest normalised rates on each library plate towards each substrate and these are recorded in the Appendix (Section 5.9).

In several cases the profiles display very high rates for a particular substrate or substrates. An example of this is shown by comparing the profiles produced from library plates 2.1 and 3.1 from the RgDAAO F58 library. These are shown in Figure 2.46 where activity profiles for variants with the highest normalised rates towards (*rac*)-*allo*-threonine are displayed.

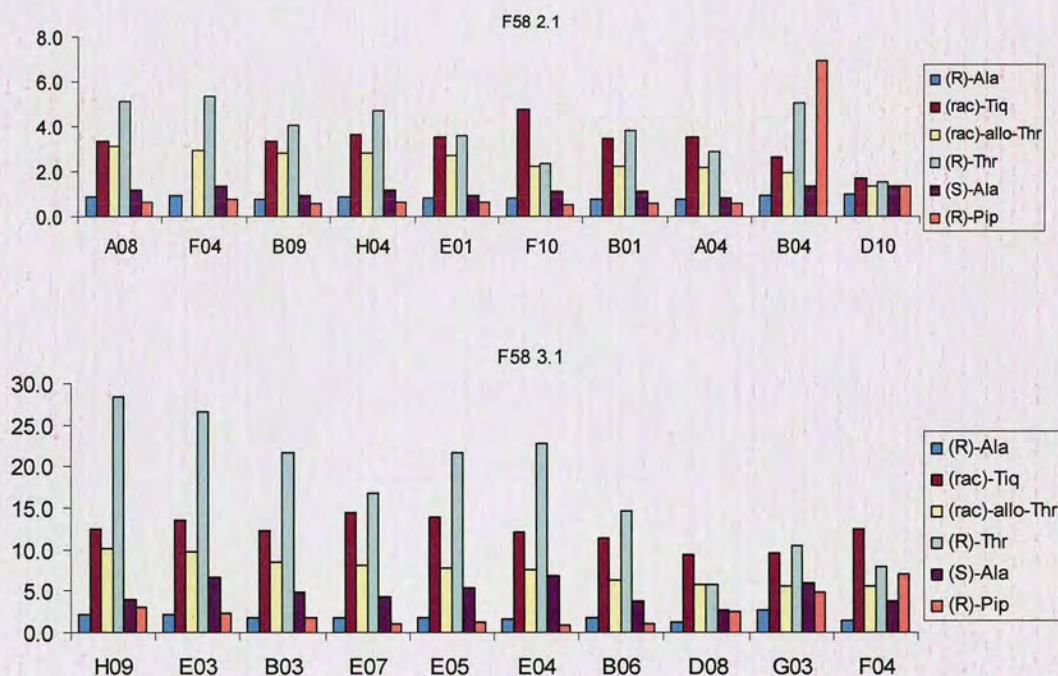


Figure 2.46 – Activity profiles for variants producing the highest rates towards (*rac*)-*allo*-threonine from saturation mutagenesis library RgDAAO F58 identified on plates-2.1 and -3.1. Parental RgDAAO activity is set as one. Any number greater than one implies improved activity over parental activity and any number smaller than one implies that the variant showed lower activity towards the test substrate than the parent. Tiq = 1,2,3,4-tetrahydroisoquinoline-3-carboxylic acid, Pip = pipercolinic acid.

Plate F58 3.1 in Figure 2.46 shows that exceptionally high activity data were observed towards (*rac*)-*allo*-threonine in this case. These are in contrast to the rate improvements seen for the plate-2.1 variants which produce data approximately a factor of 3 lower than the variants on plate 3.1.

A reason for this can be seen in the normalised rates obtained for the parental controls (wells G12 and H12 on each plate which contained assay mix, test substrate and cells expressing parental RgDAAO). For example, Figure 2.46 shows high improvements of the plate-3.1 variants towards (*R*)-threonine. However, Figure 2.47 shows that low normalised rates were obtained for parental control wells G12 and H12 toward (*R*)-threonine on this plate compared to the same wells on plate-2.1. This results in much higher apparent rate enhancements towards (*R*)-threonine being displayed by all the active variants on plate-3.1 than observed for the variants on the other RgDAAO F58 library plates (although F58 plate 6.1 variants also display high results towards this substrate for the same reason).

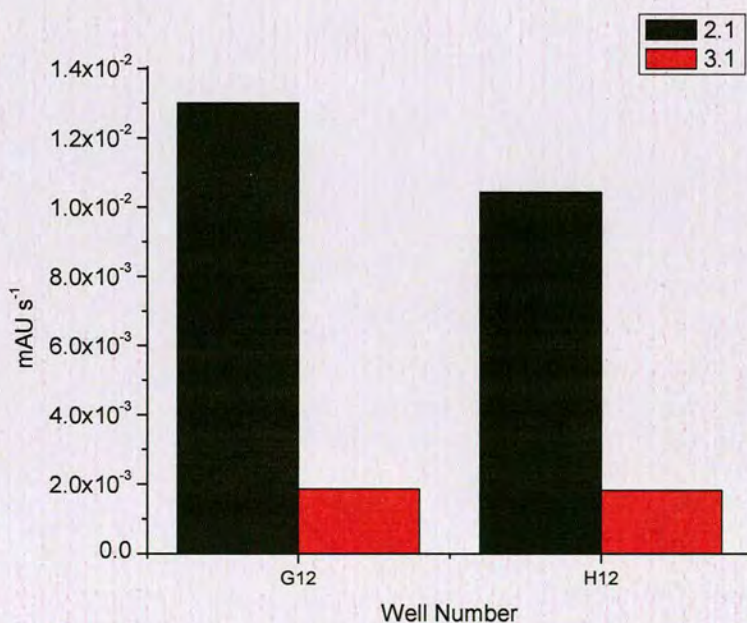


Figure 2.47 – Normalised rates for the parental control wells (assay mix, (*S*)-alanine and cells expressing parental RgDAAO) for plates 2.1 and 3.1 of the RgDAAO F58 saturation mutagenesis library.

Although these factors describe limitations of this liquid-phase assay method, the problems can easily be identified by assessing the data. This is a significant advantage over solid-phase screening which allows only a visual comparison of the responses of the positive and parental controls with those of the variants. In addition, although the limitations make it difficult to identify identical profiles on two different assay plates, similarities can be identified within the activity profiles on a single assay plate. Similar activity profiles can be identified on the plates shown in Figure 2.46, for example the profiles for variants in wells A08, B09 and H04 of plate-2.1. Figure 2.48 shows the profiles of the ten RgDAAO F58 variants displaying the highest activity towards (*rac*)-*allo*-threonine from plate 6.1. Gene-sequencing confirmed that the similar activity profiles identified for the variants in wells A09, H05 and G02 were all from RgDAAO F58I variants. (The high activity improvements shown by some variants towards (*R*)-threonine are exaggerated due to low results for control data on this assay plate.)

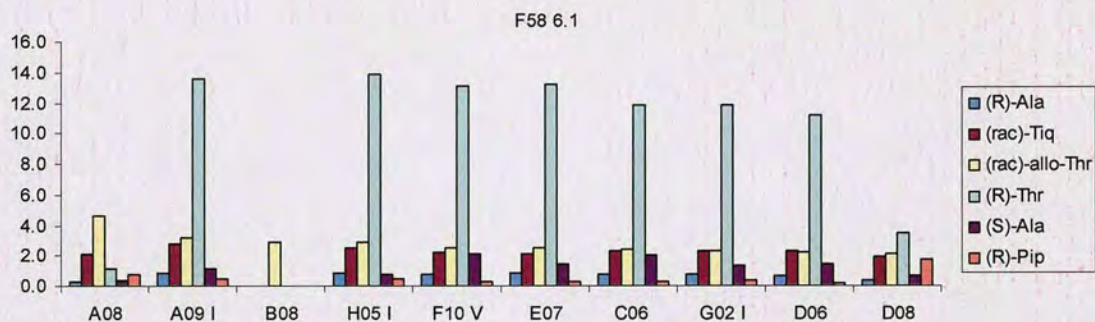


Figure 2.48 - Substrate profiles for variants producing highest rates towards (*rac*)-*allo*-threonine from saturation mutagenesis library RgDAAO F58 plate-6.1. Parental RgDAAO activity is set as one. Any number greater than one implies improved activity over parental activity and any number smaller than one implies that the variant showed lower activity towards the test substrate than the parent. Tiq = 1,2,3,4-tetrahydroisoquinoline-3-carboxylic acid, Pip = pipercolinic acid.

The activity profiles were also useful for assessing the substrates towards which parental RgDAAO showed no activity. The profiles for the 10 variants producing the highest normalised rates on each plate towards each of these substrates were assessed. Plates-2.1 and 3.1 from the RgDAAO F58 library are again used as an example in Figure 2.49, this time with the activity profiles of the variants displaying the highest activities towards (*rac*)- β -homophenylalanine. It can be seen that blank

wells (containing no cells and marked *) are listed within the top 10 results for both these plates. The top results for plate 3.1 also include parental RgDAAO (well H12). It was expected that by viewing the activity profiles of these highest results, similar profiles would be identified in cases where more than one example of the responsible variant was present on the plate, thus confirming the improved activity. On plate 2.1 the variants in wells B03 and E08 showed apparently similar profiles and on plate 3.1 the variants in wells B03 and E08 showed apparently similar profiles and on plate 3.1 the activity profiles produced by wells B10, D02 and A07 are also similar.

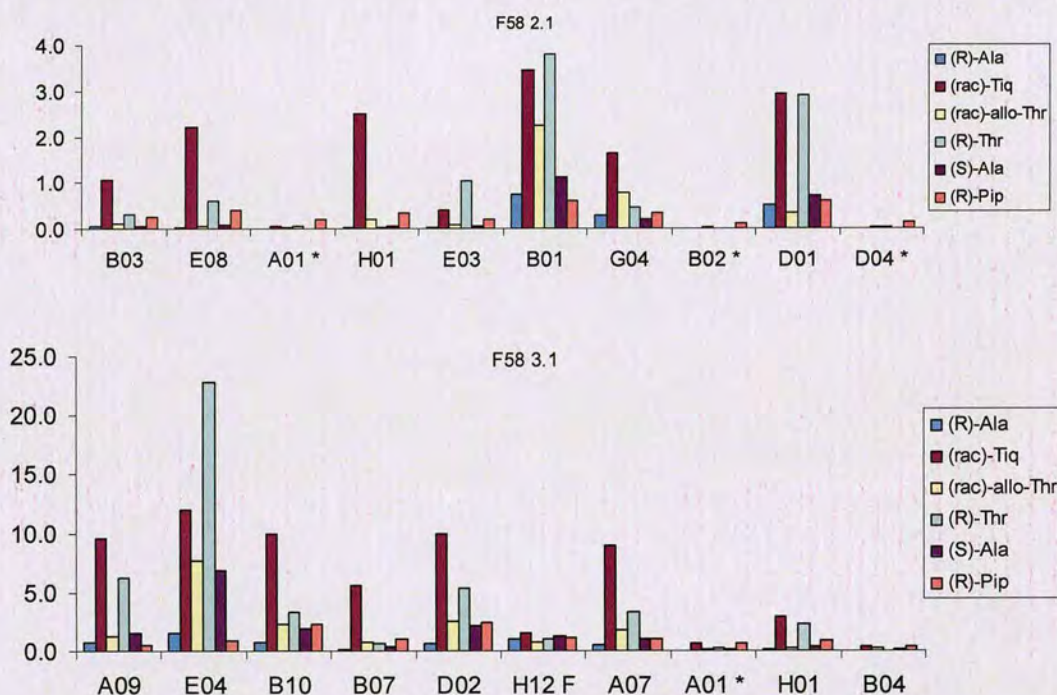


Figure 2.49 - Substrate profiles for variants producing highest rates towards (*rac*)- β -homophenylalanine from saturation mutagenesis library RgDAAO F58 plates-1.1 and -2.1. Parental RgDAAO activity is set as one. Any number greater than one implies improved activity over parental activity and any number smaller than one implies that the variant showed lower activity towards the test substrate than the parent. Tiq = 1,2,3,4-tetrahydroisoquinoline-3-carboxylic acid, Pip = pipercolinic acid, * = blank well.

The rates for these 5 variants range from 5.0×10^{-7} to 1.4×10^{-6} AU s⁻¹. According to Figure 2.22 this relates to conversion of between 0.5 and 1.4 μ M over 48 h. These conversion rates cannot be confirmed using HPLC as the error associated with the method to be used, where the oxidation is assumed to be entirely enantioselective and the unoxidised enantiomer is used as the internal standard, is around 5%. Therefore in order to confirm assay results by HPLC, a minimum conversion of

0.5 mM is required from a 20 mM racemic solution over 24 - 48 h. This relates to a change in absorbance of between 1.0×10^{-3} and $5.0 \times 10^{-4} \text{ s}^{-1}$. These changes in absorbance are visible by eye and no such change was observed for any of the variants when assayed against substrates for which the parental RgDAAO was inactive.

Summary of activity observed in the RgDAAO saturation mutagenesis libraries

As discussed, the ten highest normalised rates achieved towards each substrate for each library plate were compiled. The curves produced from the raw absorbance data against time and the influence of the positive controls (assay mix, control substrate, cells expressing parental RgDAAO) in the normalisation calculation were assessed for these variants to confirm any apparent improvements. The activity profiles were also compared to detect i) similarities in the most active variants and ii) errors caused by the influence of both positive and parental controls (assay mix, test substrate, cells expressing parental RgDAAO).

No new activity was observed in the libraries towards the β -amino acids (*rac*)- β -homophenylalanine and (*rac*)- β -phenylalanine both of which were used to screen the RgDAAO F58, M213 and R285 libraries. Neither was activity found towards (*rac*)-3-aminobutyric acid in any of the four libraries, nor towards (*rac*)-*tert*-leucine in the F58 library. No visible colour formation was observed on the assay plates for these substrates. The variants producing the highest normalised data were compiled and the activity profiles compared. In a few cases, similar activity profiles could be identified in the 10 highest results on each plate but in no case was the conversion rate sufficient for confirmation by HPLC. Tables comparing the 10 highest results from each plate with the average parental control from that plate are given in the Appendix (5.9). The compared activity profiles for a selection of these data are also shown below.

RgDAAO Y238

The RgDAAO Y238 library was difficult to analyse because of poor growth of the cells in the control wells on all of the plates, which distorted the normalised data. For this reason no conclusions can be drawn about the performance of this library. However, observations from screening of the library were; i) a range of activities was demonstrated towards the substrates (*R*)-alanine, (*S*)-alanine and (*R*)-pipecolinic acid, ii) the highest rates (prior to data normalisation) towards these substrates were comparable with those obtained for the same substrates against the RgDAAO F58 library and iii) an average of 23 % of the variants per plate were inactive towards (*R*)-alanine, compared to 7 % for the RgDAAO F58 library. The highest rates obtained for the variants on each plate towards each of the substrates are shown without normalisation in the Appendix (Section 5.9).

RgDAAO R285

This library contained an average of 53 % of variants inactive towards (*R*)-alanine per plate, suggesting that most amino acid exchanges at position R285 are deleterious. Figure 2.50 shows the activity profiles obtained for the ten variants showing the highest rates towards (*R*)-alanine on plate-5.1. Only 8 variants on this plate showed reasonable activity towards (*R*)-alanine, including the two parental controls (wells G12 and H12).

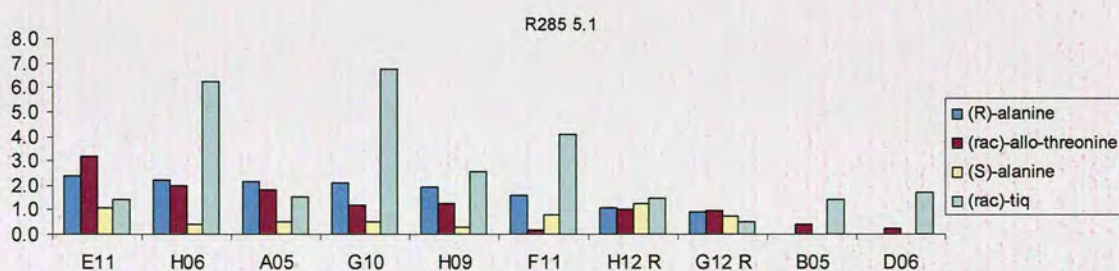


Figure 2.50 - Substrate profiles for variants producing the highest rates towards (*R*)-alanine from saturation mutagenesis library RgDAAO R285 plate-5.1. Parental RgDAAO activity is set as one. Any number greater than one implies improved activity over parental activity and any number smaller than one implies that the variant showed lower activity towards the test substrate than the parent. Tiq = 1,2,3,4-tetrahydroisoquinoline-3-carboxylic acid.

The cells in all of the assay plates for this library had overall reduced activity, including the control wells, making the data less reliable. However, comparison of the activity profiles obtained on each plate suggests that a few amino acid exchanges either maintain or improve activity towards some of the substrates screened. For example, the variants in wells H06 and G10 in Figure 2.50 have similar activity profiles and indicate an approximately 6-fold improvement towards (*rac*)-1,2,3,4-tetrahydroisoquinoline-3-carboxylic acid. The data collected on the RgDAAO R285 saturation mutagenesis library are recorded in the Appendix (Section 5.9). Due to the poor overall activity and therefore reduced accuracy observed for these assay plates, the data must be considered in conjunction with the control data and Z' values. These indicate that no improvements can be detected towards (*R*)- and (*S*)-alanine. The reduced activity in these assay plates brought detection of activity towards (*rac*)-pipercolinic acid to the limits and it was not possible to approximate any improvements towards this substrate. Moderate improvements of approximately 2-fold were detected towards (*rac*)-*allo*-threonine and rate enhancements of up to 6-fold were recorded for (*rac*)-1,2,3,4-tetrahydroisoquinoline-3-carboxylic acid.

RgDAAO M213

No rate improvements were seen towards (*rac*)-phenylalanine and only small enhancements were identified towards (*R*)-serine. Up to 3-fold improvements were observed towards (*rac*)-homophenylalanine. Some variants displayed 8-fold rate enhancements towards (*rac*)-pyridylalanine and up to 5-fold rate increases were recorded towards (*rac*)- β -methylphenylalanine. A few variants indicated exceptionally high enhancements but the curves produced by the raw data showed these to be false positives. This is also the case for several of the variants which produced high activities towards (*rac*)-1,2,3,4-tetrahydroisoquinoline-3-carboxylic acid. The more consistent rates achieved towards this substrate suggest that improvements of up to 10-fold can be achieved.

RgDAAO F58

One set of variants (plate 6) from the library produced by saturation mutagenesis at RgDAAO F58 were investigated in triplicate to assess the screening method and a description of these variants has been given above (see page 114). Additional information gained from screening the remainder of the library is discussed here. No improvements were observed towards (*R*)-alanine but one variant (well E09 on plate-5.1, see Appendix Section 5.9) indicated a 2.5-fold improvement towards (*S*)-alanine. Although the activity profiles produced for two of the library plates show very high improvements towards (*R*)-threonine, these results can be related to either poor performance of the positive control wells or of the parental control wells. The remaining data suggest rate enhancements of up to 5-fold for this substrate. Many, but not all, of the variants which demonstrated activity improvements towards (*R*)-threonine also showed similar improvements towards the stereoisomer, (*rac*)-*allo*-threonine, as shown for the highest results for both substrates on library plate-4.1 in Figure 2.51. The improvements observed in this library plate are 2.0 to 2.5-fold greater than the activity of the parental enzyme towards these substrates, although the remaining library plates suggest that up to 6-fold activity improvements may be possible. The F58 library contained variants which also showed improved activity towards (*rac*)-1,2,3,4-tetrahydroisoquinoline-3-carboxylic acid. The best improvements towards this substrate were approximately 4-fold greater than parental activity. Enhancements of up to 8-fold greater than parental activity were observed for variants from this library towards (*R*)-pipercolinic acid.

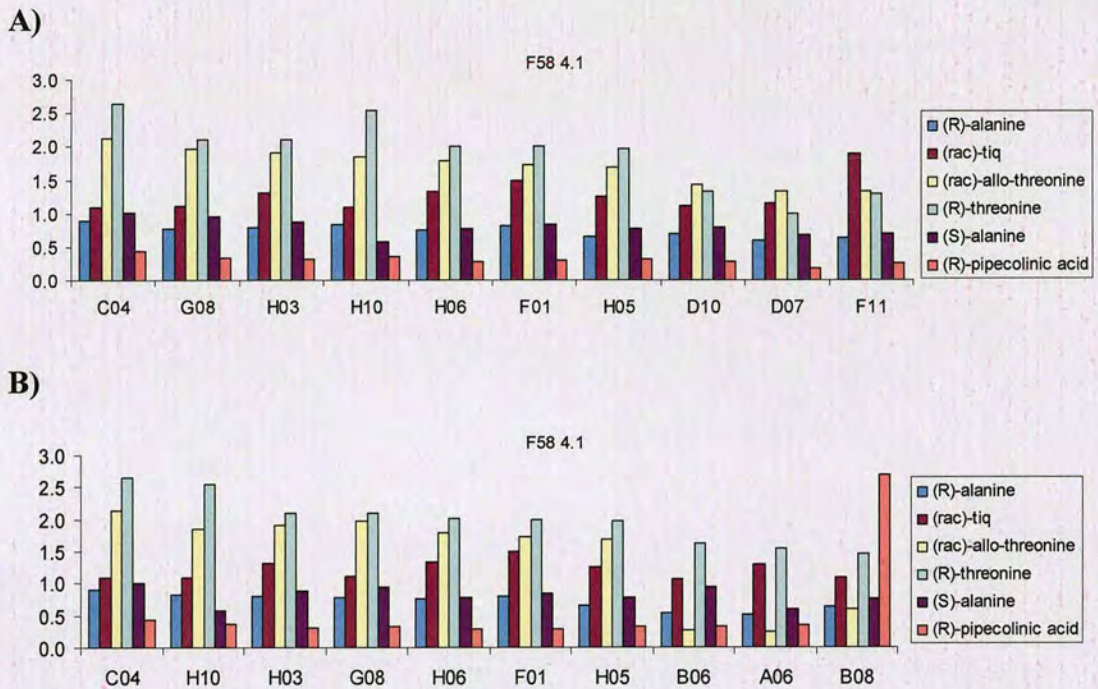


Figure 2.51 - Substrate profiles for variants producing the highest rates towards A) (*rac*)-allo-threonine and B) (*R*)-threonine from saturation mutagenesis library RgDAAO F58 plate-4.1. Parental RgDAAO activity is set as one. Any number greater than one implies improved activity over parental activity and any number smaller than one implies that the variant showed lower activity towards the test substrate than the parent. Tiq = 1,2,3,4-tetrahydroisoquinoline-3-carboxylic acid.

2.4.7 Conclusions

Four RgDAAO saturation mutagenesis libraries were prepared and the presence of each type of nucleotide exchange was confirmed by sequencing the genes. Cells expressing the corresponding variants were grown in 96-well plates for assay in liquid-phase. The libraries were assayed against a variety of substrates and the maximum slope for each variant against each substrate was determined. The data from each plate were normalised and Z' was assessed to provide an insight into the performance of the controls. The highest results towards each substrate were compared. Activity profiles for the most active variants were produced and compared. These profiles allowed the identification of identical or similar variants.

The RgDAAO variant libraries produced by saturation mutagenesis at the conserved residues R285 and Y238 both produced more inactive variants than the other active

site saturation mutagenesis libraries. Different activity profiles observed for the R285 saturation library variants indicated that this site does tolerate some amino acid exchanges. An approximately 6-fold improved activity was observed towards the substrate (*rac*)-1,2,3,4-tetrahydroisoquinoline-3-carboxylic acid by several of these variants. Additionally, no improvements were detected towards (*R*)- and (*S*)-alanine and approximately 2-fold improvements were observed towards (*rac*)-*allo*-threonine for some variants in the R285 library.

Saturation libraries were also generated at the non-conserved active site residues M213 and F58. The range of substrates used to screen these two libraries was not identical but four substrates were screened against both. These were (*rac*)-1,2,3,4-tetrahydroisoquinoline-3-carboxylic acid and three β -amino acids; (*rac*)- β -phenylalanine, (*rac*)- β -homophenylalanine and (*rac*)-3-aminobutyric acid. In addition, one plate from the F58 library (plate 6, which was used to assess the screening method and has been discussed above) was screened against (*R*)-pipercolinic acid. The full M213 library was screened against this substrate. No variant was found in either library which was active towards the β -amino acids but both libraries contained variants with improved activity towards (*rac*)-1,2,3,4-tetrahydroisoquinoline-3-carboxylic acid. The improvements towards this substrate were up to 5-fold for some variants in the F58 library and up to 10-fold for some variants in the M213 library (although the results for the M213 library towards this substrate may be over-estimated due to poor control data being obtained during screening). Both libraries also contained variants with improved activity towards (*R*)-pipercolinic acid. For example, the variant F58Q shows a 4-fold improvement over the parental enzyme and M213 variants were observed with 8-fold improvements towards (*R*)-pipercolinic acid.

The M213 saturation library also contained variants which showed improved activity towards the substrates (*rac*)-homophenylalanine (3-fold), (*rac*)-pyridylalanine (8-fold) and (*rac*)- β -methylphenylalanine (5-fold).

The RgDAAO F58 saturation library was the most closely analysed of the four libraries. F58 exchanges which proved beneficial for enzyme activity towards some of the substrates tested were those to V, T, I, M, L and Q. Variants with exchanges to C, G and A at this position were generally less active than the parental enzyme towards the substrates and exchanges from F58 to R, N and P produced variants which were inactive.

The data show that the length of the residue at amino acid 58 has an effect of the activity of the variants. For example, the variant F58Q shows some improvements in activity towards the substrates over the parental enzyme while the F58N variant is inactive towards all of the screened substrates. Additionally, branching at the β -carbon of the exchanged residue is beneficial for the activity of the variants towards (*rac*)-*allo*-threonine but detrimental for activity towards (*R*)-pipecolic acid. The variants in the screened library (plates 1 to 6) produced rate enhancements over the parental activity of up to 6-fold greater towards (*rac*)-*allo*-threonine, up to 5-fold greater for (*R*)-threonine, 4-fold greater towards (*rac*)-1,2,3,4-tetrahydroisoquinoline-3-carboxylic acid and up to 8-fold greater towards (*R*)-pipecolic acid.

The main overall observation from all of the saturation mutagenesis libraries was that no new activity was developed towards substrates, including the β -amino acids screened, for which parental RgDAAO showed no activity. Additionally, activity towards substrates upon which the parental enzyme is very active, such as (*R*)-alanine, were not improved further. However the activity for substrates towards which the parental RgDAAO performs more moderately could be improved.

The use of a heat inducible promoter for induction of protein expression was not ideal for expression in 96-well format, as this adds another level of variability in protein production from cells. If the control wells on each plate are either more or less affected by a temperature gradient than the other wells, then the normalised data will be distorted. Therefore use of an alternative expression system would improve this method. In addition, more consistent data were achieved when the initial

measurement duration was 20 to 30 min and although this time for each plate in the spectrophotometer decreases the screening throughput, the data produced are more reliable.

Although some reproducibility problems were observed in the liquid phase assay, these were easily identified. This is a significant advantage over solid-phase screening. In addition, information collected on each variant screened is recorded and stored, whereas with the solid phase assay, information only remains for those variants reassayed and sequenced. Further, the activity profiles, provided by substrates towards which the parental enzyme has activity, can be compared for the variants demonstrating the highest activities towards 'poor' substrates. This provides some insight into whether these highest results are random or produced by similar variants.

As the activity of the variants on plate-6 of the RgDAAO F58 library had been repeated in triplicate, giving the most accurate results, four of these variants were carried forward to perform biotransformation reactions with the aim of confirming the activity demonstrated by the assay by HPLC analysis.

2.5 BIOTRANSFORMATIONS USING VARIANT ENZYMES

Variant RgDAAO enzymes which were identified from the liquid-phase assay with improved oxidase activity towards selected substrates were employed in whole cell biotransformation reactions. The reaction progress was followed by HPLC analysis. These reactions were carried out using pellets (1 g wet cell mass) from cells expressing the appropriate RgDAAO variant. The initial reaction volume was 10 mL from which 1 mL samples were removed during the course of the reaction for analysis by reversed-phase chiral HPLC as described in Section 3.2.6.

2.5.1 Biotransformation of pipecolinic acid

According to the liquid-phase assay data produced by screening the F58 RgDAAO saturation mutagenesis library, the F58M and F58Q variants oxidise (*R*)-pipecolinic acid at rates approximately 2.5 and 3.5 times greater than the parental enzyme respectively. Initial biotransformations of pipecolinic acid were performed at 20 mM substrate concentration and the enantiomers separated using an Astec Chirobiotic-T reversed-phase column. As this amino acid does not contain a chromophore which allows convenient UV detection, the relative absorbance measurements produced by the enantiomers were weak compared with unidentified compounds also present in the reaction mixture. The concentration of pipecolinic acid in the biotransformation was increased to 80 mM to improve the relative signal intensity (Figure 2.52). The enantiomers of pipecolinic acid show retention times of 10.9 min (*S*) and 14.2 min (*R*).

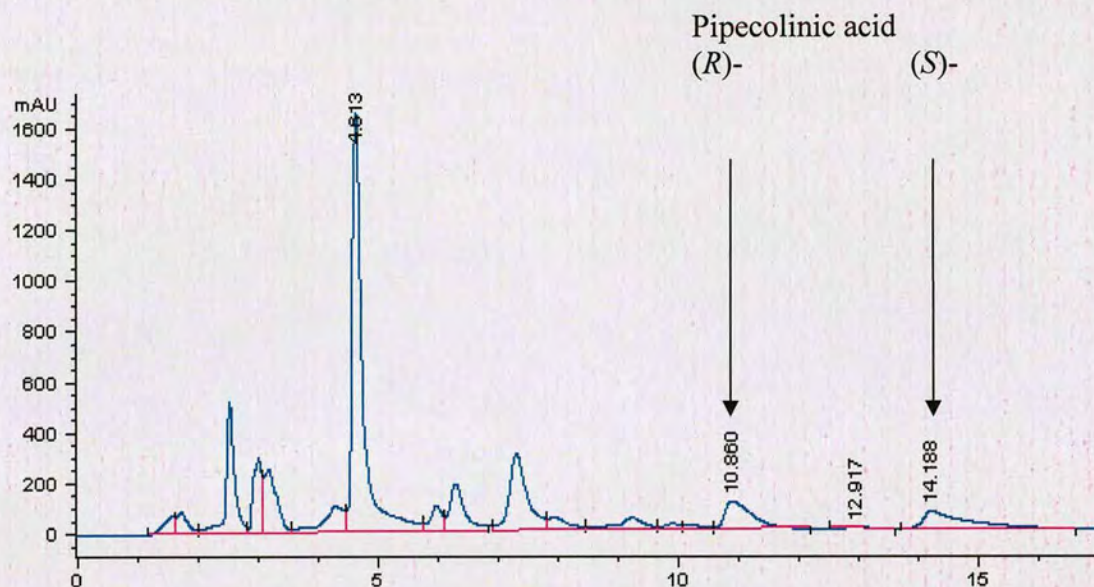


Figure 2.52 – HPLC trace produced by the separation of a sample taken from a pipecolinic acid biotransformation on a Chirobiotic-T reverse-phase column. Retention times are 10.9 min for (*S*)-pipecolinic acid and 14.2 min for (*R*)-pipecolinic acid. 80 % Acetonitrile, 20 % water, 2 mL min⁻¹, 10 °C, injection volume 5 μL. Reaction run at 80 mM substrate concentration, 100 g cells L⁻¹.

At this substrate concentration the signals for pipecolinic acid could be identified. Alternatively, a D-penicillamine ligand exchange column can be used for chiral separation of amino acids. The copper complex of pipecolinic acid observed with this analysis method shows higher absorption compared to the free amino acid observed in the previous method. This method also produces an improved peak shape (Figure 2.53). However, the negative peak which runs in advance of the (*S*)-enantiomer at 6.3 min could not be separated and the retention times of both enantiomers did not stabilise even after long equilibration times.

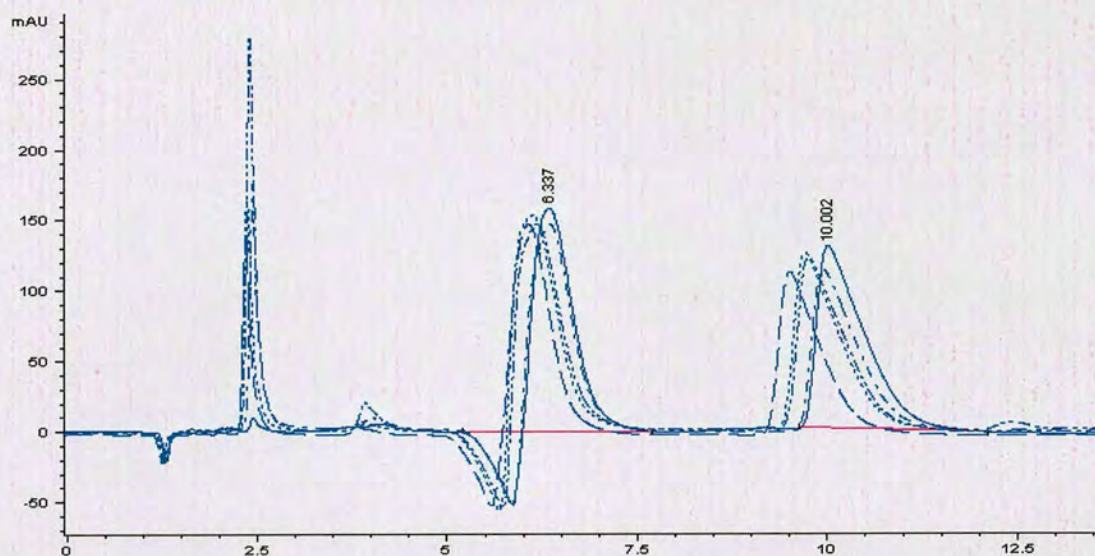


Figure 2.53 - HPLC trace produced by the separation of a sample taken from a pipercolinic acid biotransformation on a D-penicillamine ligand exchange column. Retention times of the enantiomers are approximately 6.4 and 10.0 min. It was not possible to reduce drifting retention times even after long equilibration periods. 2 mM CuSO_4 , 3 % methanol, 0.8 mL/min, injection volume 1 μL . Reaction run at 20 mM substrate concentration, 100 g cells L^{-1} .

Satisfactory data could not be obtained using either analysis method to follow the biotransformations but one example where the oxidation of pipercolinic acid was monitored using the Chirobiotic-T column for separation is shown in Figure 2.54. The oxidation is not complete for any of the RgDAAO variants after a reaction time of 41 h (F58Q 40 % conversion, F58M 31 % and parental RgDAAO 19 %). These data indicate that the F58M and F58Q variants oxidise (*R*)-pipercolinic acid 1.3 and 2.0 times faster than parental RgDAAO respectively. In comparison, the relative rate enhancements observed in the liquid phase assay were 2.5 times for F58M and 3.5 times for F58Q. However, the liquid phase assay was carried out using 10 mM (*R*)-pip and the biotransformation was carried out with 80 mM (*rac*)-pip.

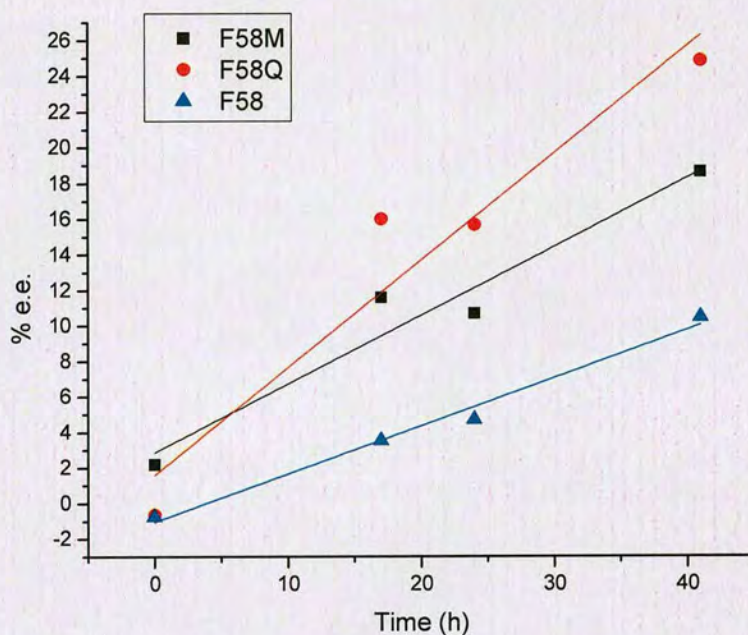


Figure 2.54 – % e.e. over time calculated from samples removed from (*rac*)-pipercolinic acid biotransformations using cells expressing F58M, F58Q and parental (F58) RgDAAO. The biotransformations were carried out at 80 mM substrate concentration, 100 g cells L⁻¹, 100 mM buffer, 37 °C, 225 rpm. Samples were separated on a Chirobiotic-T column.

The technical problems associated with monitoring the progress of the (*rac*)-pipercolinic acid biotransformations led to the selection of a substrate better suited for UV detection, (*rac*)-1,2,3,4-tetrahydroisoquinoline-3-carboxylic acid ((*rac*)-tiq), with the aim of producing more consistent HPLC data to confirm improved RgDAAO variants identified using the liquid phase assay.

2.5.2 Biotransformation of (*R*)-tiq

Liquid-phase screening of the RgDAAO F58 saturation mutagenesis library suggested respective rate enhancements of 2.8 and 2.4 times that of parental RgDAAO in the oxidation of (*rac*)-tiq by the F58L and F58I variants. The tiq enantiomers could be separated and the signals were not overlaid by signals from impurities or by-products (Figure 2.55). The analysis method allowed convenient monitoring of the biotransformation reaction.

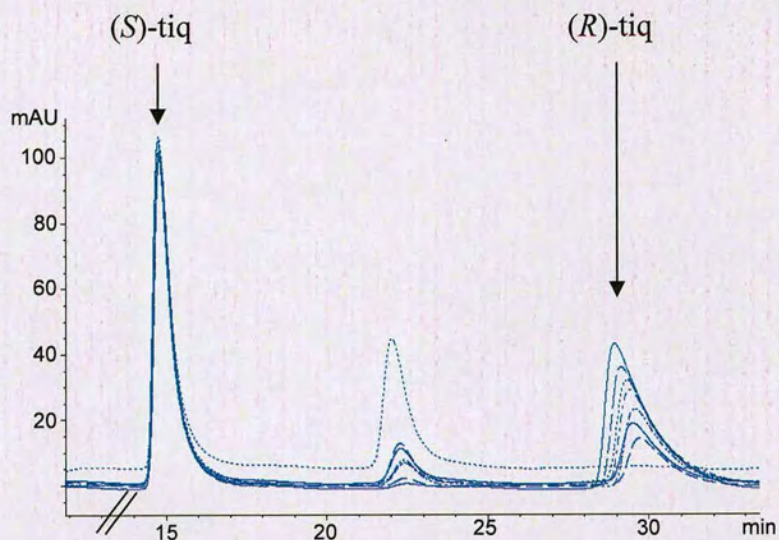


Figure 2.55 - HPLC trace produced by the Chirobiotic-T separation of samples taken over the course of a 10 mM tiq biotransformation ($100 \text{ g cells L}^{-1}$). 90% methanol, 10% water, $1 \text{ mL}\cdot\text{min}^{-1}$, $25 \text{ }^\circ\text{C}$, injection volume $1 \text{ }\mu\text{L}$.

Tiq biotransformation reactions were performed using cells expressing the RgDAAO variants F58L and F58I and parental RgDAAO. These were compared with biotransformations using empty vector cells. All reactions were carried out using 10 mM (*rac*)-tiq. The oxidation of (*R*)-tiq was monitored by HPLC and the calculated % e.e. over time is shown in Figure 2.56 for each reaction.

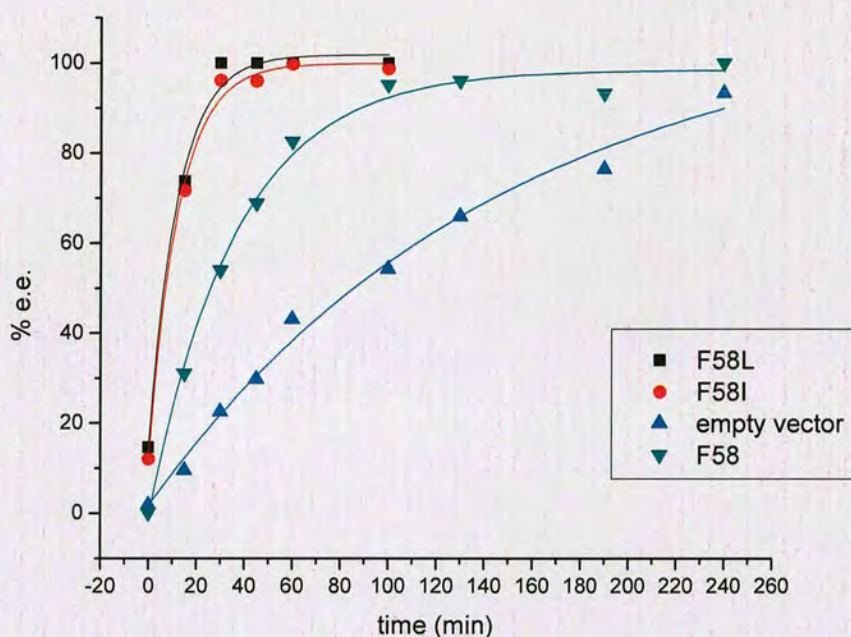


Figure 2.56 – Observed % e.e. over time obtained for samples removed from (*rac*)-*tiq* biotransformations (10 mM substrate concentration, 100 g cells L⁻¹, 100 mM buffer, 37 °C, 225 rpm) using cells expressing F58L, F58I and F58 RgDAAO and empty vector cells. The biotransformations were performed in duplicate and the data shown are the averaged results.

The biotransformation reactions demonstrated that (*R*)-*tiq* oxidation by the F58L and F58I RgDAAO reached 99 and 98 % conversion within 30 min respectively, while parental RgDAAO takes 240 min to reach 100 % conversion. The initial conversion rates observed by HPLC in whole cell biotransformation reactions are 1.5 times higher with the F58L variant and 1.6 times higher with the F58I variant compared to parental RgDAAO (activity of cells with empty vector was subtracted). These are lower than the figures suggested by the liquid-phase assay (2.8 and 2.4 times respectively). The disappearance of (*R*)-*tiq* using cells containing empty vector, shown in Figure 2.56, was not anticipated and occurs at a rate approximately 2/3 that of cells expressing parental RgDAAO. This background activity towards (*R*)-*tiq* by the *E. coli* BL21(DE3) cells was not observed in the liquid phase assay. The empty vector controls on the assay plate were assayed against a control substrate ((*R*)-serine or (*R*)-alanine) rather than the test substrate, and these control wells do not provide any information on the background reaction observed with (*R*)-*tiq*. However, several

wells on each plate contained cells expressing inactive RgDAAO variants, for example wells D01 and F01 in Figure 2.57 which shows RgDAAO F58 saturation mutagenesis variants assayed against A) (*R*)-alanine and B) (*rac*)-tiq. The OD₆₀₀ values recorded for the growth of the cells associated with these assay plates confirm that all the wells on the plate contained comparable densities of cells, with the exception of the diagonal of blank wells from A01 to G07. Rates of colour formation 1/3 lower than those produced by parental RgDAAO towards (*rac*)-tiq (wells G12 and H12) are detectable by the liquid-phase assay. Had the (*R*)-tiq background reaction been coupled to hydrogen peroxide production, colour formation would be detectable in any well containing *E. coli* cells, including those expressing inactive RgDAAO. It seems that the background activity observed here is not D-amino acid oxidase activity but some other enantioselective enzymatic system, for example, a decarboxylase.

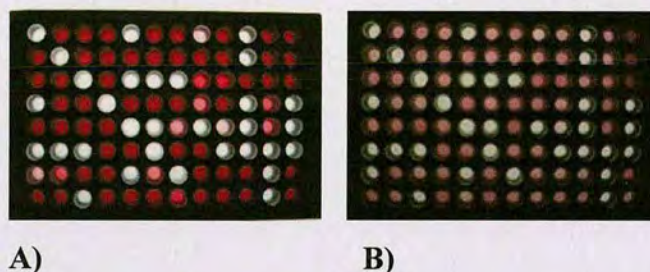


Figure 2.57 – RgDAAO F58 saturation mutagenesis library (assay plate-5) assayed against A) (*R*)-alanine and B) (*rac*)-tiq. The positive and negative control wells are in column 12 and there is a diagonal of blank wells containing no cells from A01 to G07.

2.5.3 Conclusions

RgDAAO F58 variants were selected for use in biotransformations of (*rac*)-pipecolinic acid and (*rac*)-tiq based on the enhanced oxidation rates towards these substrates displayed in the liquid-phase assay. The HPLC analysis of the pipecolinic acid biotransformation was not robust enough to provide consistent results but indicated that the F58M and F58Q RgDAAO variants oxidised (*R*)-pipecolinic acid 1.4 and 2.2 times faster than parental RgDAAO respectively. The rate enhancements in the liquid-phase assay were 2.5 and 3.5 times parental RgDAAO. The discrepancy

here could be due to the different experimental conditions. The assay was carried out using 10 mM (*R*)-pip and the biotransformation using 80 mM (*rac*)-pip).

HPLC analysis following the course of the (*rac*)-tiq biotransformations showed that (*R*)-tiq oxidation rates produced by F58L and F58I RgDAAO variants are 5.2 and 4.6 times greater than by parental RgDAAO which is greater than the rate enhancements provided by the liquid-phase assay of 2.8 and 2.4 times the parental rate. These data confirm that the liquid-phase assay can be a useful guide to detecting improved variants for use in a biotransformation experiment. (*R*)-tiq oxidation by both F58L and F58I RgDAAO variants were complete within 30 min (at 10 mM substrate concentration, $100 \text{ g cells L}^{-1}$, 100 mM buffer, 37 °C, 225 rpm).

An (*R*)-selective background reaction by *E. coli* BL21(DE3) cells was observed in biotransformations of (*rac*)-tiq using empty vector cells. The empty vector controls in future liquid phase assay experiments should be assayed against the test substrate (rather than the control substrate, (*R*)-alanine or (*R*)-serine). This will allow detection of hydrogen peroxide forming background oxidations with a particular substrate. Non-hydrogen peroxide forming background reactions will remain a possibility and should be monitored by HPLC.

No amino acid derivatisation methods were attempted in this work. A quantitative derivatisation method applied to the biotransformation samples would allow extraction of the amino acids from the reaction mixture. The samples could then be analysed by normal-phase HPLC and undesired signals caused by other compounds present in the reaction mixture could be reduced. Appropriate derivatisation, for example using Marfey's Reagent,⁽⁵⁸⁾ could also improve the monitoring of conversion of amino acids which are harder to detect by UV absorption such as pipecolinic acid.

2.6 OVERALL CONCLUSIONS

The aim of the project was to develop an oxidase enzyme for use in eventual deracemisation reactions of β -amino acids, or of unusual α -amino acids. To this end, a culture collection comprising approximately 500 microorganisms was screened with the aim of identifying β -amino acid oxidase enzymes already present in nature. As no activity towards β -phenylalanine or β -homophenylalanine was detected by this route, existing oxidase enzymes were examined for their activity towards β -amino acids.

The flavin-dependent enzymes, monoamine oxidase-N and D-amino acid oxidase were screened using an HRP-coupled solid phase assay for activity towards β -amino acids. Again, no activity was observed and D-amino acid oxidase was selected for directed evolution experiments with the aim of evolving activity. The parental profiles of TvDAAO and RgDAAO were assessed against a range of proteinogenic and non-proteinogenic amino acids. The TvDAAO gene was propagated in an *E. coli* mutator strain but as the start codon was found to be mutated in all the TvDAAO genes later sequenced it was decided to generate mutations by epPCR. EpPCR was performed on the gene encoding RgDAAO and the variant libraries produced were initially screened using a solid-phase HRP-coupled assay. This assay method proved not to be robust enough for consistent screening of the library and an HRP-coupled liquid-phase assay was therefore used as an alternative. The liquid-phase assay was favourably assessed for its suitability as a screening assay. In order to improve screening throughput a method was developed, whereby RgDAAO variants were grown in semi-solid agarose in 96-well plates. This allowed the growth of ten individual colonies per well for subsequent screening. Any active variant could later be identified by deconvoluting the variants in the active well. Throughput was further increased by the use of a robot. Approximately 100 000 colonies were screened against β -homophenylalanine but no activity towards this substrate was identified.

It was decided to reduce the number of variants which required to be screened by focussing mutations on residues around the active site. Four single-site saturation mutagenesis libraries were prepared using the RgDAAO gene, at positions F58, M213, Y238 and R285. In addition, α -amino acids were added to the substrate set to further probe the effects of the residue exchanges. Methods for screening the libraries and for handling the data produced were developed. The method was found to be reproducible within each plate and although inconsistencies were apparent between plates, the source of these could be identified.

It was found that substrate profiling was a useful method for identifying variants although these could only be reliably compared within a single plate. By comparing the profiles of the variants demonstrating the highest activity towards a particular substrate, 'hits' could be confirmed. This 'hit profiling' could potentially be useful to identify new or improved activity with higher certainty in the first round of a screen. As expected, the screening in liquid phase of mutagenesis libraries provides more information than the solid-phase assay about the effects of particular residue exchanges. In addition, this information is recorded and can be returned to for further analysis.

The main observations from the saturation mutagenesis libraries were that the libraries produced at conserved residues showed more inactive variants than those produced at the other active site residues. The substrate profiles obtained for RgDAAO R285 variants suggest that this residue will tolerate a few amino acid exchanges. No new activity was developed in any of the libraries towards the β -amino acid substrates or *tert*-leucine, for which the parental RgDAAO also shows no activity. Activity towards substrates such as (*R*)-alanine, towards which the parental enzyme is very active, could not be improved further. However the activity for substrates towards which the parental RgDAAO performs more moderately could be improved. For example, some M213 variants displayed up to 8-fold activity improvements towards (*R*)-pipercolinic acid and the F58V variant showed a 4-fold improvement towards (*R*)-threonine.

Specific variants were identified from the RgDAAO F58 saturation library by gene sequencing. Exchanges which proved beneficial for enzyme activity towards some of the substrates tested were those to V, T, I, M, L and Q. F58 variants with exchanges to C, G and A were less active than the parental enzyme towards the majority of the substrates and exchanges from F58 to R, N and P produced variants which were inactive. The length of the residue at position 58 appears to be important and the F58Q exchange improves the activity of RgDAAO towards (*R*)-pipecolinic acid and (*R*)-serine while the F58N variant is inactive towards all of the screened substrates. Branching at the β -carbon of the exchanged residue is beneficial for the activity of the variants towards the substrate (*rac*)-*allo*-threonine but detrimental for activity towards (*R*)-pipecolinic acid. For example, F58I has 3-fold better activity towards (*rac*)-*allo*-threonine but a reduced activity to (*R*)-pipecolinic acid compared with RgDAAO F58. There is no improved activity for the variant F58L towards (*rac*)-*allo*-threonine but this variant has a 3-fold better activity to (*R*)-pipecolinic acid than the parental enzyme.

Neither the random methods of mutagenesis used, nor saturation mutagenesis yielded DAAO variants active on β -amino acids. However, the reduced size of the libraries required for screening in the rational design approach allowed more substrates to be screened against each library. Substrates for which the parental enzyme showed a range of activities were selected for the screen, allowing a pattern of increased or decreased activity for each variant towards these substrates to be determined. In this way, much more information about the variants was generated. The activity observed in the substrate profiles show that another advantage of rational design is that there is a much higher chance of generating improved activities, at least towards some substrates, than in the case of random mutagenesis. While random mutagenesis allows discovery of beneficial mutations which would be difficult to predict, many of the variants generated will have no observable effect on substrate catalysis.

2.7 OVERALL FUTURE WORK

The RgDAAO gene had been cloned into the pPOT3 plasmid which contains a heat-inducible promoter. Protein production was induced by placing the growing colonies at elevated temperatures. It is possible however, that uneven heat transfer resulted in a difference in the protein production of different colonies on the same plate and therefore led to varied response in the liquid-phase assay. Heat induced expression must also be volume dependent at larger volumes. The experiments may have been more controlled using an alternative system such as IPTG-induced expression.

An alternative method of preparing the site-saturation libraries would have been to prepare distinct mutants of a single site thereby reducing the number of colonies to be screened to 20.

It is possible that further saturation mutagenesis studies at residues around the active site of RgDAAO could identify a variant active towards β -amino acids. Tishkov suggests that the Ser335 residue participates in hydrogen bonding of the α -amino group.⁽⁴⁴⁾ This residue can be seen at the bottom of Figure 2.58 (coloured light purple) which shows the active site of RgDAAO with (*R*)-alanine bound.

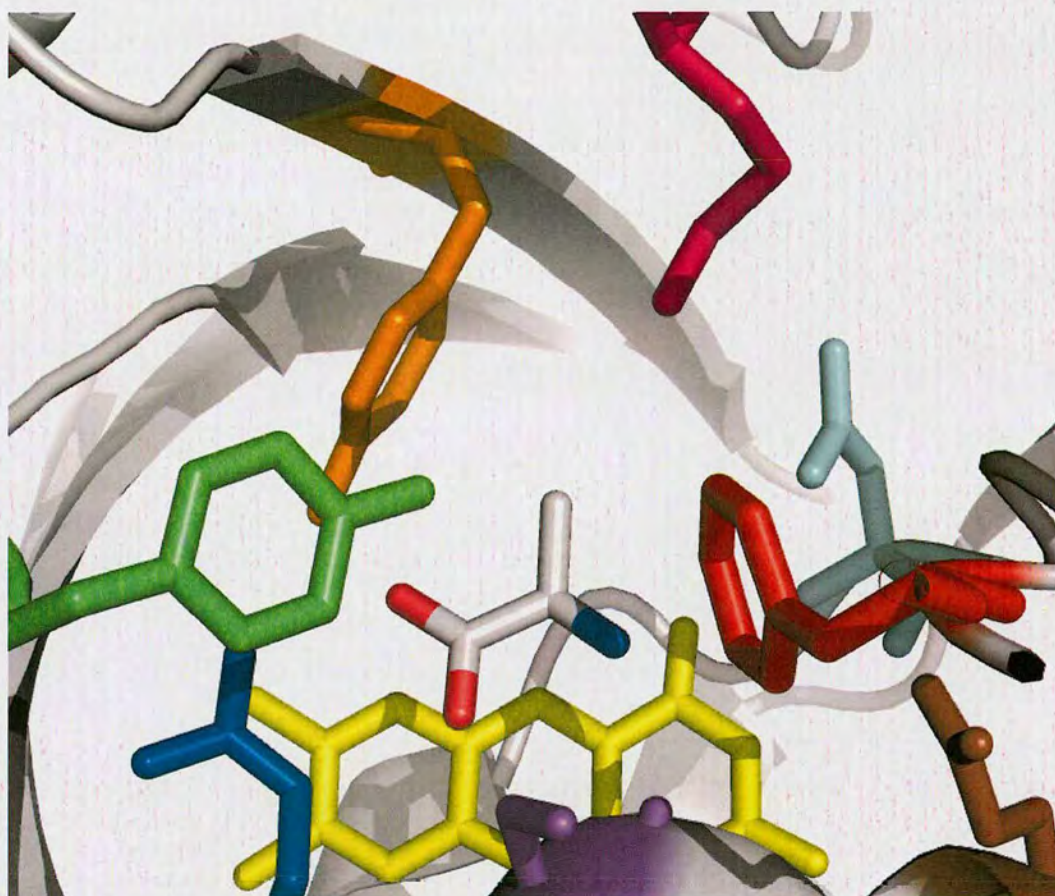


Figure 2.58 – RgDAAO crystal structure co-crystallised with (*R*)-alanine.⁽⁴⁷⁾ PDB ID code 1c0p. Residue colour code: light blue = N54, red = F58, pink = M213, orange = Y223, green = Y238, blue = R285, purple = S335, brown = Q339. The flavin molecule is shown in yellow.

Alternative enzymes could be screened for β -amino acid oxidase activity, for example, D-aspartate oxidase (EC-Number 1.4.3.1). Monoamine oxidase-N (variant D5) did not show activity towards β -amino acids but might be an interesting subject for further rounds of directed evolution or site mutagenesis. Apart from β -amino acids the substrate panel could also include derivatives such as the corresponding esters or β -amino nitriles.

Alternative screening strategies could be pursued, for example, selection growth on minimal media where all nitrogen sources apart from the β -amino acid are removed during growth of colonies containing variant RgDAAO. Only colonies processing the β -amino acid would be expected to grow in this environment.

3 EXPERIMENTAL

All reagents were purchased from Sigma-Aldrich unless otherwise stated. Sterile solutions were prepared by filtration (0.2 μ M filter) or by autoclaving (121 °C, 15 min).

3.1 INSTRUMENTS

Instrument	Make
Agarose gel electrophoresis	Biorad Minisub Cell GT gel chamber
Balances	Mettler Toldedo Analytical Balance AB204-S Mettler Toledo Balance PP1502-S/FACT
Biophotometer	Eppendorf Biophotometer
Blotting transfer cell	Biorad Transblot SD Semidry Transfer Cell
Blue-light transilluminator	Invitrogen Safe-imager
Centrifuges:	
<1.5 mL	Eppendorf 5414 R
<50 mL	Eppendorf 5810 R
<350 mL	Beckmann-Coulter Avanti J-E
96-well, 2.2 mL plates	Beckmann-Coulter Avanti J-E
Electroporator	Biorad Genepulser Xcell
FPLC	GE Healthcare Äkta Explorer 100
HPLC	Agilent 1100 series
Liquid handler	Tecan Miniprep 75
pH Meter	Hanna pH 213
Plate readers	BMG Labtech Fluostar Optima Tecan Rainbow
Polyacrylamide gel electrophoresis	Biorad Miniprotean 3 cell
Power suppliers	Biorad Powerpack 400
Robotic Sample Processor	Tecan Genesis Workstation 150

Instrument	Make
Rocker	Grant Boekel BFR25
Roller mixer	Stuart SRT1
Thermocycler	Eppendorf Mastercycler Gradient
White light transilluminator	UVP
Vortex	VWR lab dancer

3.2 METHODS

Parental RgDAAO and parental TvDAAO refer to the enzymes generated from the DNA with the sequences shown in the Appendix (sections 5.1.1 and 5.1.2 respectively). The primers used in this work are shown in the Appendices (Section 5.2).

3.2.1 DNA purification and manipulation

Plasmid DNA extraction

QIAprep Spin Miniprep Kits were purchased from Qiagen and were supplied with pre-prepared buffers and columns.

1.5 mL was removed from an overnight culture (section 3.2.3) and the cells isolated by centrifugation at 15 700 x g for 10 min. Plasmid DNA was extracted using the ‘*Plasmid DNA Purification Using the QIAprep Spin Miniprep Kit and a Microcentrifuge*’ method described in the handbook provided with the kit.⁽⁵⁹⁾ The overall procedure is: resuspension of the cell pellet, alkaline lysis of the cells, neutralisation of the resulting lysate and precipitation of unwanted cellular components at high-salt concentration. This is followed by binding of plasmid DNA to a silica column under high-salt conditions, washing in ethanol-buffer and, finally, elution of plasmid DNA in a low-salt buffer or water. Concentrations were determined by spectroscopy on a biophotometer at a wavelength of 260 nm and purity estimated using the 260 nm/280 nm ratio. The plasmid DNA was stored at -20 °C.

Restriction digest

Generic method: Restriction endonucleases and bovine serum albumin (BSA) were purchased from New England Biolabs (NEB). All restriction enzymes were supplied with the appropriate buffer (10X concentrate). Buffers for use in double digests were selected using NEB's double digest calculator (<http://www.neb.com/nebecomm/DoubleDigestCalculator.asp>). BSA was added to the reaction mixture where recommended by NEB. 1 μL of each endonuclease, 2 μL buffer (X10) and 0.2 μL BSA were placed in a 0.2 mL PCR tube and made up to a volume of 5 μL with sterile reverse osmosis (RO) H_2O . This mixture was added to 15 μL plasmid DNA and placed at 37 °C for between 1 and 4 h, or overnight at room temperature.

NcoI digest: 20 μL NEB buffer 4 (X10) and 5 μL NcoI (10 000 U mL^{-1}) were mixed in a 1.5 mL tube and made up to 100 μL with sterile RO H_2O . 10 μL of this mixture was added to 10 μL plasmid DNA obtained from each of the 10 samples, the reactions were spun briefly and placed at 37 °C for 2 h. The digested samples were analysed by agarose gel electrophoresis. The gel was run at 80 V and analysed at 30 and 50 min.

DpnI digest: The endonuclease DpnI is used to remove parental template DNA from PCR products. This is possible because the DNA generated by growth in *dam*⁺ *E. coli* strains is methylated at the adenine occurring within the sequence 5'-GATC-3', whereas the DNA produced by amplification in a PCR reaction is not. DpnI digests DNA methylated at these positions. 50 μL PCR products from site-directed, saturation or epPCR mutagenesis reactions were incubated with 1 μL DpnI (20 000 U mL^{-1}) at 37 °C for 1 h in a thermocycler.

DNA agarose gel electrophoresis

Agarose was purchased from Fisher Bioreagents, SYBR Safe DNA stain from Invitrogen and Blue/Orange Loading Dye and Benchtop 1 kb Ladder from Promega.

0.5 g agarose was added to 50 mL tris-acetate ethylene diamine tetraacetic acid buffer (TAE, Section 3.2.7), dissolved in a microwave and cooled in a water bath to 50 °C. The solution was poured into a gel mould and DNA stain was mixed in by stirring with a pipette tip (1 µL ethidium bromide (10 mg mL⁻¹) or 5 µL SYBR safe (10 000 X)). The gel was allowed to set and submerged in 1X TAE buffer in a gel tank. Blue/Orange Loading Dye (6x) was added, in a 1 in 6 dilution, to samples of digested plasmid or PCR product (20 – 200 ng DNA, maximum volume 24 µL) and to BenchTop 1 kb DNA Ladder. The samples and marker were loaded onto the gel and run at 80 to 100 V for 1 h. Ethidium bromide gels were viewed on a UV transilluminator and SYBR-safe gels on a blue-light transilluminator.

Agarose gel DNA extraction

An Agarose Gel DNA Extraction Kit was purchased from Roche, and contained agarose solubilisation buffer, nucleic acid binding buffer, washing buffer and silica matrix suspension.

Following separation of DNA fragments by agarose gel electrophoresis, the fragment of interest was cut from the gel leaving as little agarose as possible. The DNA was separated from the remaining gel by the method described in the kit manual.⁽⁶⁰⁾ The overall procedure was: solubilisation of the agarose surrounding the fragment and binding of the DNA fragment to a silica-matrix in the presence of a chaotropic salt, followed by washing of the DNA and then elution in a low-salt buffer. Absorbance was measured on a biophotometer at 260 and 280 nm to determine the concentration and purity of the DNA which was stored at -20 °C.

Preparation for DNA sequencing

ABI prism BigDye terminator V3.1 and sequencing buffer (5X) were purchased from Applied Biosystems. Samples were sequenced by either The Institute of Cell and Molecular Biology (ICMB) at The University of Edinburgh (sequencing only) or by MWG Biotech AG (amplification and sequencing). Sequencing primers are described in Section 5.2.1.

Samples submitted to ICMB were amplified by the following method. The reagents were added to a 0.2 mL thin-walled PCR tube in the following order: 2 μL sequencing buffer (5X), 1.6 μL sequencing primer ($1 \text{ pmol } \mu\text{L}^{-1}$), 4 μL template DNA ($40 - 75 \text{ ng } \mu\text{L}^{-1}$), 4 μL ABI prism BigDye terminator V3.1 (2.5X), and the volume adjusted to 10 μL with DI H_2O . The tube was placed in a thermocycler and subjected to the cycling programme shown in Table 3.1.

Table 3.1 – Thermal cycling programme used for sequencing PCR.

Step	Temperature/ $^{\circ}\text{C}$	Time/min	Repetitions
1	95	1	1
2	96	0.5	30
3	50	0.5	
4	60	4	
5	4	hold	-

The resulting PCR products were submitted to ICMB without purification. Alternatively, sequencing primers and plasmid DNA were sent to MWG Biotech AG ($10 \text{ pmol } \mu\text{L}^{-1}$ each primer and $1 \mu\text{g}$ precipitated plasmid DNA) for both the amplification and sequencing steps.

DNA plasmid precipitation

Ammonium acetate solution (5 M) was added to the purified plasmid to a final concentration of 2.5 M, followed by 2 volumes of ethanol. This mixture was placed at $-20 \text{ }^{\circ}\text{C}$ for $> 20 \text{ min}$ and centrifuged at $15\,700 \times g$ for 10 min. The supernatant was removed and the pellet washed with 70 % ethanol. The pellet was dried overnight at room temperature.

3.2.2 Mutation Protocols

Mutator strain

Transformation and subsequent growth of XL1-Red colonies on agar plates is described in Section 3.2.3. LB/KAN (2 mL) was added to the plate and the colonies were gently scraped off the surface of the agar using a sterile plastic spreader and resuspended in a further 10 mL LB/KAN. The culture was then diluted to an OD_{600} of 0.0005 in LB/KAN containing (*R*)-alanine ($250 \mu\text{M}$) and grown at $37 \text{ }^{\circ}\text{C}$ and

225 rpm for 24 h when an OD_{600} of approximately 2 was reached. This dilution and growth procedure was repeated a further 5 times and from the final culture 4 x 5 mL samples were removed. These were pelleted and the plasmid DNA extracted. For storage purposes TOP10 cells were transformed with this DNA. Following growth on agar plates the colonies were removed from the plate as described above and the DNA was re-extracted and stored at $-20\text{ }^{\circ}\text{C}$. For screening purposes, the *E. coli* expression strain BL21(DE3) was transformed with the plasmid DNA.

Error-prone PCR (epPCR)

The megaprimer PCR of whole plasmid (MEGAWHOP) method described by Miyazaki⁽⁶¹⁾ was followed. There are 6 stages; (i) an error-prone PCR to generate a library of variant genes, (ii) purification of the PCR products generated, (iii) a sub-cloning step, performed by PCR, in which the mutated genes are used as megaprimers and the parental construct is used as template, (iv) removal of parental constructs from the mixture by restriction digest, (v) repair of nicked DNA resulting from the whole plasmid PCR by transformation of highly competent cells with the products, and (vi) plasmid purification.

(i) epPCR

See Section 5.2.2 for epPCR primers. Taq polymerase and dNTPs were purchased from NEB. Reagents were added to a 1.5 mL tube in the following order: 246.6 μL DI H_2O , 1.4 μL freshly prepared RgDAAO/pPOT3 template DNA (from TOP10 cells) ($75.9\text{ ng } \mu\text{L}^{-1}$), 20 μL forward primer (10 μM), 20 μL reverse primer (10 μM), 5 μL dTTP (100 mM), 5 μL dCTP (100 mM), 1 μL dGTP (100 mM), 1 μL dATP (100 mM), 140 μL MgCl_2 (25 mM), 5 μL MnCl_2 (5 mM), 50 μL reaction buffer (10X), 5 μL Taq polymerase ($5000\text{ U } \mu\text{L}^{-1}$). These were mixed by gentle pipetting and aliquoted to 5 times 100 μL in 0.2 mL PCR tubes. The tubes were placed in a gradient thermocycler at the appropriate positions to achieve annealing temperatures of 50.0 (2 tubes), 56.1, 60.2 or 65.5 $^{\circ}\text{C}$. The thermal cycling protocol is described in Table 3.2.

Table 3.2 - epPCR thermal cycling protocol

Step	Temp/ ^o C	Time/min	Repetitions
1	95	3	1
2	95	1	16
3	50.0, 56.1, 60.2 or 65.5	1	
4	72	2	
5	72	1	1
6	4	Hold	-

(ii) PCR product purification

QIAquick PCR purification kit was purchased from Qiagen and the method ‘*QIAquick PCR Purification Kit Protocol using a microcentrifuge*’ described in the manual⁽⁶²⁾ was followed. Pre-optimised buffers and columns were provided with the kit, the principle of which was, binding of the PCR product to a silica column in the presence of a chaotropic salt, $\text{pH} \leq 7.5$, washing in ethanol-buffer and elution in low salt buffer (10 mM Tris-HCl) at pH 8.5.

(iii) MEGAWHOP

The reaction was carried out at various concentrations of mega-primer, dNTPs and polymerase as shown in Table 3.3. The reagents were added to a 0.2 mL PCR tube in the order shown and were subjected to the thermal cycles shown in Table 3.4 in a thermocycler.

Table 3.3 - Volumes of reagents added to each reaction for MEGAWHOP PCR

Reaction Reagent	vol/ μ L						
	A	B	C	D	E	F	G
RO H ₂ O	36.3	37.3	36.8	35.4	35.4	37.3	37.3
RgDAAO/pPOT3 template plasmid (75.9 ng μ L ⁻¹)	1.3	1.3	1.3	1.3	1.3	1.3	1.3
epPCR products (112 ng μ L ⁻¹)	0.4	0.4	0.9	1.8	1.8	0.9	0.9
dNTPs (10 mM each)	1	0.5	0.5	1	0.5	-	0.5
DMSO	5	5	5	5	5	5	5
Pfu turbo polymerase buffer (X10)	5	5	5	5	5	5	5
Pfu turbo polymerase (2.5 U μ L ⁻¹)	1	0.5	0.5	0.5	1	0.5	-

Table 3.4 - MEGAWHOP thermal cycling protocol

Step	Temp/ ^o C	Time/min	Repetitions
1	95	3	1
2	95	0.5	30
3	55	1	
4	68	6	
6	4	Hold	-

(iv) Digestion of methylated DNA from PCR products, (v) repair of nicked DNA by transformation of XL1-Blue cells and (vi) plasmid purification.

The PCR products were digested to remove parental DNA as described in Section 3.2.1 and then the nicked plasmid DNA produced by PCR was repaired by transforming highly competent XL1-Blue cells (chemically- or electro-competent) with the PCR products. The transformed cells were grown on 90 mm LB agar/CAP

plates (Section 3.2.3). The library of XL1-blue colonies containing variant DAAO genes were transferred from the plate to centrifuge tubes by suspending the colonies in 2 mL LB/CAP, using a sterile plastic spreader to remove them from the surface of the agar, and pipetting the mixture to the tube. This step was repeated with a further 1 mL of LB/CAP. The library DNA was extracted from the cells using the plasmid purification method described in Section 3.2.1. For the purposes of storage this plasmid DNA was used for the transformation of TOP10 cells (Section 3.2.3) from which the DNA was again extracted and stored at -20 °C. For screening purposes BL21(DE3) cells were transformed with the library DNA.

Saturation mutagenesis

Saturation mutagenesis was performed using a PCR-based method, with primers containing the degenerate NNS codon at the site selected for randomisation. This codon provides for any of the 4 nucleotides at positions 1 and 2 and either deoxycytidine monophosphate (dCMP) or deoxyguanosine monophosphate (dGMP) at position 3. This degeneracy allows access to all 20 proteinogenic amino acid residues at the selected site. PfuTurbo DNA Polymerase and 10X reaction buffer (200 mM Tris-HCl (pH 8.8), 20 mM MgSO₄, 100 mM KCl, 100 mM (NH₄)₂SO₄, 1 % Triton X-100, 1 mg mL⁻¹ nuclease-free BSA) were purchased from Stratagene.

The procedure used was a modification of that described in PfuTurbo DNA Polymerase Instruction Manual version B.⁽⁶³⁾ The following were mixed in a thin-walled 0.2 mL PCR tube placed on ice, in the order given: 5 µL reaction buffer (10X concentrate), 1 µL template DNA (55 ng µL⁻¹), 1 µL each of forward and reverse primers (10 µM), 1 µL dNTPs (10 mM ea), 40 µL sterile RO water and 1 µL pfuTurbo polymerase (2.5 U µL⁻¹). The tube was placed in a thermocycler (Eppendorf Mastercycler Gradient) and subjected to the denaturing, annealing and extension cycle shown in Table 3.5.

Table 3.5 - PCR cycling parameters for site specific saturation mutagenesis

Step	Temp/°C	Time	Repetitions
1	95	30 s	X 1
2	95	30 s	X 16
3	68	1 min	
4	68	5 min 30 s	
5	4	Hold	X 1

The PCR products were processed further as described in steps (iv), (v) and (vi) of the preparation of epPCR libraries to produce unmethylated, nick-repaired plasmid ready for the transformation of the protein expression *E. coli* strain, BL21(DE3).

3.2.3 Transformation, growth and protein expression methods

Transformation of *E. coli* BL21 (DE3) chemically competent cells.

One Shot BL21 (DE3) chemically competent *E. coli* were purchased from Invitrogen and stored at -80 °C. One vial of cells (50 µL) per transformation was thawed on ice, DNA (0.1 – 50 ng) was added, mixed by gentle tapping and the suspension incubated on ice for 30 min. The cells were heat-shocked at 42 °C for 30 s and replaced to the ice. SOC medium (250 µL) prewarmed to 42 °C was added and the vial incubated on its side at 37 °C and 225 rpm for 1 h.⁽⁶⁴⁾

Transformation of *E. coli* TOP10 chemically competent cells

One Shot TOP10 chemically competent *E. coli* (50 µL/vial) were purchased from Invitrogen, stored at -80 °C and transformed as described for BL21(DE3) cells.⁽⁶⁵⁾

Transformation of *E. coli* XL1-Blue chemically competent cells

XL1-Blue chemically competent cells (200 µL/vial) were purchased from Stratagene and stored at -80 °C. The cells were thawed on ice and aliquoted (50 µL) to pre-chilled 15 mL polypropylene tubes. 1.42 M β-mercaptoethanol (0.85 µL) was added and the suspension mixed by gentle swirling. The tube was placed on ice for 10 min, with gentle mixing every 2 min. DNA (1-3 µL PCR products) was added and mixed by tapping the tube gently. The tubes were incubated on ice for 30 min, heat-pulsed

in a 42 °C water-bath for 45 s, before a further 2 min incubation on ice. Prewarmed SOC medium (900 µL, 42 °C) was added and the tube was transferred to a shaking incubator (37 °C, 225 rpm, 1 h).⁽⁶⁶⁾

Transformation of *E. coli* XL1-Blue electrocompetent cells

XL1-Blue electrocompetent cells (200 µL/vial) were purchased from Stratagene and stored at -80 °C. The cells were thawed on ice and aliquoted (40 µL) to 1.5 mL polypropylene tubes. DNA (1-3 µL PCR products) was added to each aliquot and the cells and DNA mixed by gentle tapping of the tube. The sample was transferred to a pre-chilled electroporation cuvette (0.1 cm gap) and pulsed once (1700 V, 200 Ω, 25 µF) using an electroporator. Prewarmed SOC medium (37 °C, 960 µL) was immediately added and the cells transferred to a 15 mL polypropylene tube and incubated (37 °C, 225 rpm, 1 h).⁽⁶⁷⁾

Transformation of *E. coli* XL1-Red chemically competent cells

XL1-Red chemically competent cells (200 µL/vial) were purchased from Stratagene and stored at -80 °C. The cells were transformed as described in section 3.2.3, with the exceptions that 100 µL cells were used and 1.7 µL β-mercaptoethanol (1.42 M) was added to these.⁽⁶⁸⁾

Antibiotic solutions

Antibiotic resistance is conferred to cells by the plasmids used as vectors for the DAAO gene. Those used in this work are shown in Table 3.6 which also shows the stock concentrations prepared. These were filter-sterilized and stored at -20 °C. Working concentrations were a 1 in 1000 dilution of the stock solution for all media types.

Table 3.6- Antibiotic resistance provided by plasmids used

Plasmid	Antibiotic resistance	Supplier	Stock concentration
pJLM402	Kanamycin (KAN)	Sigma-Aldrich	50 mg mL ⁻¹ in RO H ₂ O
pPOT3	Chloramphenicol (CAP)	Fluka	34 mg mL ⁻¹ in ethanol

Growth of transformants on LB agar plates

LB or TSB agar/antibiotic plates were prepared. Transformed cells were either streaked or spread onto the plates. Volumes used were adjusted according to the efficiency of the transformation in order to ensure a sufficient number of isolated colonies. The volumes generally required for the different cell strains used are shown in Table 3.7.

Table 3.7 - Approximate transformation volume plated to ensure many isolated colonies

<i>E. coli</i> strain	90 mm plate	145 mm plate
BL21(DE3) chemically competent cells		
TOP 10 chemically competent cells		
XL1-Blue electrocompetent cells	100 μ L	
XL1-Blue chemically competent cells	100 μ L	
XL1-Red chemically competent cells		

The plates were incubated at 37 °C overnight to allow colony formation. Exceptions to this were BL21 (DE3) cells which were incubated at 30 °C and XL1-Red cells which were grown for 24 to 30 h.

Growth of transformant in semi-solid agarose.

Media and SeaPrep agarose (Lonza) were prepared at double concentration. Thus, 40 or 60 g L⁻¹ LB broth or TSB respectively and 10 g L⁻¹ SeaPrep agarose solutions were prepared, autoclaved and stored at 4 °C. The autoclaving time for SeaPrep agarose was 5 min rather than the standard 15 min to protect gelling strength. Before use, the agarose was melted in a waterbath at 60 °C and both agarose and media (TSB or LB) were equilibrated to 37 °C. The solutions were mixed in a 1 to 1 ratio in 50 mL falcon tubes and transformed XL1-Blue cells (12.5 μ L/mL) or BL21(DE3) glycerol stock (5 μ L/mL of a 1x10⁶ dilution) were added and mixed by gentle inversion of the tubes 2 to 3 times. For growth in 1.1 mL, 96-well plates, the inoculated agarose was transferred from the tube to a sterile trough and from there to the plate using a multi-channel pipette (500 μ L/well). The tubes/plates were placed at 4 °C for ~2 h to allow the agarose to gel and then overnight at 37 °C for colony formation. Where protein expression was required, this was induced by placing the tubes/plates at 45 °C for 1 h and followed by growth at 37 °C. for a further 4 h. The

tubes and plates were transferred to a shaking incubator (225 rpm, 37 °C) for 1 h to loosen the colonies and the agarose was removed by centrifugation at 3220 x g for 30 min. The cell pellets were washed twice with warm (40 °C) potassium phosphate buffer (25 mL, 0.1 M, pH 7.6).

Small scale bacterial cultures

Following BL21 (DE3) colony formation on agar plates, an isolated colony was picked with a sterile inoculation loop, inoculated to 5 to 10 mL media containing the appropriate antibiotic and grown overnight at 37 °C, 225 rpm. The resulting cultures were used for DNA isolation (Section 3.2.1), or inoculation to larger volumes of media for expression of protein (below).

Fermentation of *E. coli* expressing DAAO

Volumes of 50 to 700 mL LB/antibiotic were inoculated with a 1 in 1000 dilution of small-scale BL21 (DE3) cultures and placed at 30 °C, 225 rpm until log phase growth was reached (OD₆₀₀ of between 0.4 and 0.6). Protein expression was induced by increasing the temperature to 45 °C. The cells were grown for a further 4 h at 37 °C, 225 rpm post induction and harvested by centrifugation. 50 – 100 mL cultures were transferred directly to 50 mL falcon tubes and centrifuged at 3220 x g for 10 min. The supernatant was removed and the pellet resuspended in 30 mL potassium phosphate buffer (0.1 M, pH 7.6). The buffer was removed by a repeat of the centrifugation procedure and the cell pellets were stored at -20 °C. Larger volumes were first transferred to 500 mL centrifuge tubes and centrifuged at 6371 x g for 20 min. The supernatant was removed and the pellets were resuspended in 30 mL potassium phosphate buffer (0.1 M, pH 7.6) and transferred to 50 mL falcon tubes. The buffer was removed as above and the pellets stored at -20 °C.

For analysis of protein expression during growth, 1.5 mL samples were removed, the OD₆₀₀ recorded and the samples centrifuged at 15 700 x g for 5 min. The supernatant was removed and the pellet stored at -20 °C prior to analysis by sodium dodecylsulfate polyacrylamide gel electrophoresis (SDS-PAGE, Section 3.2.4).

Growth and fermentation of *E. coli* expressing DAAO saturation mutagenesis libraries in 96-well, 2.2 mL plates

Master plates were created by picking BL21(DE3) *E. coli* colonies containing variant DAAO genes from agar plates and transferring these individually to 800 μ L LB/CAP in 96-well, 2.2 mL plates using sterile pipette tips. The plates were covered with gas permeable membranes (Thermo Scientific) and placed overnight at 37 °C, 225 rpm. 5 μ L overnight culture from each well of the master plates was transferred to fresh 2.2 mL, 96-well plates containing 800 μ L LB/CAP using a multi-channel pipette with sterile tips. The copy plates were covered with a gas-permeable membranes and placed at 30 °C until OD₆₀₀ values of approximately 0.5 were reached, protein expression was induced and the cultures were grown overnight at 30 °C, 225 rpm. Master and copy plates were centrifuged at 3315 x g for 20 min and the supernatant removed. Master plate cell pellets were resuspended in 50 μ L sterile glycerol solution (15 % v/v in H₂O). Master and copy plates were sealed with aluminium foil and stored at -20 °C. Prior to assay, pellets in the copy plates were resuspended in 1 mL potassium phosphate buffer (0.1 M). 50 μ L of the suspension was used in the assay described in Section 3.2.5). Pellet resuspension and transfer of cells to the assay plates were carried out at 4 °C.

Expression of oxidase enzyme by heat inducible promoter (pPOT3 and pJLM402 vectors).

Upon reaching log phase growth, protein expression was induced by heating the sample to 42 °C with continued shaking at 225 rpm. Culture volumes of 50 mL were held at this elevated temperature for 15 min, 100 mL for 20 min and 700 mL for 1 h. Cultures grown in 96-well, 2.2 mL plates were held at 42 °C for 30 min.

Glycerol stocks

50 μ L samples were removed during log phase growth (Section 3.2.3) and transferred 1.5 mL storage tubes. 50 μ L sterile glycerol solution (30 % v/v in H₂O) was added and mixed by vortexing. The vials were frozen in liquid nitrogen and stored at -80 °C.

3.2.4 Protein purification and analysis

Preparation of CFE

SoluLyse Bacterial Protein Extraction Reagent was purchased from Genlantis. Frozen cell pellets produced from an expression culture (Section 3.2.3) were defrosted and resuspended in SoluLyse reagent. Pellets from 1.5 mL culture were resuspended in 150 μ L reagent. Larger pellets were resuspended in 20 mL reagent for every gram wet cell weight.⁽⁶⁹⁾ The resuspended pellets were rotated at room temperature for 10 min. 1.5 mL tubes were centrifuged at 15 700 x g for 5 min and 50 mL tubes were centrifuged at 3 220 x g for 30 min. The supernatant containing soluble protein was retained.

SDS-PAGE

SDS-PAGE was used to separate and estimate the molecular weight of proteins. Kaleidoscope 10 – 250 kD precision plus protein standard and precast polyacrylamide gels (10-20 %) were purchased from Biorad. SDS sample buffer (according to Lämelli, X2) and EZBlue gel staining reagent were purchased from Sigma-Aldrich. Cell pellets were resuspended in RO water and normalised according to the measured OD₆₀₀ at the time of sampling, with the resuspension volume given by OD₆₀₀ x 100 μ L. Resuspended pellets, cell free extracts or purification fractions were mixed in a 1 to 1 ratio with 2X SDS sample buffer. Resuspended cells were subjected to three freeze-thaw cycles using a heat block (95 °C) and liquid nitrogen and then all samples were denatured on a heat block at 95 °C for 10 min. A precast gel was placed in an SDS tank which was filled with Lämelli buffer (Section 3.2.7). 10 μ L protein standard and 25 μ L of each buffered sample was loaded onto the gel. The electrophoresis was carried out at 100 V for ~1 h. The gel was then incubated with EZBlue gel staining reagent on an orbital shaker for 1-2 h and with RO H₂O for several hours to remove background stain.

Total protein concentration

There are several methods for the determination of the total protein concentration of a sample. Measurement of UV absorbance is the quickest and easiest but also the

least accurate. For a pure sample with a known extinction coefficient (ϵ) the Beer-Lambert Law (Section 5.7.2) can be used to determine protein concentration. If the sample is not pure an approximation can be made based on the absorbance of tyrosine and tryptophan residues at ~ 280 nm. Nucleic acids also absorb at 280 nm but more strongly at 260 nm and the expression in Equation 5 has been derived to fit with experimental data.⁽⁷⁰⁾ This allows an estimation of protein concentration.

$$\text{protein concentration (mg mL}^{-1}\text{)} = (1.55 \times A_{280}) - (0.76 \times A_{260})$$

Equation 5 – A_{280} = absorbance measured at 280 nm, A_{260} = absorbance measured at 260 nm.

The protein sample was diluted until a measurement could be obtained within the linear region of the curve (less than 1.0), transferred to a measuring cuvette and the absorbance at 260 and 280 nm measured using a spectrophotometer. The measurements were blanked using the relevant buffer.

A more accurate method for determining protein concentration is the bicinchoninic acid (BCA) assay. Cu^{2+} is reduced by the amino acid residues cysteine, cystine, tyrosine and tryptophan, as well as by the peptide backbone, when in alkaline solution. Cu^+ ions complex with two molecules of BCA to form a complex with an absorbance maximum at 562 nm. A standard curve was produced using dilutions of a sample of BSA of known concentration which was measured in triplicate. These data were used to produce a standard curve from which the concentration of the experimental sample was estimated (Figure 2.18). The standard curve was reproduced each time a protein concentration estimation was made.

A BCA Protein Assay Kit was purchased from Pierce and contained BCA Reagent A (bicinchoninic acid in buffer), BCA Reagent B (4% cupric sulfate) and Albumin Standard (BSA, 2.0 mg mL⁻¹ in 0.9% saline and 0.05% sodium azide). BSA dilutions from 2000 to 0 $\mu\text{g mL}^{-1}$ were prepared as standards and BCA reagents A and B were combined in a 50 to 1 ratio. 25 μL of each standard and sample was placed in a microtitre plate in triplicate. 200 μL of the combined BCA reagents was added to

each well containing sample or standard and the plate was incubated at 37 °C for 30 min. The plate was cooled to room temperature and the absorbance measured at 562 nm on a plate reader. The readings were blanked, the standard curve was produced from the wells containing BSA dilutions and the total protein content of the sample wells was estimated against the resulting curve.

3.2.5 Colorimetric assays

Liquid-phase assay

Enzyme turnover is coupled to a peroxidase-based colorimetric assay. There are several chromogenic compounds which can be used for this purpose and here 4-amino antipyrine (AAP) and 2,4,6-tribromo-3-hydroxybenzoic acid (TBHBA), which form a red quinone-imine dye ($\lambda_{\text{max}} = 515 \text{ nm}$) upon co-oxidation, were used.⁽⁷¹⁾

Stock assay solution

140 μL AAP (1 M) and 1.85 mL TBHBA (53.4 mM in DMSO) were added to 20 mL potassium phosphate buffer (1 M, pH 7.6). This solution was made up to 45 mL with RO water and stored in a foil-covered bottle at -20 °C. Prior to use, 5 mL horseradish peroxidase (HRP) (1 mg mL⁻¹) was added to the defrosted solution.

Stock substrate solutions

Substrates were dissolved in RO water at a D-enantiomer concentration of 20 mM unless otherwise stated. The pH was adjusted to between 7.0 and 8.0 using 0.1 M NaOH or 0.1 M HCl.

Standard liquid-phase assay procedure

Assays were performed in Costar 96 well, flat-bottom microtitre plates. The stock substrate and assay mixtures were combined in a ratio of 2:1. 50 μL resuspended cells or 10 μL cell free extract (CFE) and 40 μL RO water was added to each well, followed by 150 μL of the substrate/assay mixture and the plate immediately placed

in a plate reader. Final concentrations in each reaction were 0.7 mM AAP, 0.5 mM TBHBA, 100 mM potassium phosphate, 0.025 mg mL⁻¹ HRP and 10 mM substrate (*R*-enantiomer).

Solid-phase assay

Stock assay solution

400 µL HRP (1 mg mL⁻¹) and 4 mL potassium phosphate buffer (1 M, pH 7.6) were added to 1 SIGMAFAST™ 3,3'-Diaminobenzidine tablet which had been dissolved in 15 mL RO water and the solution was made up to 20 mL using RO water.

Stock substrate solution

These were prepared as for liquid-phase assay stock substrate solutions.

Standard solid-phase assay procedure

BL21(DE3) cells were transformed with library or control DNA as described in section 3.2.3, with the exception that 900 µL SOC was added. The resulting transformed cells were spread onto PVDF membranes (Hybond-N, Amersham Biosciences) placed on LB agar plates containing the relevant antibiotic, taking care to ensure an even spread of the transformation mixture over the whole membrane. The plates were incubated overnight at 30 °C. 50 µL of cells transformed using this procedure produced approximately 3000 evenly separated colonies on a 145 mm diameter plate.

Filter paper was placed into a Petri dish and soaked with 0.1 mg mL⁻¹ HRP solution. The colony containing membrane was removed from the agar plate, frozen in liquid nitrogen for 30 s causing partial cell lysis, dried and then placed onto the HRP-soaked filter paper. The Petri dish was lidded and left to incubate at room temperature for 20 min, allowing any background HRP activity to take place.

The stock assay and stock substrate solutions described above were combined in a 1:1 ratio. A fresh filter paper was placed in a Petri dish and soaked with 2 to 3 mL of

this assay/substrate mixture. The colony-containing membrane was moved from the HRP filter to the substrate filter and allowed to develop at room temperature overnight.

Colonies showing an increase in colour development over the parental colonies with respect to test substrates were picked and grown overnight in 10 mL LB/antibiotic at 37 °C, 225 rpm. The resulting cultures were divided and used both for re-assaying in the liquid-phase as whole cells or CFE (section 3.2.4) and in preparation for DNA sequencing (section 3.2.1).

3.2.6 Biotransformations

An approximately 1.3 g pellet was resuspended in 5 mL potassium phosphate buffer (pH 7.6). 5 mL solution of racemic substrate was added (0.04 M) and the reaction placed at 37 °C, 225 rpm. Samples were removed for analysis at $T = 0$ and at appropriate time points thereafter.

Analysis - Reverse-phase chiral HPLC

Chirobiotic-T column was purchased from Astec (Sigma-Aldrich). A 0.5 mL sample of biotransformation mixture was removed and centrifuged at 15 000 x g for 5 min. The supernatant was transferred to a fresh tube and placed at 95 °C for 10 min before a further centrifugation as above. The final supernatant was filtered (0.45 μ M) and transferred to an HPLC vial.

HPLC conditions:

Column: Astec Chirobiotic-T

1,2,3,4-Tetrahydroisoquinoline-3-carboxylic acid: 90% MeOH, 10% water, using a flow rate of 1 mL.min⁻¹, at 25 °C, and an injection volume of 1 μ L. The retention time of each enantiomer was 14.2 and 27.3 min respectively.

Pipicolinic acid: 80% Acetonitrile, 20% water, using a flow rate of 2 mL.min⁻¹, at 10 °C, and an injection volume of 5 µL. The retention time of each enantiomer was 10.9 and 14.2 min respectively.

β-homophenylalanine: 95% MeOH, 5%TEA buffer (0.1%, pH 4.1), using a flow rate of 0.4 mL.min⁻¹, at 25 °C. The retention time of each enantiomer was 23.0 and 26.3 min respectively.

Phenomenex D-penicillamine

Pipicolinic acid: 2 mM CuSO₄, 3 % MeOH, 0.8 mL/min, injection volume 1 µL. The retention time of each enantiomer was 6.4 and 10.0 min respectively.

3.2.7 Buffer and reagent recipes

Growth media

Media were prepared at the concentrations specified by the supplier in DI or RO water, autoclaved and stored at 4 °C.

LB broth

Dehydrated LB (10 g L⁻¹ tryptone, 5 g L⁻¹ yeast extract, 5g L⁻¹ NaCl) was purchased from Sigma-Aldrich.

TSB

Dehydrated TSB (17.0 g L⁻¹ caseine peptone, 3.0 g L⁻¹ soya peptone, 5.0 g L⁻¹ NaCl, 2.5 g L⁻¹ K₂HPO₄, 2.5 g L⁻¹ glucose, pH 7.3) was purchased from Oxoid.

LB agar

Dehydrated LB agar (20 g L⁻¹ LB, 15 g L⁻¹ agar) was purchased from Sigma-Aldrich. Alternatively, pre-prepared, sterile LB agar was purchased from MIB stores.

Agar

Dehydrated agar (12 g L⁻¹) agar was purchased from Oxoid.

SOC medium

SOC medium (2 % tryptone, 0.5 % yeast extract, 10 mM NaCl, 2.5 mM KCl, 10 mM MgCl₂, 10 mM MgSO₄, 20 mM glucose) was purchased from Invitrogen.

Buffers

Triethylammonium acetate buffer (TEAA)

A solution of triethyl amine (0.1 %) was prepared in HPLC grade water and acetic acid was added to pH 4.1. The resulting solution was filtered (0.2 μM).

Stock ammonium acetate solution (5 M)

192.7 g ammonium acetate, purchased from BDH Laboratory Supplies, was dissolved in 0.5 L RO water (5 M) and stored at room temperature.

Potassium phosphate buffer (1 M)

Mono- and dibasic potassium phosphate were purchased from Fisher Scientific. 1 M solutions of each were prepared in RO water (136.09 g and 174.18 g respectively, 1 L each), autoclaved and stored at 4 °C. Prior to use, the solutions were combined according to the ratio given by the Henderson-Hasselbalch equation (Equation 6) to give the desired pH (pK_a = 6.88), which was checked and adjusted using a pH meter.

$$\text{pH} = \text{pK}_a + \log \left(\frac{[\text{K}_2\text{HPO}_4]}{[\text{KH}_2\text{PO}_4]} \right)$$

Equation 6 - Henderson-Hasselbalch equation

EDTA stock solution (0.5 M)

93.1 g disodium EDTA dihydrate was dissolved in 400 mL DI H₂O, the pH adjusted to 8.0 using NaOH pellets and the volume made up to 500 mL with DI H₂O.

TAE buffer (50 X)

242.2 g Tris base was dissolved in 800 mL DI H₂O. 57.1 mL glacial acetic acid and 100 mL EDTA (0.5 M, pH 8.0) were added and the volume made up to 1 L with DI H₂O.

Lämelli buffer (SDS running buffer)

30.3 g Tris-base (0.025 M), 144.1 g glycine (0.192 M) and 10.0 g SDS (1 %) were dissolved in 10 L RO water.

4 REFERENCES

1. Breuer, M., Ditrich, K., Habicher, T., Hauer, B., Kessler, M., Stuermer, R. and Zelinski, T. (2004) Industrial methods for the production of optically active intermediates. *Angewandte Chemie, International Edition*, **43**, 788-824.
2. Sunggyu Lee, L.L. (2005) *Encyclopedia of Chemical Processing*. CRC Press, London.
3. Maruoka, K. (2008) Practical aspects of recent asymmetric phase-transfer catalysis. *Organic Process Research & Development*, **12**, 679-697.
4. Najera, C. and Sansano, J.M. (2007) Catalytic asymmetric synthesis of α -amino acids. *Chemical Reviews*, **107**, 4584-4671.
5. Fotheringham, I.G., Taylor, P.P. and Ton, J.L. (1998) USA patent no. 96-723896 5728555.
6. Weiner, B., Poelarends, G.J., Janssen, D.B. and Feringa, B.L. (2008) Biocatalytic enantioselective synthesis of *N*-substituted aspartic acids by aspartate ammonia lyase. *Chemistry - a European Journal*, **14**, 10094-10100.
7. Paradisi, F., Conway, P.A., Maguire, A.R. and Engel, P.C. (2008) Engineered dehydrogenase biocatalysts for non-natural amino acids: efficient isolation of the D-enantiomer from racemic mixtures. *Organic & Biomolecular Chemistry*, **6**, 3611-3615.
8. Wegman, M.A., Janssen, M.H.A., van Rantwijk, F. and Sheldon, R.A. (2001) Towards biocatalytic synthesis of β -lactam antibiotics. *Advanced Synthesis & Catalysis*, **343**, 559-576.
9. Enright, A., Alexandre, F.-R., Roff, G., Fotheringham, I.G., Dawson, M.J. and Turner, N.J. (2003) Stereoinversion of β - and γ -substituted α -amino acids using a chemo-enzymatic oxidation-reduction procedure. *Chemical Communications*, 2636-2637.
10. Roff, G.J., Lloyd, R.C. and Turner, N.J. (2004) A versatile chemo-enzymatic route to enantiomerically pure β -branched α -amino acids. *Journal of the American Chemical Society*, **126**, 4098-4099.
11. Alexandre, F.R., Pantaleone, D.P., Taylor, P.P., Fotheringham, I.G., Ager, D.J. and Turner, N.J. (2002) Amine-boranes: effective reducing agents for the deracemisation of DL-amino acids using L-amino acid oxidase from *Proteus myxofaciens*. *Tetrahedron Letters*, **43**, 707-710.
12. Carr, R., Alexeeva, M., Enright, A., Eve, T.S.C., Dawson, M.J. and Turner, N.J. (2003) Directed evolution of an amine oxidase possessing both broad substrate specificity and high enantioselectivity. *Angewandte Chemie-International Edition*, **42**, 4807-4810.
13. Thiruvengadam, T.K., Gould, S.J., Aberhart, D.J. and Lin, H.J. (1983) Biosynthesis of streptothricin-F .5. Formation of β -lysine by *Streptomyces* L-1689-23. *Journal of the American Chemical Society*, **105**, 5470-5476.
14. von Nussbaum, F. and Spiteller, P. (2004) *β -amino acids in Nature*. Wiley VCH, Heidelberg.
15. Juaristi, E. and Soloshonok, V.A. (1997) *Enantioselective Synthesis of β -Amino Acids*. Wiley-VCH, New Jersey.

16. D'Amico, D.C., Aya, T., Human, J., Fotsch, C., Chen, J.J., Biswas, K., Riahi, B., Norman, M.H., Willoughby, C.A., Hungate, R. *et al.* (2007) Identification of a nonpeptidic and conformationally restricted bradykinin B1 receptor antagonist with anti-inflammatory activity. *Journal of Medicinal Chemistry*, **50**, 607-610.
17. Nachman, R.J., Ben Aziz, O., Davidovitch, M., Zubrzak, P., Isaac, R.E., Strey, A., Reyes-Rangel, G., Juaristi, E., Williams, H.J. and Altstein, M. (2009) Biostable β -amino acid PK/PBAN analogs: Agonist and antagonist properties. *Peptides*, **30**, 608-615.
18. Zubrzak, P., Williams, H., Coast, G.M., Isaac, R.E., Reyes-Rangel, G., Juaristi, E., Zabrocki, J. and Nachman, R.J. (2007) β -amino acid analogs of an insect neuropeptide feature potent bioactivity and resistance to peptidase hydrolysis. *Biopolymers*, **88**, 76-82.
19. Faulconbridge, S.J., Holt, K.E., Sevillano, L.G., Lock, C.J., Tiffin, P.D., Tremayne, N. and Winter, S. (2000) Preparation of enantiomerically enriched aromatic β -amino acids via enzymatic resolution. *Tetrahedron Letters*, **41**, 2679-2681.
20. Wu, B., Szymanski, W., Wietzes, P., de Wildeman, S., Poelarends, G.J., Feringa, B.L. and Janssen, D.B. (2009) Enzymatic synthesis of enantiopure α - and β -amino acids by phenylalanine aminomutase-catalysed amination of cinnamic acid derivatives. *ChemBiochem*, **10**, 338-344.
21. Kim, J., Kyung, D., Yun, H., Cho, B.K., Seo, J.H., Cha, M. and Kim, B.G. (2007) Cloning and characterization of a novel β -transaminase from *Mesorhizobium* sp Strain LUK: a new biocatalyst for the synthesis of enantiomerically pure β -amino acids. *Applied and Environmental Microbiology*, **73**, 1772-1782.
22. Krebs, H.A. (1935) Metabolism of amino acids. III. Deamination of amino acids. *Biochemical Journal*, **29**, 1620-1644.
23. Pilone, M.S. (2000) D-amino acid oxidase: new findings. *Cellular and Molecular Life Sciences*, **57**, 1732-1747.
24. Pollegioni, L., Piubelli, L., Sacchi, S., Pilone, M.S. and Molla, G. (2007) Physiological functions of D-amino acid oxidases: from yeast to humans. *Cellular and Molecular Life Sciences*, **64**, 1373-1394.
25. Alexeeva, M., Carr, R. and Turner, N.J. (2003) Directed evolution of enzymes: new biocatalysts for asymmetric synthesis. *Organic & Biomolecular Chemistry*, **1**, 4133-4137.
26. Pollegioni, L., Molla, G., Sacchi, S., Rosini, E., Verga, R. and Pilone, M.S. (2008) Properties and applications of microbial D-amino acid oxidases: current state and perspectives. *Applied Microbiology and Biotechnology*, **78**, 1-16.
27. Farinas, E.T., Bulter, T. and Arnold, F.H. (2001) Directed enzyme evolution. *Current Opinion in Biotechnology*, **12**, 545-551.
28. Stemmer, W.P.C. (1994) Rapid evolution of a protein *in vitro* by DNA shuffling. *Nature*, **370**, 389-391.
29. Arnold, F.H. (2001) Combinatorial and computational challenges for biocatalyst design. *Nature* **409**, 253.

30. Freeland, S.J. and Hurst, L.D. (1998) The genetic code is one in a million. *Journal of Molecular Evolution*, **47**, 238-248.
31. Berg, J.M., Tymoczko, J.L., Stryer, L. and Stryer, L. (2002) *Biochemistry*. W.H. Freeman, New York.
32. Wong, T.S., Roccatano, D. and Schwaneberg, U. (2007) Challenges of the genetic code for exploring sequence space in directed protein evolution. *Biocatalysis and Biotransformation*, **25**, 229-241.
33. Stratagene. (2004) *XL1-Red Competent Cells Manual*.
34. Cadwell, R.C. and Joyce, G.F. (1992) Randomization of genes by PCR-mutagenesis. *PCR-Methods and Applications*, **2**, 28-33.
35. Wong, T.S., Roccatano, D., Zacharias, M. and Schwaneberg, U. (2006) A statistical analysis of random mutagenesis methods used for directed protein evolution. *Journal of Molecular Biology*, **355**, 858-871.
36. Wong, T.S., Roccatano, D. and Schwaneberg, U. (2007) Are transversion mutations better? A Mutagenesis Assistant Program analysis on P450 BM-3 heme domain. *Biotechnology Journal*, **2**, 133-142.
37. Henriksen, A., Smith, A.T. and Gajhede, M. (1999) The structures of the horseradish peroxidase C-ferulic acid complex and the ternary complex with cyanide suggest how peroxidases oxidize small phenolic substrates. *Journal of Biological Chemistry*, **274**, 35005-35011.
38. Carr, R. (2005) PhD Thesis, University of Edinburgh.
39. Morgan, J.L. (2008) PhD Thesis, University of Edinburgh.
40. Pollegioni, L., Molla, G., Campaner, S., Martegani, E. and Pilone, M.S. (1997) Cloning, sequencing and expression in *E. coli* of a D-amino acid oxidase cDNA from *Rhodotorula gracilis* active on cephalosporin C. *Journal of Biotechnology*, **58**, 115-123.
41. Pollegioni, L., Diederichs, K., Molla, G., Umhau, S., Welte, W., Ghisla, S. and Pilone, M.S. (2002) Yeast D-amino acid oxidase: Structural basis of its catalytic properties. *Journal of Molecular Biology*, **324**, 535-546.
42. Alonso, J., Barredo, J.L., Armisen, P., Diez, B., Salto, F., Guisan, J.M., Garcia, J.L. and Cortes, E. (1999) Engineering the D-amino acid oxidase from *Trigonopsis variabilis* to facilitate its overproduction in *Escherichia coli* and its downstream processing by tailor-made metal chelate supports. *Enzyme and Microbial Technology*, **25**, 88-95.
43. Faotto, L., Pollegioni, L., Cecilian, F., Ronchi, S. and Pilone, M.S. (1995) The primary structure of D-amino acid oxidase from *Rhodotorula gracilis*. *Biotechnology Letters*, **17**, 193-198.
44. Tishkov, V.I. and Khoronenkova, S.V. (2005) D-amino acid oxidase: Structure, catalytic mechanism, and practical application. *Biochemistry-Moscow*, **70**, 40-54.
45. Rosini, E., Molla, G., Rossetti, C., Pilone, M.S., Pollegioni, L. and Sacchi, S. (2008) A biosensor for all D-amino acids using evolved D-amino acid oxidase. *Journal of Biotechnology*, **135**, 377-384.
46. Carr, R., Alexeeva, M., Dawson, M.J., Gotor-Fernandez, V., Humphrey, C.E. and Turner, N.J. (2005) Directed evolution of an amine oxidase for the preparative deracemisation of cyclic secondary amines. *ChemBiochem*, **6**, 637-639.

47. Umhau, S., Pollegioni, L., Molla, G., Diederichs, K., Welte, W., Pilone, M.S. and Ghisla, S. (2000) The X-ray structure of D-amino acid oxidase at very high resolution identifies the chemical mechanism of flavin-dependent substrate dehydrogenation. *Proceedings of the National Academy of Sciences of the United States of America*, **97**, 12463-12468.
48. Shafikhani, S., Siegel, R.A., Ferrari, E. and Schellenberger, V. (1997) Generation of large libraries of random mutants in *Bacillus subtilis* by PCR-based plasmid multimerization. *Biotechniques*, **23**, 304-310.
49. Escalettes, F. and Turner Nicholas, J. (2008) Directed evolution of galactose oxidase: generation of enantioselective secondary alcohol oxidases. *Chembiochem*, **9**, 857-860.
50. Beckman, R.A., Mildvan, A.S. and Loeb, L.A. (1985) On the fidelity of DNA-replication: manganese mutagenesis *in vitro*. *Biochemistry*, **24**, 5810-5817.
51. Patrick, W.M., Firth, A.E. and Blackburn, J.M. (2003) User-friendly algorithms for estimating completeness and diversity in randomized protein-encoding libraries. *Protein Engineering*, **16**, 451-457.
52. Alexeeva, M., Enright, A., Dawson, M.J., Mahmoudian, M. and Turner, N.J. (2002) Deracemization of α -methylbenzylamine using an enzyme obtained by *in vitro* evolution. *Angewandte Chemie-International Edition*, **41**, 3177-3180.
53. Reiss, R. (2008) PhD Thesis, University of Manchester.
54. Bailey, K.R., Ellis, A.J., Reiss, R., Snape, T.J. and Turner, N.J. (2007) A template-based mnemonic for monoamine oxidase (MAO-N) catalyzed reactions and its application to the chemo-enzymatic deracemization of the alkaloid (+/-)-crispine A. *Chemical Communications* 3640-3642.
55. Zhang, J.H., Chung, T.D.Y. and Oldenburg, K.R. (1999) A simple statistical parameter for use in evaluation and validation of high throughput screening assays. *Journal of Biomolecular Screening*, **4**, 67-73.
56. Sacchi, S., Lorenzi, S., Molla, G., Pilone, M.S., Rossetti, C. and Pollegioni, L. (2002) Engineering the substrate specificity of D-amino-acid oxidase. *Journal of Biological Chemistry*, **277**, 27510-27516.
57. Boselli, A., Sacchi, S., Job, V., Pilone, M.S. and Pollegioni, L. (2002) Role of tyrosine 238 in the active site of *Rhodotorula gracilis* D-amino acid oxidase. A site-directed mutagenesis study. *European Journal of Biochemistry*, **269**, 4762-4771.
58. Kochhar, S., Mouratou, B. and Christen, P. (2001) Amino acid analysis by high-performance liquid chromatography after derivatization with 1-fluoro-2,4-dinitrophenyl-5-L-alanine amide (Marfey's reagent). *Methods in Molecular Biology* **159**, 49-54.
59. Qiagen. (2006) *QIAprep Miniprep Handbook*. 2nd edition.
60. Roche. (2007) *Agarose Gel DNA Extraction Kit Manual*.
61. Miyazaki. (2004) *Directed Evolution Library Creation: Methods and Protocols*. Humana Press Inc., Totowa.
62. Qiagen. (2008) *QIAquick Spin Handbook*.
63. Stratagene. (2007) *PfuTurbo DNA Polymerase Instruction Manual*. Version B.

64. Invitrogen. (2002) *One Shot BL21(DE3) Competent Cells Manual*.
65. Invitrogen. (2004) *One Shot TOP10 Competent Cells Manual*.
66. Stratagene. (2004) *XL1-Blue Competent Cells Manual*.
67. Stratagene. (2004) *XL1-Blue Electroporation-Competent Cells Manual*. Revision #074003.
68. Stratagene. (2004) *XL1-Red Competent Cells Manual*. Revision #064003.
69. Genlantis. (2006) *SoluLyse Bacterial Protein Extraction Reagent Manual*.
70. Layne, E. (1957) Spectrophotometric and turbidimetric methods for measuring proteins. *Methods in Enzymology*, **3**, 447-454.
71. Moshides, J.S. (1988) Enzymic determination of the free-cholesterol fraction of high-density lipoprotein in plasma with use of 2,4,6-tribromo-3-hydroxybenzoic acid. *Clinical Chemistry*, **34**, 1799-1804.
72. Cornishbowden, A. (1985) Nomenclature for incompletely specified bases in nucleic acid sequences - Recommendations 1984. *European Journal of Biochemistry*, **150**, 1-5.

5 APPENDICES

5.1 PARENTAL DNA SEQUENCES

5.1.1 *R. gracilis* DAAO

1 ATGCACTCGCAGAAGCGCGTCGTTGTCCTCGGATCAGGCGTTATCGGTCTGAGCAGCGCCCTCATCCTCG
 M H S Q K R V V V L G S G V I G L S S A L I L
 71 CTCGGAAGGGCTACAGCGTGCATATTCGCGCGCGACTTGCCGGAGGACGTCTCGAGCCAGACTTTTCGC
 A R K G Y S V H I L A R D L P E D V S S Q T F A
 141 TTCACCATGGGCTGGCGCGAATTGGACGCCTTTCATGACGCTTACAGACGGTCCCTCGACAAGCAAATGG
 S P W A G A N W T P F M T L T D G P R Q A K W
 211 GAAGAACCGACTTTCAAGAAGTGGGTCGAGTTGGTCCCGACGGGCCATGCCATGTGGCTCAAGGGGACGA
 E E P T F K K W V E L V P T G H A M W L K G T
 281 GGGCGTTCGCGCAGAACGAAGACGGCTTGCTCGGGCACTGGTACAAGGACATCACGCCAAATTACCGCCC
 R R F A Q N E D G L L G H W Y K D I T P N Y R P
 351 CCTCCCATCTTCCGAATGTCCACCTGGCGCTATCGGCGTAACTACGACACCCTCTCCGTCCACGCACCA
 L P S S E C P P G A I G V T Y D T L S V H A P
 421 AAGTACTGCCAGTACCTTGCAAGAGAGCTGCAGAAGCTCGGCGCGACGTTTGAGAGACGGACCGTTACGT
 K Y C Q Y L A R E L Q K L G A T F E R R T V T
 491 CGCTTGAGCAGGCGTTCGACGGTGC GGATTTGGTGGTCAACGCTACGGGACTTGGCGCCAAGTCGATTGC
 S L E Q A F D G A D L V V N A T G L G A K S I A
 561 GGGCATCGACGACCAAGCCGCCGAGCCAATCCGCGCCAAACCGTCCCTCGTCAAGTCCCCATGCAAGCGA
 G I D D Q A A E P I R G Q T V L V K S P C K R
 631 TGCACGATGGACTCGTCCGACCCCGCTTCTCCCGCCTACATCATTCCCGGACCAGGTGGCGAAGTCATCT
 C T M D S S D P A S P A Y I I P R P G G E V I
 701 GCGGCGGGACGTACGGCGTGGGAGACTGGGACTTGCTGTGCAACCCAGAGACGGTCCAGCGGATCCTCAA
 C G G T Y G V G D W D L S V N P E T V Q R I L K
 771 GCACTGCTTGCGCCTCGACCCGACCATCTCGAGCGACGGAACGATCGAAGGCATCGAGGTCCCTCCGCCAC
 H C L R L D P T I S S D G T I E G I E V L R H
 841 AACGTCGGCTTGCGACCTGCACGACGAGGCGGACCCCGCGTCGAGGCAGAACGGATCGTCCCTGCCTCTCG
 N V G L R P A R R G G P R V E A E R I V L P L
 911 ACCGGACAAAGTCGCCCCCTCGCTCGGCAGGGGACGCGCACGAGCGGCGAAGGAGAAGGAGGTACGCT
 D R T K S P L S L G R G S A R A A K E K E V T L
 981 TGTGCATGCGTATGGCTTCTCGAGTACGGGATACCAGCAGAGTTGGGGCGCGGCGGAGGATGTCGCGCAG
 V H A Y G F S S T G Y Q Q S W G A A E D V A Q
 1051 CTCGTCGACGAGGCGTTCACGGGTACCACGGCGCGGCGGGAGTCGAAGTTGTAG
 L V D E A F Q R Y H G A A R E S K L *

5.1.2 *T. variabilis* DAAO

1 atggctaaaatcgtttgttattggtgccggtgttgccggtttaactacagctttcaactttcgtaag
 M A K I V V I G A G V A G L T T A L Q L L R K

71 gacatgaggttacaattgtgtccgagtttacgcccggtgatcttagtatcggatataccttgcocttgggc
 G H E V T I V S E F T P G D L S I G Y T S P W A

141 aggtgccaactggctcacatttttacgatggaggcaagtttagccgactacgatgccgtctttatcctatc
 G A N W L T F Y D G G K L A D Y D A V S Y P I

211 ttgcgagagctggctcgaagcagccccgaggctggaattcgactcatcaaccaacgctcccatgtttctca
 L R E L A R S S P E A G I R L I N Q R S H V L

281 agcgtgatttcctaaactggaaggtgccatgtcggccatctgtcaacgcaaccctggttcaaaaacac
 K R D L P K L E G A M S A I C Q R N P W F K N T

351 agtcgattctttcgagattatcgaggacaggtccaggattgtccacgatgatgtggcttatctagtcgaa
 V D S F E I I E D R S R I V H D D V A Y L V E

421 tttgcttccgtttgtatccacaccggagtctacttgaactggctgatgtccaatgcttatcgtcggcg
 F A S V C I H T G V Y L N W L M S Q C L S L G

491 ccacggtggttaaacgtcgagtgaaccatatcaaggatgccaatttactacactcctcaggatcacgccc
 A T V V K R R V N H I K D A N L L H S S G S R P

561 cgacgtgattgtcaactgtagtggttctctttgcccggttcttgggaggcgtcgaggacaagaagatgtac
 D V I V N C S G L F A R F L G G V E D K K M Y

631 cctattcgaggacaagtcgtccotttgttcgaaacttctctttcttttatggcctccttttccagcactcctg
 P I R G Q V V L V R N S L P F M A S F S S T P

701 aaaagaaaaatgaagacgaagctctatatatcatgacccgattcgatggtacttctatcattggcggttg
 E K E N E D E A L Y I M T R F D G T S I I G G C

771 tttccaacccaacaactggtcatccgaacccgatcctttctcacccatcgaatcctgtctagacctc
 F Q P N N W S S E P D P S L T H R I L S R A L

841 gaccgattcccggaactgaccaaagattggccctttgacatttgtgcgcgaatgcgttggccaccgtcctg
 D R F P E L T K D G P L D I V R E C V G H R P

911 gtagagagggcgtccccgagtagaattagagaatccccggcgttggctttgttgtccataactatgg
 G R E G G P R V E L E K I P G V G F V V H N Y G

981 tgccgccggtgctggttaccagtcctttacggcatggctgatgaagctatttcttacgtcgaaagagat
 A A G A G Y Q S S Y G M A D E A I S Y V E R A

1051 cttactcgtccaaacctttag
 L T R P N L *

5.2 PRIMERS

Primers were purchased from Sigma-Genosys or MWG Biotech AG. and, if located on a gene, are referred to by the starting position on that gene. 'f' and 'r' designate forward and reverse primers respectively.

5.2.1 Sequencing primers

TvDAAO f308	5'-CCATGTCGGCCATCTGTCAA-3' (20 bp; 55 % GC; T _m 69.4 °C; MWt 6053)
TvDAAO f648	5'-CGTCCTTGTTTCGAAACTCTC-3' (20 bp; 50 % GC; T _m 61.4 °C; MWt 6019)
TvDAAO f978	5'-TGGTGCCGCCGGTGCTGGTT-3' (20 bp; 70 % GC; T _m 79.0 °C; MWt 6172)
pPOT f4725	5'-GGCGACGTGCGTCCTCAAGC-3' (20 bp; 70 % GC; T _m 74.7 °C; MWt 6119)
RgDAAO f531	5'-CGCTACGGGACTTGG-3' (15 bp; 67 % GC; T _m 58.7 °C; MWt 4609)
RgDAAO f801	5'-GAGCGACGGAACGA-3' (14 bp; 64 % GC; T _m 57.6 °C; MWt 4346.82)
RgDAAO r150	5'-CCATGGTGAAGCGA-3' (14 bp; 57.14 % GC; T _m 55.17°C; MWt 4312.77)
RgDAAO fl	5'-ATGCACTCGCAGAAG-3' (15 bp; 53.33 % GC; T _m 53.33 °C; MWt 4585.96)
RgDAAO r1107	5'-CTACAACTTCGACTC-3' (15 bp; 46.67 % GC; T _m 40.81° C; MWt 4471.87)

5.2.2 epPCR Primers

RgDAAO fl	5'-ATGCACTCGCAGAAG-3' (15 bp; 53.33 % GC; T _m 53.33 °C; MWt 4585.96)
RgDAAO r1107	5'-CTACAACTTCGACTC-3' (15 bp; 46.67 % GC; T _m 40.81° C; MWt 4471.87)

5.2.3 Saturation mutagenesis primers

Primers for saturation mutagenesis were selected on the basis of 15 – 20 bp homology on either side of the site selected for mutagenesis. These primers are named after the amino acid subjected to mutagenesis and it's position in the enzyme amino acid sequence.

F58 f 5'-GCG AAT TGG ACG CCT **NNS** ATG ACG CTT ACA GAC-3'
(33 bp; 54.5 % GC; T_m 72.0 °C; MWt 10143)

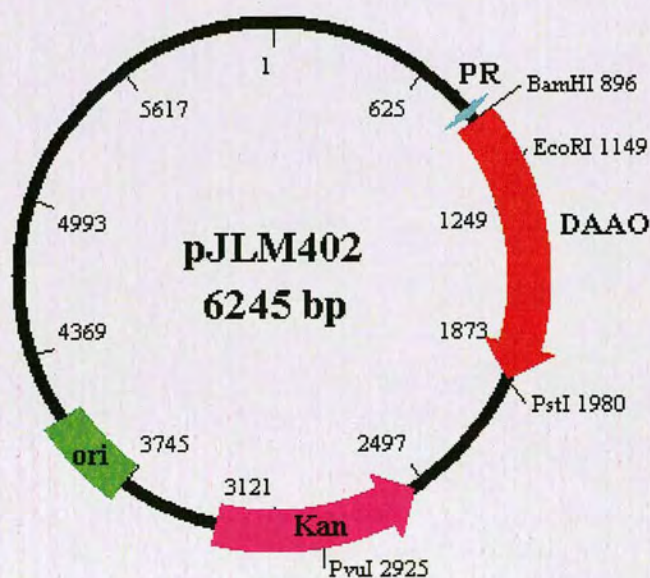
F58 r 5'-GTC TGT AAG CGT CAT **SNN** AGG CGT CCA ATT CGC-3'
(33 bp; 54.5 % GC; T_m 72.0 °C; MWt 10125)

M213 f 5'-CCA TGC AAG CGA TGC ACG **NNS** GAC TCG TCC GAC CCC-3'
(36 bp; 66.7 % GC; T_m >75 °C; MWt 10957)

M213 r 5'-GGG GTC GGA CGA GTC **SNN** CGT GCA TCG CTT GCA TGG-3'
(36 bp; 66.7 % GC; T_m >75 °C; MWt 11170)

5.3 VECTOR MAPS

5.3.1 pJLM402



5.4 GENOTYPES OF *E. COLI* STRAINS USED

5.4.1 TOP10

F- *mcrA* $\Delta(mrr-hsdRMS-mcrBC)$ $\phi 80lacZ\Delta M15$ $\Delta lacX74$ *recA1* *araD139*
 $\Delta(araleu)$ 7697 *galU* *galK* *rpsL* (Str_R) *endA1* *nupG*

5.4.2 BL21 (DE3)

F- *ompT* *hsdS_B* (r_B-m_B-) *gal* *dcm*

5.4.3 XL1-Blue

recA1 *endA1* *gyrA96* *thi-1* *hsdR17* *supE44* *relA1* *lac* [F' *proAB* *lacI^fZ\Delta M15* Tn10
 (Tet_r)]

5.4.4 XL1-Red

endA1 *gyrA96* *thi-1* *hsdR17* *supE44* *relA1* *lac* *mutD5* *mutS* *mutT* Tn10 (Tet^f)a

5.5 SYMBOLS OF THE NATURALLY OCCURRING AMINO ACIDS

Letter	Code	Amino acid	Letter	Code	Amino acid
A	Ala	Alanine	M	Met	Methionine
C	Cys	Cysteine	N	Asn	Asparagine
D	Asp	Aspartic acid	P	Pro	Proline
E	Glu	Glutamic acid	Q	Gln	Glutamine
F	Phe	Phenylalanine	R	Arg	Arginine
G	Gly	Glycine	S	Ser	Serine
H	His	Histidine	T	Thr	Threonine
I	Ile	Isoleucine	V	Val	Valine
K	Lys	Lysine	W	Trp	Tryptophan
L	Leu	Leucine	Y	Tyr	Tyrosine

5.6 SINGLE LETTER NUCLEOTIDE CODES

(Codes of the International Union of Biochemistry).⁽⁷²⁾

Base	Name	Bases	Complementary base
T	Thymine	T	A
C	Cytosine	C	G
A	Adenine	A	T
G	Guanine	G	C
Y	pYrimidine	C T	R
R	puRine	A G	Y
S	Strong (3H)	G C	S
W	Weak (2H)	A T	W
K	Keto	T G	M
M	aMino	A C	K
B	not A	C G T	V
D	not C	A G T	H
H	not G	A C T	D
V	not T	A C G	B
N	aNy	A C G T	N

5.7 CALCULATIONS

5.7.1 Pearson Product moment correlation coefficient (R^2)

Linear relationships between two sets of variables were assessed using R^2 values. These were produced in MS Excel using the expression below. It is described as “the proportion of the variance in Y attributable to the variance in X”.

$$R^2 = \left(\frac{\sum (x - \bar{x})(y - \bar{y})}{\sqrt{\sum (x - \bar{x})^2 \sum (y - \bar{y})^2}} \right)^2$$

5.7.2 Beer-Lambert Law

$$A = \epsilon cl$$

A = absorbance, ϵ = molar extinction coefficient, l = pathlength

5.8 MICROORGANISMS SCREENED FOR ACTIVITY TOWARDS (*rac*)- β -PHENYLALANINE AND (*rac*)- β -HOMOPHENYLALANINE

The microorganisms screened form part of the Chirotech Technology Limited culture collection.

Name	Classification	Name	Classification
<i>Achromobacter denitrificans</i>	Bacteria	<i>Beauveria densa</i>	Fungi
<i>Achromobacter xylosoxidans</i> ssp. <i>xylosoxidans</i>	Bacteria	<i>Beauveria stephanoderis</i>	Fungi
<i>Acinetobacter baumannii</i>	Bacteria	<i>Blakeslea trispora</i>	Fungi
<i>Acinetobacter calcoaceticus</i>	Bacteria	<i>Botryotinia narcissicola</i>	Fungi
<i>Acinetobacter junii</i>	Bacteria	<i>Calcarisporium antibioticum</i>	Fungi
<i>Acinetobacter</i> sp.	Bacteria	<i>Caldariomyces fumago</i>	Fungi
<i>Actinoplanes utahensis</i>	Bacteria	<i>Cephalotrichum stemonitis</i>	Fungi
<i>Agrobacterium radiobacter</i>	Bacteria	<i>Ceratocystis allantospora</i>	Fungi
<i>Agromyces mediolanus</i>	Bacteria	<i>Ceratocystis cainii</i>	Fungi
<i>Alcaligenes denitrificans</i> ssp. <i>denitrificans</i>	Bacteria	<i>Ceratocystis clavata</i>	Fungi
<i>Alcaligenes eutrophus</i>	Bacteria	<i>Ceratocystis ips</i>	Fungi
<i>Alcaligenes faecalis</i> ssp. <i>Faecalis</i>	Bacteria	<i>Ceratocystis moniliformis</i>	Fungi
<i>Alcaligenes</i> or <i>Pseudomonas</i> sp.	Bacteria	<i>Ceratocystis olivacea</i>	Fungi
<i>Alcaligenes</i> sp.	Bacteria	<i>Ceratocystis pilifera</i>	Fungi
<i>Alcaligenes</i> sp.	Bacteria	<i>Ceratocystis prolifera</i>	Fungi
<i>Amycolatopsis orientalis</i> ssp. <i>orientalis</i>	Bacteria	<i>Ceratocystis pseudoeuropioides</i>	Fungi
<i>Aneurinibacillus migulanus</i>	Bacteria	<i>Ceratocystis radicolica</i>	Fungi
<i>Arthrobacter aurescens</i>	Bacteria	<i>Ceratocystis stenoceras</i>	Fungi
<i>Arthrobacter globiformis</i>	Bacteria	<i>Ceratocystis tetropii</i>	Fungi
<i>Arthrobacter nicotianae</i>	Bacteria	<i>Chaetomium globosum</i>	Fungi
<i>Arthrobacter oxydans</i>	Bacteria	<i>Circinella simplex</i>	Fungi
<i>Arthrobacter</i> sp.	Bacteria	<i>Cochliobolus sativus</i>	Fungi
<i>Arthrobacter sulfureus</i>	Bacteria	<i>Coniochaeta nepalica</i>	Fungi
<i>Arthrobacter viscosus</i>	Bacteria	<i>Coniochaeta nodulisporioides</i>	Fungi
<i>Aureobacterium</i> sp.	Bacteria	<i>Corynascus sepedonium</i>	Fungi
<i>Azospirillum brasiliense</i>	Bacteria	<i>Cryptosporiopsis tarraconensis</i>	Fungi
<i>Bacillus aminovorans</i>	Bacteria	<i>Cunninghamella elegans</i>	Fungi
<i>Bacillus cereus</i>	Bacteria	<i>Cylindrocarpon didymum</i>	Fungi
<i>Bacillus coagulans</i>	Bacteria	<i>Cyptospora chrysosperma</i>	Fungi
<i>Bacillus fastidiosus</i>	Bacteria	<i>Diheterospora cylindrospora</i>	Fungi
<i>Bacillus gibsonii</i>	Bacteria	<i>Dimargaris verticillata</i>	Fungi
<i>Bacillus licheniformis</i>	Bacteria	<i>Embellisia proteae</i>	Fungi
<i>Bacillus megaterium</i>	Bacteria	<i>Exserohilum heteropogonicola</i>	Fungi

Name	Classification	Name	Classification
<i>Bacillus polymyxa</i>	Bacteria	<i>Filosporaella fistucella</i>	Fungi
<i>Bacillus pseudofirmus</i>	Bacteria	<i>Filosporaella viersimorpha</i>	Fungi
<i>Bacillus smithii</i>	Bacteria	<i>Fomes fomentarius</i>	Fungi
<i>Bacillus</i> sp.	Bacteria	<i>Fusarium oxysporum</i>	Fungi
<i>Bacillus sphaericus</i>	Bacteria	<i>Fusarium oxysporum</i> f.sp. <i>Pisi</i>	Fungi
<i>Bacillus stearothermophilus</i>	Bacteria	<i>Fusidium coccineum</i>	Fungi
<i>Bacillus subtilis</i>	Bacteria	<i>Gibberella fujikuroi</i> var. <i>Moniliformis</i>	Fungi
<i>Bacillus subtilis</i> ssp. <i>Subtilis</i>	Bacteria	<i>Gliocladium virens</i>	Fungi
<i>Bacillus thuringiensis</i>	Bacteria	<i>Gloeotinia granigena</i>	Fungi
<i>Beijerinckia indica</i> ssp. <i>lacticogenes</i>	Bacteria	<i>Gloephyllum seiparium</i>	Fungi
<i>Brevibacterium lactofermentum</i>	Bacteria	<i>Glomerella cingulata</i>	Fungi
<i>Brevibacterium linens</i>	Bacteria	<i>Gnomonia comari</i>	Fungi
<i>Brevibacterium</i> sp.	Bacteria	<i>Gonotobotryum apiculatum</i>	Fungi
<i>Burkholderia cepacia</i>	Bacteria	<i>Harknessia hawaiiensis</i>	Fungi
<i>Burkholderia cepacia</i>	Bacteria	<i>Hypomyces rosellus</i>	Fungi
<i>Cellulomonas flavigena</i>	Bacteria	<i>Isaria felina</i>	Fungi
<i>Cellulosimicrobium cellulans</i>	Bacteria	<i>Keratinophyton terreum</i>	Fungi
<i>Chryseobacterium indoltheticum</i>	Bacteria	<i>Leptographium serpens</i>	Fungi
<i>Citrobacter koseri</i>	Bacteria	<i>Leptographium wageberi</i>	Fungi
<i>Comamonas terrigena</i>	Bacteria	<i>Mariannaea elegans</i>	Fungi
<i>Corynebacterium flavescens</i>	Bacteria	<i>Melanospora zamiae</i>	Fungi
<i>Corynebacterium glutamicum</i>	Bacteria	<i>Memnoniella echinata</i>	Fungi
<i>Corynebacterium</i> sp	Bacteria	<i>Microascus trigonosporus</i>	Fungi
<i>Curtobacterium albidum</i>	Bacteria	<i>Monodisma fragilis</i>	Fungi
<i>Curtobacterium citreum</i>	Bacteria	<i>Mortierella elongata</i>	Fungi
<i>Curtobacterium pusillum</i>	Bacteria	<i>Mucor circinelloides</i>	Fungi
<i>Deinococcus radiodurans</i>	Bacteria	<i>Myceliophthora lutea</i>	Fungi
<i>Deinococcus radiophilus</i>	Bacteria	<i>Mycosphaerella pinodes</i>	Fungi
<i>Delftia acidovorans</i>	Bacteria	<i>Neosartorya fischeri</i>	Fungi
<i>Enterobacter intermedius</i>	Bacteria	<i>Nomuraea rileyi</i>	Fungi
<i>Enterococcus</i> sp.	Bacteria	<i>Ophiostoma novo-ulmi</i>	Fungi
<i>Erwinia</i> sp.	Bacteria	<i>Paecilomyces variotii</i>	Fungi
<i>Escherichia coli</i>	Bacteria	<i>Penicillium aurantiogriseum</i>	Fungi
<i>Escherichia coli</i>	Bacteria	<i>Penicillium citrinum</i>	Fungi
<i>Flavimonas oryzihabitans</i>	Bacteria	<i>Penicillium thomii</i>	Fungi
<i>Flavobacterium lutescens</i>	Bacteria	<i>Pestalotia microspora</i>	Fungi
<i>Geobacillus stearothermophilus</i>	Bacteria	<i>Petriella sordida</i>	Fungi
<i>Geobacillus thermoglucosidasius</i>	Bacteria	<i>Phanerochaete chrysosporium</i>	Fungi
<i>Gluconobacter oxydans</i>	Bacteria	<i>Phialophora fastigiata</i>	Fungi
<i>Gordonia rubripertincta</i>	Bacteria	<i>Phialophora japonica</i>	Fungi
<i>Hafnia alvei</i>	Bacteria	<i>Phomopsis obscurans</i>	Fungi
<i>Halomonas</i> sp.	Bacteria	<i>Phycomyces blakesleeanus</i>	Fungi
<i>Hyphomicrobium</i> sp.	Bacteria	<i>Pithomyces chartarum</i>	Fungi
<i>Janthinobacterium lividum</i>	Bacteria	<i>Pithomyces graminicola</i>	Fungi
<i>Jensenia canicruria</i>	Bacteria	<i>Poitrasia circinans</i>	Fungi
<i>Klebsiella</i> sp.	Bacteria	<i>Ramichloridium anceps</i>	Fungi
<i>Kurthia gibsonii</i>	Bacteria	<i>Readeriella mirabilis</i>	Fungi

Name	Classification	Name	Classification
<i>Lysobacter</i> sp.	Bacteria	<i>Rhinochlorella indica</i>	Fungi
<i>Methylobacterium organophilum</i>	Bacteria	<i>Rhizopus oryzae</i>	Fungi
<i>Methylomonas clara</i>	Bacteria	<i>Sarophorum palmicola</i>	Fungi
<i>Microbacterium liquefaciens</i>	Bacteria	<i>Scopulariopsis brevicaulis</i>	Fungi
<i>Micrococcus luteus</i>	Bacteria	<i>Sordaria fimicola</i>	Fungi
<i>Micrococcus varians</i>	Bacteria	<i>Spegazzinia lobulata</i>	Fungi
<i>Nocardia</i> sp.	Bacteria	<i>Sphacelotheca destruens</i>	Fungi
<i>Ochrobactrum anthropi</i>	Bacteria	<i>Stachybotrys chartarum</i>	Fungi
<i>Paenibacillus polymyxa</i>	Bacteria	<i>Stilbella fimetaria</i>	Fungi
<i>Pediococcus</i> sp.	Bacteria	<i>Thamnidium elegans</i>	Fungi
<i>Pseudomonas aeruginosa</i>	Bacteria	<i>Tolyposcladium cylindrosporium</i>	Fungi
<i>Pseudomonas alcaligenes</i>	Bacteria	<i>Trichocladium asperum</i>	Fungi
<i>Pseudomonas fluorescens</i>	Bacteria	<i>Trichocladium pyriforme</i>	Fungi
<i>Pseudomonas fragi</i>	Bacteria	<i>Trichoderma harzianum</i>	Fungi
<i>Pseudomonas oleovorans</i>	Bacteria	<i>Trichoderma reesei</i>	Fungi
<i>Pseudomonas putida</i>	Bacteria	<i>Wallemia sebi</i>	Fungi
<i>Pseudomonas</i> sp.	Bacteria	<i>Zygorhynchus moelleri</i>	Fungi
<i>Pseudomonas testosteroni</i>	Bacteria	<i>Phanerochaete chrysosporium</i>	Recombinant Yeast
<i>Rhizobium</i> sp.	Bacteria	<i>Candida albicans</i>	Yeast
<i>Rhodococcus equi</i>	Bacteria	<i>Candida apis</i> var. <i>galacta</i>	Yeast
<i>Rhodococcus erythropolis</i>	Bacteria	<i>Candida boidinii</i>	Yeast
<i>Rhodococcus globerulus</i>	Bacteria	<i>Candida curvata</i>	Yeast
<i>Rhodococcus rhodochrous</i>	Bacteria	<i>Candida etchellsii</i>	Yeast
<i>Rhodococcus</i> sp.	Bacteria	<i>Candida glabrata</i>	Yeast
<i>Saccharopolyspora hordei</i>	Bacteria	<i>Candida glabrata</i>	Yeast
<i>Salmonella enterica</i> ssp. <i>enterica</i>	Bacteria	<i>Candida magnoliae</i>	Yeast
<i>Serratia liquifaciens</i>	Bacteria	<i>Candida maltosa</i>	Yeast
<i>Serratia marcescens</i>	Bacteria	<i>Candida parapsilosis</i>	Yeast
<i>Sporosarcina pasteurii</i>	Bacteria	<i>Candida rugosa</i>	Yeast
<i>Staphylococcus aureus</i> ssp. <i>aureus</i>	Bacteria	<i>Candida sonorensis</i>	Yeast
<i>Staphylococcus</i> sp.	Bacteria	<i>Candida tropicalis</i>	Yeast
<i>Streptococcus faecium</i>	Bacteria	<i>Candida utilis</i>	Yeast
<i>Streptococcus</i> sp.	Bacteria	<i>Exophiala</i> sp.	Yeast
<i>Streptomyces avidinii</i>	Bacteria	<i>Hanseniaspora occidentalis</i>	Yeast
<i>Streptomyces cinnamomeus</i>	Bacteria	<i>Hanseniaspora osmophilia</i>	Yeast
<i>Streptomyces clavuligerus</i>	Bacteria	<i>Hyphopichia burtonii</i>	Yeast
<i>Streptomyces coeruleorubidus</i>	Bacteria	<i>Issatchenkia orientalis</i>	Yeast
<i>Streptomyces espinosus</i>	Bacteria	<i>Kluyveromyces thermotolerans</i>	Yeast
<i>Streptomyces griseoruber</i>	Bacteria	<i>Komagataella pastoris</i>	Yeast
<i>Streptomyces hiroshimensis</i>	Bacteria	<i>Lipomyces starkeyi</i>	Yeast
<i>Streptomyces lincolnensis</i>	Bacteria	<i>Phaffia rhodozyma</i>	Yeast
<i>Streptomyces peucetius</i>	Bacteria	<i>Pichia angusta</i>	Yeast
<i>Streptomyces peucetius</i> ssp. <i>caesius</i>	Bacteria	<i>Pichia finlandica</i>	Yeast
<i>Streptomyces thermovulgaris</i>	Bacteria	<i>Pichia holstii</i>	Yeast
<i>Streptomyces tuius</i>	Bacteria	<i>Pichia methanolica</i>	Yeast
<i>Vibrio cyclospites</i>	Bacteria	<i>Pichia</i> sp.	Yeast
<i>Vibrio proteolyticus</i>	Bacteria	<i>Pichia trehalophila</i>	Yeast

Name	Classification	Name	Classification
<i>Absidia anomala</i>	Fungi	<i>Rhodospiridium toruloides</i>	Yeast
<i>Acrocalymma medicaginis</i>	Fungi	<i>Rhodotorula glutinis</i>	Yeast
<i>Acrophialophora fusispora</i>	Fungi	<i>Rhodotorula glutinis</i> var. <i>glutinis</i>	Yeast
<i>Allantonectria miltina</i>	Fungi	<i>Rhodotorula mucilaginoso</i>	Yeast
<i>Alpakesa uniseptata</i>	Fungi	<i>Rhodotorula rubra</i>	Yeast
<i>Alternaria alternata</i>	Fungi	<i>Rhodotorula</i> sp.	Yeast
<i>Amerosporium concinnum</i>	Fungi	<i>Saccharomyces cerevisiae</i>	Yeast
<i>Amorphotheca resinae</i>	Fungi	<i>Saccharomyces uvarum</i>	Yeast
<i>Aphanoascus biplantanus</i>	Fungi	<i>Sporidiobolus johnsonii</i>	Yeast
<i>Apiospora montagnei</i>	Fungi	<i>Sporidiobolus salmonicolor</i>	Yeast
<i>Arthrinium phaeospermum</i>	Fungi	<i>Trichosporon cutaneum</i>	Yeast
<i>Ascodesmis sphaerospora</i>	Fungi	<i>Trichosporon laibachii</i>	Yeast
<i>Ascotricha xyliina</i>	Fungi	<i>Trichosporon monoliliiforme</i>	Yeast
<i>Aspergillus flavus</i> var. <i>columnaris</i>	Fungi	<i>Trigonopsis variabilis</i>	Yeast
<i>Aspergillus japonicus</i>	Fungi	Unidentified (x2)	Yeast
<i>Aspergillus niger</i>	Fungi	<i>Williopsis saturnus</i> var. <i>saturnus</i>	Yeast
<i>Aspergillus quadricinctus</i>	Fungi	<i>Xanthophyllomyces dendrorhous</i>	Yeast
<i>Aspergillus tamaris</i>	Fungi	<i>Yamadazyma farinosa</i>	Yeast
<i>Aspergillus terreus</i>	Fungi	<i>Yarrowia lipolytica</i>	Yeast
<i>Aspergillus versicolor</i>	Fungi	Unidentified (x22, Aquapharm)	Fungi
<i>Aureobasidium pullulans</i>	Fungi	Unidentified (x 208, Aquapharm)	Bacteria

5.9 PROFILES AND HIGHEST NORMALISED RATES FOR RGDAAO SATURATION MUTAGENESIS LIBRARIES

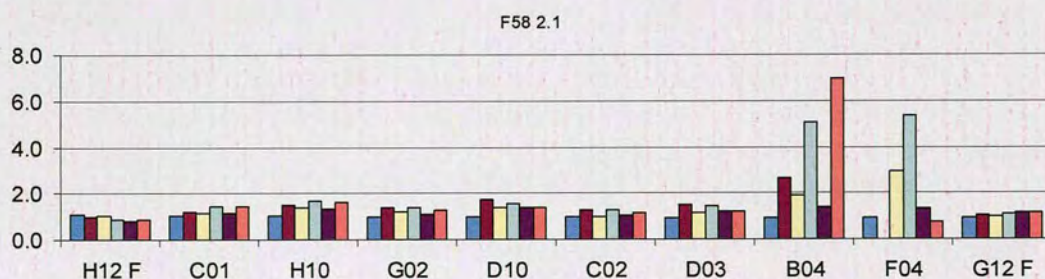
The assays were performed only once as a screening exercise. Exaggerated activities were observed in cases where the activity of the cells in the positive control wells was much lower than expected. This gives very high activity data for some variants towards some substrates. This particularly relates to the data obtained for the RgDAAO R285 and Y238 libraries but examples can also be seen in the M213 and Y238 libraries.

5.9.1 RgDAAO F58: (*R*)-alanine

Key:

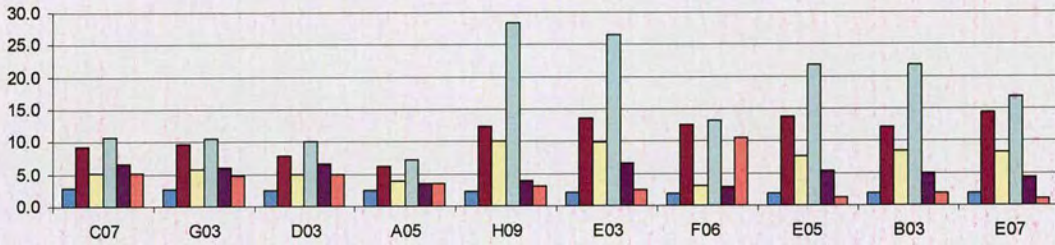
WT	RgDAAO F58
Blank or *	Blank well containing assay mix and substrate with no cells.
Pos	Positive control well containing assay mix, control substrate and cells expressing parental RgDAAO
Neg	Negative control well containing assay mix, control substrate and empty vector cells.
n.m.	Not measured.

(<i>R</i>)-Ala	(<i>rac</i>)-1,2,3,4-tetrahydroisoquinoline-3-carboxylic acid	(<i>rac</i>)- <i>allo</i> -Thr	(<i>R</i>)-Thr	(<i>S</i>)-Ala	(<i>R</i>)-Pipicolinic acid

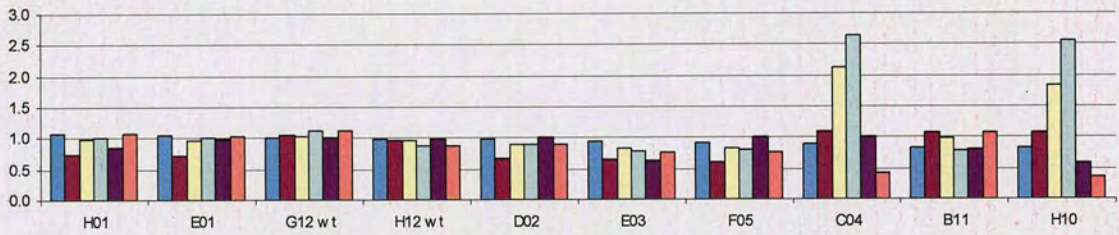


(R)-Ala	(rac)-1,2,3,4-tetrahydroisoquinoline-3-carboxylic acid	(rac)-allo-Thr	(R)-Thr	(S)-Ala	(R)-Pipicolinic acid

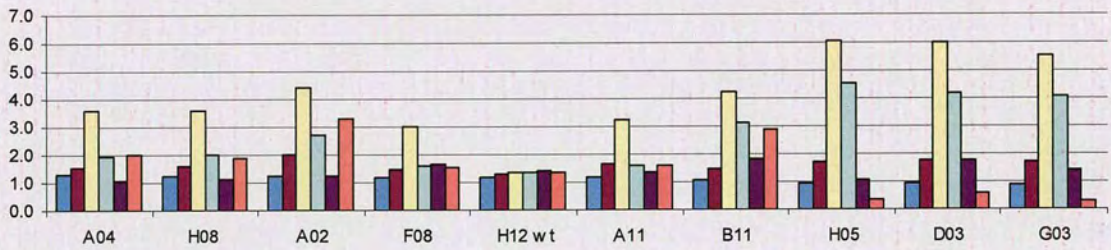
F58 3.1



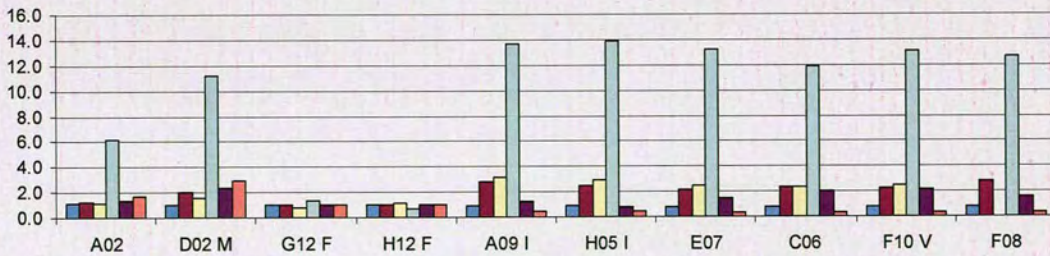
F58 4.1



F58 5.1



F58 6.1

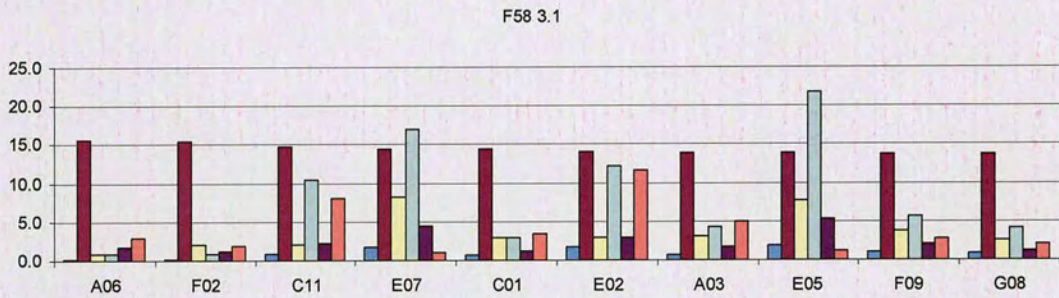
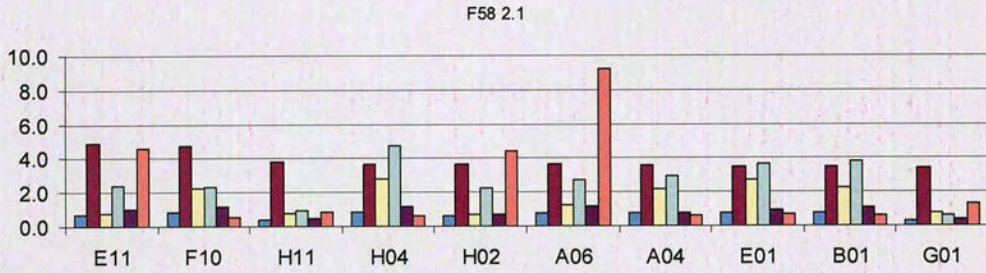
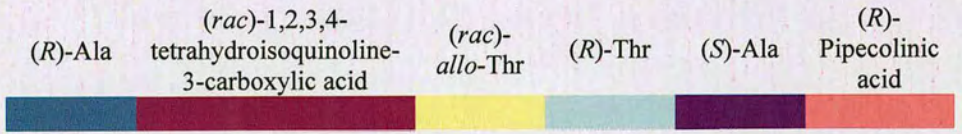


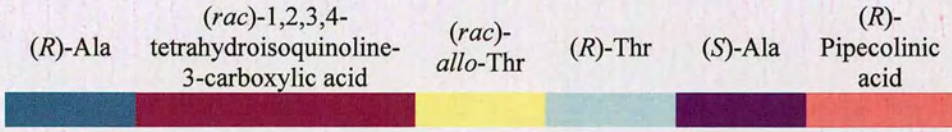
RgDAAO F58: highest rates towards (*R*)-alanine

Plate-2.1	Normalised rate	Plate-3.1	Normalised rate
H12 wt	1.2E+00	C07	2.5E+00
C01	1.1E+00	G03	2.5E+00
H10	1.1E+00	D03	2.3E+00
G02	1.1E+00	A05	2.2E+00
D10	1.0E+00	H09	2.0E+00
C02	1.0E+00	E03	1.9E+00
D03	1.0E+00	F06	1.8E+00
B04	1.0E+00	E05	1.7E+00
F04	9.9E-01	B03	1.7E+00
G12 wt	9.8E-01	E07	1.6E+00
Av F58	1.1E+00	Av F58	9.1E-01

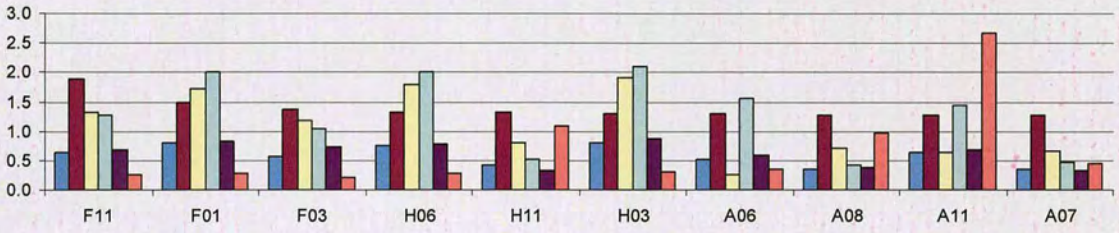
Plate-4.1	Normalised rate	Plate-5.1	Normalised rate	Plate-6.1	Normalised rate
H01	1.2E+00	A04	1.4E+00	A02	1.1E+00
E01	1.0E-04	H08	1.4E+00	D02 M	1.0E+00
G12 wt	9.3E-06	A02	1.3E+00	G12 WT	1.0E+00
H12 wt	2.3E-05	F08	1.3E+00	H12 WT	9.9E-01
D02	7.8E-05	H12 wt	1.3E+00	A09 I	9.1E-01
E03	9.1E-05	A11	1.3E+00	H05 I	8.4E-01
F05	4.4E-05	B11	1.2E+00	E07	8.2E-01
C04	5.0E-05	H05	1.1E+00	C06	7.8E-01
B11	4.3E-05	D03	1.0E+00	F10 V	7.8E-01
H10	8.7E-05	G03	1.0E+00	F08	7.8E-01
Av F58	1.1E+00	Av F58	1.1E+00	Av F58	9.9E-01

5.9.2 RgDAAO F58: (*rac*)-tetrahydroisoquinoline-3-carboxylic acid

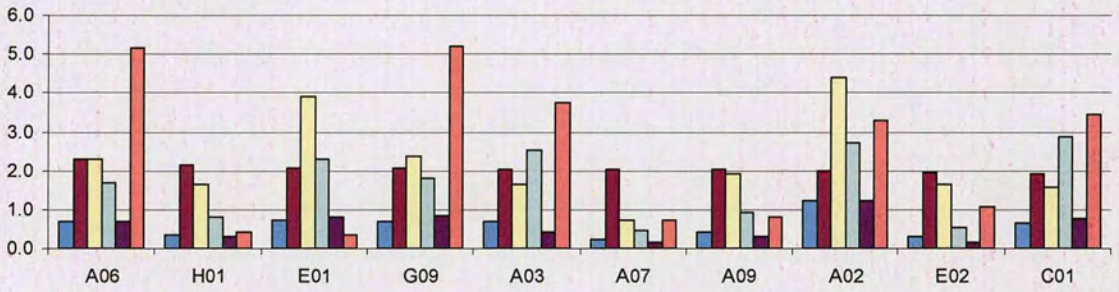




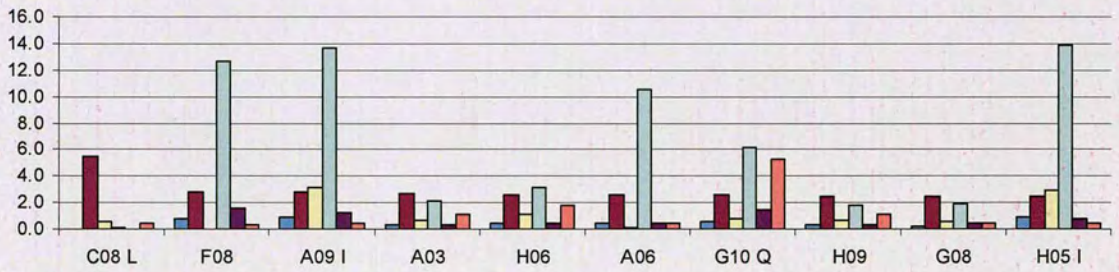
F58 4.1



F58 5.1



F58 6.1



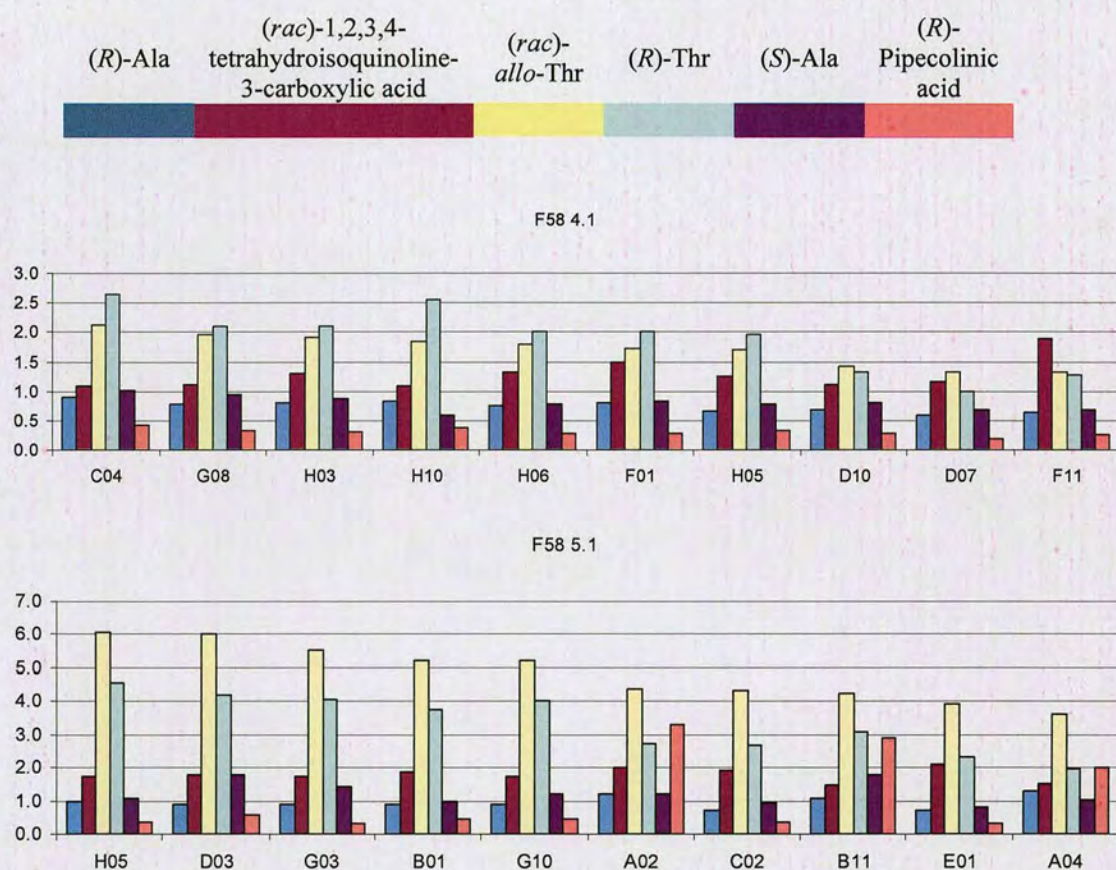
RgDAAO F58: highest rates towards (*rac*)-tetrahydroisoquinoline

Plate-2.1	Normalised rate	Plate-3.1	Normalised rate
E11	5.6E-02	A06	2.3E-01
F10	5.5E-02	F02	2.3E-01
H11	4.3E-02	C11	2.1E-01
H04	4.2E-02	E07	2.1E-01
H02	4.2E-02	C01	2.1E-01
A06	4.2E-02	E02	2.0E-01
A04	4.1E-02	A03	2.0E-01
E01	4.0E-02	E05	2.0E-01
B01	4.0E-02	F09	2.0E-01
G01	3.9E-02	G08	2.0E-01
Av F58	1.2E-02	Av F58	1.5E-02

Plate-4.1	Normalised rate	Plate-5.1	Normalised rate	Plate-6.1	Normalised rate
F11	1.1E-01	A06	1.1E-01	C08 L	1.9E-01
F01	8.8E-02	H01	1.0E-01	F08	1.0E-01
F03	8.0E-02	E01	9.9E-02	A09 I	9.8E-02
H06	7.8E-02	G09	9.7E-02	A03	9.7E-02
H11	7.8E-02	A03	9.6E-02	H06	9.3E-02
H03	7.7E-02	A07	9.6E-02	A06	9.1E-02
A06	7.6E-02	A09	9.6E-02	G10 Q	9.0E-02
A08	7.5E-02	A02	9.4E-02	H09	8.9E-02
A11	7.5E-02	E02	9.2E-02	G08	8.8E-02
A07	7.4E-02	C01	9.1E-02	H05 I	8.8E-02
Av F58	5.9E-02	Av F58	4.7E-02	Av F58	3.6E-02

5.9.3 RgDAAO F58: (*rac*)-*allo*-threonine

The activity profiles relating to the variants displaying the highest activities towards (*rac*)-*allo*-threonine from plates 2.1, 3.1 and 6.1 are shown in the main text (Figure 2.46 and Figure 2.48).

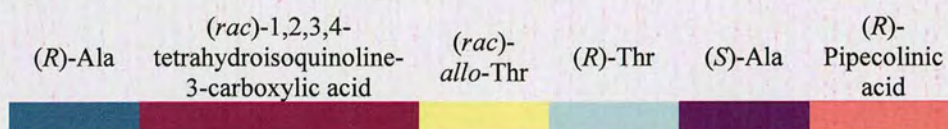


RgDAAO F58: highest normalised rates towards (*rac*)-*allo*-threonine

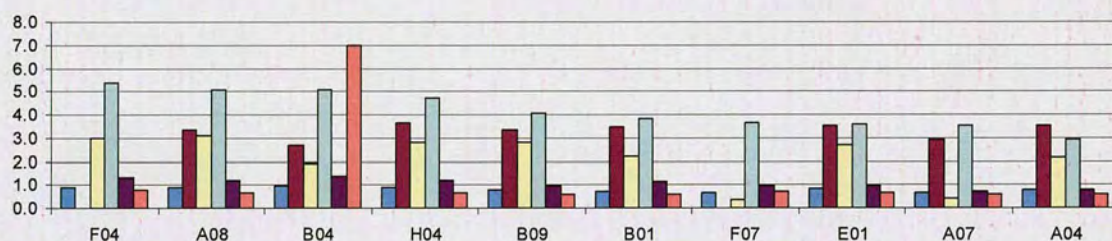
Plate-2.1	Normalised rate	Plate-3.1	Normalised rate
A08	3.2E-01	H09	7.3E-01
F04	3.1E-01	E03	7.1E-01
B09	2.9E-01	B03	6.2E-01
H04	2.9E-01	E07	5.9E-01
E01	2.8E-01	E05	5.6E-01
F10	2.3E-01	E04	5.5E-01
B01	2.3E-01	B06	4.7E-01
A04	2.3E-01	D08	4.2E-01
B04	2.0E-01	G03	4.1E-01
D10	1.4E-01	F04	4.0E-01
Av F58	1.0E-01	Av F58	7.3E-02

Plate-4.1	Normalised rate	Plate-5.1	Normalised rate	Plate-6.1	Normalised rate
C04	3.1E-01	H05	3.7E-01	A08	4.4E-01
G08	2.9E-01	D03	3.6E-01	A09 I	3.0E-01
H03	2.8E-01	G03	3.3E-01	B08	2.7E-01
H10	2.7E-01	B01	3.1E-01	H05 I	2.7E-01
H06	2.6E-01	G10	3.1E-01	F10 V	2.4E-01
F01	2.5E-01	A02	2.6E-01	E07	2.4E-01
H05	2.5E-01	C02	2.6E-01	C06	2.3E-01
D10	2.1E-01	B11	2.6E-01	G02 I	2.2E-01
D07	1.9E-01	E01	2.4E-01	D06	2.1E-01
F11	1.9E-01	A04	2.2E-01	D08	2.0E-01
Av F58	1.5E-01	Av F58	6.0E-02	Av F58	9.5E-02

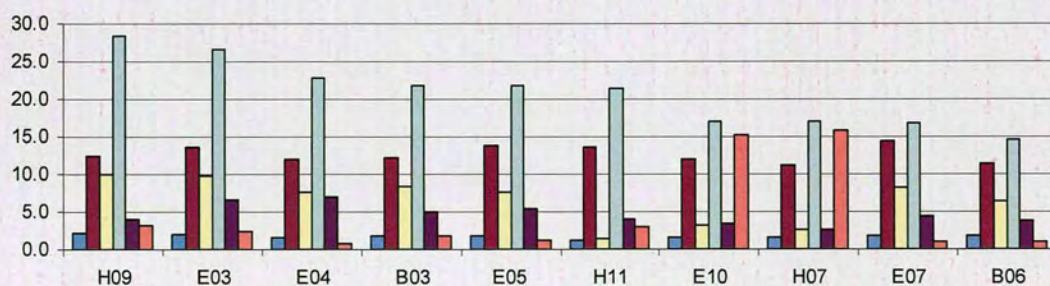
5.9.4 RgDAAO F58: (*R*)-threonine

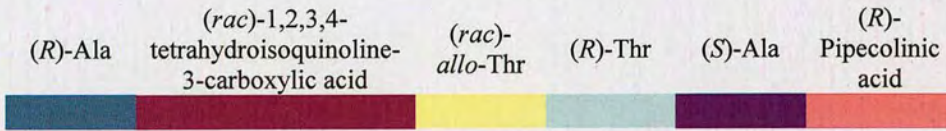


F58 2.1

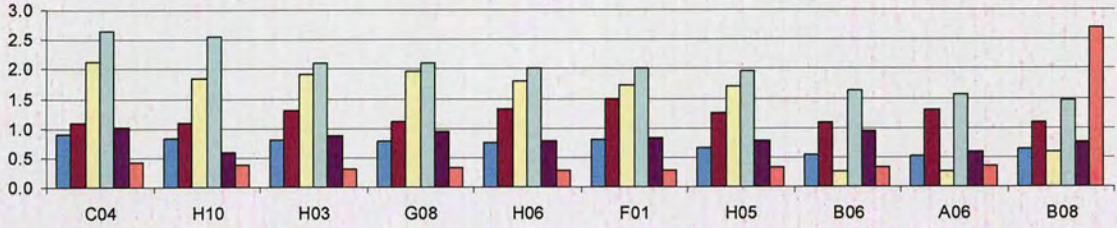


F58 3.1

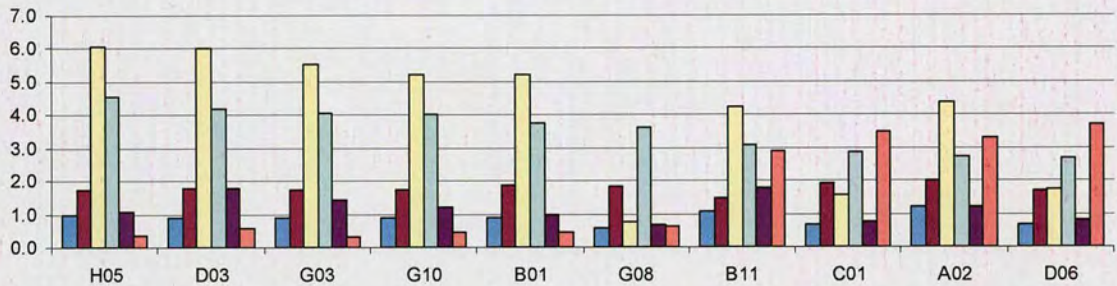




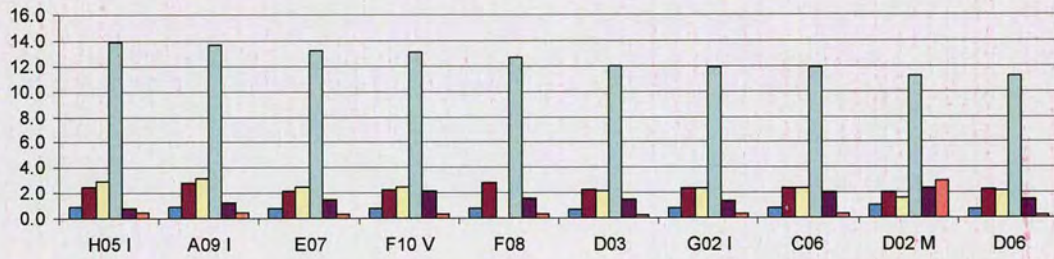
F58 4.1



F58 5.1



F58 6.1

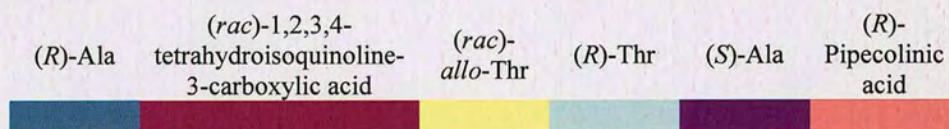


RgDAAO F58: highest rates towards *(R)*-threonine

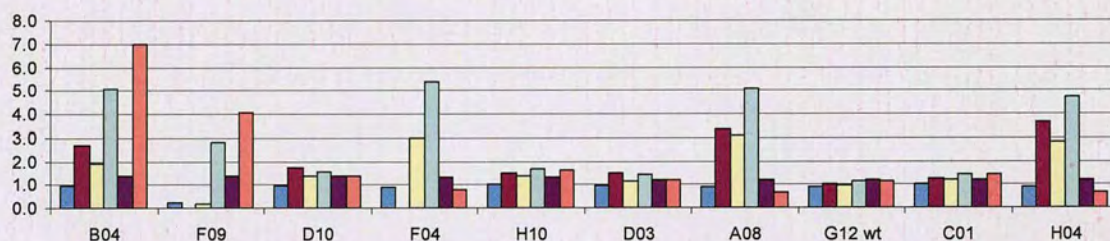
Plate-2.1	Normalised rate	Plate-3.1	Normalised rate
F04	1.0E-02	H09	1.8E-02
A08	9.9E-03	E03	1.6E-02
B04	9.8E-03	E04	1.4E-02
H04	9.1E-03	B03	1.3E-02
B09	7.9E-03	E05	1.3E-02
B01	7.4E-03	H11	1.3E-02
F07	7.1E-03	E10	1.1E-02
E01	7.0E-03	H07	1.0E-02
A07	6.8E-03	E07	1.0E-02
A04	5.7E-03	B06	9.0E-03
Av F58	1.9E-03	Av F58	6.2E-04

Plate-4.1	Normalised rate	Plate-5.1	Normalised rate	Plate-6.1	Normalised rate
C04	9.9E-03	H05	4.1E-02	H05 I	3.6E-02
H10	9.5E-03	D03	3.8E-02	A09 I	3.5E-02
H03	7.8E-03	G03	3.7E-02	E07	3.4E-02
G08	7.8E-03	G10	3.6E-02	F10 V	3.3E-02
H06	7.5E-03	B01	3.4E-02	F08	3.2E-02
F01	7.5E-03	G08	3.2E-02	D03	3.1E-02
H05	7.3E-03	B11	2.8E-02	G02 I	3.0E-02
B06	6.1E-03	C01	2.6E-02	C06	3.0E-02
A06	5.8E-03	A02	2.5E-02	D02 M	2.9E-02
B08	5.5E-03	D06	2.4E-02	D06	2.9E-02
Av F58	3.7E-03	Av F58	9.0E-03	Av F58	2.6E-03

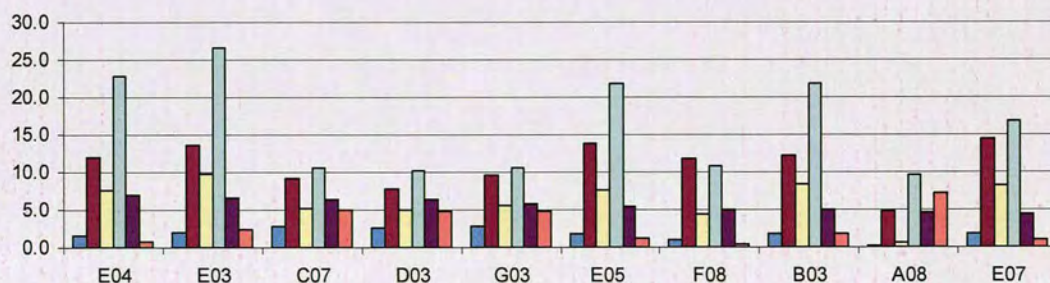
5.9.5 RgDAAO F58: (S)-alanine

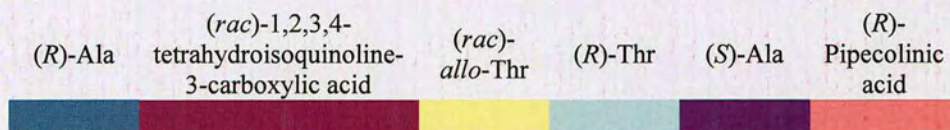


F58 2.1

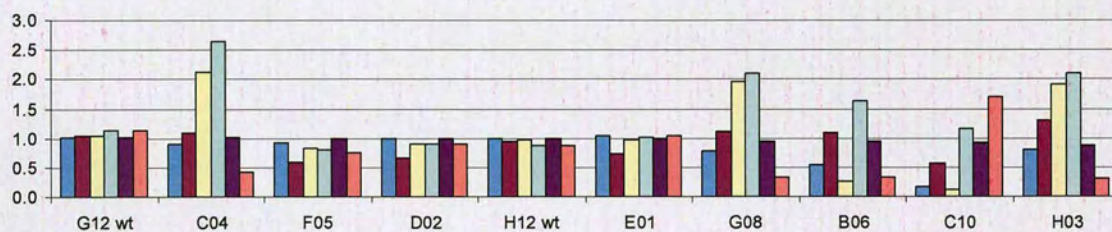


F58 3.1

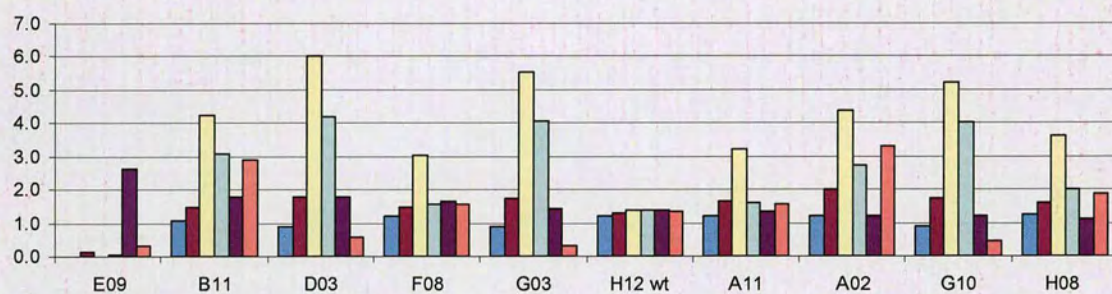




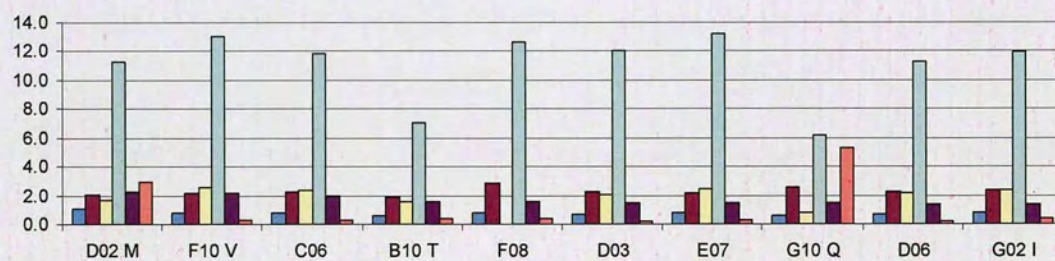
F58 4.1



F58 5.1



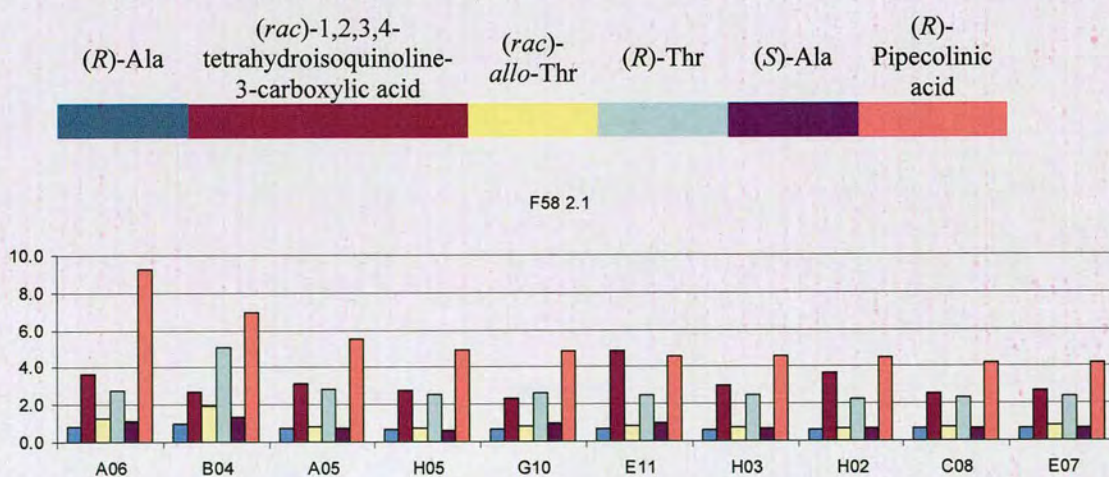
F58 6.1

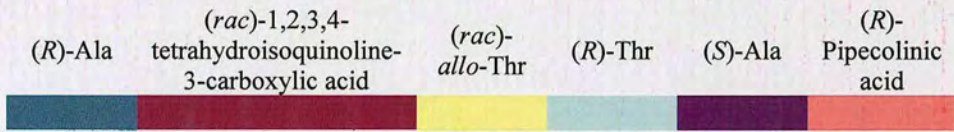


RgDAAO F58: highest rates towards (*S*)-alanine

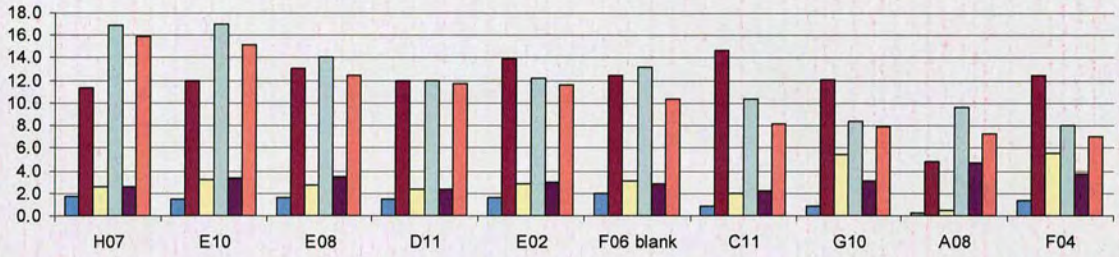
Plate-2.1	Normalised rate	Plate-3.1	Normalised rate
B04	1.2E-02	E04	2.2E-02
F09	1.2E-02	E03	2.1E-02
D10	1.2E-02	C07	2.1E-02
F04	1.2E-02	D03	2.1E-02
H10	1.2E-02	G03	1.9E-02
D03	1.1E-02	E05	1.7E-02
A08	1.1E-02	F08	1.6E-02
G12 wt	1.1E-02	B03	1.6E-02
C01	1.1E-02	A08	1.5E-02
H04	1.1E-02	E07	1.4E-02
Av F58	9.1E-03	Av F58	3.2E-03

Plate-4.1	Normalised rate	Plate-5.1	Normalised rate	Plate-6.1	Normalised rate
G12 wt	1.1E-02	E09	4.4E-02	D02 M	3.1E-02
C04	1.1E-02	B11	3.0E-02	F10 V	3.0E-02
F05	1.1E-02	D03	3.0E-02	C06	2.7E-02
D02	1.1E-02	F08	2.8E-02	B10 T	2.1E-02
H12 wt	1.1E-02	G03	2.4E-02	F08	2.1E-02
E01	1.1E-02	H12 wt	2.3E-02	D03	2.1E-02
G08	1.0E-02	A11	2.2E-02	E07	2.0E-02
B06	1.0E-02	A02	2.0E-02	G10 Q	2.0E-02
C10	1.0E-02	G10	2.0E-02	D06	1.9E-02
H03	9.6E-03	H08	1.9E-02	G02 I	1.8E-02
Av F58	1.1E-02	Av F58	1.7E-02	Av F58	1.4E-02

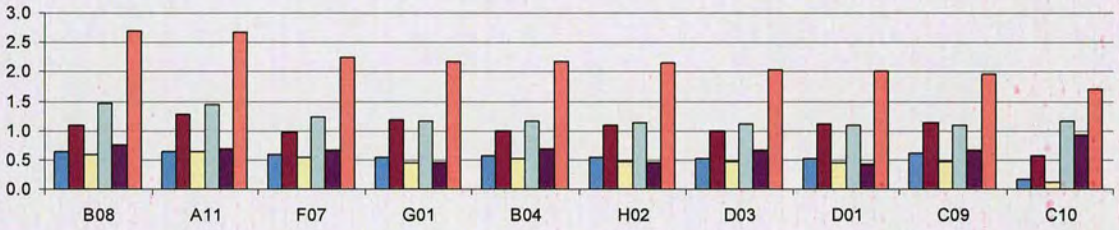
5.9.6 RgDAAO F58: (*R*)-pipecolinic acid



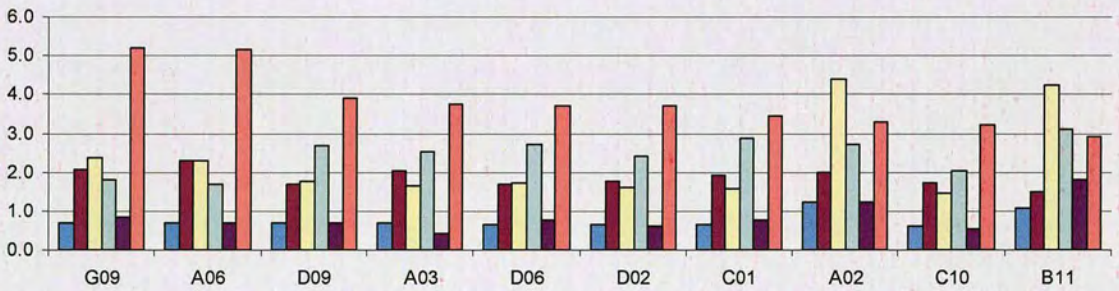
F58 3.1



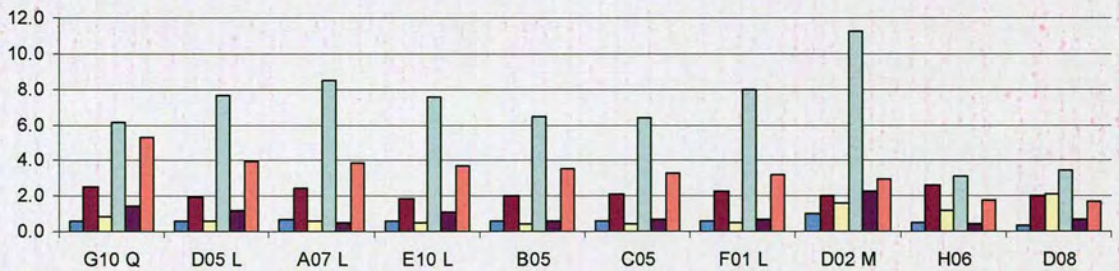
F58 4.1



F58 5.1



F58 6.1



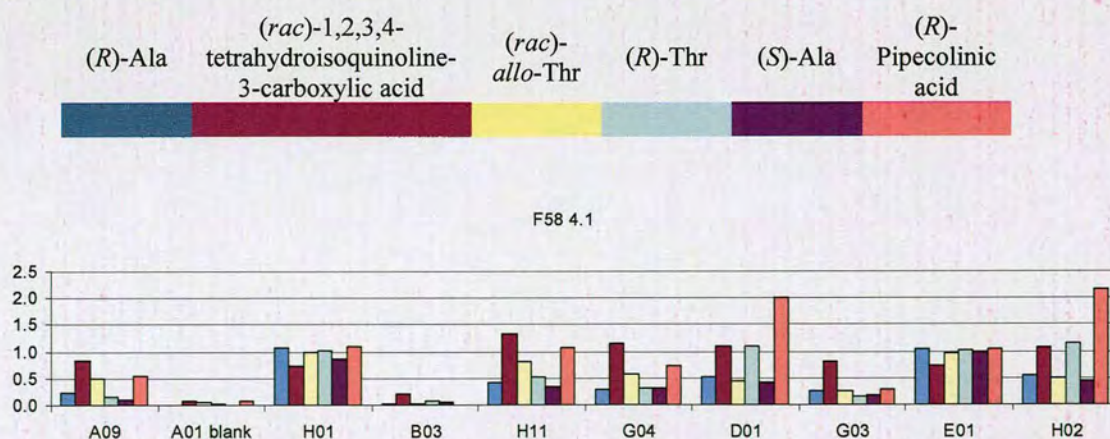
RgDAAO F58: highest rates towards (*R*)-pipecolinic acid

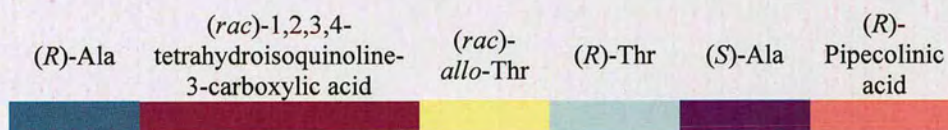
Plate-2.1	Normalised rate	Plate-3.1	Normalised rate
A06	7.6E-03	H07	6.4E-03
B04	5.7E-03	E10	6.1E-03
A05	4.5E-03	E08	5.0E-03
H05	4.0E-03	D11	4.7E-03
G10	4.0E-03	E02	4.7E-03
E11	3.8E-03	F06 blank	4.2E-03
H03	3.7E-03	C11	3.3E-03
H02	3.7E-03	G10	3.2E-03
C08	3.4E-03	A08	2.9E-03
E07	3.4E-03	F04	2.8E-03
Av F58	8.2E-04	Av F58	4.0E-04

Plate-4.1	Normalised rate	Plate-5.1	Normalised rate	Plate-6.1	Normalised rate
B08	4.2E-03	G09	2.2E-02	G10 Q	1.6E-02
A11	4.2E-03	A06	2.2E-02	D05 L	1.2E-02
F07	3.5E-03	D09	1.7E-02	A07 L	1.2E-02
G01	3.4E-03	A03	1.6E-02	E10 L	1.1E-02
B04	3.4E-03	D06	1.6E-02	B05	1.1E-02
H02	3.4E-03	D02	1.6E-02	C05	9.9E-03
D03	3.2E-03	C01	1.5E-02	F01 L	9.7E-03
D01	3.1E-03	A02	1.4E-02	D02 M	9.0E-03
C09	3.0E-03	C10	1.4E-02	H06	5.5E-03
C10	2.7E-03	B11	1.2E-02	D08	5.2E-03
Av F58	1.6E-03	Av F58	4.3E-03	Av F58	3.1E-03

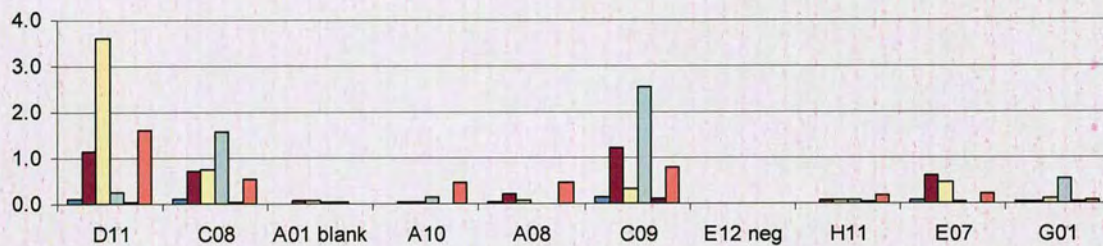
5.9.7 RgDAAO F58: (*rac*)- β -homophenylalanine

The activity profiles relating to the variants displaying the highest activities towards (*rac*)- β -homophenylalanine from plates 2.1 and 3.1 are shown in the main text (Figure 2.49).

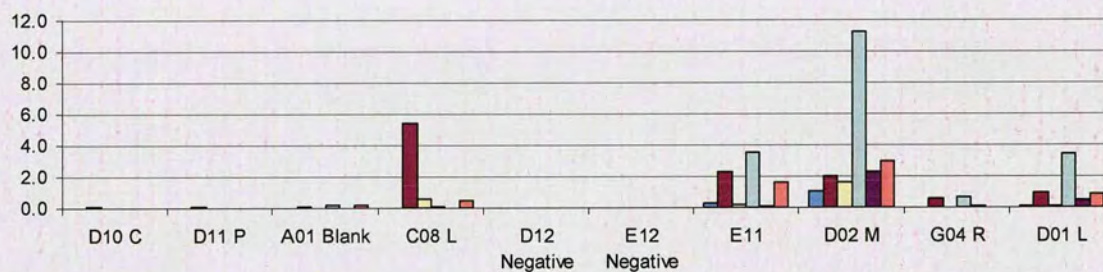




F58 5.1



F58 6.1

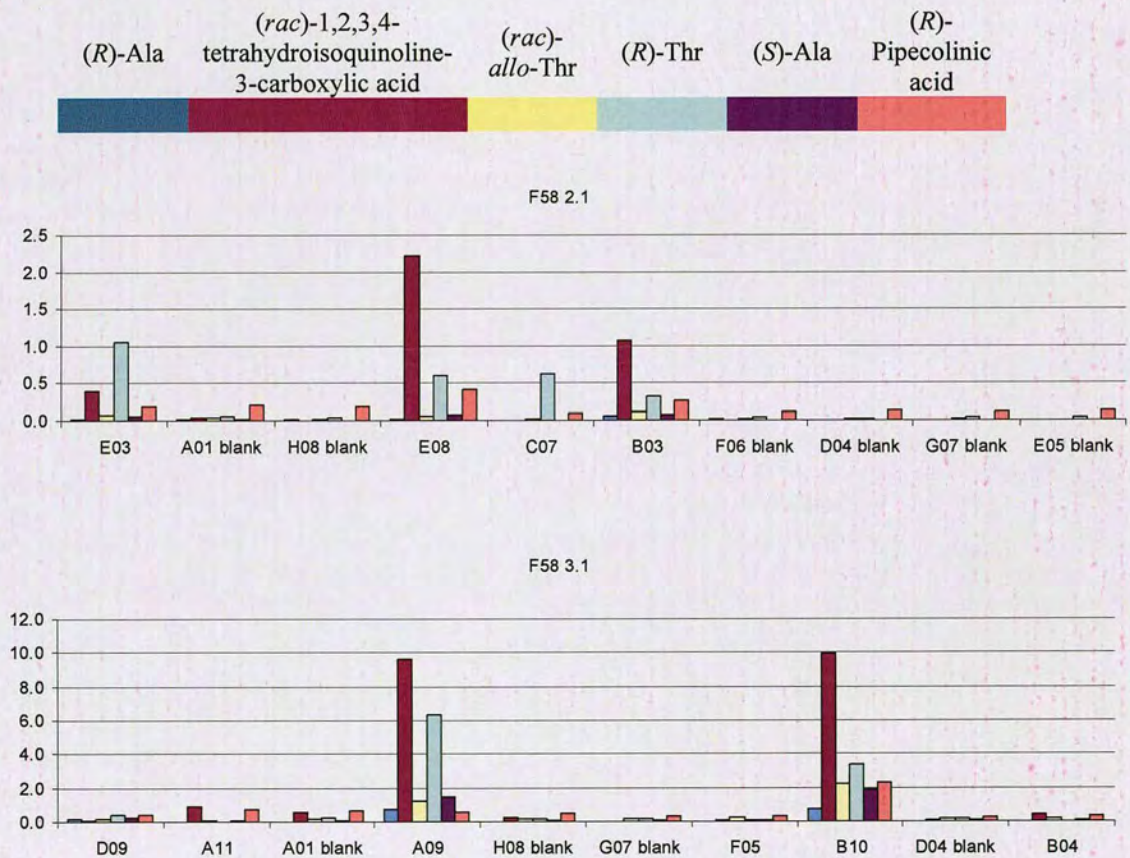


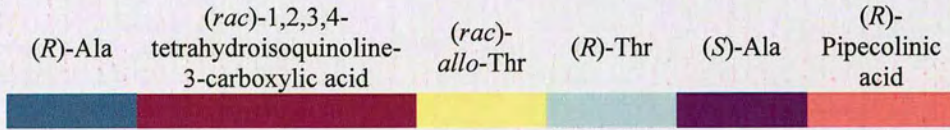
RgDAAO F58: highest rates towards *(rac)*- β -homophenylalanine

Plate-2.1	Normalised rate	Plate-3.1	Normalised rate
B03	2.5E-04	A09	6.5E-04
E08	2.1E-04	E04	5.1E-04
A01 blank	2.0E-04	B10	5.1E-04
H01	1.9E-04	B07	4.8E-04
E03	1.6E-04	D02	4.5E-04
B01	9.9E-05	H12 wt	4.2E-04
G04	9.5E-05	A07	4.0E-04
B02 blank	8.7E-05	A01 blank	3.9E-04
D01	8.2E-05	H01	3.8E-04
D04 blank	7.9E-05	B04	3.7E-04
Av F58	2.2E-07	av F58	3.2E-04

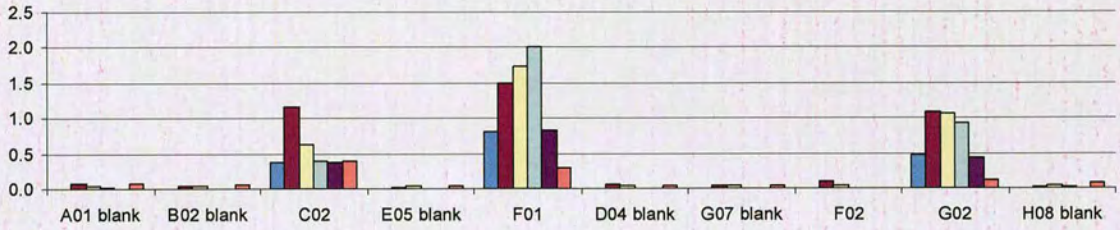
Plate-4.1	Normalised rate	Plate-5.1	Normalised rate	Plate-6.1	Normalised rate
A09	2.4E-04	D11	1.5E-04	D10 C	1.2E-04
A01 blank	2.2E-04	C08	1.3E-04	D11 P	1.1E-04
H01	2.0E-04	A01 blank	1.1E-04	A01 Blank	5.9E-05
B03	1.2E-04	A10	9.3E-05	C08 L	4.8E-05
H11	1.1E-04	A08	8.3E-05	D12 Negative	4.3E-05
G04	1.1E-04	C09	6.1E-05	E12 Negative	4.3E-05
D01	1.1E-04	E12 neg	4.8E-05	E11	4.0E-05
G03	1.1E-04	H11	4.7E-05	D02 M	4.0E-05
E01	1.0E-04	E07	4.1E-05	G04 R	3.4E-05
H02	1.0E-04	G01	3.5E-05	D01 L	3.4E-05
Av F58	1.6E-05	Av F58	1.6E-05	Av F58	1.1E-06

5.9.8 RgDAAO F58: (*rac*)-*tert*-leucine

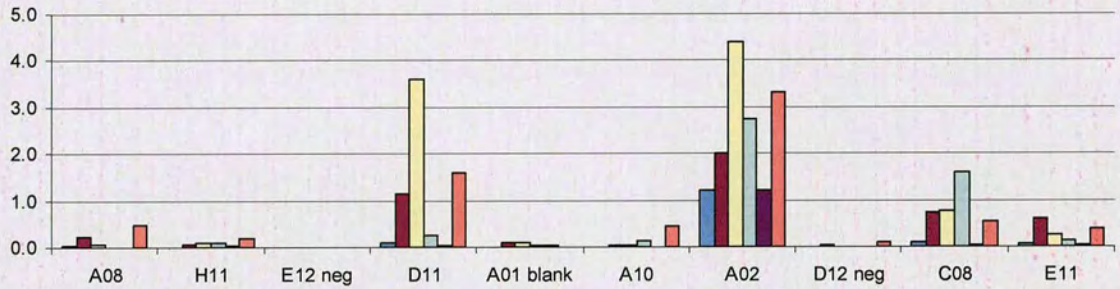




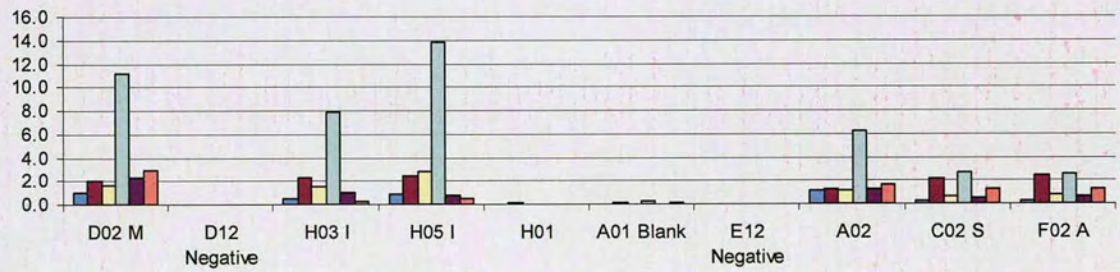
F58 4.1



F58 5.1



F58 6.1



RgDAAO F58: highest rates towards (*rac*)-*tert*-leucine

Plate-2.1	Normalised rate	Plate-3.1	Normalised rate
E03	1.1E-04	D09	2.0E-04
A01 blank	7.8E-05	A11	1.8E-04
H08 blank	7.0E-05	A01 blank	1.7E-04
E08	6.7E-05	A09	1.6E-04
C07	6.0E-05	H08 blank	1.6E-04
B03	5.9E-05	G07 blank	1.3E-04
F06 blank	4.7E-05	F05	1.3E-04
D04 blank	4.5E-05	B10	1.2E-04
G07 blank	4.4E-05	D04 blank	1.2E-04
E05 blank	4.3E-05	B04	1.1E-04
Av F58	0.0E+00	Av F58	4.4E-05

Plate-4.1	Normalised rate	Plate-5.1	Normalised rate	Plate-6.1	Normalised rate
A01 blank	1.0E-02	A08	1.3E-03	D02 M	9.3E-05
B02 blank	7.3E-03	H11	8.4E-05	D12 Negative	4.4E-05
C02	7.1E-03	E12 neg	5.0E-05	H03 I	4.3E-05
E05 blank	6.4E-03	D11	3.7E-05	H05 I	4.2E-05
F01	6.2E-03	A01 blank	3.1E-05	H01	3.7E-05
D04 blank	5.9E-03	A10	2.7E-05	A01 Blank	2.7E-05
G07 blank	5.1E-03	A02	1.4E-05	E12 Negative	2.4E-05
F02	4.8E-03	D12 neg	1.1E-05	A02	2.3E-05
G02	4.8E-03	C08	9.2E-06	C02 S	2.1E-05
H08 blank	4.8E-03	E11	8.9E-06	F02 A	2.0E-05
Av F58	7.6E-04	Av F58	0.0E+00	Av F58	0.0E+00

5.9.9 RgDAAO F58:(*rac*)- 3-aminobutyric acid

Plate-2.1	Normalised rate	Plate-3.1	Normalised rate
E03	2.1E-04	A09	3.8E-04
C07	1.9E-04	B07	3.1E-04
A01 *	1.3E-04	A11	2.7E-04
B03	1.0E-04	G01	2.7E-04
E08	8.9E-05	H12 F	2.4E-04
H08 *	8.8E-05	G02	2.4E-04
G07 *	7.3E-05	H08 *	2.2E-04
E05 *	6.6E-05	A01 *	2.1E-04
C03 *	6.3E-05	E04	2.0E-04
F06 *	6.1E-05	B10	1.9E-04
Av F58	0.0E+00	Av F58	1.6E-04

Plate-4.1	Normalised rate	Plate-5.1	Normalised rate	Plate-6.1	Normalised rate
A01 *	9.1E-05	H11	1.5E-04	D11 P	1.1E-04
H08 *	8.1E-05	A10	1.1E-04	E12 neg	8.7E-05
H01	8.0E-05	G01	9.7E-05	D10 C	7.1E-05
H12 F	7.9E-05	A08	8.0E-05	A01 *	7.0E-05
G07 *	6.6E-05	D11	7.7E-05	C09 T	6.0E-05
D04 *	6.0E-05	E11	6.2E-05	B09 T	4.6E-05
F06 *	5.4E-05	F11	6.0E-05	A09 I	4.2E-05
E05 *	4.8E-05	A01 *	4.3E-05	A11 S	2.8E-05
C03 *	4.6E-05	C09	3.6E-05	B10 T	2.4E-05
B02 *	4.4E-05	E12 neg	3.5E-05	A06	2.0E-05
Av F58	3.9E-05	Av F58	0.0E+00	Av F58	0.0E+00

5.9.10 RgDAAO F58: (*rac*)- β -phenylalanine

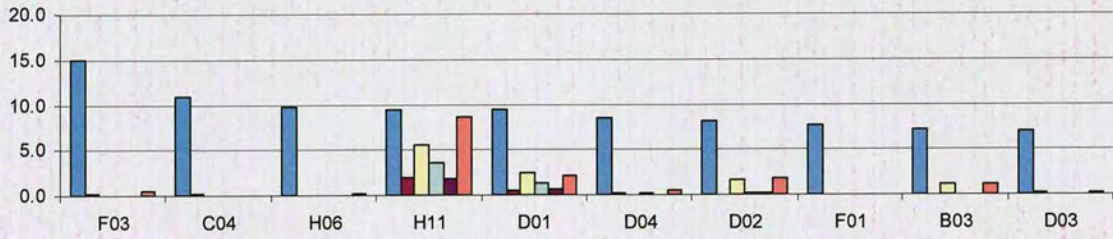
Plate-2.1	Normalised rate	Plate-3.1	Normalised rate
n.m.	n.m.	D09	3.9E-04
n.m.	n.m.	A01 *	3.8E-04
n.m.	n.m.	B07	3.7E-04
n.m.	n.m.	G02	2.4E-04
n.m.	n.m.	G01	2.4E-04
n.m.	n.m.	A11	2.3E-04
n.m.	n.m.	D05	2.2E-04
n.m.	n.m.	D02	2.2E-04
n.m.	n.m.	H12 F	2.0E-04
n.m.	n.m.	H08 *	1.8E-04
n.m.	n.m.	Av F58	1.4E-04

Plate-4.1	Normalised rate	Plate-5.1	Normalised rate	Plate-6.1	Normalised rate
A01 *	1.9E-04	A01 *	1.7E-04	A01 *	1.2E-04
H01	1.7E-04	H11	1.6E-04	E08	8.8E-05
H04	9.3E-05	A10	1.0E-04	D10 C	8.2E-05
D01	8.4E-05	G01	8.4E-05	D11 P	3.7E-05
H08 *	8.3E-05	E11	8.1E-05	H08 *	3.4E-05
B02 *	7.0E-05	A08	6.4E-05	C08 L	3.1E-05
B01	6.7E-05	E07	6.4E-05	D12 neg	2.7E-05
H02	6.6E-05	B10	6.2E-05	B02 *	2.7E-05
A04	6.1E-05	D11	5.9E-05	H12 F	2.0E-05
D02	5.9E-05	C08	5.8E-05	E12 neg	1.8E-05
Av F58	0.0E+00	Av F58	7.6E-06	Av F58	1.0E-05

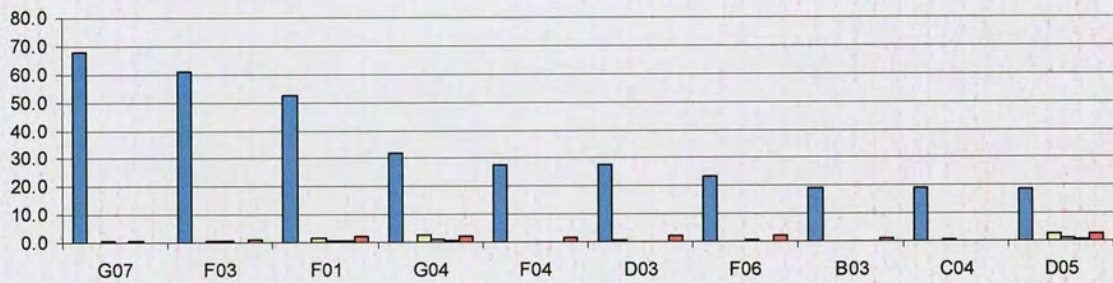
5.9.11 RgDAAO M213: (*rac*)-tetrahydroisoquinoline-3-carboxylic acid

(<i>rac</i>)-1,2,3,4-tetrahydroisoquinoline-3-carboxylic acid	(<i>R</i>)-Ser	(<i>rac</i>)-pyridylalanine	(<i>rac</i>)-homo-phenylalanine	(<i>R</i>)-Phe	(<i>rac</i>)- β -methylphenylalanine

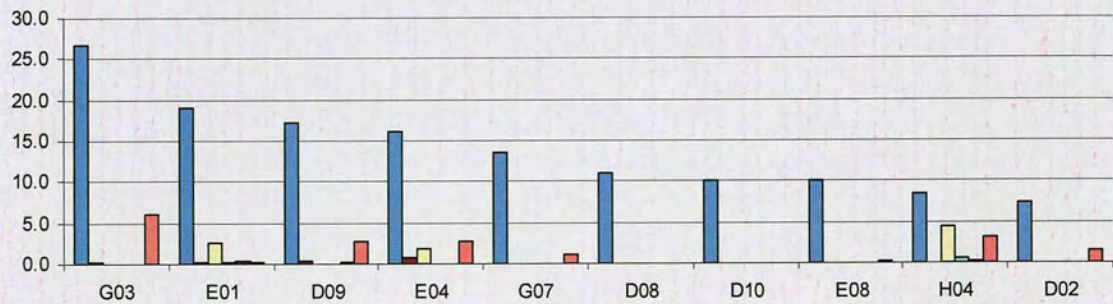
M213 1.1



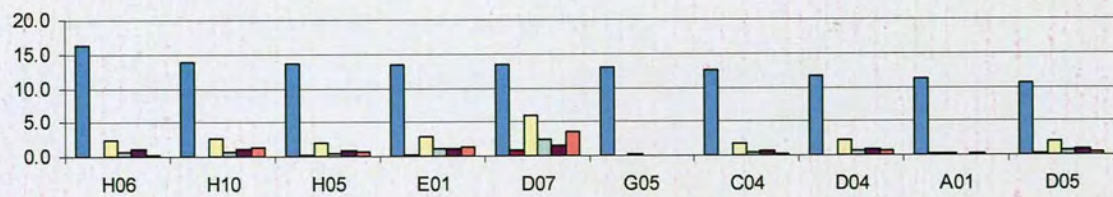
M213 2.1



M213 3.1



M213 5.1



RgDAAO M213: highest rates towards (*rac*)-tetrahydroisoquinoline-3-carboxylic acid

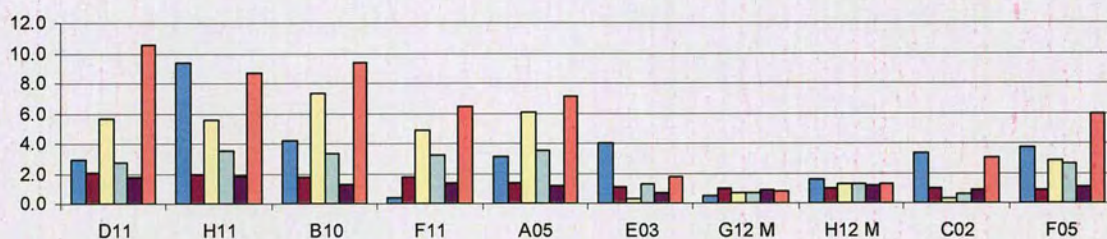
Plate-1.1	Normalised rate	Plate-2.1	Normalised rate	Plate-3.1	Normalised rate
F03	4.9E-01	G07	6.9E-01	G03	9.2E-01
C04	3.6E-01	F03	6.1E-01	E01	6.5E-01
H06	3.2E-01	F01	5.3E-01	D09	5.9E-01
H11	3.1E-01	G04	3.2E-01	E04	5.5E-01
D01	3.1E-01	F04	2.8E-01	G07	4.6E-01
D04	2.8E-01	D03	2.8E-01	D08	3.7E-01
D02	2.7E-01	F06	2.4E-01	D10	3.5E-01
F01	2.5E-01	B03	2.0E-01	E08	3.4E-01
B03	2.3E-01	C04	2.0E-01	H04	2.9E-01
D03	2.3E-01	D05	1.9E-01	D02	2.5E-01
Av M213	3.3E-02	Av M213	1.0E-02	Av M213	3.4E-02

Plate-5.1	Normalised rate
H06	2.4E-01
H10	2.0E-01
H05	2.0E-01
E01	2.0E-01
D07	1.9E-01
G05	1.9E-01
C04	1.8E-01
D04	1.7E-01
A01	1.6E-01
D05	1.5E-01
Av M213	1.5E-02

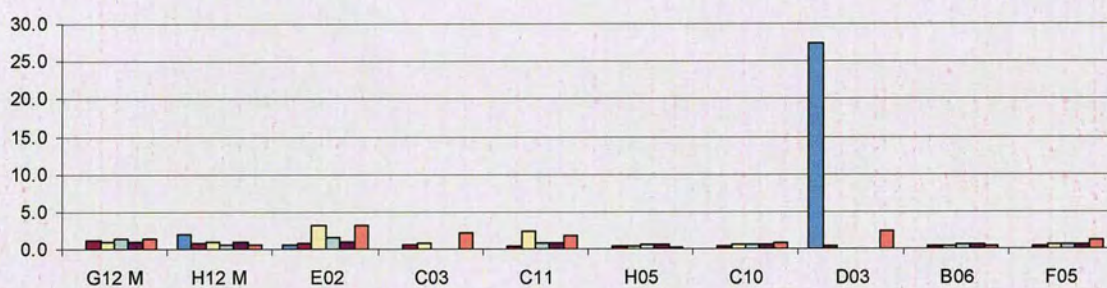
5.9.12 RgDAAO M213: (*R*)-serine

<i>(rac)</i> -1,2,3,4-tetrahydroisoquinoline-3-carboxylic acid	(<i>R</i>)-Ser	<i>(rac)</i> -pyridylalanine	<i>(rac)</i> -homophenylalanine	(<i>R</i>)-Phe	<i>(rac)</i> - β -methylphenylalanine

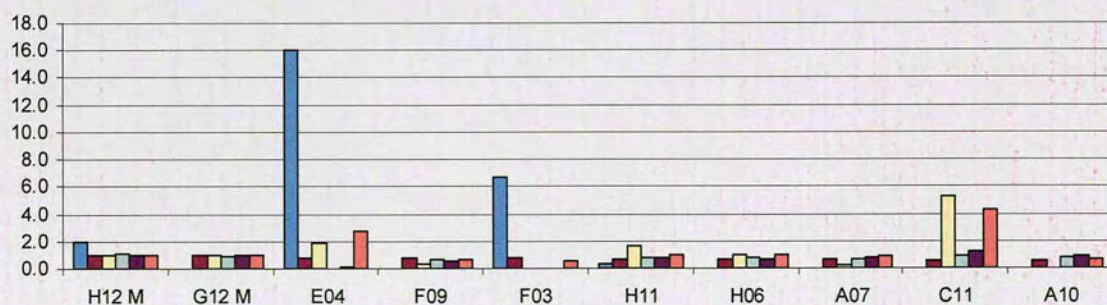
M213 1.1

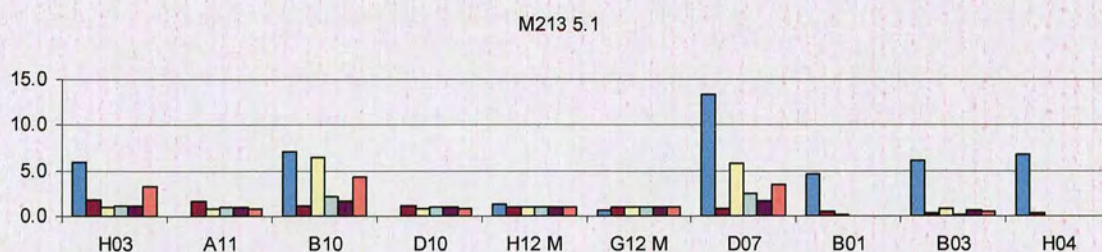


M213 2.1



M213 3.1





RgDAAO M213: highest rates towards (*R*)-serine

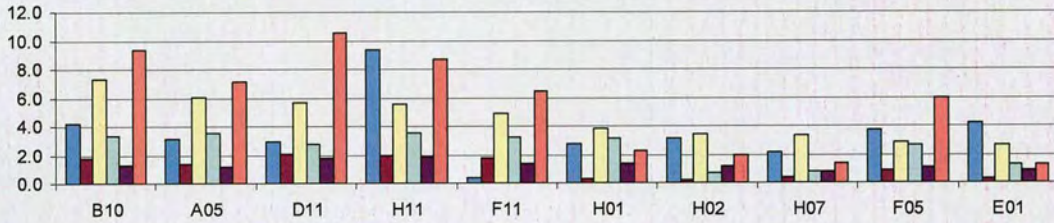
Plate-1.1	Normalised rate	Plate-2.1	Normalised rate	Plate-3.1	Normalised rate
D11	1.8E+00	G12 M	1.1E+00	H12 M	1.2E+00
H11	1.7E+00	H12 M	7.4E-01	G12 M	1.1E+00
B10	1.6E+00	E02	7.0E-01	E04	8.7E-01
F11	1.5E+00	C03	4.8E-01	F09	8.4E-01
A05	1.2E+00	C11	3.9E-01	F03	8.4E-01
E03	9.8E-01	H05	3.8E-01	H11	7.5E-01
G12 M	8.9E-01	C10	3.5E-01	H06	7.2E-01
H12 M	8.8E-01	D03	3.4E-01	A07	7.1E-01
C02	8.2E-01	B06	3.1E-01	C11	6.7E-01
F05	8.0E-01	F05	2.8E-01	A10	6.6E-01
Av M213	8.8E-01	Av M213	9.2E-01	Av M213	1.2E+00

Plate-5.1	Normalised rate
H03	1.5E+00
A11	1.4E+00
B10	1.0E+00
D10	1.0E+00
H12 M	8.9E-01
G12 M	8.4E-01
D07	7.0E-01
B01	4.1E-01
B03	3.4E-01
H04	2.6E-01
Av M213	8.6E-01

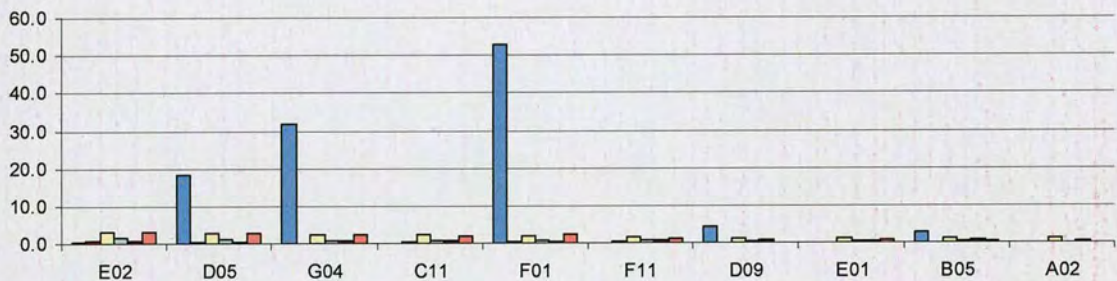
5.9.13 RgDAAO M213: (*rac*)- β -pyridylalanine

<i>(rac)</i> -1,2,3,4-tetrahydroisoquinoline-3-carboxylic acid	(<i>R</i>)-Ser	<i>(rac)</i> -pyridylalanine	<i>(rac)</i> -homo-phenylalanine	(<i>R</i>)-Phe	<i>(rac)</i> - β -methylphenylalanine

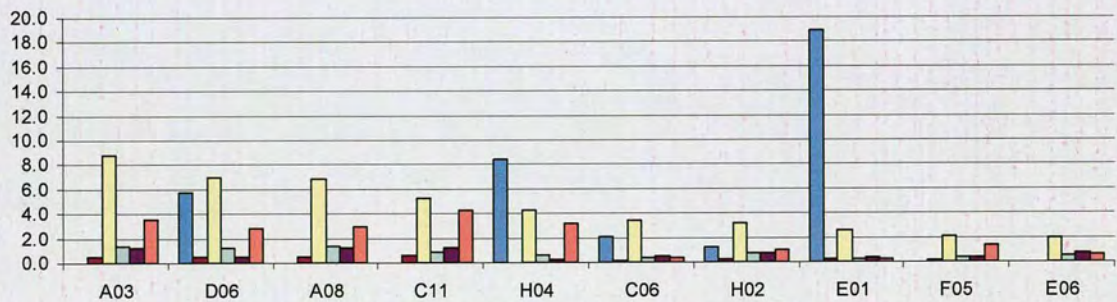
M213 1.1



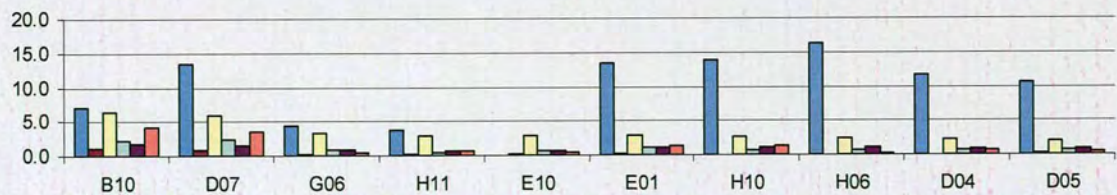
M213 2.1



M213 3.1



M213 5.1



RgDAAO M213: highest rates towards (*rac*)- β -pyridylalanine

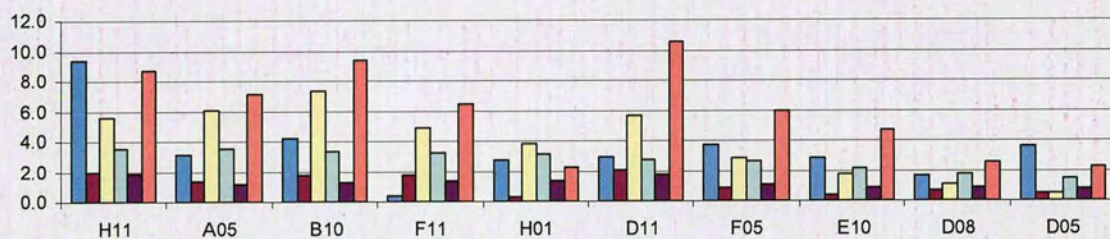
Plate-1.1	Normalised rate	Plate-2.1	Normalised rate	Plate-3.1	Normalised rate
B10	2.5E+00	E02	6.7E-01	A03	1.1E+00
A05	2.1E+00	D05	5.6E-01	D06	9.0E-01
D11	1.9E+00	G04	5.2E-01	A08	8.8E-01
H11	1.9E+00	C11	5.1E-01	C11	6.7E-01
F11	1.6E+00	F01	3.8E-01	H04	5.5E-01
H01	1.3E+00	F11	3.6E-01	C06	4.3E-01
H02	1.2E+00	D09	2.7E-01	H02	4.1E-01
H07	1.1E+00	E01	2.5E-01	E01	3.2E-01
F05	9.5E-01	B05	2.4E-01	F05	2.6E-01
E01	9.0E-01	A02	2.3E-01	E06	2.4E-01
Av M213	3.4E-01	Av M213	2.1E-01	Av M213	1.3E-01

Plate-5.1	Normalised rate
B10	1.9E+00
D07	1.7E+00
G06	9.6E-01
H11	8.6E-01
E10	8.4E-01
E01	8.4E-01
H10	7.7E-01
H06	7.3E-01
D04	6.2E-01
D05	6.1E-01
Av M213	3.0E-01

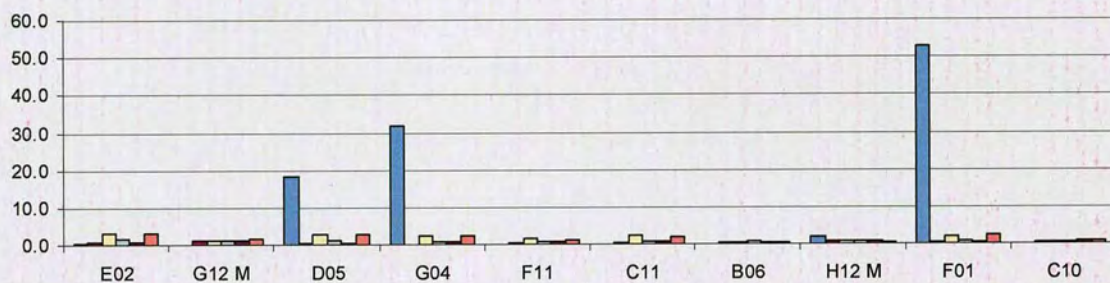
5.9.14 RgDAAO M213: (*rac*)-homophenylalanine

<i>(rac)</i> -1,2,3,4-tetrahydroisoquinoline-3-carboxylic acid	(<i>R</i>)-Ser	<i>(rac)</i> -pyridylalanine	<i>(rac)</i> -homophenylalanine	(<i>R</i>)-Phe	<i>(rac)</i> - β -methylphenylalanine

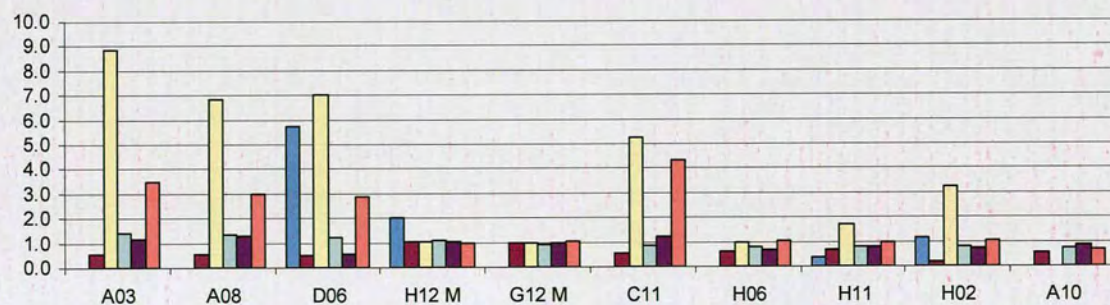
M213 1.1



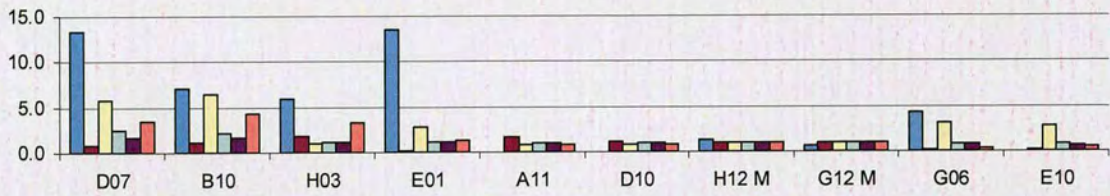
M213 2.1



M213 3.1



M213 5.1



RgDAAO M213: highest rates towards (*rac*)-homophenylalanine

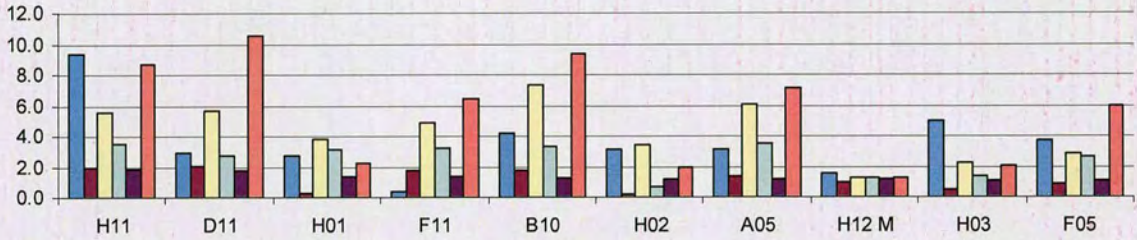
Plate-1.1	Normalised rate	Plate-2.1	Normalised rate	Plate-3.1	Normalised rate
H11	3.8E+00	E02	1.4E+00	A03	2.2E+00
A05	3.8E+00	G12 M	1.1E+00	A08	2.2E+00
B10	3.5E+00	D05	9.0E-01	D06	2.0E+00
F11	3.4E+00	G04	8.3E-01	H12 M	1.7E+00
H01	3.4E+00	F11	7.1E-01	G12 M	1.5E+00
D11	2.9E+00	C11	6.2E-01	C11	1.3E+00
F05	2.8E+00	B06	5.6E-01	H06	1.3E+00
E10	2.3E+00	H12 M	5.5E-01	H11	1.3E+00
D08	1.8E+00	F01	5.5E-01	H02	1.2E+00
D05	1.6E+00	C10	5.0E-01	A10	1.2E+00
Av M213	1.1E+00	Av M213	8.5E-01	Av M213	1.6E+00

Plate-5.1	Normalised rate
D07	5.4E+00
B10	4.6E+00
H03	2.4E+00
E01	2.3E+00
A11	2.3E+00
D10	2.2E+00
H12 M	2.1E+00
G12 M	2.1E+00
G06	1.8E+00
E10	1.6E+00
Av M213	2.1E+00

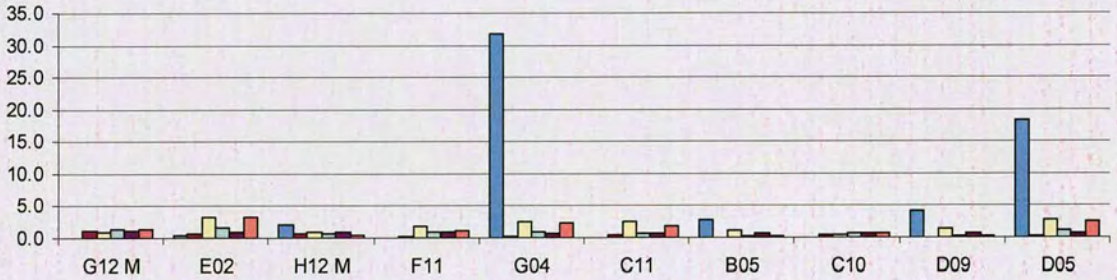
5.9.15 RgDAAO M213: (*rac*)-phenylalanine

<i>(rac)</i> -1,2,3,4-tetrahydroisoquinoline-3-carboxylic acid	(<i>R</i>)-Ser	<i>(rac)</i> -pyridylalanine	<i>(rac)</i> -homophenylalanine	(<i>R</i>)-Phe	<i>(rac)</i> - β -methylphenylalanine
--	------------------	------------------------------	---------------------------------	------------------	---

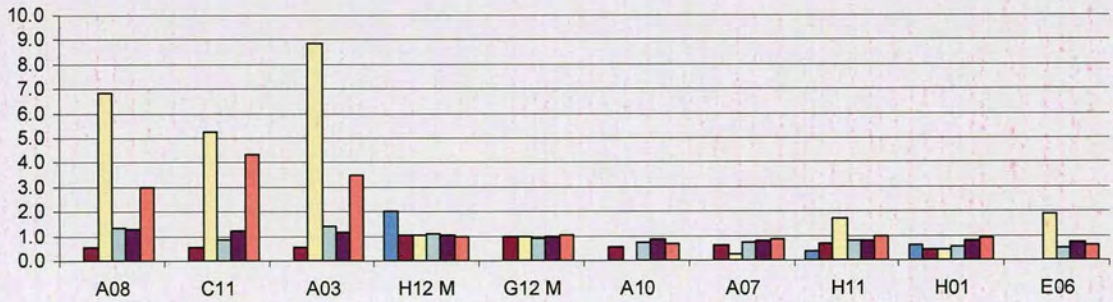
M213 1.1



M213 2.1

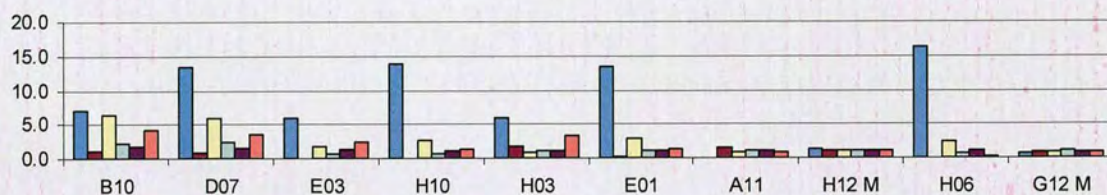


M213 3.1



<i>(rac)</i> -1,2,3,4-tetrahydroisoquinoline-3-carboxylic acid	<i>(R)</i> -Ser	<i>(rac)</i> -pyridylalanine	<i>(rac)</i> -homo-phenylalanine	<i>(R)</i> -Phe	<i>(rac)</i> - β -methylphenylalanine

M213 5.1



RgDAAO M213: highest rates towards *(rac)*-phenylalanine

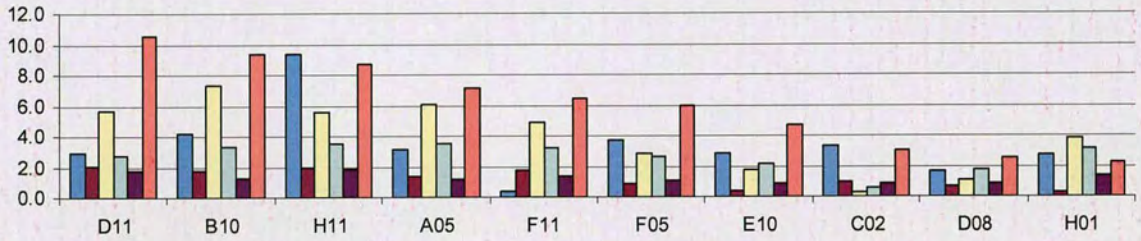
Plate-1.1	Normalised rate	Plate-2.1	Normalised rate	Plate-3.1	Normalised rate
H11	1.0E+01	G12 M	4.1E+00	A08	7.6E+00
D11	9.7E+00	E02	3.7E+00	C11	7.3E+00
H01	7.8E+00	H12 M	3.6E+00	A03	7.0E+00
F11	7.7E+00	F11	3.3E+00	H12 M	6.1E+00
B10	7.3E+00	G04	2.9E+00	G12 M	5.8E+00
H02	6.5E+00	C11	2.8E+00	A10	5.0E+00
A05	6.4E+00	B05	2.4E+00	A07	4.8E+00
H12 M	6.2E+00	C10	2.4E+00	H11	4.7E+00
H03	6.2E+00	D09	2.3E+00	H01	4.6E+00
F05	5.9E+00	D05	2.2E+00	E06	4.5E+00
Av M213	5.5E+00	Av M213	3.8E+00	Av M213	6.0E+00

Plate-5.1	Normalised rate
B10	1.5E+01
D07	1.4E+01
E03	1.2E+01
H10	1.0E+01
H03	1.0E+01
E01	9.6E+00
A11	9.3E+00
H12 M	9.3E+00
H06	9.2E+00
G12 M	8.5E+00
Av M213	8.9E+00

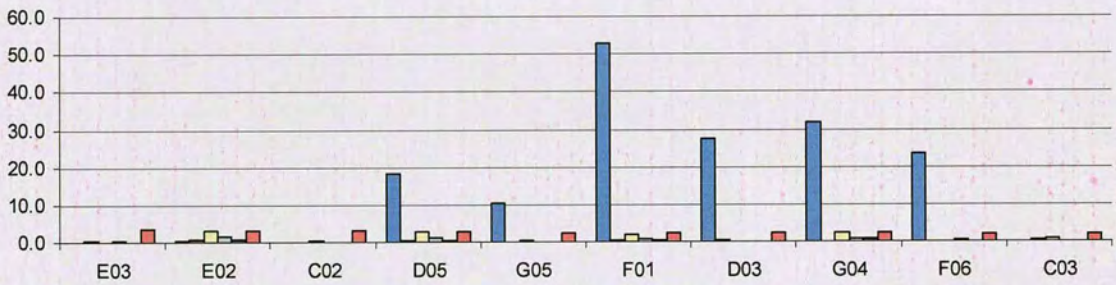
5.9.16 RgDAAO M213: (*rac*)- β -methylphenylalanine

<i>(rac)</i> -1,2,3,4-tetrahydroisoquinoline-3-carboxylic acid	(<i>R</i>)-Ser	<i>(rac)</i> -pyridylalanine	<i>(rac)</i> -homo-phenylalanine	(<i>R</i>)-Phe	<i>(rac)</i> - β -methylphenylalanine

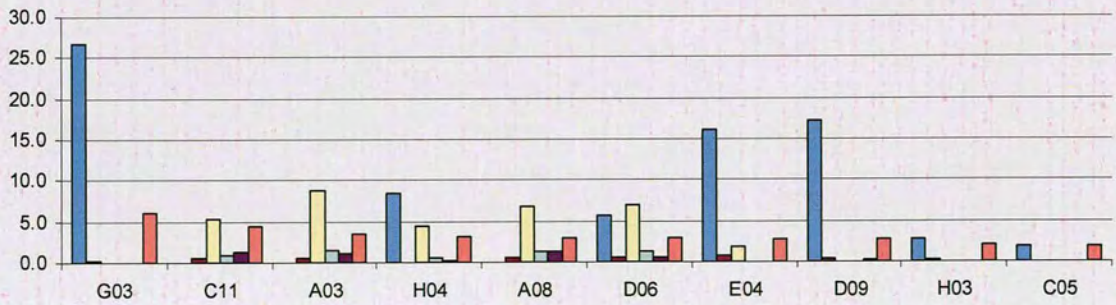
M213 1.1



M213 2.1

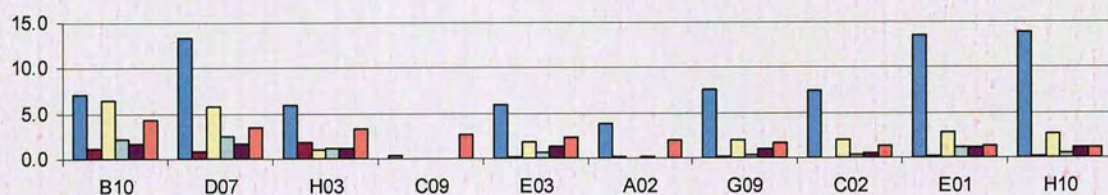


M213 3.1



<i>(rac)</i> -1,2,3,4-tetrahydroisoquinoline-3-carboxylic acid	<i>(R)</i> -Ser	<i>(rac)</i> -pyridylalanine	<i>(rac)</i> -homo-phenylalanine	<i>(R)</i> -Phe	<i>(rac)</i> - β -methylphenylalanine

M213 5.1



RgDAAO M213: highest rates towards *(rac)*- β -methylphenylalanine

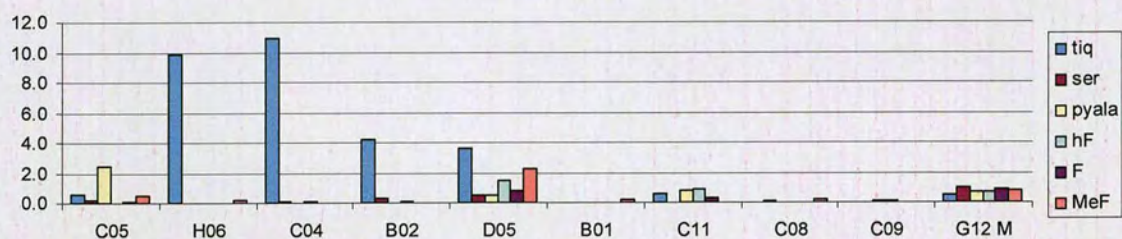
Plate-1.1	Normalised rate	Plate-2.1	Normalised rate	Plate-3.1	Normalised rate
D11	1.3E+00	E03	6.1E-01	G03	8.8E-01
B10	1.2E+00	E02	5.4E-01	C11	6.4E-01
H11	1.1E+00	C02	5.1E-01	A03	5.2E-01
A05	9.0E-01	D05	4.4E-01	H04	4.7E-01
F11	8.1E-01	G05	4.0E-01	A08	4.4E-01
F05	7.5E-01	F01	3.9E-01	D06	4.2E-01
E10	6.0E-01	D03	3.9E-01	E04	4.1E-01
C02	3.8E-01	G04	3.7E-01	D09	4.0E-01
D08	3.2E-01	F06	3.5E-01	H03	3.1E-01
H01	2.9E-01	C03	3.5E-01	C05	2.8E-01
Av M213	1.3E-01	Av M213	1.7E-01	Av M213	1.5E-01

Plate-5.1	Normalised rate
B10	7.3E-01
D07	6.0E-01
H03	5.6E-01
C09	4.7E-01
E03	4.0E-01
A02	3.5E-01
G09	3.0E-01
C02	2.4E-01
E01	2.2E-01
H10	2.1E-01
Av M213	1.7E-01

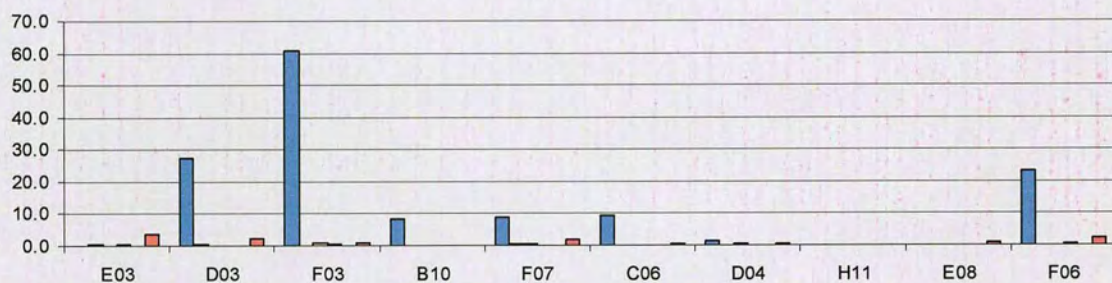
5.9.17 RgDAAO M213: (*rac*)- β -homophenylalanine

<i>(rac)</i> -1,2,3,4-tetrahydroisoquinoline-3-carboxylic acid	(<i>R</i>)-Ser	<i>(rac)</i> -pyridylalanine	<i>(rac)</i> -homophenylalanine	(<i>R</i>)-Phe	<i>(rac)</i> - β -methylphenylalanine

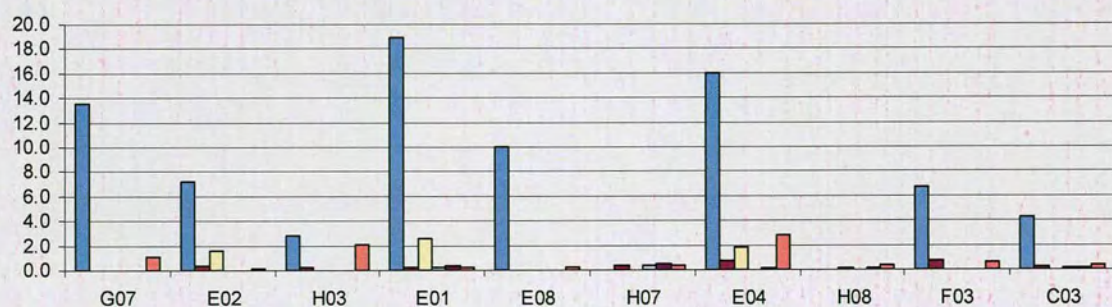
M213 1.1

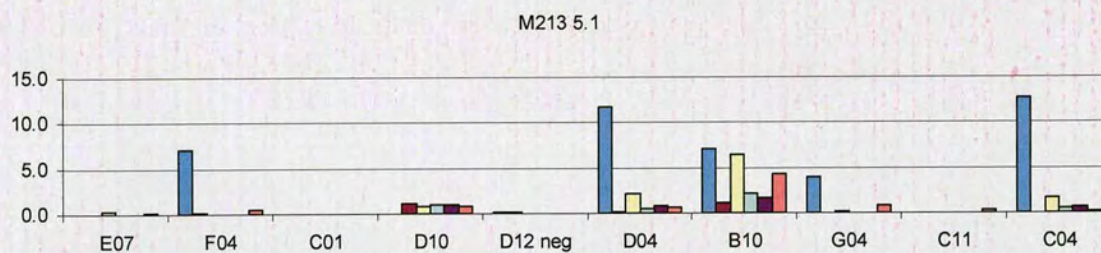


M213 2.1



M213 3.1





RgDAAO M213: highest rates towards (*rac*)- β -homophenylalanine

Plate-1.1	Normalised rate	Plate-2.1	Normalised rate	Plate-3.1	Normalised rate
C05	2.4E-01	E03	3.9E-01	G07	1.2E+00
H06	2.2E-01	D03	3.2E-01	E02	3.7E-01
C04	2.1E-01	F03	2.1E-01	H03	3.3E-01
B02	2.0E-01	B10	1.7E-01	E01	2.9E-01
D05	1.9E-01	F07	1.5E-01	E08	2.3E-01
B01	1.8E-01	C06	1.5E-01	H07	2.1E-01
C11	1.7E-01	D04	1.1E-01	E04	2.1E-01
C08	1.6E-01	H11	1.0E-01	H08	1.9E-01
C09	1.4E-01	E08	9.8E-02	F03	1.9E-01
G12 M	1.4E-01	F06	8.9E-02	C03	1.1E-01
Av M213	6.8E-02	Av M213	0.0E+00	Av M213	0.0E+00

Plate-5.1	Normalised rate
E07	6.6E-02
F04	5.5E-02
C01	5.2E-02
D10	2.7E-02
D12 neg	1.9E-02
D04	1.7E-02
B10	1.6E-02
G04	1.5E-02
C11	8.8E-03
C04	5.6E-03
Av M213	0.0E+00

5.9.18 RgDAAO M213: (*rac*)- 3-aminobutyric acid

Plate-1.1	Normalised rate	Plate-2.1	Normalised rate	Plate-3.1	Normalised rate
C04	1.4E+00	F06	3.0E-01	E04	8.4E-02
F01	1.1E+00	E03	2.2E-01	F09	7.4E-02
C06	7.0E-01	F03	2.0E-01	C04	4.1E-02
C11	6.2E-01	D02	2.0E-01	G07	4.0E-02
A08	5.7E-01	C02	1.7E-01	F02	3.4E-02
C08	5.2E-01	D03	1.7E-01	F03	2.4E-02
A06	2.0E-01	C05	1.6E-01	F05	2.3E-02
B01	1.8E-01	G04	1.3E-01	D11	2.1E-02
E06	1.6E-01	G06	1.3E-01	E10	2.1E-02
B06	1.4E-01	F07	1.2E-01	H01	1.9E-02
Av M213	1.6E-02	Av M213	2.4E-02	Av M213	6.1E-03

Plate-5.1	Normalised rate
D02	4.7E-01
C07	2.9E-01
G05	2.6E-01
H05	2.4E-01
A05	2.2E-01
C02	2.1E-01
H04	1.9E-01
F06	1.5E-01
E09	1.4E-01
G08	1.4E-01
Av M213	1.3E-02

5.9.19 RgDAAO M213: (*rac*)- β -phenylalanine

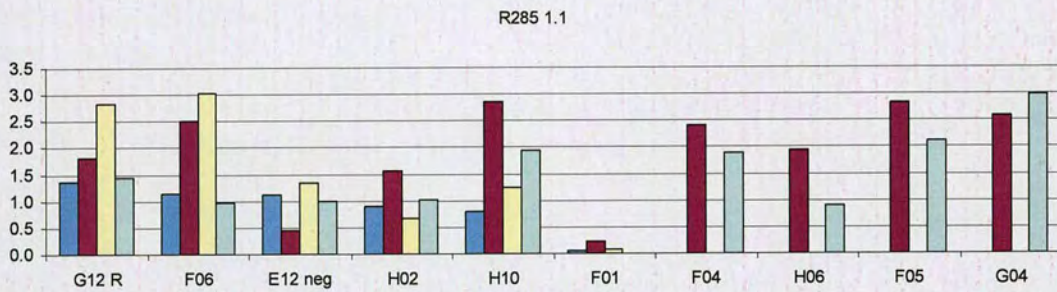
Plate-1.1	Normalised rate	Plate-2.1	Normalised rate	Plate-3.1	Normalised rate
E05	8.0E-01	C05	6.6E-01	E03	9.7E-01
E03	5.8E-01	E06	5.4E-01	G07	8.5E-01
C11	5.5E-01	E07	5.0E-01	G05	8.1E-01
C04	5.4E-01	G06	4.2E-01	G04	7.9E-01
C05	3.7E-01	E05	4.2E-01	F11	7.8E-01
D02	3.3E-01	H03	4.0E-01	E07	7.8E-01
G03	3.3E-01	H08	3.7E-01	C03	7.8E-01
F05	3.2E-01	D02	3.6E-01	E02	7.3E-01
D05	3.0E-01	H07	3.5E-01	G03	7.2E-01
H06	2.9E-01	A07	3.5E-01	D03	7.1E-01
Av M213	7.1E-02	Av M213	1.9E-02	Av M213	0.0E+00

Plate-5.1	Normalised rate
C06	2.3E-01
E01	9.7E-02
C04	9.2E-02
F04	9.1E-02
E03	7.8E-02
C01	7.0E-02
E02	6.5E-02
G04	6.4E-02
C02	6.0E-02
G01	6.0E-02
Av M213	0.0E+00

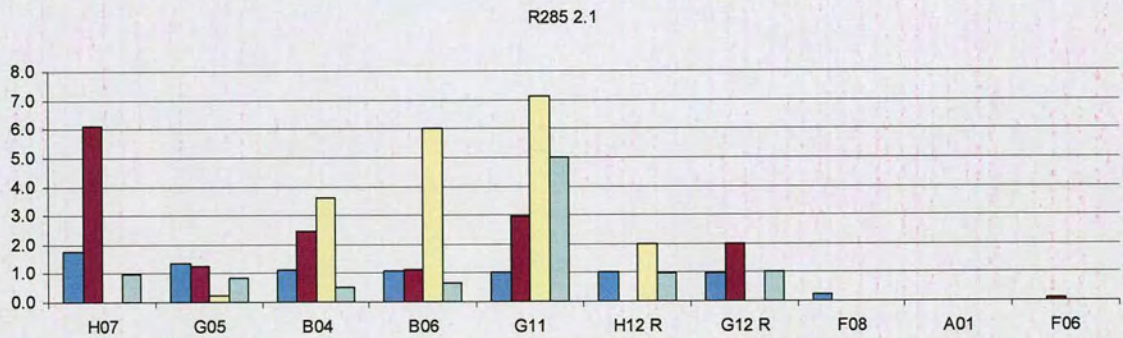
5.9.20 RgDAAO R285: (*R*)-alanine

The activity profiles relating to the variants displaying the highest activities towards (*R*)-alanine from plate 5.1 is shown in the main text (Figure 2.50).

(<i>R</i>)-Ala	(<i>rac</i>)- <i>allo</i> -Thr	(<i>S</i>)-Ala	(<i>rac</i>)-1,2,3,4-tetrahydroisoquinoline-3-carboxylic acid

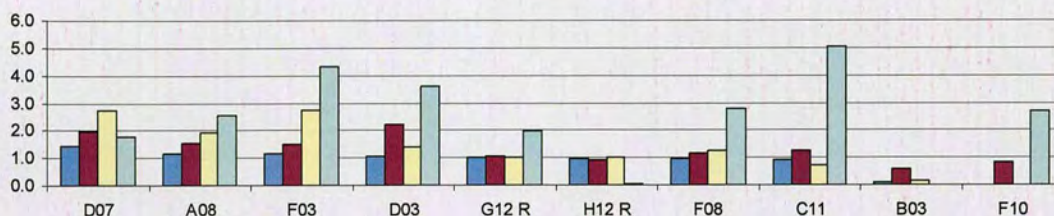


The negative control well E12 contained a contamination carried from the growth plate R285 1.1 to all assay plates.

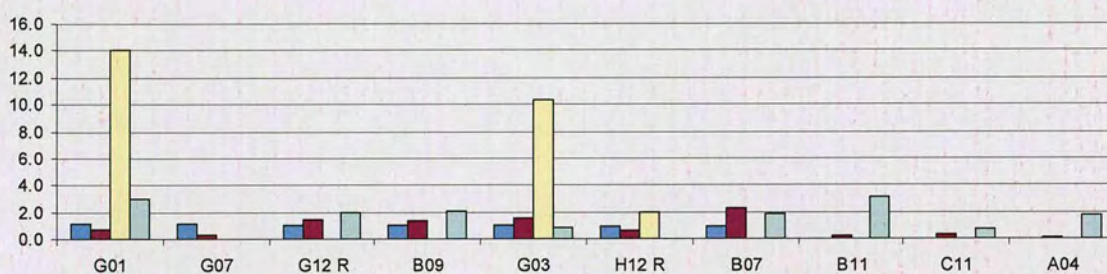


(<i>R</i>)-Ala	(<i>rac</i>)- <i>allo</i> -Thr	(<i>S</i>)-Ala	(<i>rac</i>)-1,2,3,4-tetrahydroisoquinoline-3-carboxylic acid

R285 3.1



R285 6.1



RgDAAO R285: highest rates towards (*R*)-alanine

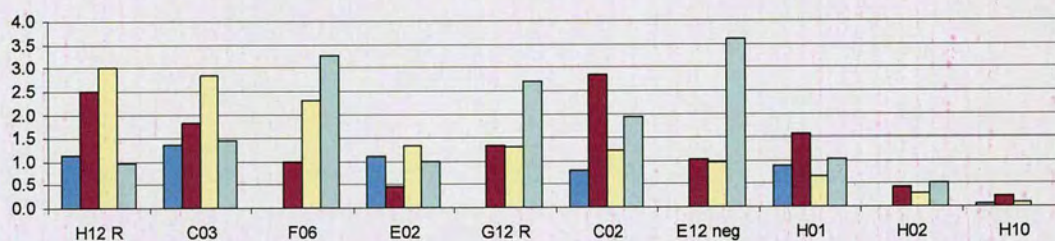
Plate-1.1	Normalised rate	Plate-2.1	Normalised rate	Plate-3.1	Normalised rate
G12 R	1.4E+00	H07	1.8E+00	D07	1.5E+00
F06	1.2E+00	G05	1.4E+00	A08	1.2E+00
E12 neg	1.1E+00	B04	1.1E+00	F03	1.2E+00
F09	9.0E-01	B06	1.1E+00	D03	1.1E+00
D01	8.0E-01	G11	1.0E+00	G12 R	1.1E+00
H10	4.9E-02	H12 R	1.0E+00	H12 R	1.0E+00
D08	0.0E+00	G12 R	1.0E+00	F08	1.0E+00
G06	0.0E+00	F08	2.1E-01	C11	9.7E-01
A02	0.0E+00	A01	5.0E-04	B03	1.1E-01
B10	0.0E+00	F06	4.8E-04	F10	1.1E-02
Av R285	1.0E+00	Av R285	1.0E+00	Av R285	1.0E+00

Plate-5.1	Normalised rate	Plate-6.1	Normalised rate
E11	1.7E+00	G01	1.4E+00
H06	1.6E+00	G07	1.4E+00
A05	1.5E+00	G12 R	1.3E+00
G10	1.5E+00	B09	1.3E+00
H09	1.4E+00	G03	1.2E+00
F11	1.1E+00	H12 R	1.2E+00
H12 R	7.8E-01	B07	1.1E+00
G12 R	6.3E-01	B11	5.1E-02
B05	6.7E-03	C11	3.9E-02
D06	4.3E-03	A04	3.6E-02
Av R285	7.0E-01	Av R285	1.2E+00

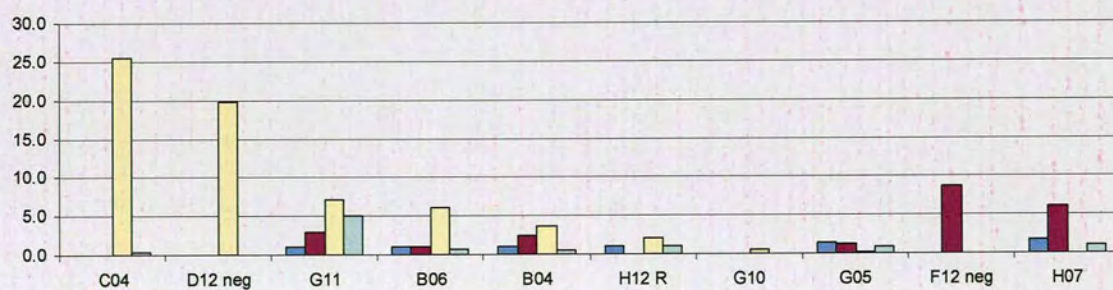
5.9.21 RgDAAO R285: (*S*)-alanine

(<i>R</i>)-Ala	(<i>rac</i>)- <i>allo</i> -Thr	(<i>S</i>)-Ala	(<i>rac</i>)-1,2,3,4-tetrahydroisoquinoline-3-carboxylic acid

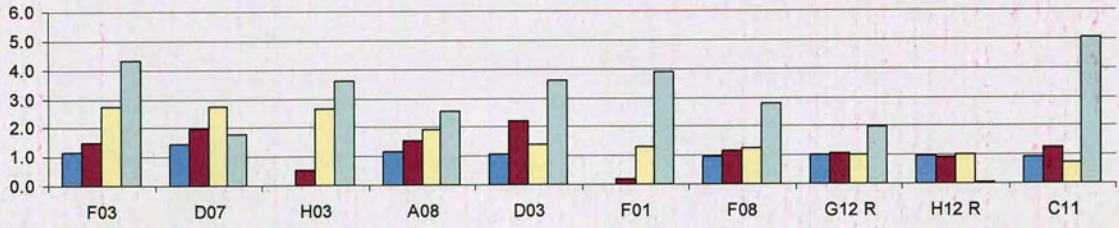
R285 1.1



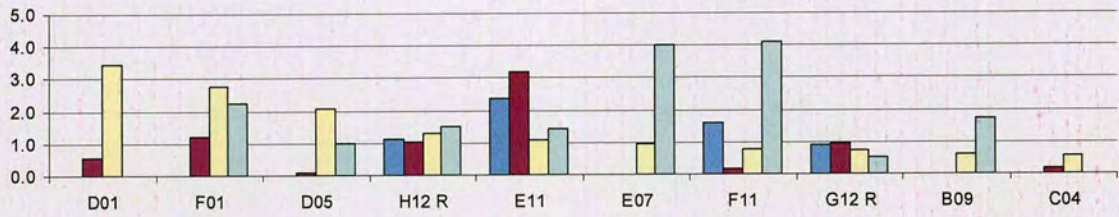
R285 2.1



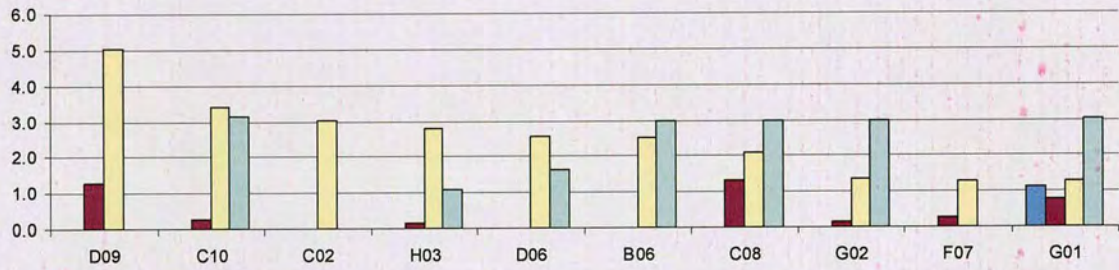
R285 3.1



R285 5.1



R285 6.1



RgDAAO R285: highest rates towards (S)-alanine

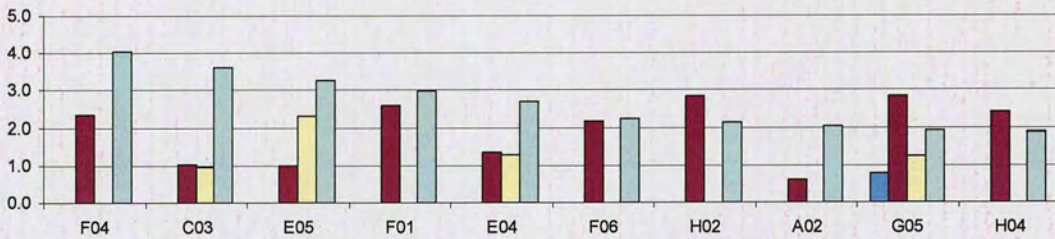
Plate-1.1	Normalised rate	Plate-2.1	Normalised rate	Plate-3.1	Normalised rate
H12 R	6.3E-03	C04	4.2E-03	D09	1.6E+00
C03	5.9E-03	D12 neg	3.3E-03	A09	1.5E+00
F06	4.8E-03	G11	1.2E-03	D05	1.5E+00
E02	2.8E-03	B06	1.0E-03	F03	1.0E+00
G12 R	2.7E-03	B04	6.0E-04	A08	1.4E-01
C02	2.6E-03	H12 R	3.3E-04	H12 R	1.1E-01
E12 neg	2.0E-03	G10	9.3E-05	E07	9.3E-02
H01	1.4E-03	G05	3.5E-05	F10	9.1E-02
F01	6.0E-04	F12 neg	0.0E+00	E11	9.1E-02
F04	1.8E-04	H07	0.0E+00	H07	8.7E-02
Av R285	2.1E-03	Av R285	1.7E-04	Av R285	6.0E-02

Plate-5.1	Normalised rate	Plate-6.1	Normalised rate
D01	1.6E-02	D09	4.8E-02
F01	1.3E-02	C10	3.3E-02
D05	9.4E-03	C02	2.9E-02
H12 R	5.8E-03	H03	2.7E-02
E11	4.9E-03	D06	2.5E-02
E07	4.4E-03	B06	2.4E-02
F11	3.6E-03	C08	2.0E-02
G12 R	3.3E-03	G02	1.3E-02
B09	2.7E-03	F07	1.2E-02
C04	2.6E-03	G01	1.2E-02
Av R285	4.5E-03	Av R285	9.6E-03

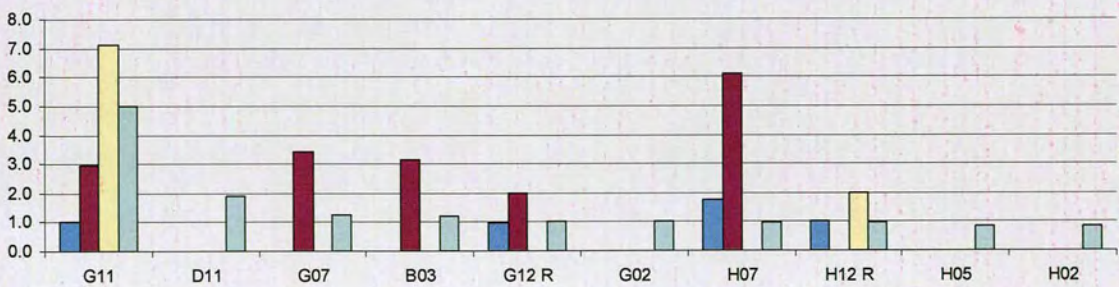
5.9.22 RgDAAO R285: (*rac*)-tetrahydroisoquinoline-3-carboxylic acid

(<i>R</i>)-Ala	(<i>rac</i>)- <i>allo</i> -Thr	(<i>S</i>)-Ala	(<i>rac</i>)-1,2,3,4-tetrahydroisoquinoline-3-carboxylic acid

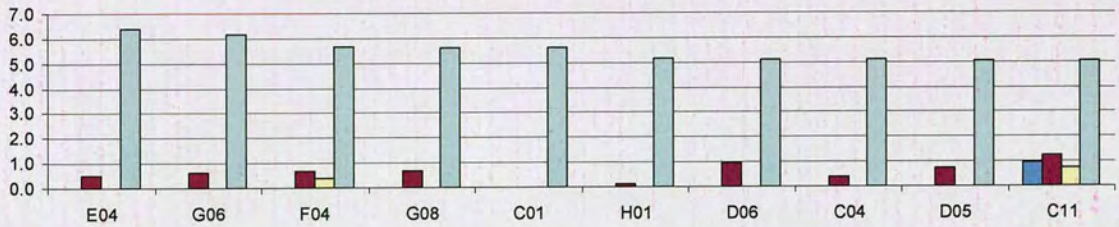
R285 1.1



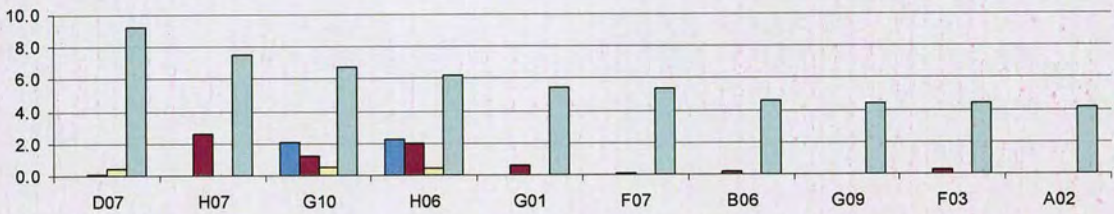
R285 2.1



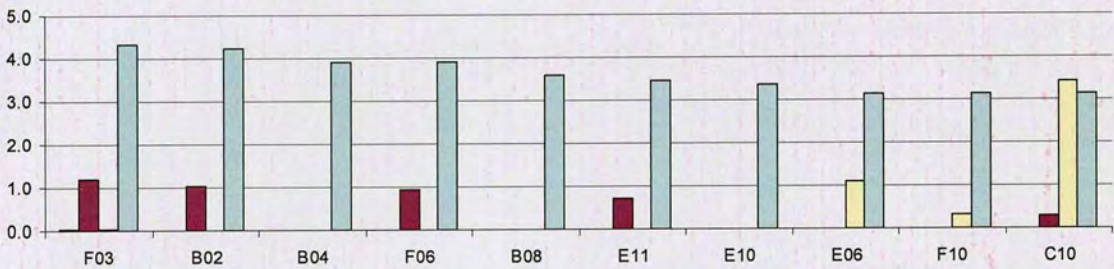
R285 3.1



R285 5.1



R285 6.1



RgDAAO R285: highest rates towards (*rac*)-tetrahydroisoquinoline-3-carboxylic acid

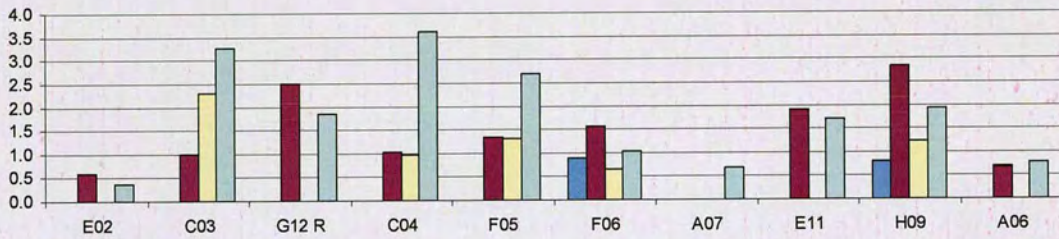
Plate-1.1	Normalised rate	Plate-2.1	Normalised rate	Plate-3.1	Normalised rate
F04	1.7E-01	G11	4.0E-02	E04	1.6E-01
C03	1.5E-01	D11	1.5E-02	G06	1.5E-01
E05	1.4E-01	G07	1.0E-02	F04	1.4E-01
F01	1.2E-01	B03	9.5E-03	G08	1.4E-01
E04	1.1E-01	G12 R	8.1E-03	C01	1.4E-01
F06	9.3E-02	G02	8.1E-03	H01	1.3E-01
H02	8.8E-02	H07	8.0E-03	D06	1.3E-01
A02	8.4E-02	H12 R	8.0E-03	C04	1.2E-01
G05	8.0E-02	H05	6.8E-03	D05	1.2E-01
H04	7.8E-02	H02	6.5E-03	C11	1.2E-01
Av R285	4.2E-02	Av R285	8.0E-03	Av R285	2.4E-02

Plate-5.1	Normalised rate	Plate-6.1	Normalised rate
D07	9.1E-02	F03	1.6E-01
H07	7.4E-02	B02	1.6E-01
G10	6.6E-02	B04	1.5E-01
H06	6.1E-02	F06	1.5E-01
G01	5.3E-02	B08	1.3E-01
F07	5.3E-02	E11	1.3E-01
B06	4.5E-02	E10	1.3E-01
G09	4.3E-02	E06	1.2E-01
F03	4.3E-02	F10	1.2E-01
A02	4.1E-02	C10	1.2E-01
Av R285	9.8E-03	Av R285	3.8E-02

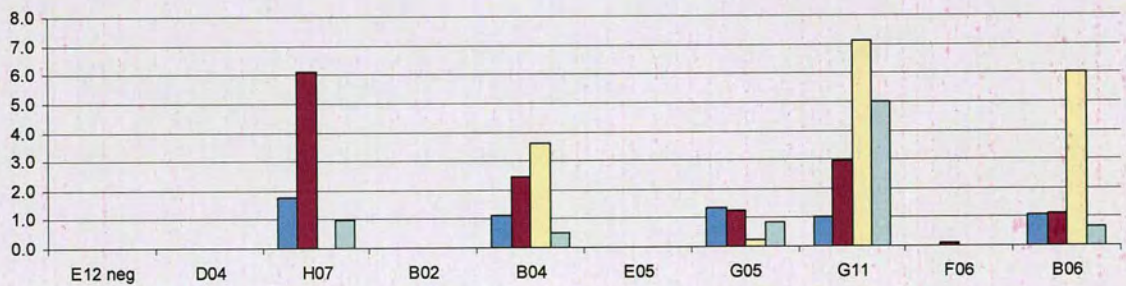
5.9.23 RgDAAO R285: (*R*)-pipecolinic acid

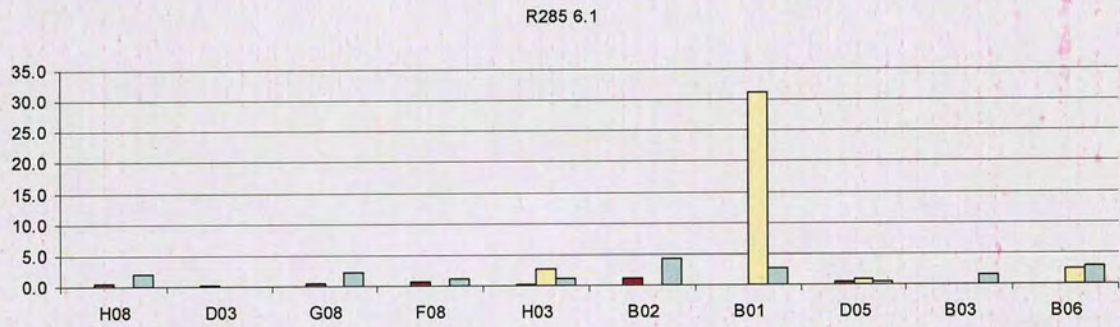
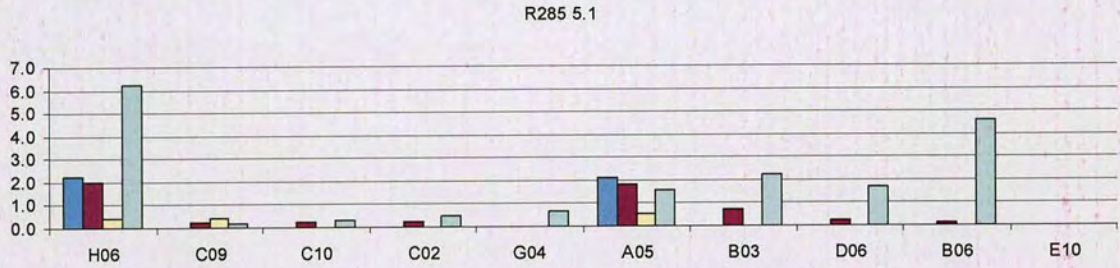
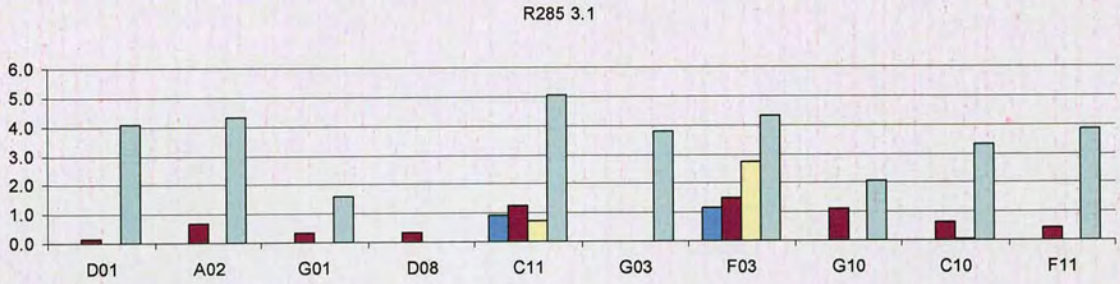
(<i>R</i>)-Ala	(<i>rac</i>)- <i>allo</i> -Thr	(<i>S</i>)-Ala	(<i>rac</i>)-1,2,3,4-tetrahydroisoquinoline-3-carboxylic acid

R285 1.1



R285 2.1





RgDAAO R285: highest rates towards (*R*)-pipercolinic acid

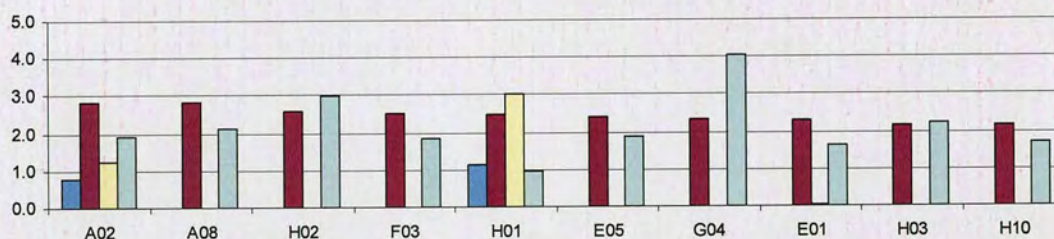
Plate-1.1	Normalised rate	Plate-2.1	Normalised rate	Plate-3.1	Normalised rate
E02	5.3E-03	E12 neg	2.8E-02	D01	5.2E-03
C03	4.8E-03	D04	9.7E-04	A02	3.5E-03
G12 R	4.1E-03	H07	9.3E-04	G01	3.2E-03
C04	4.1E-03	B02	8.4E-04	D08	2.6E-03
F05	4.1E-03	B04	4.3E-04	C11	2.3E-03
F06	3.7E-03	E05	4.1E-04	G03	2.0E-03
A07	2.3E-03	G05	3.8E-04	F03	1.8E-03
E11	2.3E-03	G11	3.5E-04	G10	1.3E-03
H09	2.0E-03	F06	3.3E-04	C10	1.2E-03
A06	1.6E-03	B06	2.8E-04	F11	1.2E-03
Av R285	1.9E-03	Av R285	1.7E-04	Av R285	3.1E-04

Plate-5.1	Normalised rate	Plate-6.1	Normalised rate
H06	9.9E-03	H08	9.8E-02
C09	7.7E-03	D03	2.7E-02
C10	6.8E-03	G08	2.2E-02
C02	5.4E-03	F08	1.1E-02
G04	5.4E-03	H03	1.0E-02
A05	4.6E-03	B02	5.8E-03
B03	4.5E-03	B01	5.5E-03
D06	4.4E-03	D05	5.4E-03
B06	3.2E-03	B03	5.1E-03
E10	3.0E-03	B06	5.1E-03
Av R285	1.1E-04	Av R285	1.6E-04

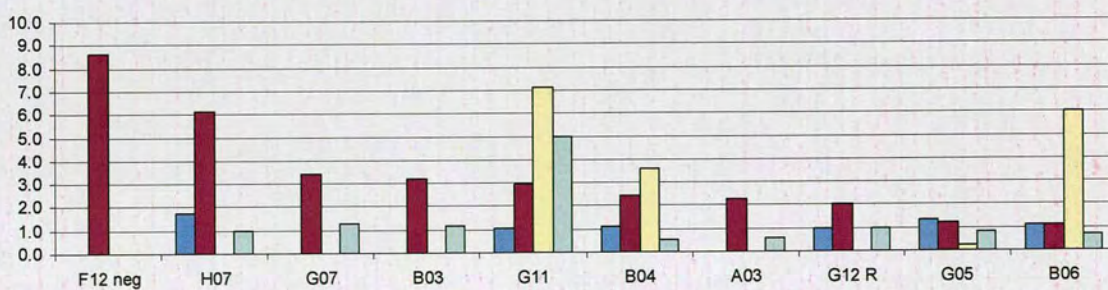
5.9.24 RgDAAO R285: (*rac*)-*allo*-threonine

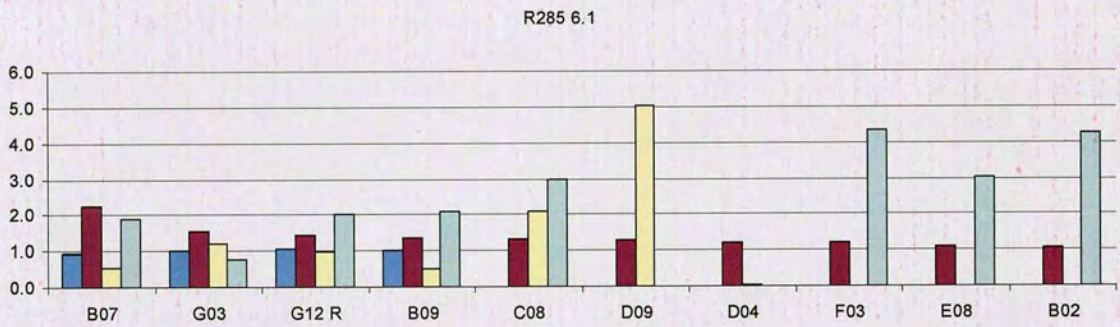
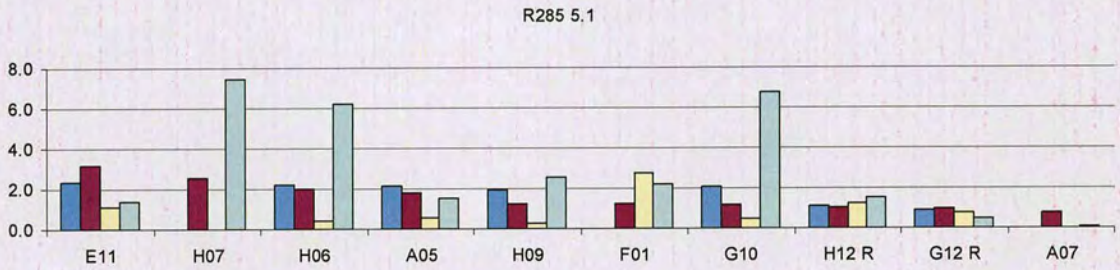
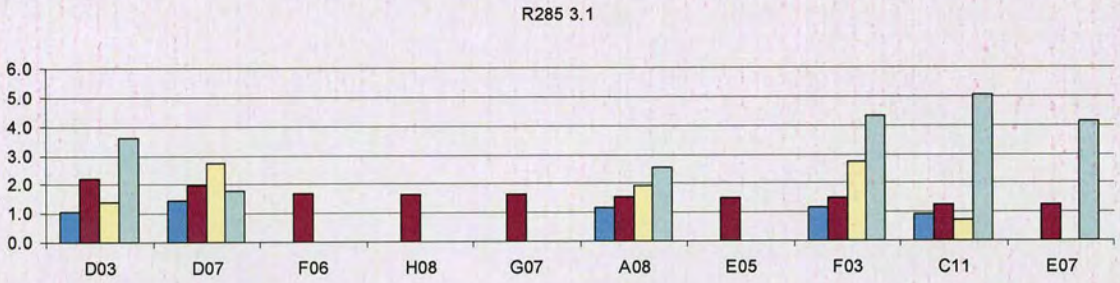
(<i>R</i>)-Ala	(<i>rac</i>)- <i>allo</i> -Thr	(<i>S</i>)-Ala	(<i>rac</i>)-1,2,3,4-tetrahydroisoquinoline-3-carboxylic acid

R285 1.1



R285 2.1





RgDAAO R285: highest rates towards (*rac*)-*allo*-threonine

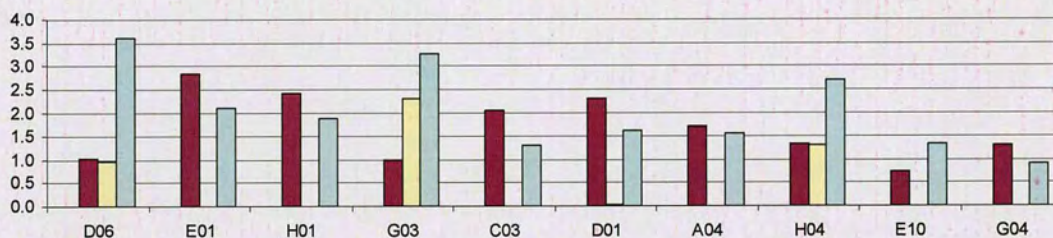
Plate-1.1	Normalised rate	Plate-2.1	Normalised rate	Plate-3.1	Normalised rate
A02	2.1E-01	F12 neg	2.4E-01	D03	2.3E-01
A08	2.1E-01	H07	1.7E-01	D07	2.1E-01
H02	1.9E-01	G07	9.4E-02	F06	1.8E-01
F03	1.9E-01	B03	8.7E-02	H08	1.7E-01
H01	1.9E-01	G11	8.2E-02	G07	1.7E-01
E05	1.8E-01	B04	6.7E-02	A08	1.6E-01
G04	1.7E-01	A03	6.2E-02	E05	1.6E-01
E01	1.7E-01	G12 R	5.5E-02	F03	1.6E-01
H03	1.6E-01	G05	3.4E-02	C11	1.3E-01
H10	1.6E-01	B06	3.1E-02	E07	1.3E-01
Av R285	7.4E-02	Av R285	2.8E-02	Av R285	1.0E-01

Plate-5.1	Normalised rate	Plate-6.1	Normalised rate
E11	1.4E-01	B07	7.5E-02
H07	1.1E-01	G03	5.2E-02
H06	8.5E-02	G12 R	4.8E-02
A05	7.7E-02	B09	4.6E-02
H09	5.4E-02	C08	4.4E-02
F01	5.2E-02	D09	4.3E-02
G10	5.1E-02	D04	4.0E-02
H12 R	4.5E-02	F03	4.0E-02
G12 R	4.1E-02	E08	3.6E-02
A07	3.2E-02	B02	3.5E-02
Av R285	4.3E-02	Av R285	3.4E-02

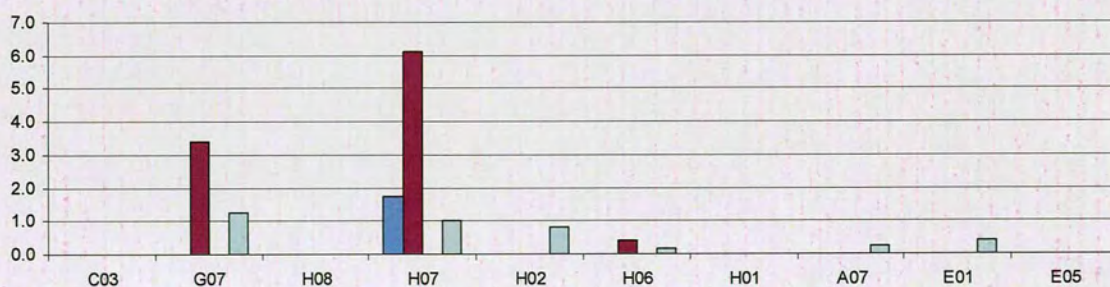
5.9.25 RgDAAO R285: (*rac*)- β -homophenylalanine

(<i>R</i>)-Ala	(<i>rac</i>)- <i>allo</i> -Thr	(<i>S</i>)-Ala	(<i>rac</i>)-1,2,3,4-tetrahydroisoquinoline-3-carboxylic acid

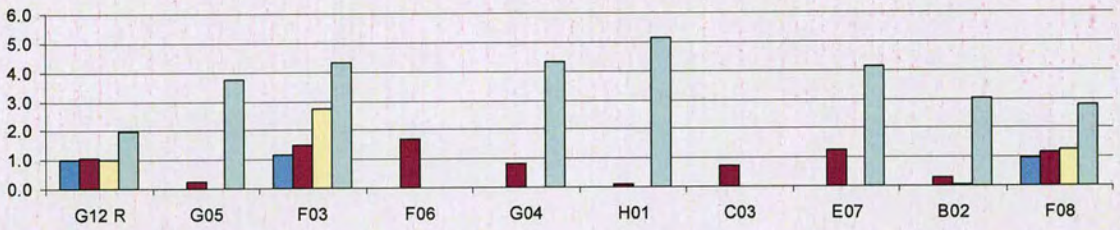
R285 1.1



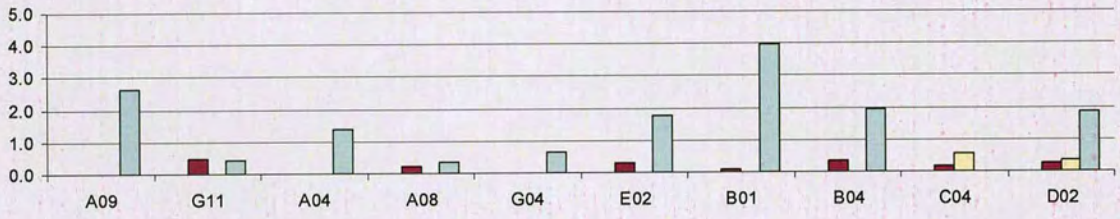
R285 2.1



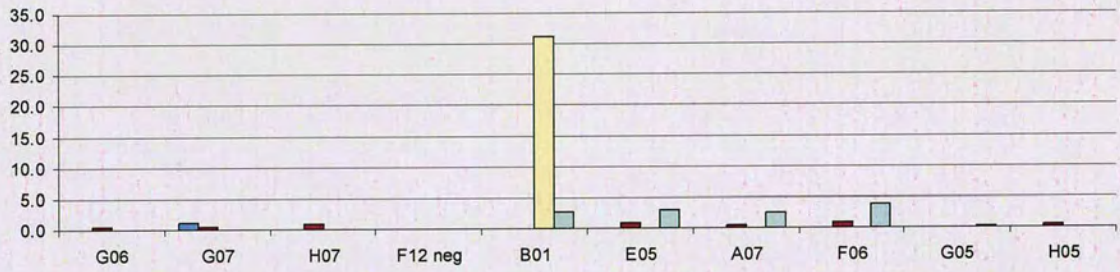
R285 3.1



R285 5.1



R285 6.1



(R)-Ala	(rac)-allo-Thr	(S)-Ala	(rac)-1,2,3,4-tetrahydroisoquinoline-3-carboxylic acid

RgDAAO R285: highest rates towards (*rac*)- β -homophenylalanine

Plate-1.1	Normalised rate	Plate-2.1	Normalised rate	Plate-3.1	Normalised rate
D06	3.2E-01	C03	4.2E-01	G12 R	8.9E-02
E01	1.9E-01	G07	3.1E-01	G05	7.6E-02
H01	1.7E-01	H08	3.0E-01	F03	7.0E-02
G03	1.6E-01	H07	2.9E-01	F06	5.9E-02
C03	1.6E-01	H02	2.4E-01	G04	5.6E-02
D01	1.5E-01	H06	2.3E-01	H01	5.6E-02
A04	1.4E-01	H01	2.2E-01	C03	5.6E-02
H04	1.4E-01	A07	2.2E-01	E07	5.3E-02
E10	1.4E-01	E01	2.0E-01	B02	5.3E-02
G04	1.3E-01	E05	2.0E-01	F08	5.3E-02
Av R285	1.2E-02	Av R285	4.6E-02	Av R285	5.2E-02

Plate-5.1	Normalised rate	Plate-6.1	Normalised rate
A09	1.8E-01	G06	5.2E-02
G11	1.3E-01	G07	5.1E-02
A04	8.7E-02	H07	4.4E-02
A08	7.0E-02	F12 neg	3.5E-02
G04	7.0E-02	B01	3.3E-02
E02	7.0E-02	E05	3.1E-02
B01	6.8E-02	A07	2.6E-02
B04	6.6E-02	F06	2.5E-02
C04	6.5E-02	G05	2.1E-02
D02	6.4E-02	H05	2.1E-02
Av R285	1.5E-03	Av R285	0.0E+00

5.9.26 RgDAAO R285: (*rac*)- 3-aminobutyric acid

Plate-1.1	Normalised rate	Plate-2.1	Normalised rate	Plate-4.1	Normalised rate
B10	1.7E-02	F06	4.1E-02	F06*	2.0E-01
E08	1.3E-02	E05	4.1E-02	H08*	1.5E-01
G04	1.2E-02	A01	3.7E-02	E05*	1.5E-01
D09	1.2E-02	D04	3.3E-02	G07*	1.4E-01
C08	1.2E-02	F02	3.0E-02	A01*	1.2E-01
F05	1.2E-02	B02	3.0E-02	D04*	8.2E-02
D06	1.1E-02	G02	2.5E-02	H04	6.6E-02
A10	1.1E-02	H08	2.5E-02	E07	6.4E-02
H06	1.1E-02	B11	2.2E-02	G06	5.9E-02
C10	1.1E-02	B05	2.2E-02	C01	5.7E-02
Av R285	7.1E-03	Av R285	0.0E+00	Av R285	9.3E-03

Plate-5.1	Normalised rate	Plate-6.1	Normalised rate
A04	3.5E-01	A02	1.8E-01
G04	4.7E-02	B02*	1.5E-01
H02	4.5E-02	H06	1.1E-01
A09	4.3E-02	F03	9.8E-02
F04	4.1E-02	D04*	9.8E-02
E01	4.1E-02	F06*	9.6E-02
A05	3.9E-02	A01*	9.5E-02
C01	3.9E-02	A07	7.7E-02
F05	3.7E-02	C01	7.2E-02
A02	3.6E-02	E08	7.0E-02
Av R285	1.3E-02	Av R285	2.0E-02

5.9.27 RgDAAO R285: (*rac*)- β -phenylalanine

Plate-1.1	Normalised rate	Plate-2.1	Normalised rate	Plate-3.1	Normalised rate
F04	4.0E-01	F12 neg	5.7E-02	F06*	1.7E-01
H06	3.4E-01	D04*	3.1E-02	B02*	1.4E-01
F05	3.3E-01	B02*	3.1E-02	E05*	1.4E-01
G04	3.3E-01	H08*	2.7E-02	D04*	1.4E-01
A02	3.3E-01	G07*	1.8E-02	A01*	1.3E-01
H07	3.2E-01	F06*	1.5E-02	A04	1.3E-01
E04	3.2E-01	H09	1.4E-02	H02	1.2E-01
D01	3.0E-01	A01*	1.4E-02	H01	1.2E-01
D06	3.0E-01	A03	8.3E-03	H06	1.2E-01
H04	3.0E-01	E05*	8.2E-03	A05	1.2E-01
Av R285	3.0E-02	Av R285	0.0E+00	Av R285	6.4E-03

Plate-5.1	Normalised rate	Plate-6.1	Normalised rate
H07	8.9E-02	F02	3.4E-01
C01	8.8E-02	F06*	2.3E-01
G06	8.1E-02	E05*	2.2E-01
A06	8.0E-02	F03	1.8E-01
H09	7.7E-02	G06	1.7E-01
H06	7.6E-02	D08	1.7E-01
B05	7.2E-02	E04	1.7E-01
B03	7.1E-02	D04*	1.5E-01
E04	7.0E-02	H10	1.4E-01
E03	6.7E-02	D09	1.4E-01
Av R285	3.9E-03	Av R285	3.8E-02

5.9.28 RgDAAO Y238: Rates shown prior to normalisation

(R)-alanine	1.1	2.1	3.1	4.1	5.1
F3	6.0E-03	D7 4.5E-03	A5 1.7E-03	D6 5.1E-03	A6 2.2E-03
E2	5.9E-03	E9 1.9E-03	G1 1.1E-03	D10 4.8E-03	D6 1.6E-03
D6	5.2E-03	A8 1.5E-03	G4 9.2E-04	B4 4.2E-03	G3 4.7E-04
E8	5.0E-03	E11 1.0E-03	B3 9.0E-04	F11 3.4E-03	H12 Y 3.8E-04
C5	3.5E-03	G4 1.0E-03	H12 Y 8.4E-04	E10 3.2E-03	G4 2.8E-04
A5	3.5E-03	H10 8.9E-04	C1 3.9E-04	A4 3.0E-03	G12 Y 2.7E-04
F5	2.9E-03	F7 7.9E-04	D6 3.7E-04	E4 2.4E-03	E4 1.2E-04
F9	1.3E-03	B9 7.3E-04	G12 Y 2.6E-04	C7 2.2E-03	G1 1.0E-04
G10	1.0E-03	A7 6.1E-04	D11 1.5E-04	H6 1.9E-03	C2 9.6E-05
H9	6.9E-04	G9 5.0E-04	A4 1.3E-04	B9 1.9E-03	H10 7.8E-05
Av Y	2.3E-04	Av Y 1.3E-04	Av Y 5.5E-04	Av Y 2.1E-04	Av Y 3.3E-04

(S)-alanine	1.1	2.1	3.1	4.1	5.1
F12 neg	5.2E-04	A8 3.8E-04	B3 7.4E-05	F12 neg 2.7E-04	D6 9.9E-04
F3	2.6E-04	D7 1.1E-04	D6 2.0E-05	D6 1.9E-04	H3 6.2E-04
E2	1.5E-04	E9 3.2E-05	H12 Y 1.7E-05	B4 1.6E-04	A6 2.7E-04
D6	1.1E-04	E1 2.9E-05	A5 1.4E-05	D10 1.3E-04	H10 6.8E-05
C5	8.7E-05	G4 2.7E-05	G3 1.2E-05	F11 8.2E-05	D10 9.1E-06
E8	7.2E-05	E11 2.0E-05	G1 1.2E-05	E10 6.5E-05	G12 Y 6.6E-06
F5	5.1E-05	A7 1.4E-05	C1 9.7E-06	C7 6.4E-05	A3 6.4E-06
A5	4.6E-05	F7 1.3E-05	G12 Y 7.8E-06	A4 5.9E-05	G3 5.0E-06
B1	2.1E-05	B9 1.0E-05	A4 7.6E-06	B9 5.5E-05	C2 4.7E-06
D4	2.0E-05	C4 9.1E-06	G6 7.4E-06	B6 5.4E-05	C10 4.5E-06
Av Y	2.8E-06	Av Y 2.2E-06	Av Y 1.3E-05	Av Y 6.4E-06	Av Y 5.4E-06

(R)-pipecolinic acid	1.1	2.1	3.1	4.1	5.1
E2	1.3E-05	D7 7.0E-06	D12 neg 1.7E-04	D10 9.5E-06	H10 5.4E-06
F3	1.2E-05	H10 5.3E-06	E9 8.9E-06	A4 7.9E-06	B2 5.2E-06
G7	1.0E-05	A4 4.8E-06	E5 7.7E-06	B4 7.6E-06	D4 4.9E-06
F6	8.6E-06	E5 4.6E-06	G7 6.8E-06	G7 7.1E-06	A1 4.0E-06
E5	8.5E-06	C4 3.7E-06	B2 6.3E-06	F11 7.0E-06	G7 3.8E-06
D4	8.3E-06	E9 3.6E-06	F6 5.1E-06	F6 6.3E-06	C3 3.6E-06
B2	8.1E-06	D4 3.6E-06	D4 5.0E-06	D6 6.0E-06	D10 3.3E-06
C3	7.5E-06	C3 3.6E-06	A1 4.9E-06	E5 5.9E-06	E7 3.3E-06
H8	6.9E-06	G7 3.4E-06	C3 4.8E-06	B2 5.2E-06	G3 3.1E-06
G10	5.8E-06	B2 3.0E-06	H8 4.7E-06	C3 4.6E-06	C10 2.9E-06
Av Y	1.2E-06	Av Y 1.6E-07	Av Y 4.4E-07	Av Y 2.4E-07	Av Y 2.6E-07

<i>(rac)</i> -3-aminobutyric acid	1.1	2.1	3.1	4.1	5.1
D4	6.3E-06	E5 6.7E-06	E9 9.0E-06	E5 6.9E-06	D4 8.0E-06
F6	5.9E-06	D4 5.2E-06	D4 7.8E-06	D4 5.8E-06	H8 7.1E-06
E5	5.5E-06	A4 5.1E-06	G7 7.5E-06	F6 5.8E-06	F6 6.9E-06
C3	5.4E-06	B2 4.7E-06	F6 6.2E-06	B2 5.1E-06	A1 6.0E-06
B2	5.1E-06	G7 4.6E-06	C3 6.0E-06	H8 5.0E-06	B6 5.9E-06
A1	2.8E-06	H8 4.4E-06	B2 5.9E-06	C3 4.8E-06	B2 5.8E-06
G7	2.4E-06	H10 4.3E-06	A1 5.4E-06	G7 4.6E-06	C3 5.6E-06
A10	1.3E-06	G11 3.5E-06	E5 4.7E-06	A1 2.4E-06	H10 4.6E-06
G10	1.2E-06	C4 3.4E-06	H11 2.6E-06	G1 4.5E-07	D10 4.6E-06
F12 neg	1.1E-06	A1 3.2E-06	H8 2.1E-06	G4 2.7E-07	E5 3.8E-06
Av Y	1.1E-07	Av Y 7.8E-08	Av Y 0.0E+00	Av Y 0.0E+00	Av Y 0.0E+00

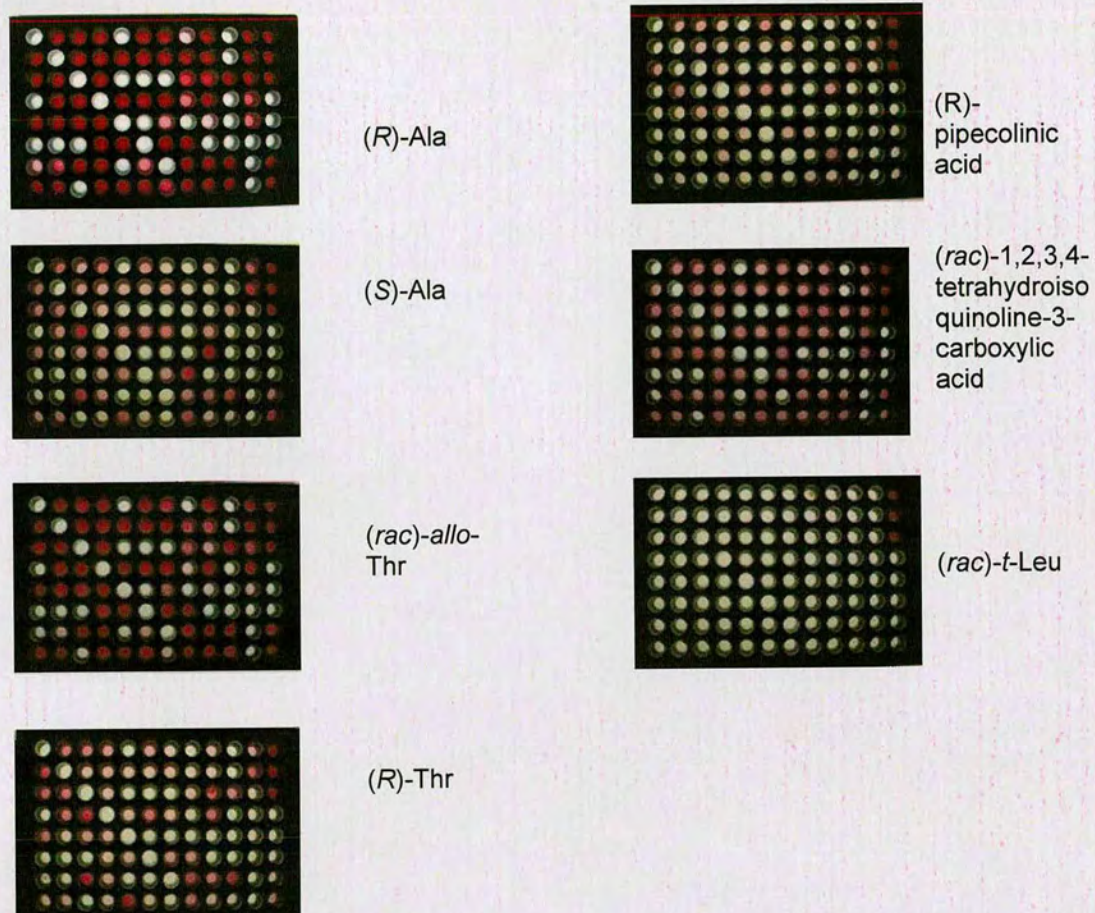


Figure 5.1- RgDAAO F58 plate 5.1